

HYDROGEOLOGICAL CHARACTERIZATION AND INVESTIGATION
OF THE ÇELTİKÇİ COAL BASIN IN CENTRAL ANATOLIA

A THESIS SUBMITTED TO
THE GRADUATE SCHOOL OF NATURAL AND APPLIED SCIENCES
OF
MIDDLE EAST TECHNICAL UNIVERSITY

BY

CANSU KAHRAMAN

IN PARTIAL FULFILLMENT OF THE REQUIREMENTS
FOR
THE DEGREE OF MASTER OF SCIENCE
IN
GEOLOGICAL ENGINEERING

JUNE 2014

Approval of the thesis:

**HYDROGEOLOGICAL CHARACTERIZATION AND
INVESTIGATION OF THE ÇELTİKÇİ COAL BASIN IN CENTRAL
ANATOLIA**

submitted by **CANSU KAHRAMAN** in partial fulfillment of the requirements for
the degree of **Master of Science in Geological Engineering Department, Middle
East Technical University** by,

Prof. Dr. Canan Özgen
Dean, Graduate School of **Natural and Applied Science**

Prof. Dr. Erdin Bozkurt
Head of Department, **Geological Engineering**

Prof. Dr. Hasan Yazıcıgil
Supervisor, **Geological Engineering Dept., METU**

Examining Committee Members:

Prof. Dr. M. Zeki Çamur
Geological Engineering Dept., METU

Prof. Dr. Hasan Yazıcıgil
Geological Engineering Dept., METU

Prof. Dr. M. Lütfi Süzen
Geological Engineering Dept., METU

Assist. Prof. Dr. Koray K. Yılmaz
Geological Engineering Dept., METU

Assist. Prof. Dr. Özlem Yağbasan
Geography Education, Gazi University

Date:

I hereby declare that all information in this document has been obtained and presented in accordance with academic rules and ethical conduct. I also declare that, as required by these rules and conduct, I have fully cited and referenced all material and results that are not original to this work.

Name, Last name: Cansu Kahraman

Signature :

ABSTRACT

HYDROGEOLOGICAL CHARACTERIZATION AND INVESTIGATION OF THE ÇELTİKÇİ COAL BASIN IN CENTRAL ANATOLIA

Kahraman, Cansu

M.S., Department of Geological Engineering

Supervisor: Prof. Dr. Hasan YAZICIGİL

June 2014, 191 pages

Coal exploration activities continue in the vicinity of Çeltikçi town located at 20 km southeast of Kızılcahamam district in Ankara province. The purpose of this study is conduct hydrogeological characterization and investigation of the watershed of Çeltikçi coal basin. In order to accomplish this purpose (1) existing data related to study area were compiled and reviewed; (2) monthly instantaneous flow measurements were conducted to evaluate runoff and surface water flow potential in the study area, (3) exploration wells and pump wells were opened and aquifer tests and groundwater level measurements were conducted at these wells, (4) field quality parameters were measured from all monitoring points and water sampling were conducted from these monitoring wells for detailed laboratory analysis, and (5) water bearing units and relation between them were identified, spatial distribution of aquifer hydraulic parameters, spatial and temporal variation of water levels, spatial and temporal variation of water quality, boundary conditions and conceptual groundwater budget were analyzed. The results of this study present the groundwater problems which can be encountered in future mining operations planned in the field.

Key Words: Çeltikçi Coal Basin, Hydrogeological Characterization, Aquifer Tests

ÖZ

İÇ ANADOLU'DA YER ALAN ÇELTİKÇİ KÖMÜR HAVZASININ HİDROJEOLOJİK ETÜDÜ VE KARAKTERİZASYONU

Kahraman, Cansu

Yüksek Lisans, Jeoloji Mühendisliği Bölümü

Tez Yöneticisi: Prof. Dr. Hasan YAZICIGİL

Haziran 2014, 191 sayfa

Kömür arama faaliyetleri Ankara İli, Kızılcahamam İlçesi'nin 20 km güneydoğusunda yer alan Çeltikçi Beldesi civarında devam etmektedir. Bu çalışmanın amacı Çeltikçi kömür havzasının hidrojeolojik etüdü ve karakterizasyonunu yapmaktır. Bu amaçlar doğrultusunda (1) çalışma alanına ait mevcut veriler toplanıp değerlendirilmiş, (2) anlık akım ölçümleri sahasının su toplama havzasının hidrolojik yapısını ve yüzey suyu potansiyelini belirlemek için gerçekleştirilmiş, (3) gözlem kuyuları ve pompa kuyuları açılarak akifer testleri ve yeraltı suyu seviye ölçümleri gerçekleştirilmiş, (4) tüm yüzey suyu gözlem noktalarından saha kalite parametreleri aylık olarak ölçülmüş su örnekleri alınarak ayrıntılı laboratuvar analizleri gerçekleştirilmiş ve (5) su taşıyan birimler ve bunlar arasındaki ilişkiler ortaya konularak akifer hidrolik parametrelerin, yeraltı suyu seviyelerinin ve su kalitesinin zamansal ve alansal değişimleri analiz edilmiştir. Çalışmanın sonuçları sahada planlanan madencilik faaliyetlerinin yeraltı suyu ile ilgili karşılaşılabilecek sorunları ortaya koymuştur.

Anahtar Kelimeler: Çeltikçi Kömür Havzası, Hidrojeolojik Karakterizasyon, Akifer Testleri

TO MY BELOVED FAMILY...

ACKNOWLEDGEMENTS

The author is grateful to the supervisor, Prof. Dr. Hasan Yazıcıgil, for giving an opportunity to work under his guidance. His theoretical support, guidance, criticism, trust and encouragement have continued at all stages of this study.

The author also would like to thank Prof. Dr. M. Zeki Çamur, Prof. Dr. M. Lütfi Süzen and Assist. Prof. Dr. Koray K. Yılmaz for their valuable contributions to the project number 11-03-09-2-00-36 entitled as “Hydrogeological Investigation and Characterization of the Çeltikçi Coal Basin”. This master thesis was a part of this project which is supported by “İKA Mining Inc. Therefore, most sincere gratitude and appreciation are expressed to each manager and employee of Asia Minor Mining Inc. and İKA Mining Inc. for their support to conduct this thesis.

The author extends her gratitude to Prof. Dr. F. Bora Rojay for his valuable geological study of the Çeltikçi coal basin.

The author would also like to wish deepest thanks to her colleagues; Burcu Ünsal, Çidem Argunhan, Mert Onursal Çatak, Egemen Fırat, Yağmur Derin and Ayşe Peksezer Sayıt for their supports.

The author extends her gratitude to Uygur Duru for his valuable support and encouragement at the initial steps of her career.

Finally, the author would like to express her sincere appreciation to her parents, Haluk Kahraman and Emine Kahraman for their patience, love and encouragement of a life time. Also, the author wants to express her deepest gratitude to her spouse, Cem Ünüştü, for his love and patience in every step of her life.

TABLE OF CONTENTS

ABSTRACT	v
ACKNOWLEDGEMENTS.....	viii
TABLE OF CONTENTS	ix
LIST OF TABLES.....	xii
LIST OF FIGURES	xiv
1. INTRODUCTION	1
1.1. PURPOSE AND SCOPE.....	1
1.2. GEOGRAPHICAL LOCATION OF THE STUDY AREA.....	2
1.3. EXISTING STUDIES.....	2
2. DESCRIPTION OF THE STUDY AREA	5
2.1. TOPOGRAPHY AND LAND COVER.....	5
2.2. SETTLEMENT AREAS AND POPULATION	9
2.3. CLIMATE AND METHODOLOGY	10
2.3.1. Precipitation.....	12
2.3.2. Temperature.....	24
2.3.3. Relative Humidity.....	26
2.3.4. Evaporation.....	27
2.4. GEOLOGY.....	30
2.4.1. Regional Geology	30
2.4.2. Stratigraphy.....	31
2.4.3. Structural Geology.....	44

3. SURFACE WATER HYDROLOGY	51
3.1. REGIONAL AND STUDY AREA DRAINAGE NETWORK	51
3.2. OBSERVED FLOW DATA.....	52
3.2.1. Stream Gauging Stations.....	53
3.2.2. Surface Water Monitoring Points.....	63
3.3. CONCEPTUAL WATER BUDGET OF THE STUDY AREA	73
3.4. EXISTING AND PLANNED WATER STRUCTURES.....	81
4. HYDROGEOLOGY	85
4.1. WATER POINTS	85
4.1.1. Surface Waters	85
4.1.2. Springs and Fountains.....	86
4.1.3. Wells	95
4.2. HYDROGEOLOGY OF THE STUDY AREA.....	100
4.2.1. Hydraulic Parameters	102
4.2.2. Groundwater Elevations	111
4.2.3. Hydrogeological Cross-sections.....	128
4.2.4. Fluid Pressure under the Coal Seam	129
4.3. CONCEPTUAL GROUNDWATER BUDGET	141
4.4. EXISTING AND PLANNED GROUNDWATER USAGE.....	145
4.5. THERMAL WATER RESOURCE.....	146
5. HYDROCHEMISTRY AND WATER QUALITY	149
5.1. STUDIES CONDUCTED	149
5.2. SURFACE WATER HYDROCHEMISTRY	149
5.2.1. Analysis of Field Parameters.....	150
5.2.2. Analysis of Laboratory Parameters	154

5.3. GROUNDWATER HYDROCHEMISTRY	157
5.3.1. Spring and Fountains	157
5.3.2. Wells	164
5.3.3. Villages Water Depots	171
5.4. WATER QUALITY	174
5.4.1. Surface Water.....	174
5.4.2. Spring and Fountain.....	177
5.4.3. Wells	178
5.4.4. Water Depots	182
6. CONCLUSIONS AND RECOMMENDATIONS	185
6.1. CONCLUSIONS	185
6.2. RECOMMENDATIONS	187
REFERENCES	189

LIST OF TABLES

TABLES

Table 2.1. General information of meteorological stations related to the study area	11
Table 2.2. Estimation of monthly total precipitation value of long term Çeltikçi meteorological station by using %error value between Kızılcahamam and Çeltikçi meteorological station.....	20
Table 3.1. Data of stream gauging stations	54
Table 3.2. Instantaneous flow measurement data of surface water monitoring points	66
Table 3.3. Catchment area of the surface water monitoring points and water structures	68
Table 3.4. Curve Number calculation for sub-basins	77
Table 3.5. Monthly conceptual water budget of the study area	79
Table 3.6. Annual water budget results	80
Table 3.7. Calculation of total unit surface runoff of the study area in 2013.....	81
Table 3.8. Information of the dams which are located in the vicinity of the study area	83
Table 3.9. Information of the ponds which are located in the vicinity of the study area	83
Table 3.10. Information of the dam/pond which are located in the vicinity of the study area.....	84
Table 4.1. Information of springs in the study area.....	89
Table 4.2. Flow rates of the fountains vicinity of the study area	90
Table 4.3. Information of the Bank of Provinces Wells.....	96
Table 4.4. Well detail of pump wells and monitoring wells in the study area	100
Table 4.5. Aquifer tests and target geological units	102
Table 4.6. Aquifer test results.....	107

Table 4.7. Hydraulic conductivity and storativity values of the each geological unit	109
Table 4.8. Anisotropy ratio of the wells.....	110
Table 4.9. Fluid pressures calculated at the wells.....	141
Table 4.10. Conceptual Groundwater Budget of the study area	142
Table 5.1. Average hydrochemical field parameters analysis result of surface water monitoring points (nm: not measurement, sm: single measurement)	153
Table 5.2. Average hydrochemical field parameters analysis result of fountains (nm: not measurement, sm: single measurement).....	159
Table 5.3. Field parameters of the fountain monitoring points which are located out of the tenements	161
Table 5.4. Probable lithological units which interact with fountain water and cation facies of the fountain monitoring points	164
Table 5.5. Hydrochemical field parameters of the monitoring wells which were measured at sampling.....	166
Table 5.6. Electrical conductivity (EC) and Temperature (T) values of the wells at the bottom and top of the screen level	167
Table 5.7. Hydrochemical field parameters of the village water depots.....	172
Table 5.8. Surface water quality classification	176
Table 5.9. Water quality classification of fountain monitoring points	179
Table 5.10. Water quality classification of well samples.....	181
Table 5.11. Water quality classification of water depots of the villages	183

LIST OF FIGURES

FIGURES

Figure 1.1. Site location map.....	3
Figure 2.1. Geographic position of the study area	6
Figure 2.2. Elevation map of the study area.....	7
Figure 2.3. Soil properties of the study area.....	8
Figure 2.4. Land use and vegetation cover of the study area	8
Figure 2.5. Population distribution of the villages near the study area	9
Figure 2.6. Meteorological stations in vicinity of the study area	10
Figure 2.7. Automated meteorological station which was installed in south of Binkoz village.....	12
Figure 2.8. Graph of annual total precipitation (mm) and cumulative deviation from the annual average (mm)	13
Figure 2.9. Comparison of the annual total precipitation between 1970 and 1991.	14
Figure 2.10. Comparison of the cumulative precipitation between 1970 and 1991	15
Figure 2.11. Comparison of the meteorological stations near the study area between the years 1987-1993	16
Figure 2.12. Comparison of monthly average precipitation of Kızılcahamam, Çeltikçi and Kurtboğazi stations (a) line graph, (b) bar graph and precipitation values.....	17
Figure 2.13. Scatter diagrams of monthly total precipitation of Kızılcahamam and Çeltikçi meteorological station between the years of 1986 and 1994.....	19
Figure 2.14. Scatter diagrams of daily total precipitation values of Binkoz meteorological station and Kızılcahamam and Etimesgut meteorological stations (June-August 2013).....	21
Figure 2.15. Scatter diagrams of daily average temperature of Binkoz meteorological station and Kızılcahamam and Etimesgut meteorological stations (June-August 2013).....	22

Figure 2.16. Scatter diagrams of daily minimum temperature of Binkoz meteorological station and Kızılcahamam and Etimesgut meteorological stations (June-August 2013).....	22
Figure 2.17. Scatter diagrams of daily maximum temperature of Binkoz meteorological station and Kızılcahamam and Etimesgut meteorological stations (June-August 2013).....	23
Figure 2.18. Scatter diagrams of relative humidity of Binkoz meteorological station and Kızılcahamam and Etimesgut meteorological stations (June-August 2013)	23
Figure 2. 19. Distribution of the monthly average temperature values for Çeltikçi and Kızılcahamam stations	24
Figure 2. 20. Distribution of the average monthly minimum temperature values for Çeltikçi and Kızılcahamam stations.....	25
Figure 2.21. Distribution of the average monthly maximum temperature values for Çeltikçi and Kızılcahamam stations.....	26
Figure 2.22. Distribution of the average relative humidity values for Çeltikçi and Kızılcahamam stations	27
Figure 2.23. Average monthly total open surface precipitation values of Kızılcahamam, Kurtboğazi and Beypazarı stations (Only the months which have at least 15-year data).....	28
Figure 2.24. Correlation coefficient of linear relation between monthly average temperature and monthly total evaporation of Kızılcahamam meteorological station	29
Figure 2.25. Distribution of monthly total precipitation and monthly total evaporation in a year of Kızılcahamam meteorological station between 1973 and 2011	29
Figure 2.26. Tectonic setting of Galatian Volcanic Province (GVP) (Rojay, 2013)	30
Figure 2.27. Generalized columnar section of the study area (Rojay, 2013).....	34
Figure 2.28. Geological map of the study area (Rojay, 2013)	35

Figure 2.29. Miocene Çavuşlar mudrocks-clastics on top of the Miocene volcanic (to the left) and cross-cutting relations with Miocene volcanics (to the right) manifesting intrusive contact (Rojay, 2013)	36
Figure 2.30. Miocene Çavuşlar Sequence on top of Miocene volcanics (Rojay, 2013).....	36
Figure 2.31. View of Miocene andesitic lavas and pyroclastics, dipping NNW (Rojay, 2013).....	37
Figure 2.32. General view of Miocene Çeltikçi sequences (Rojay, 2013).....	39
Figure 2.33. Pumice fragments bearing tuff layers within mudrocks (Rojay, 2013)	39
Figure 2.34. Silicification of Miocene Çavuşlar Mudrocks (north of Aşağıadaköy village) (Rojay, 2013).....	40
Figure 2.35. Basalt dyke (B dyke) intruded into a) Abacı İgnimbite (Çavuşlar village) and b) Çavuşlar member (Mahkemeağıcın village) (Rojay, 2013)....	41
Figure 2.36. General view of Bezci member a) Bezci mb on Miocene Kocalar carbonates (Bezcikuzören village), b) Quaternary terraces conglomerates on top of Bezci mb (northwest of Gümele) (Rojay, 2013).....	42
Figure 2.37. The Quaternary terrace cobble conglomerates unconformably overlies the Plio-Quaternary units (Rojay, 2013)	44
Figure 2.38. Kocalar landslide (Rojay, 2013)	44
Figure 2.39. The view of the Çavuşlar fault-2 (ÇF-2) (Rojay, 2013)	47
Figure 2.40. Binkoz normal faults (Rojay, 2013).....	48
Figure 2.41. EW trending Aşağıadaköy normal fault (Rojay, 2013)	48
Figure 3.1. Map of catchment basins of Kirmir Stream and Kurt Creek, gauging stations and water structures in the vicinity of the study area.....	52
Figure 3. 2. Information of number of days of available data of stream gauging stations.....	54
Figure 3.3. Hydrograph of the daily average flow rates of Kızılcahamam – Mandra (12-017) station (a) arithmetic scale, (b) logarithmic scale.....	55

Figure 3.4. Monthly average flow rates of Kızılcahamam – Mandra (12-017) station (a) 1960-2013 water years, (b) 1960-1991 water years (uncontrolled flow), (c) 1992-2013 water years (controlled flow).....	56
Figure 3.5. Flow duration curve of Kızılcahamam – Mandra (12-017) station (a) arithmetic scale, (b) logarithmic scale (1960-2013)	57
Figure 3.6. (a) Annual lowest flow rate, (b) first date of the lowest flow rate of the Kızılcahamam – Mandra (12-017) station	58
Figure 3.7. Annual flow duration curves by using the lowest flow rates.....	59
Figure 3.8. For Kızılcahamam – Mandra (12-017) station (a) the longest period of continuous low flow in a year, (b) total number of days of the daily average flow remain under the low flow threshold ($0.21 \text{ m}^3/\text{s}$)	60
Figure 3.9. Data of annual total precipitation measured at Kızılcahamam (17664) and annual average flow measured at Kızılcahamam – Mandra (12-017) stations	61
Figure 3.10. Data of annual total precipitation measured at Kızılcahamam (17664) and annual average flow measured at Sey - Saray (12-030) stations.....	62
Figure 3.11. Data of annual total precipitation measured at Kızılcahamam (17664) and annual average flow measured at Bulak - Derince (12-081) stations.....	62
Figure 3.12. Data of annual total precipitation measured at Kızılcahamam (17664) and annual average flow measured at Kirmir - Gdl (12-139) stations.....	63
Figure 3.13. Catchment area of the surface water monitoring points of the study area	64
Figure 3.15. The fountain which was determined at the field study conducted on 25 April 2013	71
Figure 3.16. Daily precipitation and average temperature data of Kızılcahamam (January 2012-May 2013) and Binkoz (June 2012-December 2013) meteorological stations (a) and flow rates of surface water monitoring points (b-f)	72
Figure 3.17. Comparison of flow rates at 12-07 and SW1.....	73
Figure 4.1. Distributions of the drainage areas, water structures and surface water monitoring points	86

Figure 4.2. Fountain locations on the topographic map	87
Figure 4.3. Fountain locations on the geological map.....	88
Figure 4.4. Variations of the discharge rates of the fountains.....	91
Figure 4.5. Location map of the wells in the study area.....	95
Figure 4.6. Monitoring wells, pump wells and The Bank of Provinces wells in the study area.....	97
Figure 4.7. Distribution map of the monitoring, pump and The Bank of Provinces Wells on the geological map	98
Figure 4. 8. Groundwater elevation contours on geological map of the study area	103
Figure 4. 9. Locations of the wells which were conducted aquifer tests.....	106
Figure 4.10. Calculated hydraulic conductivity values of the study area.....	110
Figure 4.11. Groundwater elevation map of the study area	113
Figure 4.12. Temporal changes of the groundwater measurements at pump and monitoring wells.....	115
Figure 4.13. Temporal changes of the groundwater levels at PW1-PW2	127
Figure 4.14. Temporal changes of the groundwater levels at CEL19A-CEL19B- CEL19D.....	127
Figure 4.15. Temporal changes of the groundwater levels at CEL47-CEL47A ...	128
Figure 4.16. Temporal changes of the groundwater levels at CEL59-CEL59A- CEL59B.....	128
Figure 4.17. A-A' cross section	131
Figure 4.18. B-B' cross section.....	133
Figure 4.19. C-C' cross section.....	135
Figure 4.20. D-D' cross section	137
Figure 4.21. Hydraulic pressure distribution of the study area	139
Figure 4.22. Water supply locations in or vicinity of the study area	146
Figure 4.23. Water points which have thermal potential in the study area	147
Figure 5.1. Surface water, groundwater and water depot monitoring points	151
Figure 5.2. Average pH, EC, DO and ORP parameters (single measurement at SW7 and SW17).....	154

Figure 5.3. Relative distributions of the major ion concentrations of the surface water in 2012 and 2013	156
Figure 5.4. Hydrochemical facies distribution according to surface water major ion average concentrations	156
Figure 5. 5. Average pH, EC, DO and ORP parameters of fountain monitoring points	160
Figure 5.6. Relative distributions of the major ion concentrations of the fountains in 2012 and 2013	162
Figure 5.7. Areal distributions of hydrochemical facies according to major ion average concentrations of fountain monitoring points.....	163
Figure 5.8. Distribution of the average temperature of the wells in the screen level	168
Figure 5.9. Distribution of the average electrical conductivity of the wells in the screen level.....	168
Figure 5.10. Relative distributions of the major ion concentrations of the well waters in 2012 and 2013	170
Figure 5.11. Areal distributions of hydrochemical facies according to major ion average concentrations of well monitoring points	170
Figure 5.12. Average pH, EC, DO and ORP parameters of village water depots	173
Figure 5.13. Relative distributions of the major ion concentrations of the water depots in the villages	174
Figure 5.14. Areal distribution of the surface water monitoring points according to inland water classification.....	177
Figure 5.15. Areal distribution of the fountain monitoring points according to inland water classification.....	178
Figure 5.16. Areal distribution of the well monitoring points according to inland water classification.....	182

CHAPTER 1

INTRODUCTION

1.1. PURPOSE AND SCOPE

The İKA Mining Inc. has been conducting coal exploration activities in the vicinity of the Çeltikçi Town in Kızılcahamam District in Ankara Province. A thermal power plant is planned to be constructed because the preliminary findings of the exploration activities are positive. Before the feasibility and environmental impact assessment studies, it is necessary to conduct a hydrogeological study to investigate the physical, chemical and hydraulic parameters of the watershed area and hydrogeologically characterize the coal basin. The following had been carried out within the scope of this study:

1- Existing topographical, meteorological, geological, hydrological, hydrogeological, geotechnical and water quality data related to or in the vicinity of the project area were compiled and reviewed.

2- Surface water monitoring stations were established to evaluate runoff and surface water flow potential in the project area; measure monthly instantaneous flow rates over the project duration.

3- Hydrogeological investigation and physical, chemical and hydraulic characterization of the project area have been done by converting exploration holes into piezometers, drilling pump wells, conducting aquifer tests, and monitoring groundwater levels.

4- Water quality and hydrogeochemical characterization were done by measuring field water quality parameters (pH, T, EC, DO etc.) on a monthly basis for all surface water and spring monitoring points as well as for some of the

groundwater monitoring wells. In addition, water samples were collected twice a year during the project for detailed laboratory chemical analyses in order to classify water for various usage purposes.

5- Water bearing units and relation between them were identified, spatial distribution of aquifer hydraulic parameters, spatial and temporal variation of water levels, spatial and temporal variation of water quality, boundary conditions and conceptual groundwater budget were analyzed.

1.2. GEOGRAPHICAL LOCATION OF THE STUDY AREA

The project area is located 50 km northwest of the Ankara province (Figure 1.1). Access to the study area is provided with Ankara – İstanbul TEM motorway which divides the study area into two segments. The largest settlement in the vicinity of the study area is Çeltikçi town which is located between the Kirmir and Pazar Streams. The villages located near the study area are Bezcikuzören, Kocalar, Doğanöz, Aşağıadaköy, Demirciören, Kızılca, Alibey, Binkoz, Çavuşlar, Mahkemeağcin, Değirmenönü, Bağören, Kuşçuören, Bağlıca and Gümele.

Project area covers H28a3, H28b3, H28b4, H28c1, H28d2, H29a3 and H29a4 sheets in 1/25 000 scaled topographic map.

1.3. EXISTING STUDIES

Existing hydrological and hydrogeological studies near the study area are limited. Geological maps at scales of 1/100.000 and 1/25.000 have been mapped by General Directorate of Mineral Research and Exploration (MTA). Detailed geological and structural studies of the study area have been conducted by Asia Minor Energy in the scope of the 43-101 Technical Report (2012) and Rojay (2013).

Planning report of the Doğanöz Dam which was constructed at the upstream of the Kirmir Stream by V. Regional Directorate of State Hydraulic Works had been prepared by Akarsu Engineering and Consultancy Co. Ltd. Bank of Provinces drilled

three pump wells in the alluvium of the Pazar Stream and conducted pumping tests. The purpose of the opening of the wells was to provide water to the Çeltikçi Town.

The first hydrogeological study in the Çeltikçi coal basin and the vicinity of the area was conducted by Yazıcıgil et al. (2014). Within the context of this project which is entitled as "Hydrogeological Investigation and Characterization of the Çeltikçi Coal Basin" a series of studies have been conducted including monitoring and pump well installations, aquifer tests, monitoring and sampling of surface and groundwaters. This thesis is a part of this study.

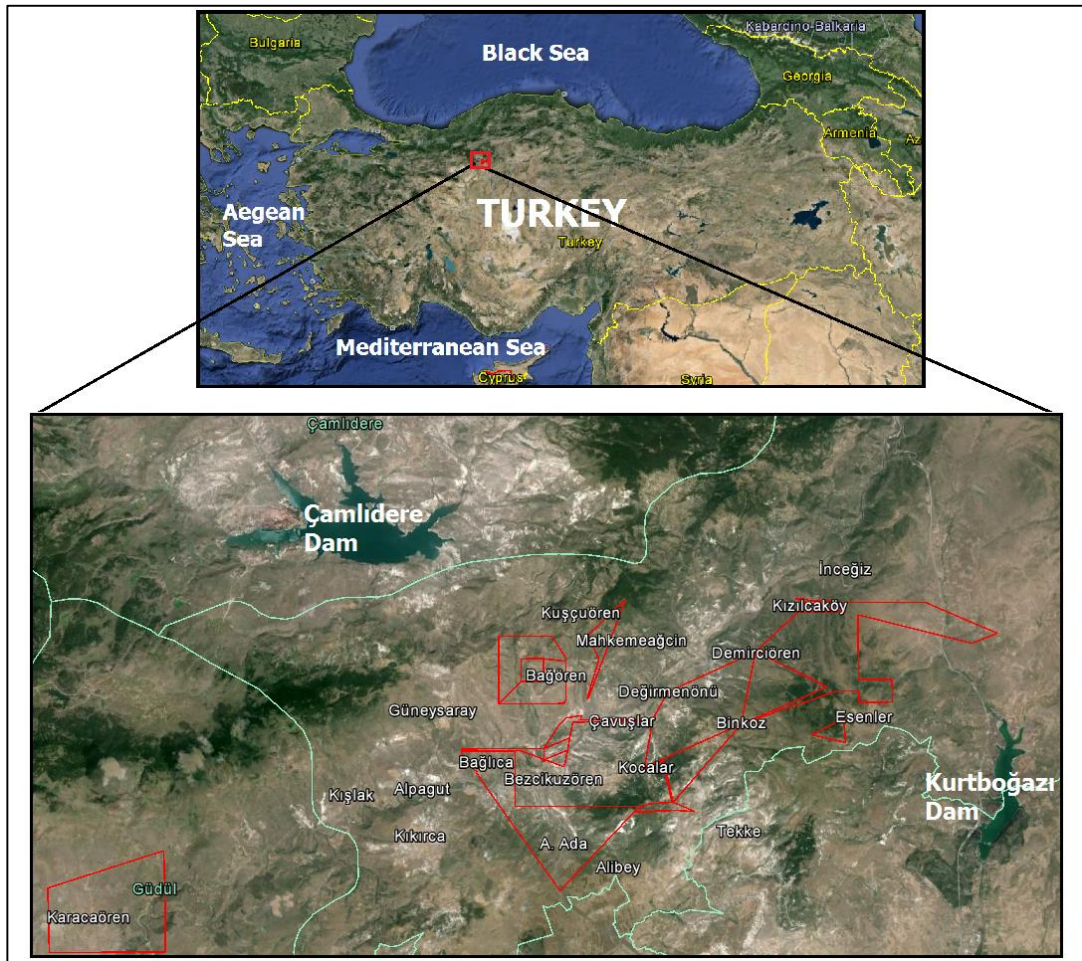


Figure 1.1. Site location map

CHAPTER 2

DESCRIPTION OF THE STUDY AREA

2.1. TOPOGRAPHY AND LAND COVER

Project area is located on steep and rugged terrain. Elevation changes in the ranges between 760-790 m near the Kirmir Stream to 1690 m on Hıdırdede Hill which is at the north of the area (Figure 2.1). Major elevations in the study area are Hıdırdede (1690 m), Yumru (1566 m), Tekçam (1484 m), Erenler (1477 m), Karakuz (1433 m), Tonrul (1432 m), Gür (1408 m), Höyükü (1368 m), Dededoruk (1364 m), Beyce (1353 m), Kırınkaya (1349 m), Dikmen (1341 m), Aktepe (1323 m), Işkınlı (1310 m), Örencikbaşı (1306 m), Asar (1301 m), Ada (1280 m), Tuzluca (1254 m), Kazankaya (1245 m) and Erikliyatak (1206 m) Hills. The digital elevation model of the study area is presented in Figure 2.2.

Information on land usage, soil and vegetation cover in the study area are obtained from 1/25.000 scaled The National Soil Database (NSDB) and they are presented in Figure 2.3 and 2.4, respectively. As can be seen in Figure 2.3, brown forest soil covers the area between Demirciören, Binkoz and Çeltikçi villages. Non-calcareous brown forest soil covers the northern side of the Demirciören village and alluvial soil covers along the floodplain of the Kirmir Stream.

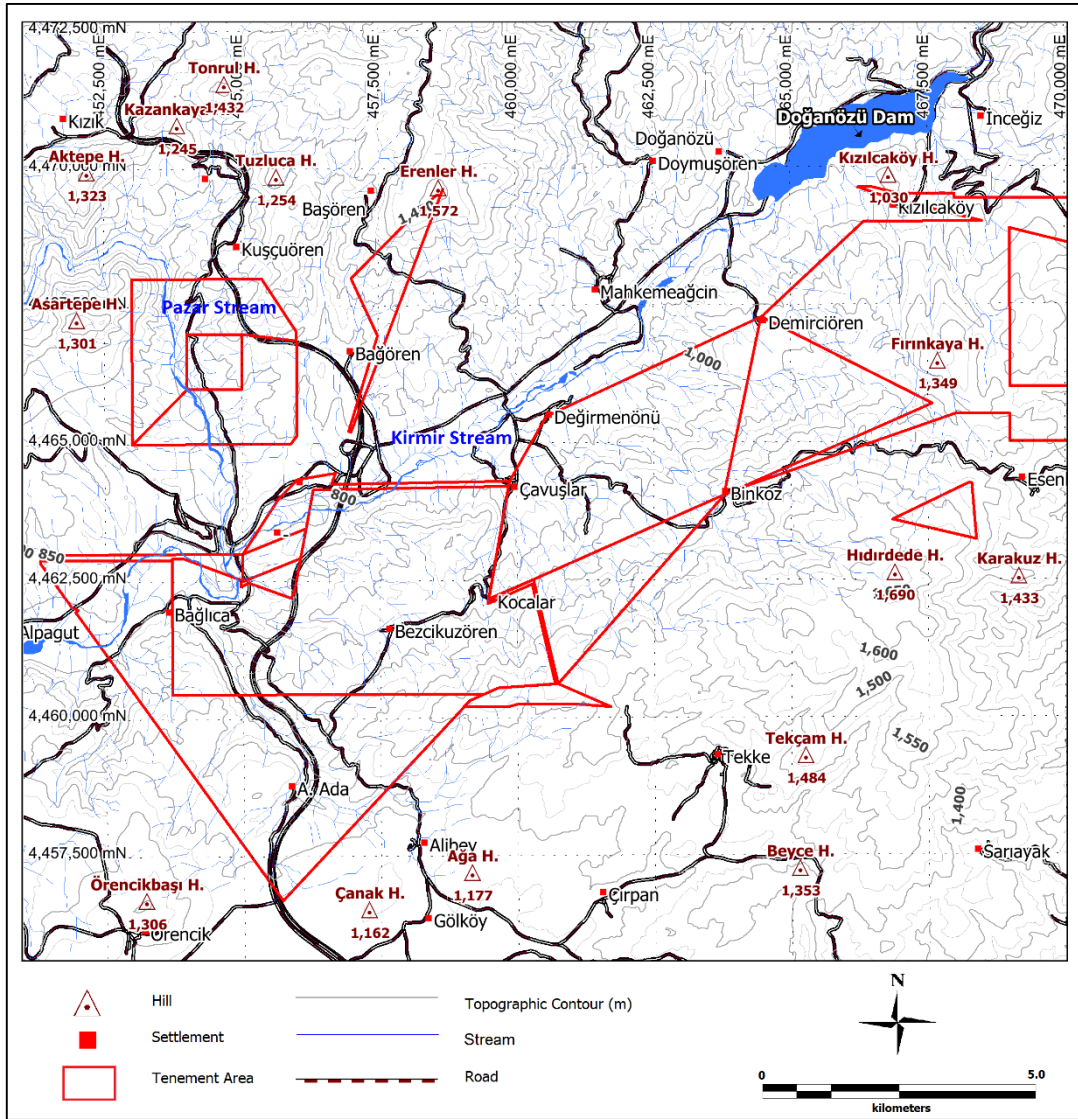


Figure 2.1. Geographic position of the study area

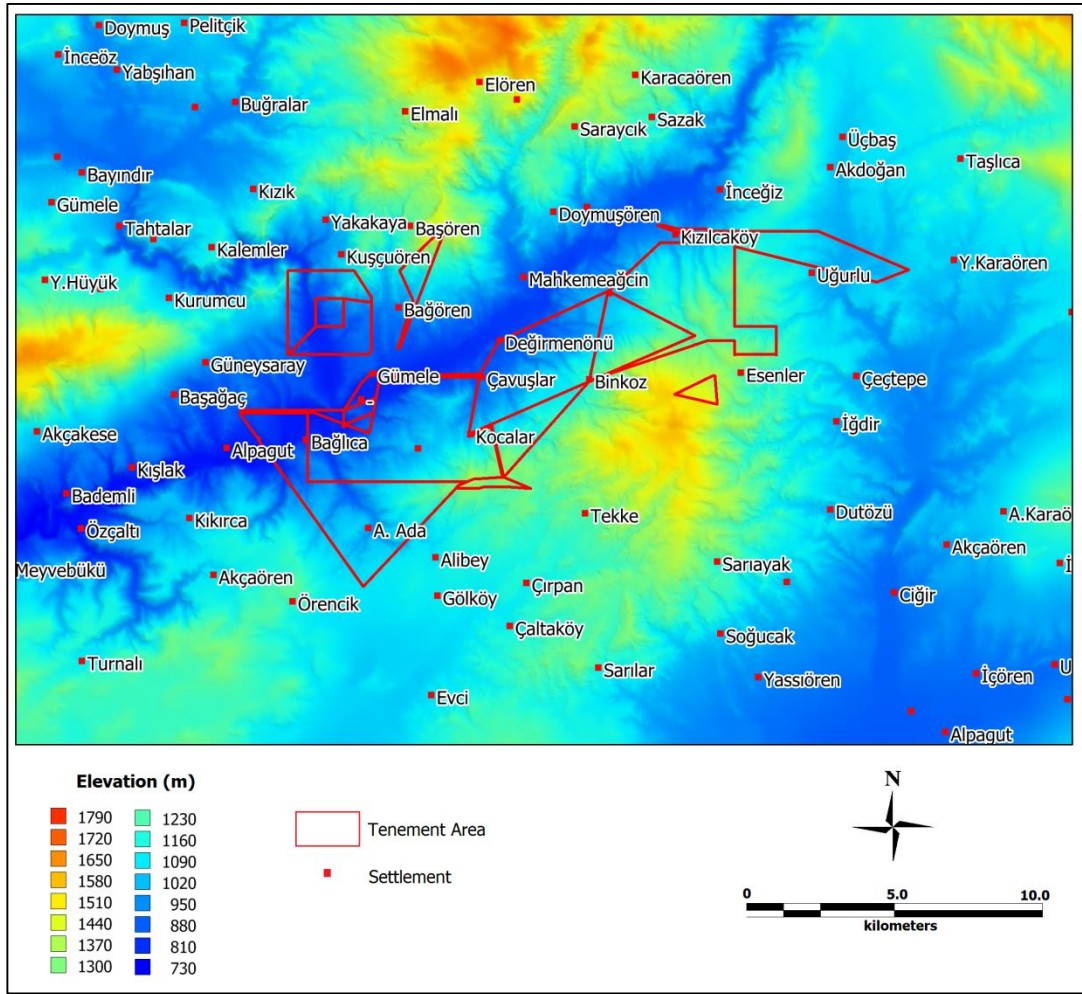


Figure 2.2. Elevation map of the study area

As can be seen in Figure 2.4, the land cover in the southern side of the Kirmir Stream and nearby the Binkoz village is heaths. Dry farming has been done in the vicinity of the Dimirciören village and Kirmir Stream. Brown forestland is dominant in the area between Kızılca and Demirciören villages and irrigated farming is dominant along the Kirmir Stream and around the Çeltikçi Town.

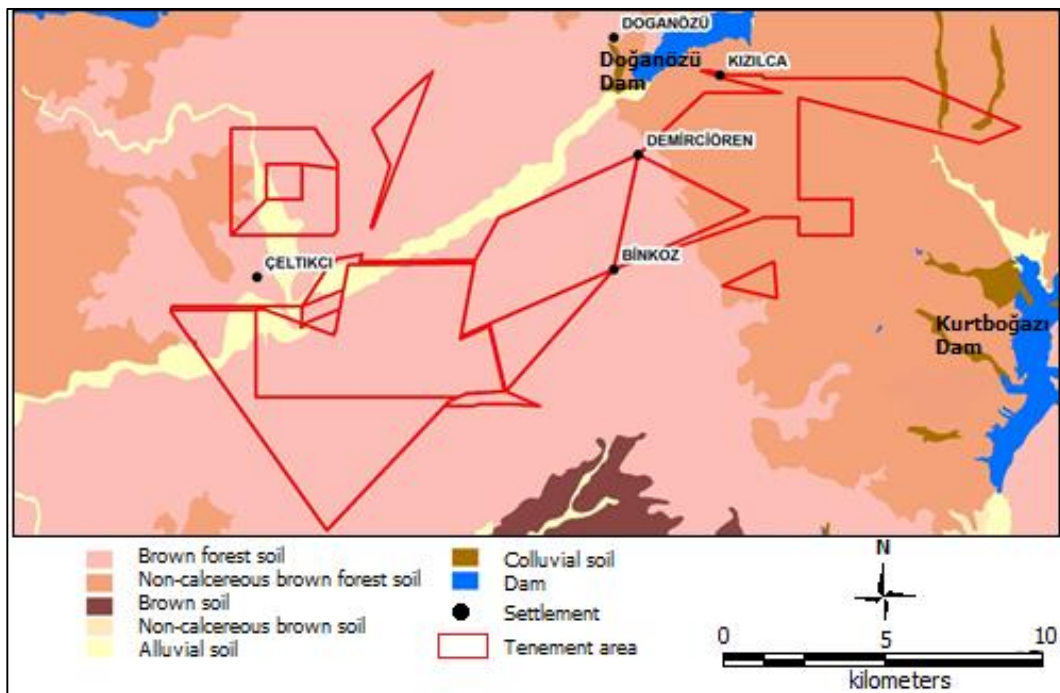


Figure 2.3. Soil properties of the study area

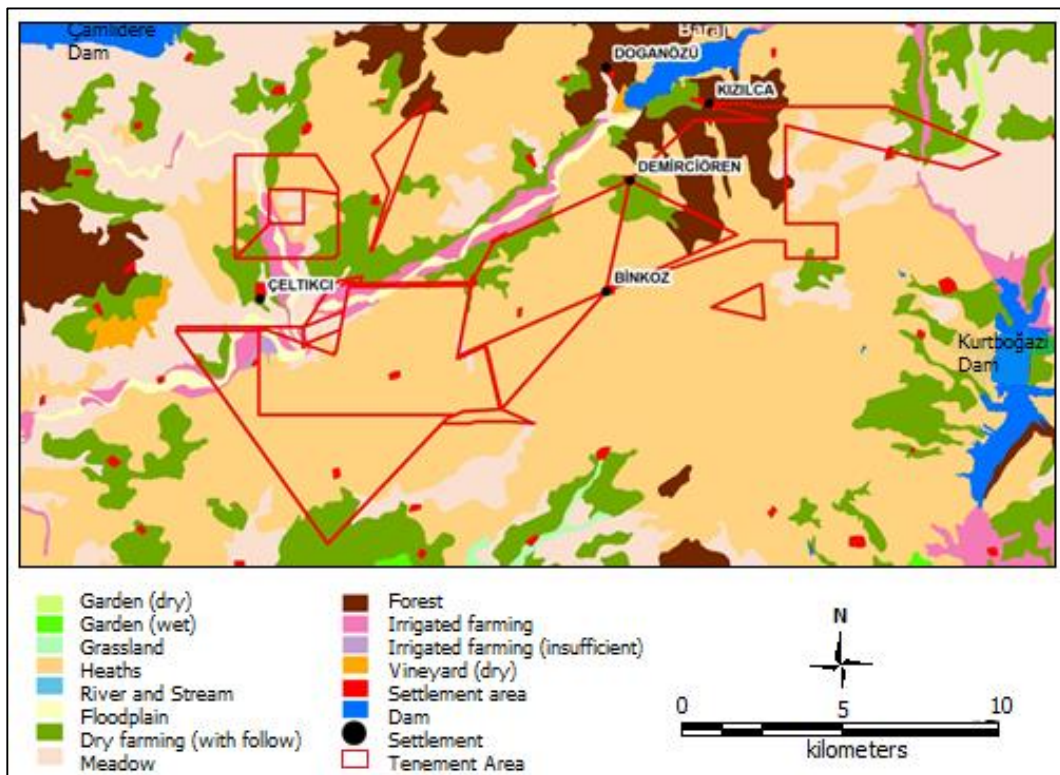


Figure 2.4. Land use and vegetation cover of the study area

2.2. SETTLEMENT AREAS AND POPULATION

Kızılcahamam is the largest district within the study area with a population of 24,635. Because it is located 30 kms away from the project area it is within the socio-cultural influence area of the mining activities. The other settlements in or in the vicinity of the study area are; Kızılcaören, Gümele, Başağaç, Kırkırca, Bağlıca, Kuşcuören, Bağören, Değirmenönü, Güneysaray, Mahkemeağcin, Alpagut, Kışlak, Çavuşlar, Binkoz, Alibey, İnceğiz, Demirciören, Esenler, Aşağıada, Doğanözü, Kocalar and Bezikuzören, villages and Çeltikçi Town. Population statistics of the year 2012 were taken by Address Based Population Registration System of TÜİK (Turkish Statistical Institute). The total population of these villages is 1721. In Figure 2.5, total population and male/female distribution of the villages in the study area is presented graphically.

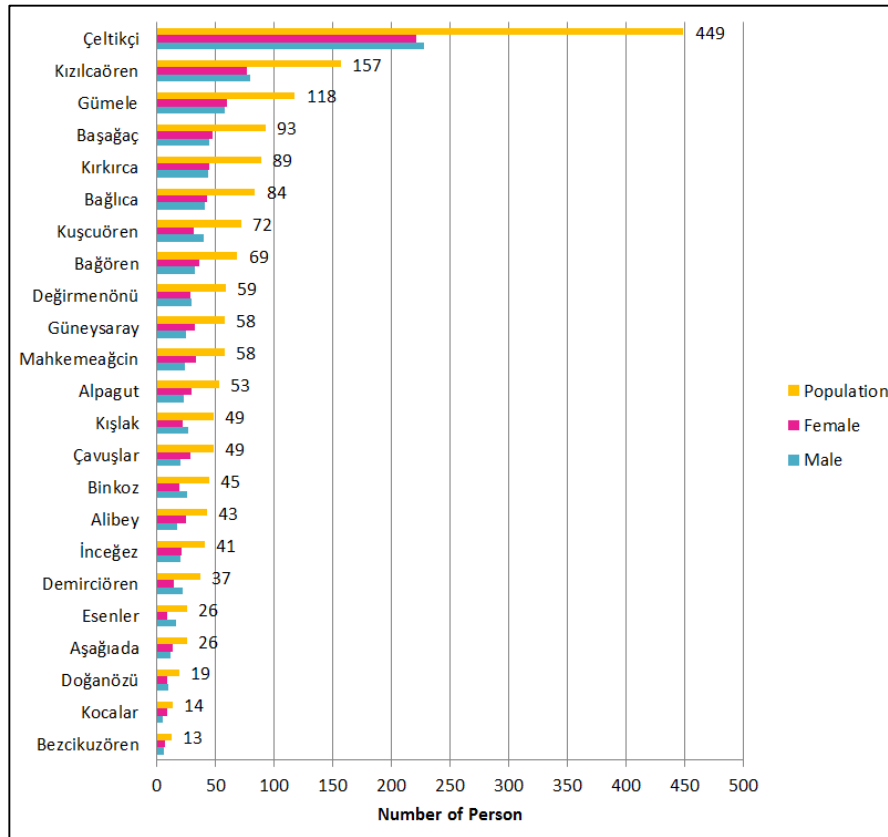


Figure 2.5. Population distribution of the villages near the study area

2.3. CLIMATE AND METHODOLOGY

The study area, located at the northeast of the Sakarya River basin in the Central Anatolian Region is characterized by the continental climate. On the other hand, because of the closeness of the Black Sea Region, moisture content is relatively high. According to Thorntwaite climate classification which is done by Turkish State Meteorological Service (MGM), the area is classified as semiarid-mesothermal climate. Hot and dry summer months and cold, snowy winter months are the characteristics of this type of climate. The majority of the total rainfall occurs in winter, spring and fall seasons.

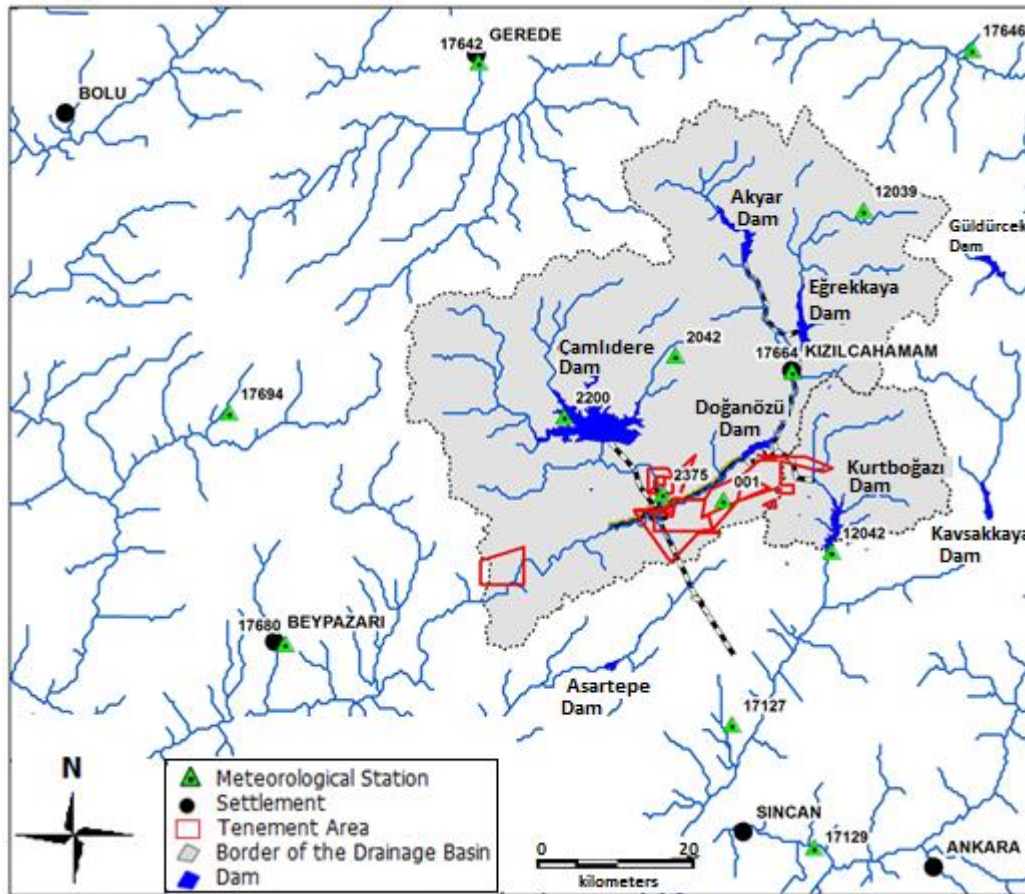


Figure 2.6. Meteorological stations in vicinity of the study area

In order to analyze the spatial and temporal variations in the meteorological data, several stations were selected (Figure 2.6). These are Kızılcahamam, Akıncı-

Mürted, Beypazarı, Kıbrısçık, Gerede, Çerkeş, Etimesgut, Çeltikçi, Peçenek, Çamlıdere-Ankara, Kurtboğazı, Yağcılıhüseyin and Binkoz meteorological stations. The pertinent information about these stations is presented in Table 2.1.

Binkoz meteorological station was established by İKA Mining Inc. in the Binkoz village (Figure 2.7). Meteorological data has been collected since 23 May 2013 at this station. Average wind speed, average wind direction, air temperature (average, minimum and maximum), relative humidity (average, minimum and maximum), dew point temperature (average, minimum and maximum), barometric pressure (average, minimum and maximum), solar radiation (average, minimum and maximum), total rain, and evapotranspiration values have been recorded in 10 minute intervals. Unfortunately, due to the short period of observation, it could not be used for the long-term analysis. Also, in most of the other stations except Kızılcahamam meteorological station, long term data does not exist. Because of the closeness to the study area and the presence of the long term data, Kızılcahamam meteorological station gains more importance. In addition to this, Çeltikçi meteorological station is also important due to its location. Unfortunately it had been operated only the years between 1986 and 1994. Although it was not operated for a long period, it is the most representative station with respect to the meteorological properties of the study area.

Table 2.1. General information of meteorological stations related to the study area

Institution	Station no.	Station name	Easting	Northing	Elevation(m)	Distance between project site (km)	Data Type			
							Precipitation	Temperature	Relative Humidity	Evaporation
MGM	17664	Kızılcahamam M.S.	326500	404667	1033	11	√	√	√	√
MGM	17127	Akıncı-Mürted	325667	400833	831	21	√	√	√	
MGM	17680	Beypazarı	319333	401667	682	47	√	√	√	
MGM	17694	Kıbrısçık	318500	404167	682	47		√	√	
MGM	17642	Gerede	322000	408000	1270	53	√	√	√	
MGM	17646	Çerkeş	329050	408167	1126	53	√	√	√	
MGM	17129	Etimesgut	326833	399500	806	38	√	√	√	
MGM	2375	Çeltikçi	324667	403333	775	0	√	√	√	
MGM	2200	Peçenek	323166	404167	1042	12	√	√	√	
MGM/DSİ	2042	Çamlıdere-Ankara	324833	404833	1175	14	√	√	√	
DSİ	12042	Kurtboğazı	327065	402712	981	8	√			√
DSİ	12039	Yağcılıhüseyin	327503	406418	1550	31	√			
İKA Mining Inc.	001	Binkoz	325492	403264	1083	0	√	√	√	√

2.3.1. Precipitation

Annual total precipitation recorded at the Kızılcahamam meteorological station was evaluated for analyzing the long term precipitation regime of the study area drainage basin. The long-term (1957-2012) average annual rainfall is 580 mm; 1977 is the driest year with 340 mm of annual precipitation and 2009 is the wettest year with 876 mm of annual precipitation. The analyses of the cumulative deviation from the annual average precipitation curve shows that the years between 1962-1972, 1995-1999 and 2009-2012 represent wet period, whereas the years 1957-1961, 1973-1994 and 2002-2008 represent dry period (Figure 2.8).



Figure 2.7. Automated meteorological station which was installed in south of Binkoz village

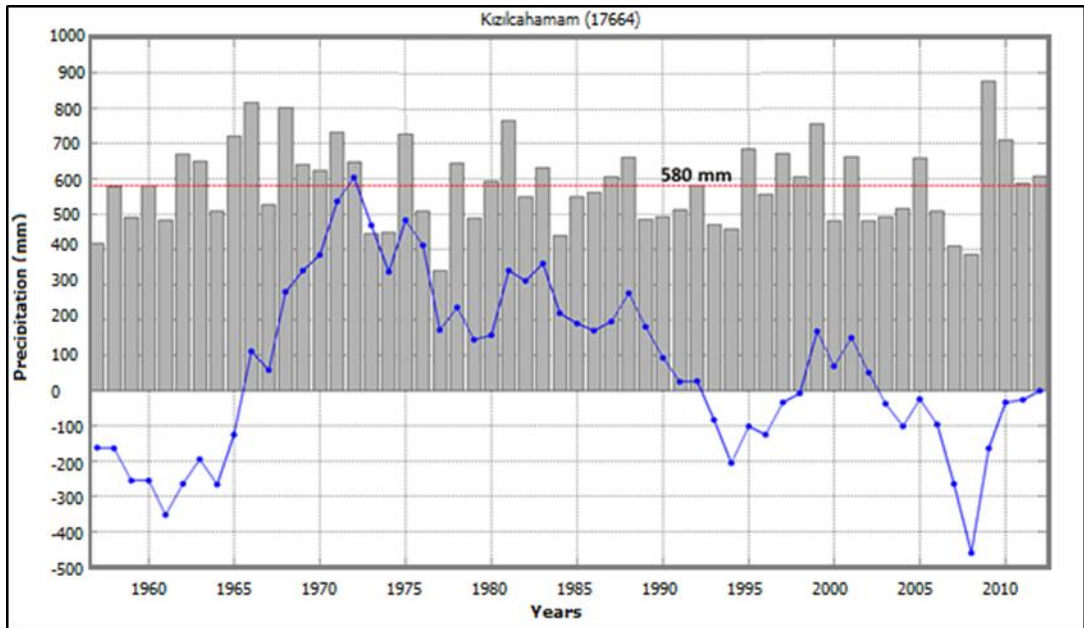


Figure 2.8. Graph of annual total precipitation (mm) and cumulative deviation from the annual average (mm)

In order to analyze the long term trend of the precipitation regime, common time interval (1970-1991) of the meteorological stations, which have long years of precipitation data, was determined. Figure 2.9 shows the total precipitation measured at these stations. As it can be seen in this figure, Kızılcahamam meteorological station has received the highest precipitation compared to the other stations except for the year 1977. Annual trend is similar for all meteorological stations. Kurtboğazi and Etimesgut meteorological stations have the lowest precipitation rate while Akıncı-Mürted and Beypazarı meteorological stations have higher values.

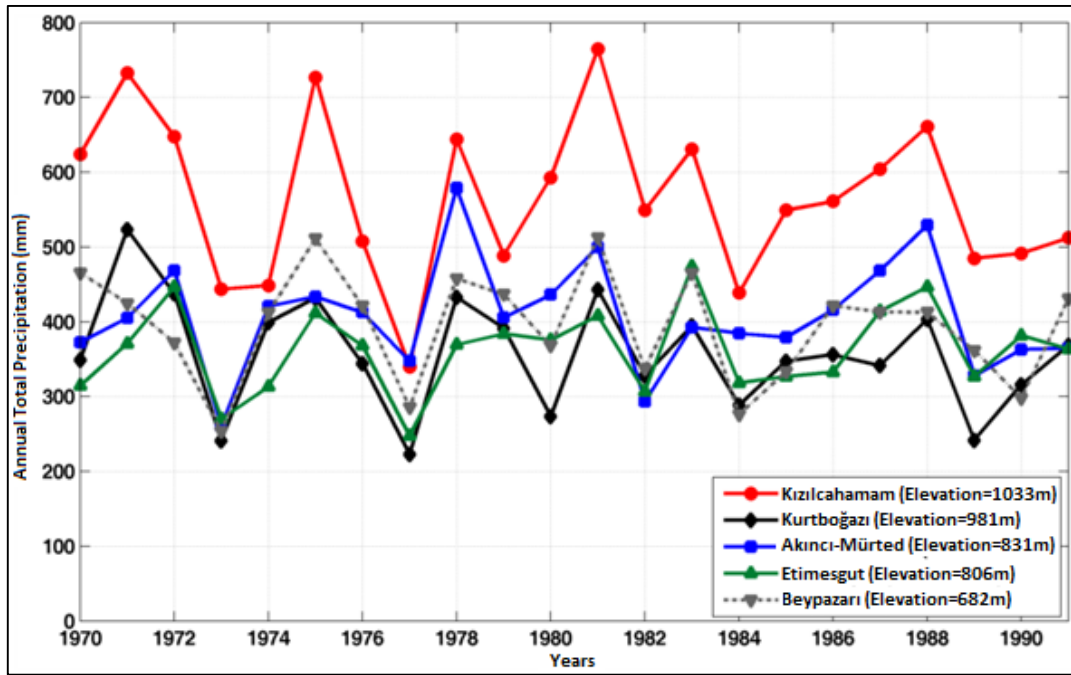


Figure 2.9. Comparison of the annual total precipitation between 1970 and 1991

The cumulative precipitations at the same stations between 1970 and 1991 were compared in Figure 2.10. As it can be seen in this figure, the total precipitation in 1970-1991 period is 12440 mm in Kızılcahamam, 8670 mm in Akıncı-Mürted, 8670 mm in Beypazarı, 7971 mm in Etimesgut and 7876 mm in Kurtboğazi meteorological stations. It was noticed that the precipitation regime in the area is more affected from a north-south position rather than the topographic elevation of the meteorological stations. Precipitation generally decreases from north to south. For instance, although Etimesgut meteorological station (Elevation=806 m) is located at higher elevation than Beypazarı meteorological station (Elevation=682 m), it has lower precipitation than Beypazarı. The only exception to this condition is the Kurtboğazi meteorological station. The reasons why higher precipitation is measured in the Kızılcahamam meteorological station can be listed as closeness to the Black Sea region, forestry vegetation and local climate property.

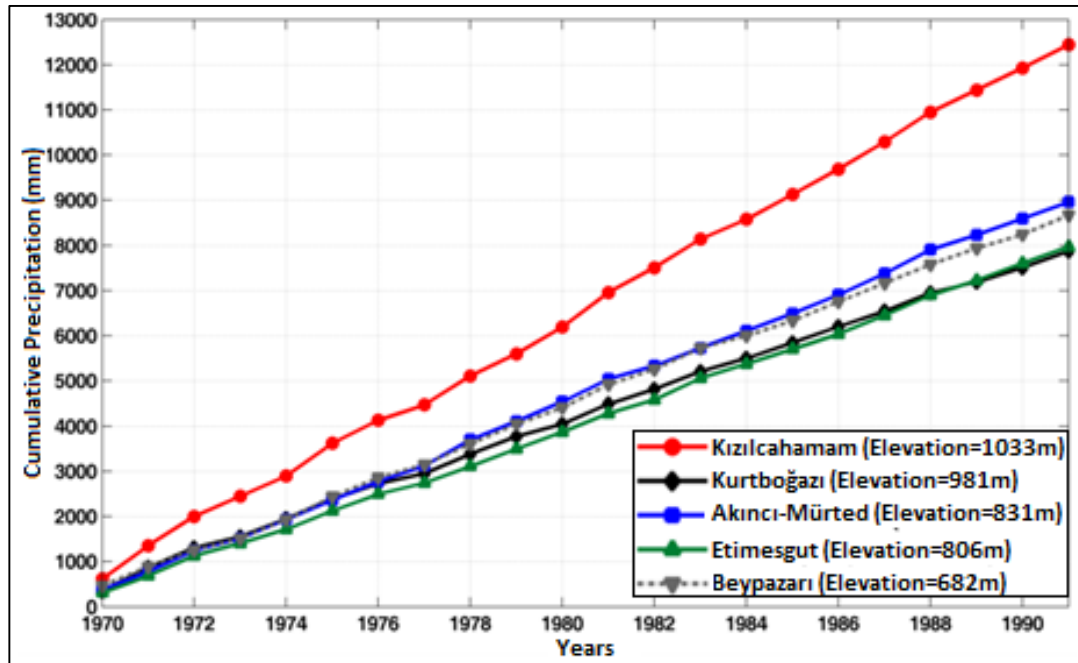


Figure 2.10. Comparison of the cumulative precipitation between 1970 and 1991

Although Çeltikçi, Peçenek, Çamlıdere, Kurtboğazi and Kızılcahamam meteorological stations are the most important stations because of the closeness to the study area, except Kızılcahamam station, they had been operated only a limited time period. In order to analyze the precipitation regime of the study area, common years (1987-1993) of data at these meteorological stations were compared (Figure 2.11). As can be seen in this figure, the precipitation in the vicinity of the study area changes in north-south direction rather than the elevation. Kızılcahamam and Çamlıdere meteorological stations which are located in the north have more precipitation than the others. In addition to these, Kızılcahamam station has the highest annual total precipitation due to the reason which is mentioned above. Even though there are differences between the total precipitations of each station, general trend is similar.

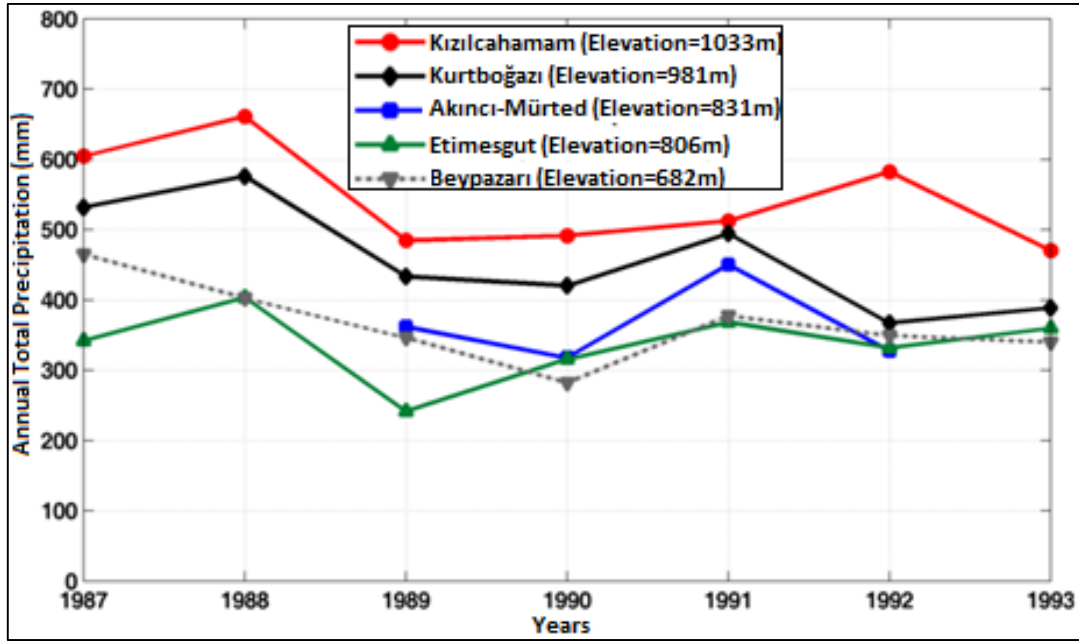


Figure 2.11. Comparison of the meteorological stations near the study area between the years 1987-1993

The variation in the average monthly precipitation is analyzed for the meteorological stations in or in the vicinity of the study area (Figure 2.12). Because the Çeltikçi meteorological station is the closest station to the study area; it is primarily considered and compared with other nearby stations for the same period. The long term (1957-2012) average monthly precipitation data of the Kızılcahamam meteorological station were also calculated and presented in Figure 2.12. It was observed that, generally monthly average precipitation data of the Çeltikçi and Kurtboğazi stations are similar in short term (1987-1992), but only in winter seasons, the Çeltikçi station has more precipitation than the Kurtboğazi station. For short term precipitation data of the Çeltikçi station, December received the highest average precipitation while August and September received the lowest amount. The monthly variations of the average precipitation for short term data indicate similar patterns for Çeltikçi, Kurtboğazi and Kızılcahamam stations. However, Kızılcahamam station has the highest monthly average precipitation amount. The similarity between the changes of the average monthly precipitation data of Kızılcahamam and Çeltikçi stations suggest that the similarity is also expected in the long term. Therefore,

December is the wettest and August is the driest months for the study area as in long term (1957-2012) precipitation measurement of Kızılcahamam station. Precipitation generally occurs in winter and spring months between December-May and in this time period 67% of the total annual precipitation falls. July, August and September are the driest months and only 11% of the total annual precipitation falls in this period.

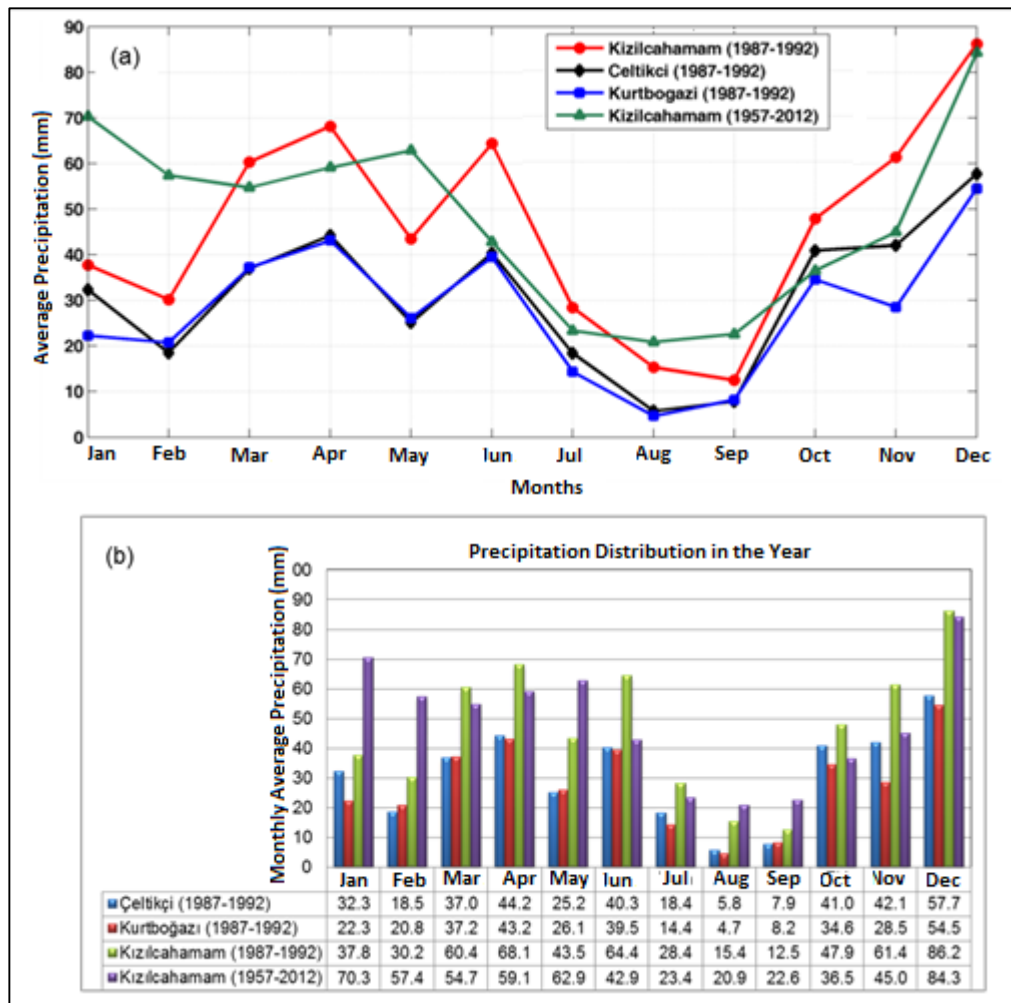


Figure 2.12. Comparison of monthly average precipitation of Kızılcahamam, Çeltikçi and Kurtboğazi stations (a) line graph, (b) bar graph and precipitation values

2.3.1.1. Estimation of the Long Term Average Precipitation for the Study Area

The long term precipitation data which is representative for the study area is very important for the hydrogeological studies. Although Çeltikçi meteorological station is located in the study area, it had been operated only between 1986 and 1994. Similarly, Binkoz meteorological station which was installed by İKA Mining Inc within the study area has been in operation since May 2013. Thus, the long term (1929-2013) Kızılcahamam meteorological station data is very important for this hydrogeological study. As mentioned earlier, while monthly changes of Kızılcahamam and Çeltikçi meteorological stations precipitation data are similar, in terms of monthly total precipitation amounts, Kızılcahamam station is quite high. Therefore, representative precipitation data for the study area can be estimated by correlating the measured data of the Kızılcahamam meteorological station to Çeltikçi meteorological station. In this study, 1986-1994 periods' monthly percentage error (%Bias) values between Kızılcahamam and Çeltikçi meteorological stations were used as the estimation method.

Scatter graph of the monthly total precipitation of Kızılcahamam and Çeltikçi meteorological stations between 1986 and 1994 is presented in Figure 2.13. In this figure, diagonal red line is 1:1 line and represents equal precipitation of vertical and horizontal axis. Also, statistical values are shown in this figure. In these comparisons correlation coefficient (CORR), %error (%Bias) and %absolute error (% |Bias|) values were used. The best statistics are obtained when correlation coefficient (CORR) is one and %error (%Bias) and %absolute error (% |Bias|) are zero. The condition of %Bias is below zero means that precipitation of Çeltikçi station is less than the precipitation of Kızılcahamam station. The comparisons show that in winter, spring and fall seasons when precipitation is relatively higher there is a good linear relationship (close to 1:1 line and $CORR > 0.67$; except April) between precipitation data of both stations. However, the relation decreases ($CORR < 0.60$) in dry summer months. It is also noted that the precipitation of Kızılcahamam station is continuously higher than the Çeltikçi station (below 1:1 line and %error < 0). Precipitation values for the Çeltikçi station were obtained by decreasing the precipitation values of Kızılcahamam station by using %error (%Bias) values calculated in these graphs

(Table 2.2). According to the results which were obtained from this method, the long term precipitation value in the study area is 393 mm.

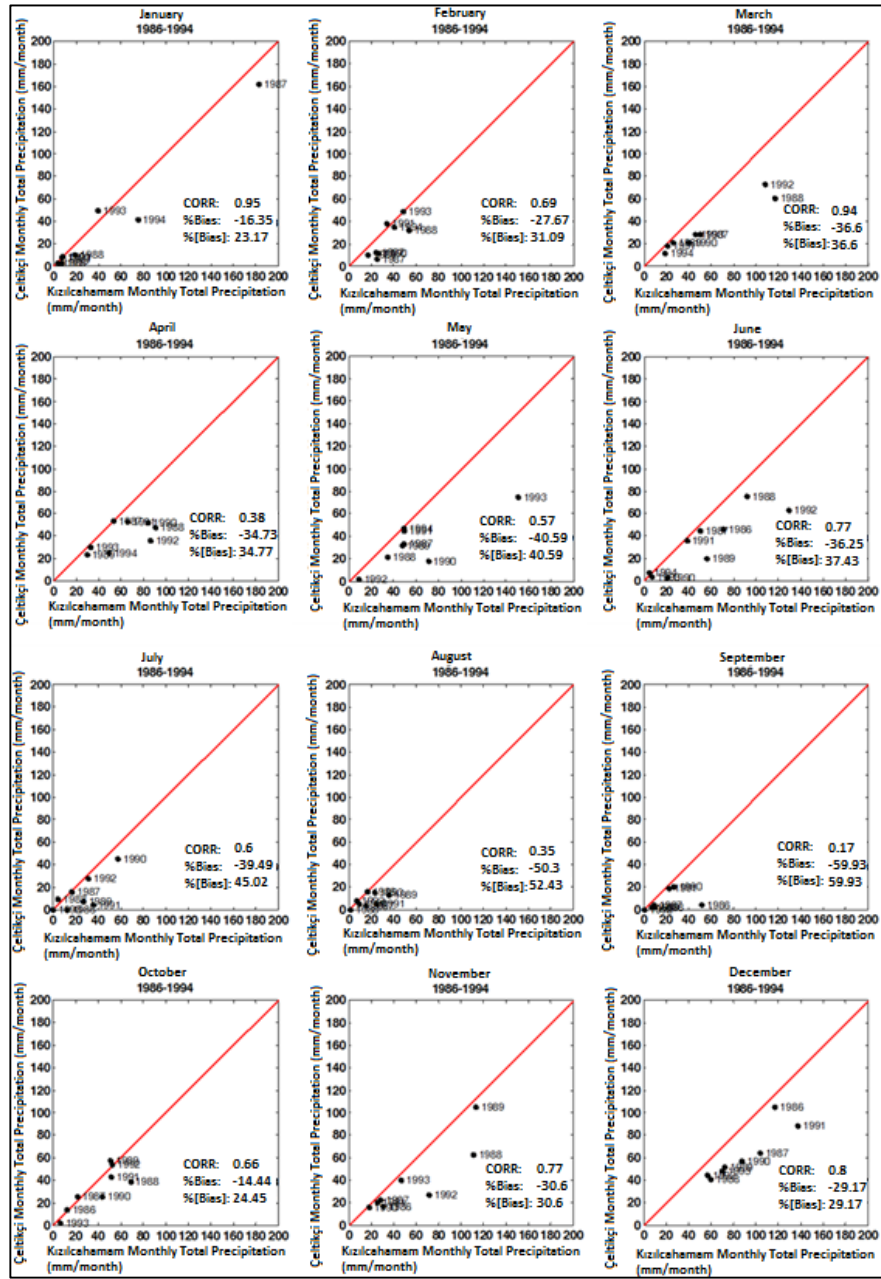


Figure 2.13. Scatter diagrams of monthly total precipitation of Kızılcahamam and Çeltikçi meteorological station between the years of 1986 and 1994

Table 2.2. Estimation of monthly total precipitation value of long term Çeltikçi meteorological station by using %error value between Kızılcahamam and Çeltikçi meteorological station

	Long Term Average Monthly Precipitation Values (mm/month)											
	Jan	Feb	Mar	Apr	May	Jun	Jul	Aug	Sep	Oct	Nov	Dec
Kızılcahamam (1957-2012)	70.3	57.4	57.4	59.1	62.9	42.9	23.4	20.9	22.6	36.5	45.0	84.3
Kızılcahamam-Çeltikçi (%error)	-16.4	-27.6	-38.6	-34.7	-40.9	-36.3	-39.5	-50.3	-59.9	-14.4	-30.6	-29.2
Çeltikçi-Estimated (1957-2012)	58.8	41.6	33.6	38.6	37.2	27.3	14.1	10.4	9.1	31.2	31.2	59.7

2.3.1.2. Analyses of Binkoz Meteorological Station Data

Binkoz meteorological station was installed on 23 May 2013 at the south of Binkoz village and it has been recording data since then. Because this station has not been operated long enough time to use in hydrogeological study, only pre-analysis of the data could be done.

In this analysis, the comparison of daily data between Binkoz station and Kızılcahamam and Etimesgut stations was done for common time interval (Figure 2.14-Figure 2.18). These figures show the scatter diagrams of measured daily meteorological data of Binkoz meteorological stations versus Kızılcahamam and Etimesgut meteorological stations in the periods between July and August 2013. Diagonal red line is the 1:1 line representing equal values of horizontal and vertical axes. As can be seen in Figure 2.14, although precipitation during the summer is less, abrupt local (convective) precipitation can be expected; for instance in July a high precipitation was observed in Kızılcahamam station while other stations did not record it. In June, the precipitation values are quite similar in Kızılcahamam and Binkoz meteorological stations. There is no relation between the low intensity precipitations which were observed in Etimesgut and Binkoz meteorological stations. The reliability of this analysis is quite less because precipitation occurred only a few times in the observation period. This analysis should be repeated when long term data of the Binkoz meteorological station is available.

As can be seen in Figure 2.15 - Figure 2.17, measured minimum, maximum and average temperature values are quite similar at Binkoz and Kızılcahamam meteorological stations. Daily air temperature of Etimesgut station is higher than others because the continental climate is more dominated in that area. For the same reason, daily average relative humidity values measured at Etimesgut station are less than Binkoz station and measured values at Kızılcahamam station are similar with Binkoz station (Figure 2.18).

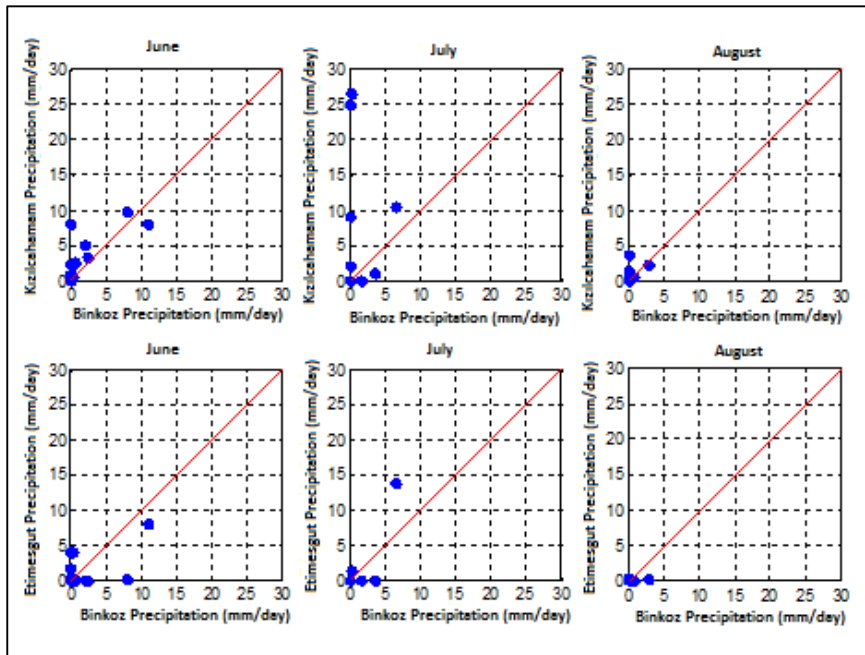


Figure 2.14. Scatter diagrams of daily total precipitation values of Binkoz meteorological station and Kızılcahamam and Etimesgut meteorological stations (June-August 2013)

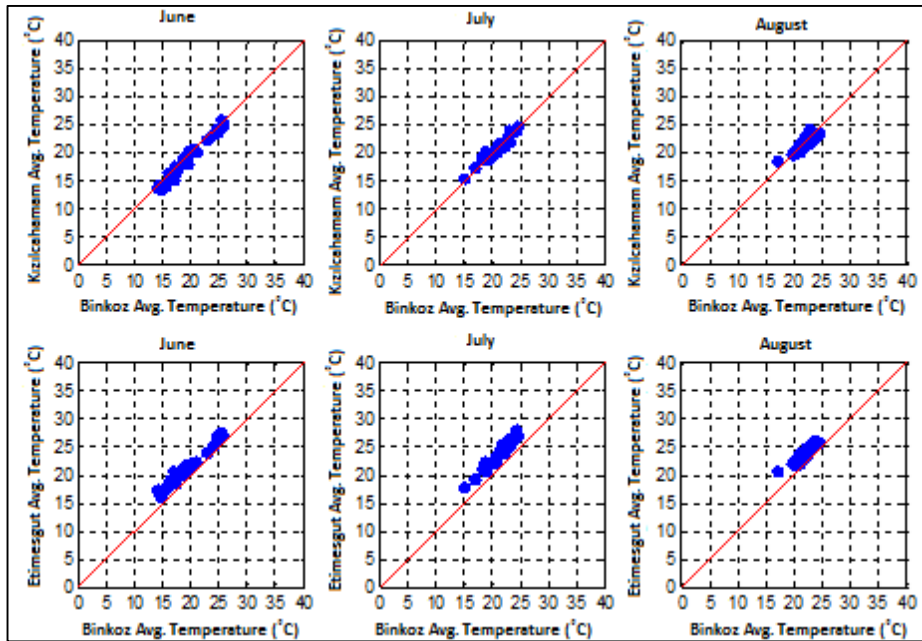


Figure 2.15. Scatter diagrams of daily average temperature of Binkoz meteorological station and Kızılcahamam and Etimesgut meteorological stations (June-August 2013)

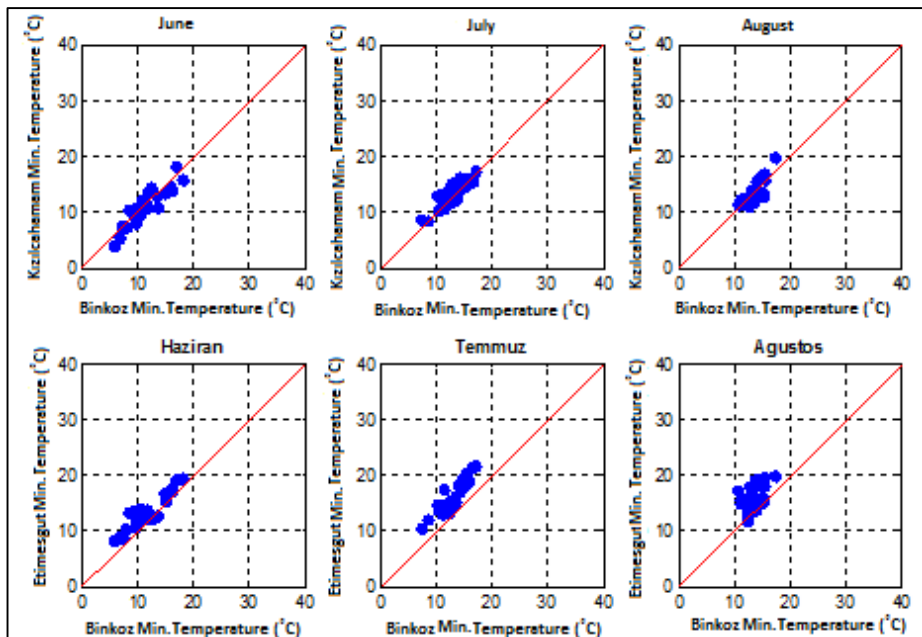


Figure 2.16. Scatter diagrams of daily minimum temperature of Binkoz meteorological station and Kızılcahamam and Etimesgut meteorological stations (June-August 2013)

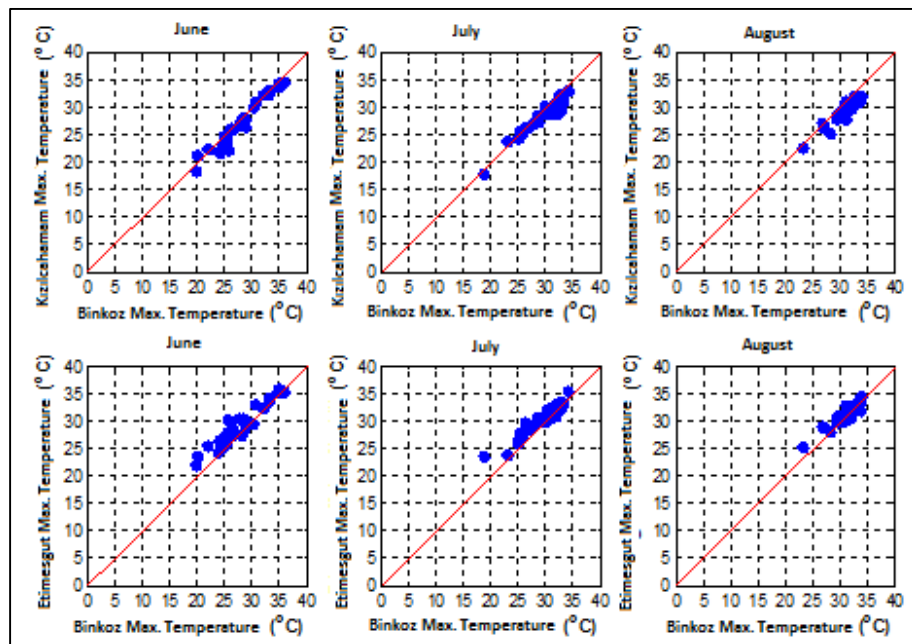


Figure 2.17. Scatter diagrams of daily maximum temperature of Binkoz meteorological station and Kızılcahamam and Etimesgut meteorological stations (June-August 2013)

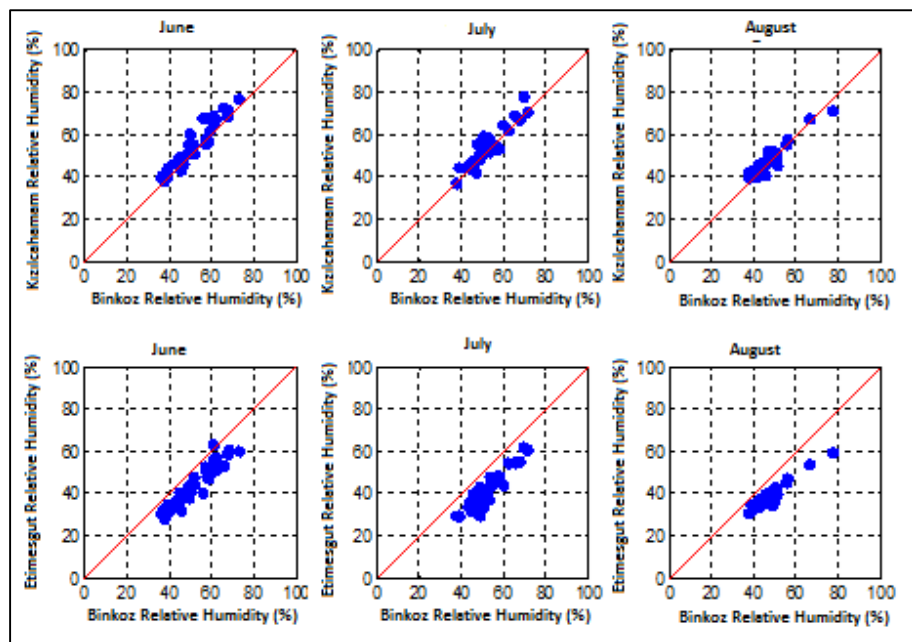


Figure 2.18. Scatter diagrams of relative humidity of Binkoz meteorological station and Kızılcahamam and Etimesgut meteorological stations (June-August 2013)

2.3.2. Temperature

Minimum, maximum and average temperature values of both Çeltikçi and Kızılcahamam meteorological stations are shown in Figure 2.19-2.22. In these graphs average monthly values were calculated by using short term (1987-1993) data of Çeltikçi station and long term (1959-2012) data of Kızılcahamam station. The results show that the calculated long term and short term average monthly temperature values are very similar to each other for the Kızılcahamam station.

Monthly average temperature values of Kızılcahamam and Çeltikçi stations are presented in Figure 2.19. In short term (1987-1993), monthly average temperature value in Çeltikçi station is approximately 1-1.5 °C higher than the Kızılcahamam station. For Çeltikçi station, the highest monthly average temperature is seen in August as 22.4 °C and the lowest monthly average temperature is seen in January as -1.5 °C. In this station, except for January, monthly average temperatures are above the freezing point. For Kızılcahamam station, measured long term monthly average temperature values especially in winter months are higher than the short term monthly average temperature values. For this reason it is expected that long term monthly average temperature values would be 0.5 °C higher than the short term data, especially in winter months.

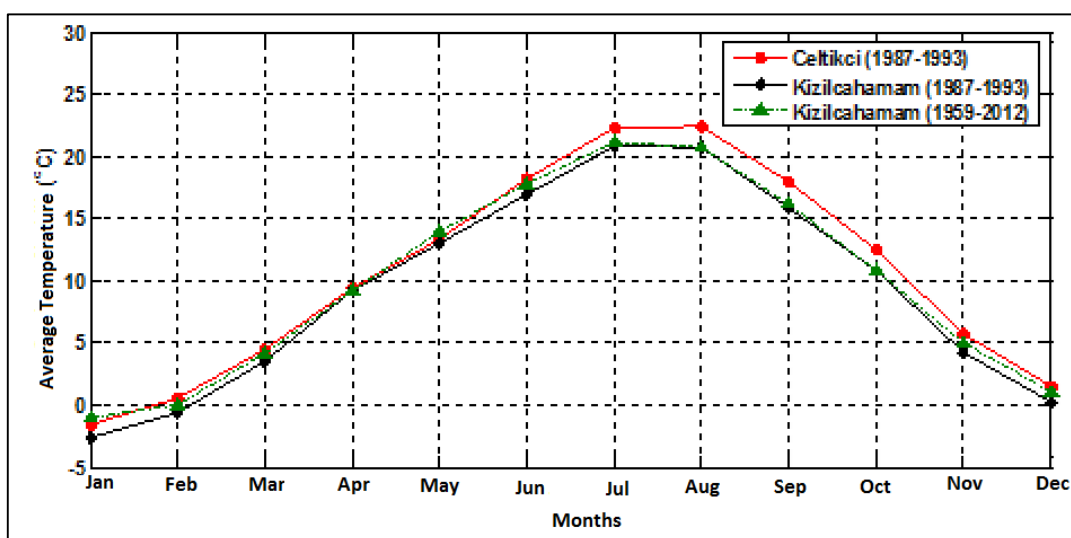


Figure 2. 19. Distribution of the monthly average temperature values for Çeltikçi and Kızılcahamam stations

Average monthly minimum temperature data of Çeltikçi and Kızılcahamam stations are presented in Figure 2.20. In short term (1987-1993), average monthly minimum temperature of Çeltikçi station is measured 1 °C higher than Kızılcahamam station. The highest average monthly minimum temperature is measured in August as 8.4 °C and lowest value is measured in January as -15 °C. As can be seen in this figure, except for May-September period, temperature may drop below zero in other months. Because of this reason, in these months frosting and snow cover possibility occurs. In Kızılcahamam station, long term and short term average monthly minimum temperature values are very similar in summer but long term value is 1-2 °C higher than the short term value in winter months.

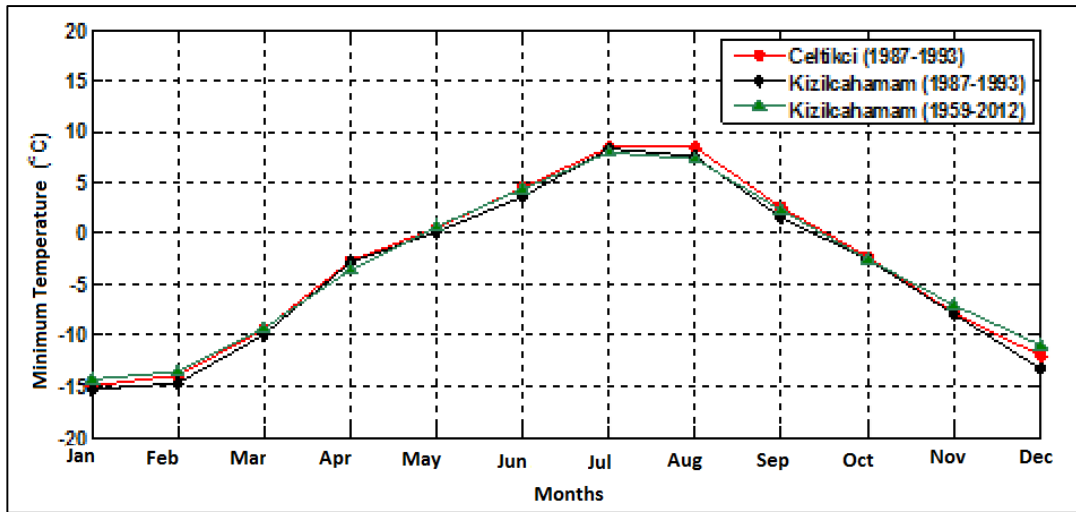


Figure 2. 20. Distribution of the average monthly minimum temperature values for Çeltikçi and Kızılcahamam stations

Average monthly maximum temperature data of Çeltikçi and Kızılcahamam stations are presented in Figure 2.21. In short term (1987-1993), average monthly maximum temperature of Çeltikçi station is measured 1 °C higher than the Kızılcahamam station. The highest average monthly maximum temperature is measured in July as 35.8 °C and lowest value is measured in January as 8 °C. As can be seen in this figure, temperature values are higher than 30 °C in July-September months. In Kızılcahamam station, long term monthly maximum temperature values are 1 °C higher than short term data. Similarly, it is expected that long term monthly

maximum temperature values would be 1 °C higher than the short term data for Çeltikçi station.

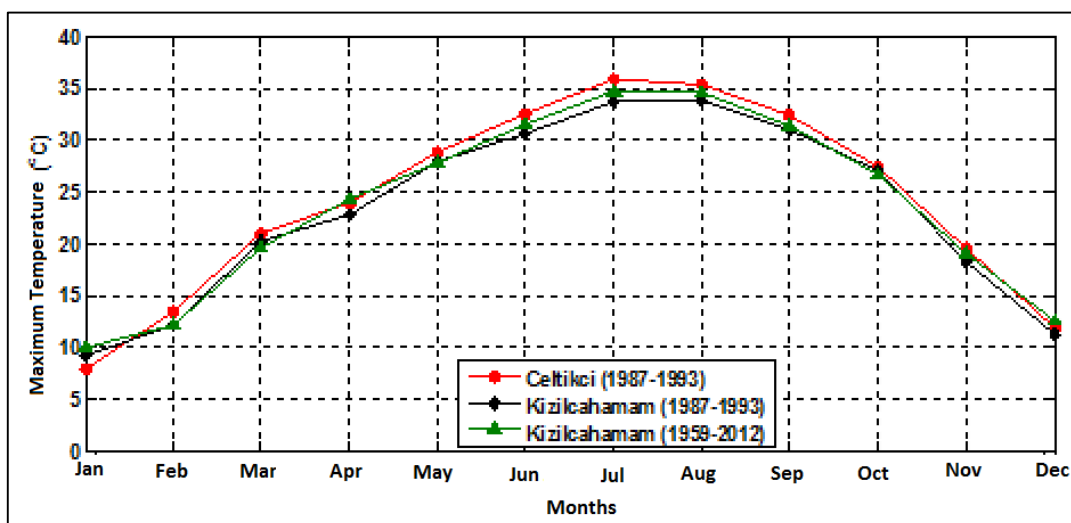


Figure 2.21. Distribution of the average monthly maximum temperature values for Çeltikçi and Kızılcahamam stations

In summary, temperature values significantly show seasonality. In summer, monthly average temperature values are in the range between 20-25 °C while maximum values may be over 35 °C. In winter months, monthly average temperature values change between -2 and 5 °C. In the periods between October and May, temperatures may fall below freezing point; especially in January and February it may decrease down to -15 °C. For this reason, in these months freezing and snow cover possibility occurs and this condition may be more effective in higher elevations.

2.3.3. Relative Humidity

Monthly average relative humidity values for Kızılcahamam and Çeltikçi stations are presented in Figure 2.22. For Kızılcahamam station, short term (1987-1993) and long term (1959-2012) monthly average relative humidity values are very similar. Short term monthly average relative humidity in Kızılcahamam station is higher than Çeltikçi station for all months. Especially in summer months Kızılcahamam stations have 7% to 10% higher values. This condition shows that the vicinity of the study area has relatively lower humid air than Kızılcahamam. In

Çeltikçi station, the highest monthly average relative humidity is observed in December as 75% and lowest value is observed in August as 46%.

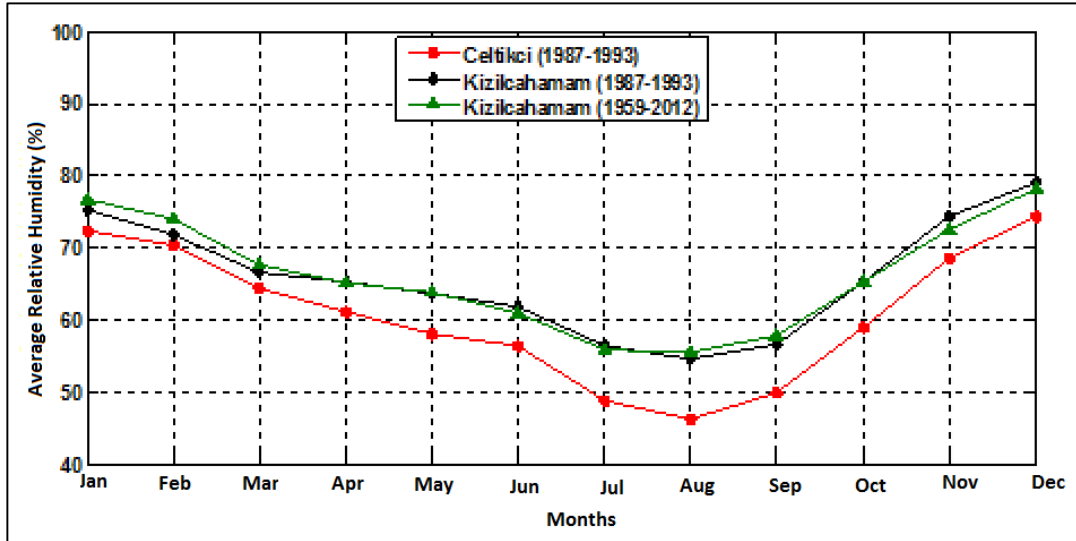


Figure 2.22. Distribution of the average relative humidity values for Çeltikçi and Kızılcahamam stations

2.3.4. Evaporation

Monthly total open surface evaporation value could be obtained from only Kızılcahamam (1974-2011), Kurtboğazı (1966-2000) and Beypazarı (1975-2011) stations among the regional meteorological stations. In these stations, evaporation measurement was not conducted in winter months (November-March). Average monthly total open surface evaporation of Kızılcahamam, Kurtboğazı and Beypazarı stations are presented in Figure 2.23. Monthly average values were calculated for the month which has at least 15 years of data. As can be seen in this figure, evaporation values show seasonality within a year. In Kızılcahamam station, the highest open surface evaporation value is seen in July as 212 mm, lowest value is seen in October as 79.5 mm. Average monthly open surface evaporation of Kurtboğazı station is higher than Kızılcahamam station; especially in summer months it has %50 higher values. The highest open surface evaporation is seen in August as 308 mm and the lowest value is seen in May as 144 mm. The measured open surface evaporation values in Beypazarı station show similarity with Kızılcahamam station. The highest open surface evaporation is seen in July as 236 mm and the lowest value is seen in

October as 72 mm. The expected open surface evaporation in winter months in which measurements were not conducted is expected to be quite low with decreasing temperature and increasing relative humidity.

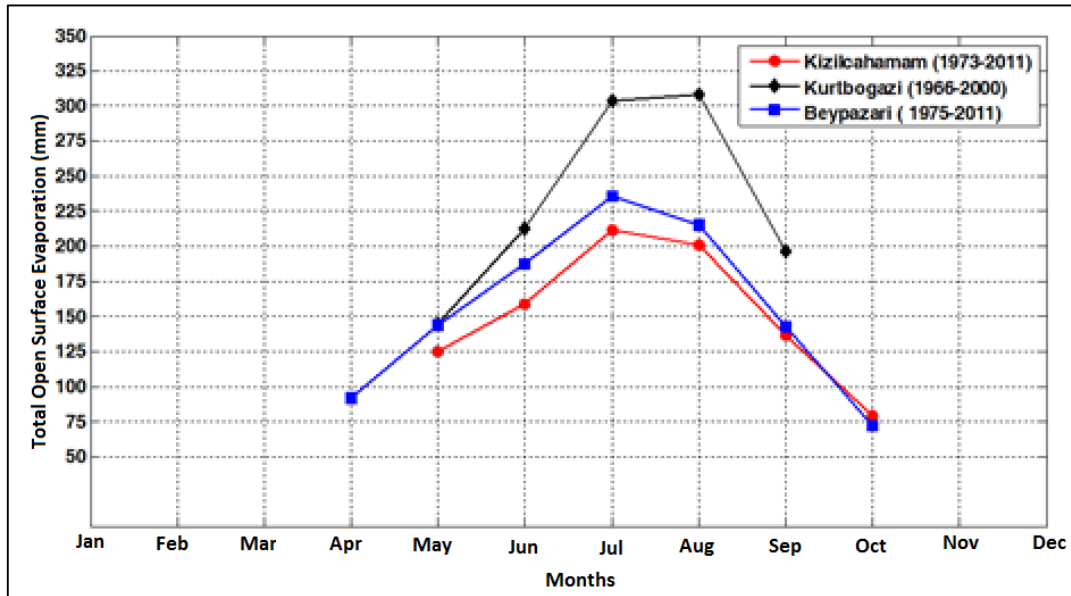


Figure 2.23. Average monthly total open surface precipitation values of Kızılcahamam, Kurtboğazi and Beypazari stations (Only the months which have at least 15-year data)

The relation between monthly total open surface evaporation and monthly average temperature at Kızılcahamam meteorological station was explored. The correlation coefficient for a linear relationship between monthly total evaporation and monthly average temperature for the period between 1973 and 2011 is given in Figure 2.24. As can be seen in this figure, the correlation coefficient is generally greater than 0.9. For each year, the evaporation values of the months, for which measurement were not conducted, were estimated by using the linear relation between monthly total temperature and monthly total evaporation. Monthly total evaporation and monthly total precipitation values obtained from the method is presented in Figure 2.25.

The results in Figure 2.25 show that the precipitation is greater than the evaporation between November and April; in other months precipitation is lower than the evaporation. In December, January and February months evaporation values are quite low. According to this comparison, it is expected that the groundwater recharge from surface is expected to occur between November-April months.

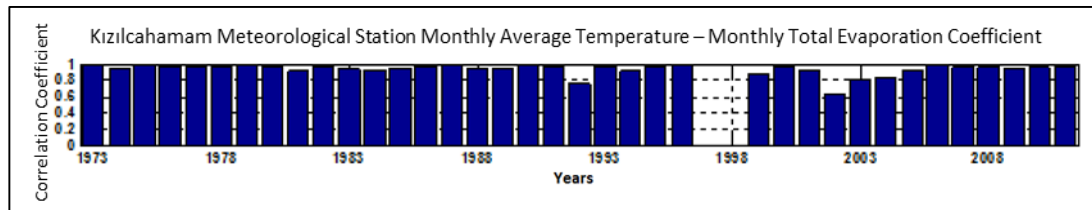


Figure 2.24. Correlation coefficient of linear relation between monthly average temperature and monthly total evaporation of Kızılcahamam meteorological station

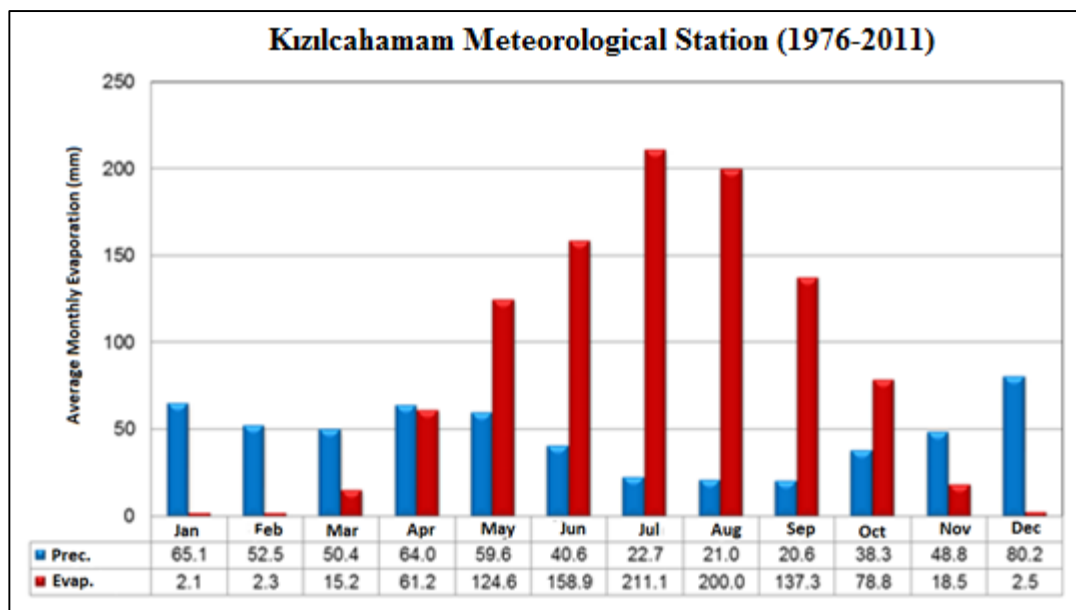


Figure 2.25. Distribution of monthly total precipitation and monthly total evaporation in a year of Kızılcahamam meteorological station between 1973 and 2011

2.4. GEOLOGY

The rock units and structural geological data of the study area were mapped at 1:25000 scale by Rojay (2013). The following sections were summarized from this study.

2.4.1. Regional Geology

The project area is located on the southern margin of a volcanic terrain known as “Galatian Volcanic Province” (GVP). GVP is located on top of the Cretaceous accretionary prism within the Pontides and to the south of seismogenic North Anatolian Fault Zone (NAFZ) along the “Çeltikçi graben” (Öngür 1976; 1977) (Figure 2.2626). These volcanics were also named as “Kızılcahamam volcanics” or “Koroğlu volcanics” (Türkecan et al 1991). However, informal but tectonically well-fit name “Galatian Volcanic Province” is preferred to address the terrain (Toprak et al 1996).

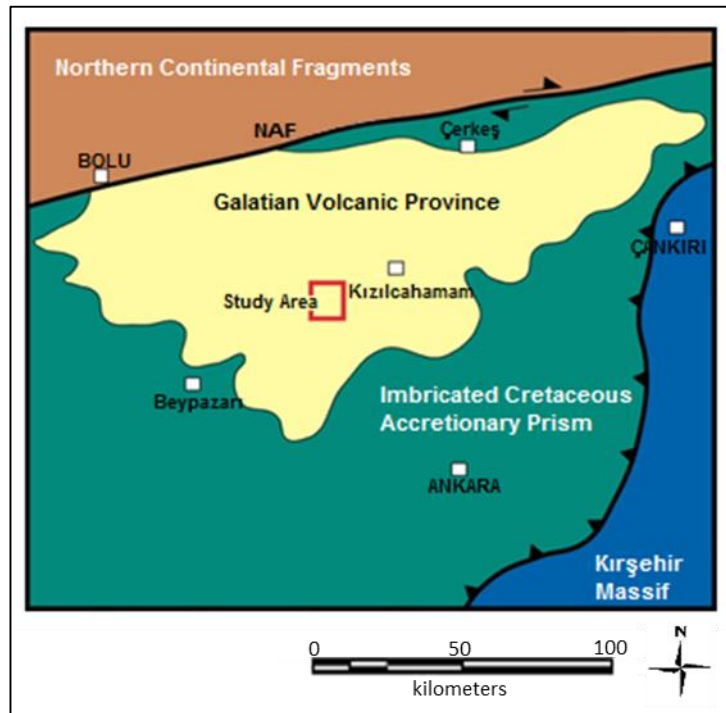


Figure 2.26. Tectonic setting of Galatian Volcanic Province (GVP) (Rojay, 2013)

2.4.1.1. Regional Stratigraphy

The rock units of pre-Miocene age are pre-Triassic metamorphics, Triassic Complex, Jurassic-Cretaceous Atlantic type margin sequences, Upper Cretaceous-Paleogene ophiolitic *mélange* with Upper Cretaceous-Paleogene forearc volcano-sedimentary sequences and piggyback to peripheral Eocene basins (Koçyiğit, 1991). The pre-Miocene units are unconformably overlain by Miocene clastics and volcanics. Miocene age several eruptive phase volcanic products as lavas and volcanoclastics of GVP are inter-fingering with and unconformably overlain by Miocene sequences (Figure 2.27). The organic layers and coal beds were deposited within Miocene and Pliocene sequences. All the units are unconformably overlain by Quaternary deposits (Figure 2.27) (Rojay, 2013).

Two eruptive cycles of the volcanic activity are observed within the GVP. The older one is calc-alkaline volcanics that comprise of lavas and pyroclastics of felsic to intermediate composition (Tankut et al., 1990; Türkecan et al., 1991; Keller et al., 1992) and dated as 16 to 24 Ma (Early Miocene) (Ercan et al, 1990; Türkecan et al., 1991, Keller et al., 1992) (Figure 2. 27). The second and final eruptions are dated as 10 Ma and in alkaline character. Paleontological analysis was done in the region on clastics inter-fingering with volcanic rocks that show younger ages as Middle to Late Miocene (in the mammalian time scale which is 11.1 Ma to 6.8 Ma; MN-9 to MN-13 time interval) (Ozansoy, 1961; Akyol, 1968; Turgut, 1978; Gürbüz, 1981; Inci et al 1988; Turkecan et al 1991; Agusti et al 2001).

2.4.2. Stratigraphy

Stratigraphy of the study area was done based on the 1:25 000 scale geological mapping (Figure 2.28). Instead of establishing the stratigraphy in the area, the main emphasis is give to the continuous and major structures like bedding planes/folds, ignimbrite-green tuffaceous sandstone levels, faults with fault planes and slip data (Rojay, 2013).

The units exposed in the area are classified as, from bottom to top, Miocene volcanics, Çeltikçi Formation, Plio-Quaternary and Quaternary units (Figure 2.27). The coal beds are located in the Çeltikçi Formation.

2.4.2.1. Volcanic Rocks

Andesitic-andesitic basaltic volcanics are extensively exposed in the study area. Volcanic rocks are taken as one unit regardless of being lavas, eruption centers or pyroclastics. However, the base of volcanic rocks is not observed within the boundaries of the study area. The nature of upper boundary is different in various parts of the area. In some parts, the mudrocks-clastics unconformably overlie the volcanics, but in some other areas it is totally silicified with cross-cutting relations manifesting intrusive contacts (Figure 2.29) (Rojay, 2013).

All these relations can be seen along the motor highway within the limits of the study area (east and south of Aşağıadaköy village along the motorway) (Figure 2.29). The sedimentary contacts are changing from one place to another where mudrocks dominantly onlap the volcanics.

The volcanic rocks are dominantly composed of lava flows and pyroclastics of andesitic to andesitic basaltic composition with volcanic centers around Binkoz village (Figure 3.28-3.31). Total thickness is more than 500 m as observed in the northern side of the Çeltikçi town along Pazar Stream valley. Along this valley and around Binkoz village, alternating flows of lava and pyroclastics are well orderly cropped out. The lavas and pyroclastics are overlying Neogene mudrocks to the east of the mapped area (northeast of Binkoz village) where they are overlain by Miocene Çavuşlar mudrocks bearing coals (Figure 2.27-2.29).

Two stages of volcanism with different tectonic settings in the GVP are proposed by various researchers (Türkecan et al,1991; Tankut et al,1993, 1995; Wilson et al, 1997; Koçyiğit et al, 2003). The volcanism is interpreted as being generated from a subducting slab and a continuous rifting process related to subduction in two intermittent or successive stages. The older volcanic cycle, which is the major phase, is calc-alkaline in character ranging in composition from K-rich basaltic trachyandesite to rhyolite with minor occurrences of alkali-basalts (Türkecan et al, 1991). This volcanic cycle was taken place between 25 Ma to 10 Ma (Early-Late Miocene) (Türkecan et al, 1991; Wilson et al, 1997) or even much older (since Paleocene, 65 Ma) (Koçyiğit et al 2003). The older volcanism is interpreted as sourced from lithospheric mantle that is modified by earlier subduction during the

first volcanic cycle in the GVP in the northern Neotethys. The parental magmas of the Early Miocene volcanism in the Galatian province were generated in a post-collisional tectonic setting from a previously subduction-modified mantle source (asthenospheric mantle) (Tankut et al, 1990; Tankut et al, 1998). This latest cycle, whose age is 8.5 Ma to 11 Ma, consists of small volume of alkali basaltic flows capping the older volcanic sequences (Türkecan et al, 1991). The Upper Miocene alkaline basalts of the latest phase in GVP simply correspond to typical rift volcanism related to extensional tectonics. It is stressed that Mid-Miocene hiatus in volcanic activity in the area strongly suggests a major change in the geodynamic setting as manifested in changes in eruptive style and geochemical characteristics of the volcanics.

Age	Name	Thickness (m)	Symbol	Description	Depositional Setting	
Quaternary		>20		Alluvium, Alluvial fan, Talus, Terraces, Landslides, ...	Fluvial Setting	
Plio-Q				Red Clastics	Lacustrine to Fluvial Setting	
				U (Unconformity) Red Clastics		
Middle - Late Miocene	Bezci	28		Red Clastics	Lacustrine Setting	
		40		Cherty clayey limestones, dolomitic mudrocks		
	Kocalar Member	60		Mudrocks with clastics		
		12		Green tuffaceous sandstone		
	Abacı	27		"Ignimbrite"		Volcanism
		5		Silicified tuff layer Basalts		
Early (?) - Middle Miocene	Çavuşlar Member	200		Mudrocks with sandstone and Tuff layers	Lacustrine with swampy conditions	
				Mudrocks with limnic and coal beds		
Early Miocene	Galatian volcanics			Volcanics (Lavas, pyroclastics, volcanic intrusives, ...)	Volcanism	

Figure 2.27. Generalized columnar section of the study area (Rojay, 2013)

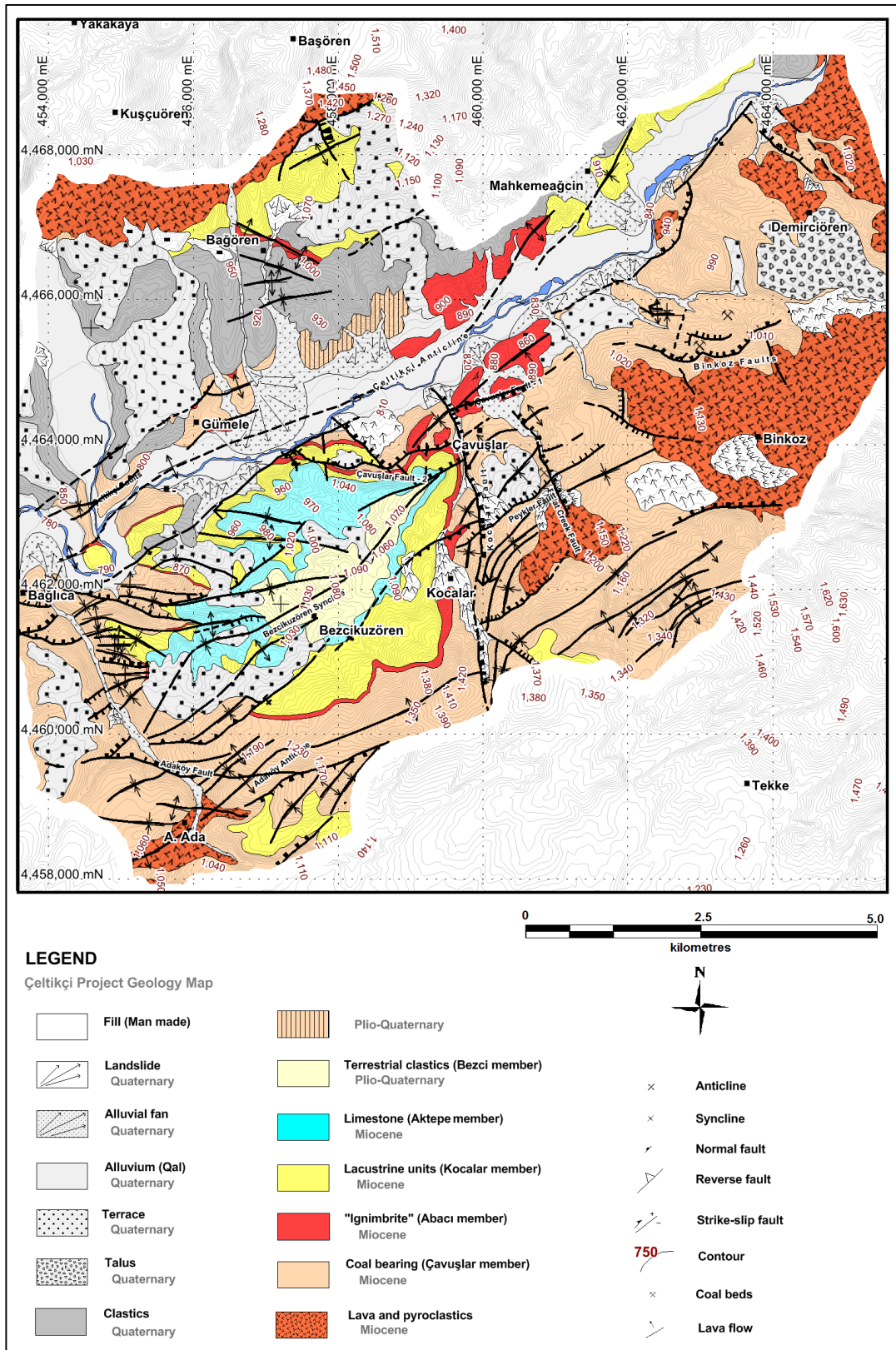


Figure 2.28. Geological map of the study area (Rojay, 2013)



Figure 2.29. Miocene Çavuşlar mudrocks-clastics on top of the Miocene volcanic (to the left) and cross-cutting relations with Miocene volcanics (to the right) manifesting intrusive contact (Rojay, 2013)

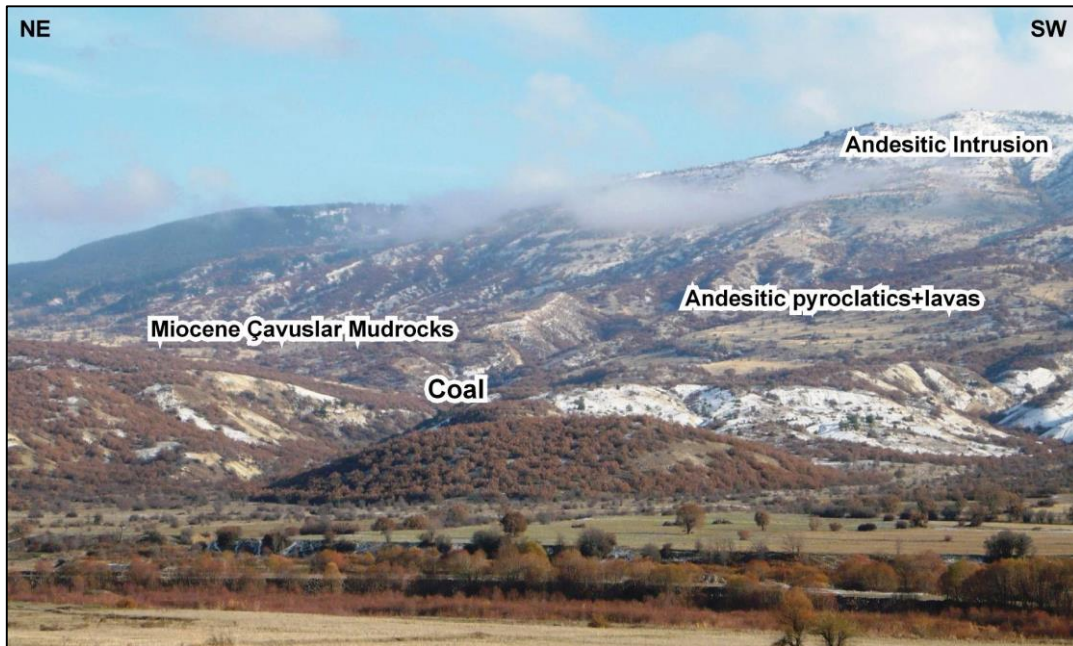


Figure 2.30. Miocene Çavuşlar Sequence on top of Miocene volcanics (Rojay, 2013)



Figure 2.31. View of Miocene andesitic lavas and pyroclastics, dipping NNW (Rojay, 2013)

2.4.2.2. Çeltikçi Formation

The formation is divided into five members. According to the stratigraphic position, it is listed from bottom to top as; Çavuşlar, Abacı (“Ignimbrite”), Kocalar, Aktepe and Bezci members (Figure 2.27). The unit displays unconformable relationships in various parts of the Galatian volcanic terrain. Abacı ignimbrite is a marker unit that differentiates lower mudrocks (almost no carbonate input) from upper mudrocks that are alternating with carbonates.

Miocene units are aged as Middle-Late Miocene by correlating a mammalian fossil site in the study area with paleontological and lithological equivalent levels in the type locality (Ozansoy, 1961; Gürbüz, 1981). It corresponds to Middle-Late Miocene age (MN-9 to MN-13 time interval in the mammalian time scale which is 11.1 Ma to 6.8 Ma; Agusti et al 2001). However, there are wide ranges of age calibrations done with palynological and radiometric age dating. The results of the palynological analyses done on coal layers alternating with mudrocks reveal Middle to Late Miocene age (Akyol, 1968; Turgut, 1978). Age dating analyses on tuff samples alternating with lacustrine units yielded an age interval of 25 Ma to 21 Ma (Türkecan et al. 1991), 16.2 Ma (Ercan et al 1990), 20.9 to 9.6 Ma (Keller et al 1992).

Altogether, the age of the Miocene sequence alternating with volcanics is accepted as Early (?) to Late Miocene.

Interbedded sequences of volcanics/volcanoclastics and terrestrial sediments imply that the paleogeographic setting is composed of a continental depositional setting with lakes around the terrestrial volcanic vents in an inter-arc depositional system on İzmir-Ankara Suture Belt in the central Anatolia during Neogene period (Koçyiğit et al 1988). The alkaline lakes covered quite large areas with calc-alkaline volcanism at the northwest of Ankara. The volcanism affected entire central Anatolia.

2.4.2.2.1. Çavuşlar member

Çavuşlar member overlies the andesitic volcanic rocks and underlies the Abacı member conformably (Figure 2.32). Although the member is strongly deformed, the thickness is around 200 m after reconstructing the sequence by using the immature coal bearing levels (South of Çavuşlar village). Almost a perfect section can be documented to the north of Binkoz village to the Kirmir Stream. However, the thickness should be more than 350 m based on borehole surveys.

The member is composed of cream-white-light green mudrocks with sandstones, tuffs and organic-coal bearing levels. The target coal layers are located within this member. The thickness of the coal seams is a few cm to a few tens of cm.

Gray to white crossbedded, pumice bearing tuffaceous sandstone and tuff layers interlayered with the mudrocks are common in the Çavuşlar member (eg. northeast of Kocalar village) (Figure 2.32-2.33). They are traceable laterally for long distances from Kocalar to north of Gümele.

Silicification is commonly observed within the Çavuşlar member. The silicified levels occur as lenses and layers of silica in mudrocks and as silicified sequences due to intense volcanic activity and faulting (Figure 2.34). To sum up, the silica is present in the system as primary (layers and lenses of silica) and secondary (results of volcanism and faulting). The silicification is intense in Demirciören area, north-northeast of Peykler, north of Alibeyköy and Çeltikçi-Bağlıca-Aşağıadaköy areas (Rojay, 2013).

Çavuşlar member as a whole is deposited in a lacustrine environment with frequently evolved swampy conditions cooperated with andesitic volcanism. The palynological analyses suggest an age of Middle Miocene in the region (Akyol, 1968; Turgut, 1978). The coals in Beypazarı area is deposited within Early (?)-Middle Miocene age coarse clastics named as Çoraklar Formation (Yağmurlu et al. 1988).

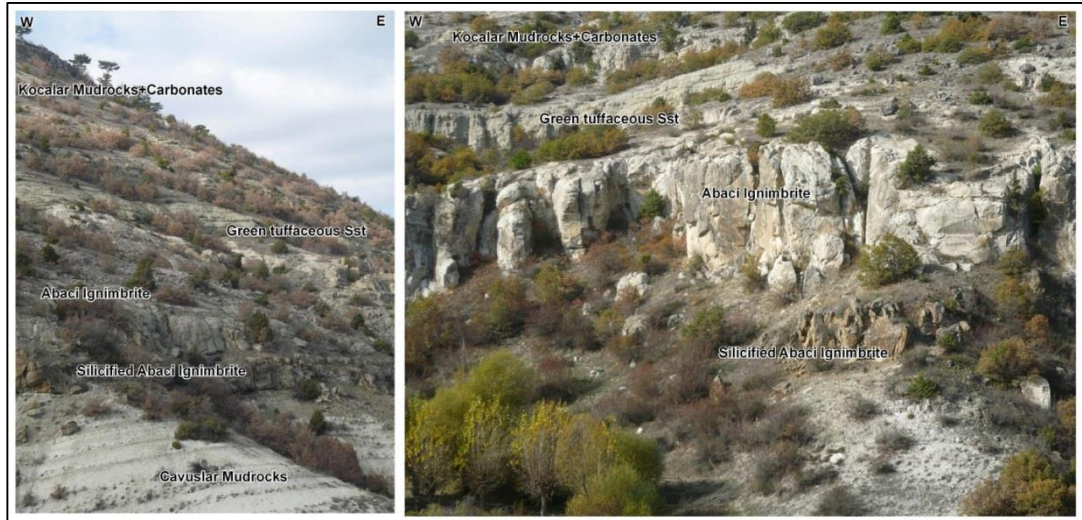


Figure 2.32. General view of Miocene Çeltikçi sequences (Rojay, 2013)



Figure 2.33. Pumice fragments bearing tuff layers within mudrocks (Rojay, 2013)



Figure 2.34. Silicification of Miocene Çavuşlar Mudrocks (north of Aşağıadaköy village) (Rojay, 2013)

2.4.2.2.2. Abacı “İgnimbrite”

Abacı member is a layer stratigraphically located in the middle of the Neogene lacustrine sequence between underlying Çavuşlar and overlying Kocalar members.

The maximum thickness of the Abacı member in the area is about 27 m. The thickness varies; gets thinner and diminishes towards east and west of the study area (Figure2.28). However, the member is used as a key bed and highly helpful in the interpretation of structures.

Lithologically the member is composed of two parts: 1) lower; silicified, impervious massive tuff layer of maximum 5 m; and 2) upper; highly porous, light colored pumice fragment bearing tuff (“İgnimbrite”) layer of maximum 22 m (Çavuşlar area) (Figure2.32). In some areas, “İgnimbrites” are hydrothermally altered along the preexisting joints and cross cut by basaltic dykes (Figure 2.35).

The unit overlies mudrocks of the Çavuşlar member with a sharp contact and gradational to overlying mudrocks of the Kocalar member.

Thick, green colored tuffaceous sandstone is deposited above Abacı “İgnimbrite” layer that can be correlative in the area. The upper contact is transitional

part of the Abacı member to upper clastic sequence. Cross-bedding observed within the sandstones. The average thickness is about maximum 12 m within the study area.

“Ignimbrite” is erupted into the lake onto mudrocks of the Çavuşlar formation where sedimentation continues without any drought in sedimentation period during Middle Miocene.

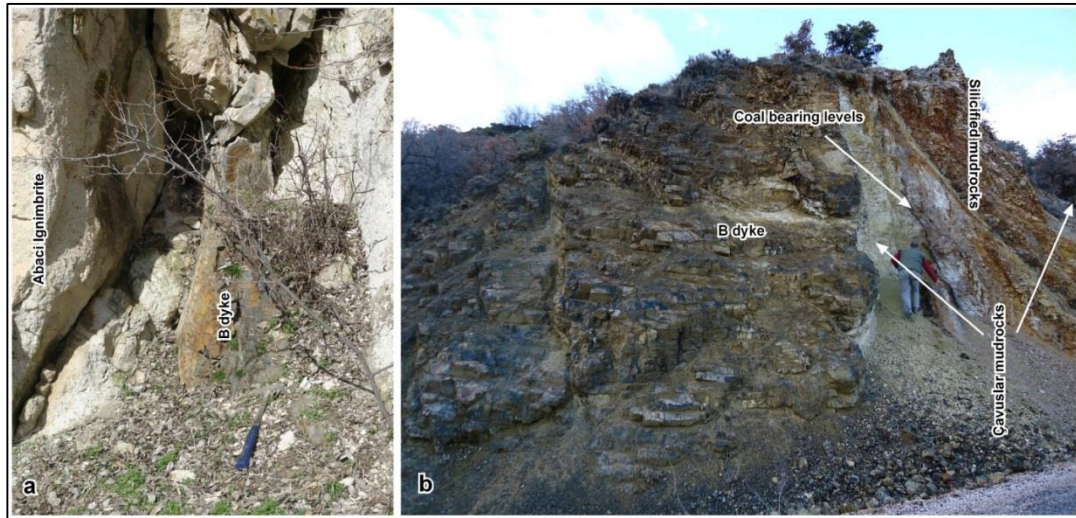


Figure 2.35. Basalt dyke (B dyke) intruded into a) Abacı Ignimbrite (Çavuşlar village) and b) Cavaşlar member (Mahkemeağıcın village) (Rojay, 2013)

2.4.2.2.3. Kocalar member

Kocalar member conformably overlies Abacı member and underlies the carbonates of the Aktepe member and clastics of the Bezci member. A typical section of the Kocalar member is exposed to the SW of Çavuşlar village where both bottom and top boundaries of the unit are clear (Figure 2.32). The thickness of the unit is about 60 m.

Kocalar member is composed of beige-cream colored mudrocks containing sandstone beds and tuff layers. It is deposited in a silica rich lacustrine environment having frequent clastic influx.

2.4.2.2.4. Aktepe member

Aktepe member overlies Kocalar member and underlies clastics of the Bezci member. The thickness of the unit is about 40 m. High silicification is observed at

the western side of the study area (Çeltikçi-Aşağıadaköy). The reason of the silicification is hydrothermal interaction resulting from volcanism and low angle faulting (Rojay, 2013).

The unit is composed of two distinct levels. The lower part is composed of beige-cream colored mudrocks with sandstone beds and tuff layers, and the upper part is dominated by beige-light gray to white colored, thick bedded limestones-dolomitic mudrocks with silica nodules-lenses (Rojay, 2013). Lithostratigraphically it can be correlated with the carbonates of the Upper Miocene cropping out in Central Anatolia.

2.4.2.2.5. Bezci member

The Bezci member composed of clastics can easily be recognized with their pinkish red color and soft morphologies with gentle dip amounts (especially around Bezcikuzören village) except in intensely faulted areas (far Northeast of Çeltikçi) (Figure 2.36). Polygenetic sandstone-siltstones with some limnic-organic horizons and conglomerate are common lithologies. The unit is observed in highly elevated areas relative to the recent river bottom (Bezcikuzören-Çavuşlar-SE of Çeltikçi and Çeltikçi-İnişdibi-Bağören-Abacı areas to Mahkemeağıcı village). However, to the west of Mahkemeağıcı and Abacı villages, it is hard to differentiate the outcrops from Kocalar member. The total thickness is more than 30 m.

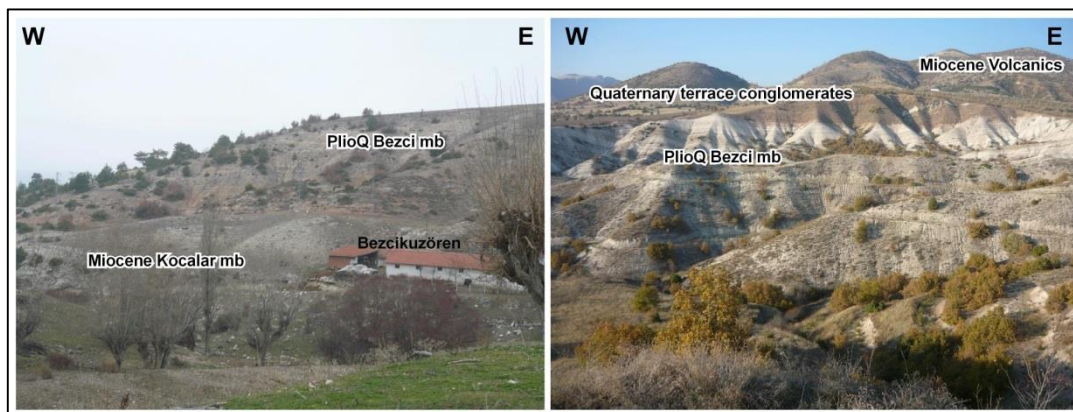


Figure 2.36. General view of Bezci member a) Bezci mb on Miocene Kocalar carbonates (Bezcikuzören village), b) Quaternary terraces conglomerates on top of Bezci mb (northwest of Gümele) (Rojay, 2013)

The unit deposited in a terrestrial setting with short-lived lacustrine periods. The age of the unit is anticipated to be post-Miocene, as Plio-Quaternary. The unit is dated as Early Pliocene with mammalian fossils in the region (Ozansoy, 1961; Tekkaya, 1973; 1974 a, b; Şen and Rage, 1979; Tatlı, 1975). However, the Pliocene age is accepted as questionable due to the difficulties of correlating terrestrial clastics over long distances.

2.4.2.3. Plio-Quaternary Units

The Plio-Quaternary clastics can be easily recognized with their pinkish red color, soft morphologies and gentle dip amounts (NW of Gümele) (Figure 2.37). Hence, due to these properties it is difficult to separate it from the Bezci member for the mapping purposes.

It is commonly observed in highly elevated areas to the recent river bottoms (Bezci-kuzören-Çavuşlar-SE of Çeltikçi and Çeltikçi-İnişdibi-Bağören-Abacı areas to Mahkemeağıcı village). The total thickness is more than 60 m. It is composed of polygenetic sandstone-siltstones with some limnic-organic horizons.

The unit is deposited in a terrestrial setting having locally developed swampy environments. The age of the unit is anticipated to be post-Miocene, as Plio-Quaternary. The unit is dated as Plio-Quaternary after lithologic and lithostratigraphic correlations (especially in Kazan, Ankara) (Ozansoy, 1961; Tekkaya, 1973; 1974 a, b; Şen and Rage, 1979; Tatlı, 1975). However, the Pliocene age is accepted as questionable due to the difficulties of correlating terrestrial clastics over long distances.

2.4.2.4. Quaternary Units

Relatively old Quaternary (Holocene) units are elevated river terraces (Çeltikçi to north of Gümele) (Figure 2.37). The river terraces are composed of horizontally lying, well-rounded, poorly sorted, dominantly basaltic volcanic cobbles bearing conglomerates. They are situated at 80 m above the Kirmir Stream. They unconformably overlie the Plio-Quaternary clastics (Çeltikçi and north of Gümele). Recent alluvial fans, recent alluvium, talus and active landslides are the present day units deposited in the channels of the recent drainage systems (Figure 2.38).



Figure 2.37. The Quaternary terrace cobble conglomerates unconformably overlies the Plio-Quaternary units (Rojay, 2013)



Figure 2.38. Kocalar landslide (Rojay, 2013)

2.4.3. Structural Geology

Rojay (2013) analyzed the faults and folds in so called “Çeltikçi Graben”. It is seen that most of the structures that strike in NE-SW to ENE-WSW direction are cut with faults trending in NNW-SSE to NW-SE. (Figure 2.28).

2.4.3.1. Fault patterns and Faulting

Rojay (2013) differentiated the types of faults using slickenlines, drag folds, offsets, juxtaposition of rock units and cross-cutting relations of geological structures. Overprinting in the slickenlines is important to differentiate the order of

deformational phases. Cross cutting relationships of folds and faults and irregularities in the attitude of beds were other important elements for the differentiation of faults (Figure 2.28).

The faults that are mostly confined to the Miocene units are compressional structures, like strike-slip and reverse faults with dextral components trending in ENE-WSW orientation. However, most of the much younger faults developed in a parallel array with the Miocene confined faults. This possibly indicates reactivation of the post-Miocene structures during extension (Rojay, 2013). The faults can be grouped based on their attitudes as NS-trending, EW-trending, Kirmir Stream valley and Northern margin faults in the study area (Figure 2.28). NS-trending faults are; Kocalar Fault, Polat Creek Fault, EW-trending ones are; Çavuşlar Fault-1, Çavuşlar Fault-2, Binkoz Faults, Peykler Fault, Aşağı Adaköy Fault, and Kirmircayi valley faults (Çeltikçi Faults) and Northern margin Fault.

2.4.3.1.1. N-S Trending Faults

N-S to NW-SE trending faults are developed usually perpendicular to the strikes of the stratigraphic units, folds and high angle normal faults. The faults are oblique-slip (having both dextral strike-slip and dip-slip components) or dextral strike-slip faults. The initiation age of faulting must be Post-Miocene - Pre-Holocene (Rojay, 2013).

Kocalar Fault (KF); N-S to NNW-SSE (N030W) trending east facing faults are high angle oblique normal faults. The fault extends from Erenler Hill (south of Kocalar village) to Kayabasi Hill (west of Çavuşlar village) and to Kirmir Stream for 5.5 km. No slip data could be obtained from the fault surfaces due to the soft and clayey nature of the sediments. However, the faults are interpreted as oblique normal faults with their normal offsets (west of Çavuşlar village) and dragfolds in regional scale (north of Erenler hill). Offset amount along the fault should be more than 50 m where eastern block is downthrown. Landslides, truncation of Abacı ignimbrite, truncation and downthrown of syncline, region wide drag folds and linear narrow valleys are the indication of the fault. The age of the faulting must be post-Miocene (post-Kocalar and Bezci members), which is post-Plio-Quaternary- pre-Holocene

(Rojay, 2013). The observations however indicate that this fault has moved several times in the geologic past (Rojay, 2013).

Polatcreek Fault (PcF); N23°W trending fault extending along Polat creek (Peykler village) for 2 km is manifested with truncation of target coal beds (N45E striking coal beds are truncated), sudden changes in strikes of beds and actual landslides. Possibly a 500 m of right lateral offset is proposed where western block is uplifted. However, no slip data could be measured (Rojay, 2013).

2.4.3.1.2. N-S Trending Faults

Çavuşlar Fault-1 (CF-1); N65°E trending left lateral fault with normal components extends for 2 km to the north of Çavuşlar village where southern block is downthrown. The fault crosscuts the Abacı ignimbrite (Figure 2.28). The slip data manifests a left lateral strike slip fault with normal components developed under NE-SW compression where lately post-dated by right lateral strike slip faulting developed under almost WNW-ESE compression (Rojay, 2013).

Çavuşlar Fault-2 (CF-2); N72°E trending right lateral fault with normal components extends for 3 km to the east of Gümele village where northern block is downthrown (Figure 2.39). The fault crosscuts the Abacı ignimbrite with a fresh morphology (Figure 2.28). The slip data manifests a right lateral strike slip fault with normal components developed under WNW-ESE compression. Landslides, rock falls and hanging Quaternary terraces are the indication of faulting with slip data (Rojay, 2013). The possible throw along the fault is estimated at more than 40 m. Both left and right lateral motion recorded along the Çavuşlar faults. Therefore idealized 3:1 ratio for strike slip faulting can not be applied and actual throw can not be calculated (Rojay, 2013).

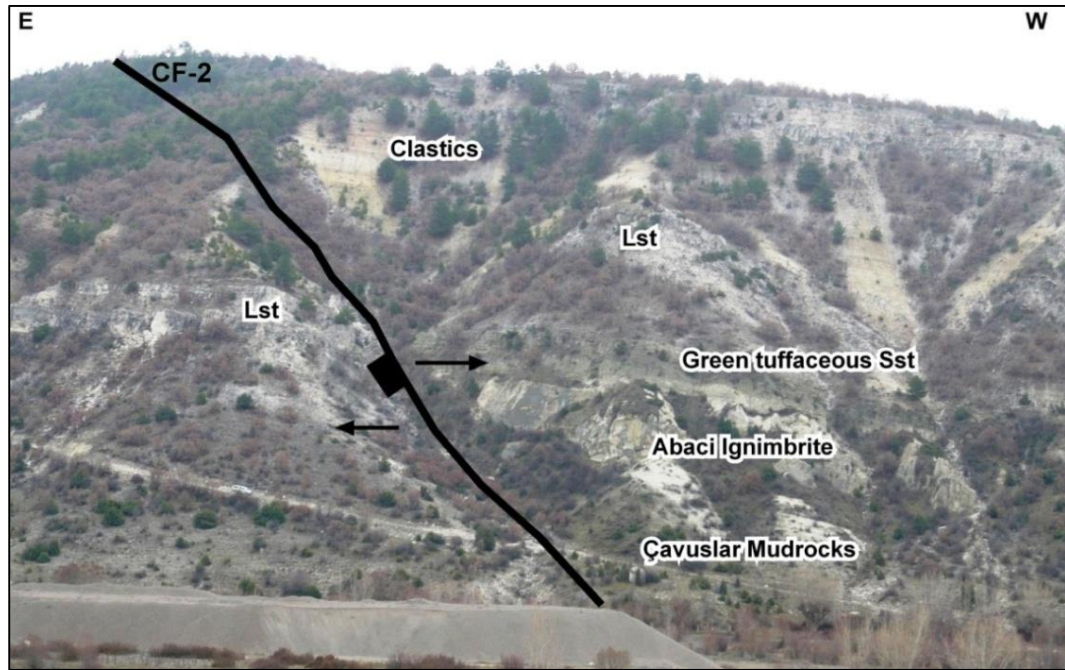


Figure 2.39. The view of the Çavuşlar fault-2 (ÇF-2) (Rojay, 2013)

Binkoz Faults (BF); The Binkoz faults are composed of two parallel normal faults with N76°E and N82°E trends. Both are located to the north of Binkoz village (Figure 2.28). The normal faults are possibly oblique slip faults; however, there are no slip data. The northern blocks are downthrown. Normal drags, linear vegetation, diminishing of coal beds and sudden change in topographic slopes are the indication of faulting (Figure 2.40). Coal beds are on the footwall block in the northern Binkoz fault and on the downthrown block in the southern Binkoz fault. The faults have observable length of more than 3 km. There is no slip data (Rojay, 2013).

Peykler Fault (PF); N60°E trending normal fault observed parallel to the Binkoz faults is possibly the same type. Silicification, linear vegetation, normal drags, landslides, talus deposits, rock falls and sudden slope changes are the indication of faulting. However, there is no slip data. The coal beds are on the footwall block (Rojay, 2013).

Aşağıadaköy Fault (AF); EW trending normal fault has an observable length of 2 km to the north of Aşağı Adaköy village (Figure 2.28). The fault is morphologically the most impressive structure in the area with well-preserved fault

planes and fills. Brecciation, mylonites, travertine development and slickenlines are the indications of the fault (Figure 2.41). The slip data shows a normal faulting developed under NNE-SSW extension where the northern block is downthrown. The age of faulting is post-Plio-Quaternary – pre-Holocene (Rojay, 2013).

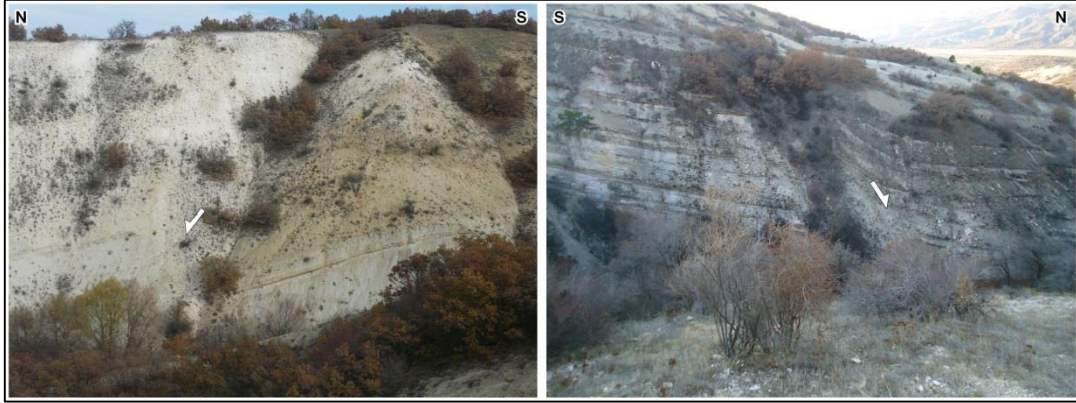


Figure 2.40. Binkoz normal faults (Rojay, 2013)



Figure 2.41. EW trending Aşağıdaköy normal fault (Rojay, 2013)

2.4.3.1.3. Kirmir Stream Valley Faults

Çeltikçi Faults (CeF); N69°E trending faults effect the Plio-Quaternary units and overlain by Holocene terrace deposits where Miocene sequences are fully silicified. The faults extend from Çeltikçi to north of Gümele for more than 3 km. Silicifications, brecciation, Fe-staining, silica veins/dykes, “travertines” and slip data are the indication of faulting. The faults are reverse to right lateral strike slip faults

with reverse components developed under NNW-SSE to WSW-ENE compression where northern blocks are uplifted (Rojay, 2013).

A possible buried/hidden fault along the Kirmir Stream—without any direct evidence- probably controls the southern margin of the Kirmir Stream (Figure 2.2828). The fault extends for 11 km between south of Çeltikçi town and south of Mahkemeağıcın village being a morphologically distinct structure (Figure 2.28). The Miocene units are elevated where northern block is downthrown.

2.4.3.1.4. Northern Margin Faults

The northern margin of the Çeltikçi graben is highly elevated. The fault extends for more than 6 km between İnışdibi (far north of Çeltikçi) to Tepebaşı ridge (far north of Abacı village). The sudden topographic slope change, spatial distribution of Holocene terraces, Quaternary talus deposits and landslides are the indication of faulting with slip data. The slip data manifests right lateral strike slip and reverse faulting developed under NW-SE compression. The fault is lately crosscut by a normal fault trending N14°W developed under NNE-SSW extension.

CHAPTER 3

SURFACE WATER HYDROLOGY

In order to determine the hydrologic nature of the drainage basin and surface water potential of the study area, surface water drainage network, flow rates of important streams and creeks, precipitation-runoff relation and water structures located in the upstream and downstream were analyzed. In the following, regional scale surface water hydrology will be presented first. The study area hydrologic observations, evaluations, and conceptual water budget will follow. Finally, information about the existing and planned water structures in the study area and its vicinity will be given.

3.1. REGIONAL AND STUDY AREA DRAINAGE NETWORK

Study area is located at the southeast of the Sakarya River Basin. Regional scale drainage network, catchment areas and water structures can be seen in Figure 3.1. The ponds in the vicinity of the coal tenements are shown with numbers and their names are presented in Chapter 3.4.

The creeks that originate from piedmonts of Işık Hill and Çiçekliyayla Hill on the north of the Kızılcahamam flow toward south and join the Hamam Stream. This stream continues to flow in northeast-southwest direction in the vicinity of the Doğanözü village where it is named as Kirmir Stream. The most important surface water unit in the study area is the Kirmir Stream which forms approximately the northern border of the coal tenements in the south. The second important surface water unit is the Pazar Stream which flows from the northern side of the Çeltikçi Town toward south and joins the Kirmir Stream. Pazar and Kirmir streams have 2000 km² catchment area in the vicinity of the Çeltikçi town. Both Kirmir Stream and Pazar Stream are controlled by important water structures (Figure 3.1). These water

structures are; Çamlıdere Dam which controls the Pazar Stream and Doğanözü Dam, Eğrekkaya Dam and Akyar Dam which control the Kirmir Stream, respectively. The streams which drain the east of the tenements are located in the Kurt Stream watershed and recharge the Kurtboğazi Dam Lake. Kurt Stream has approximately 300 km² catchment area. All dams are used for potable water supply by the Ankara Metropolitan Municipality. The water stored in these dams is transported by pipelines which pass through the study area (Figure 3.1). The general information about dams and other water structures are presented in Chapter 3.4.

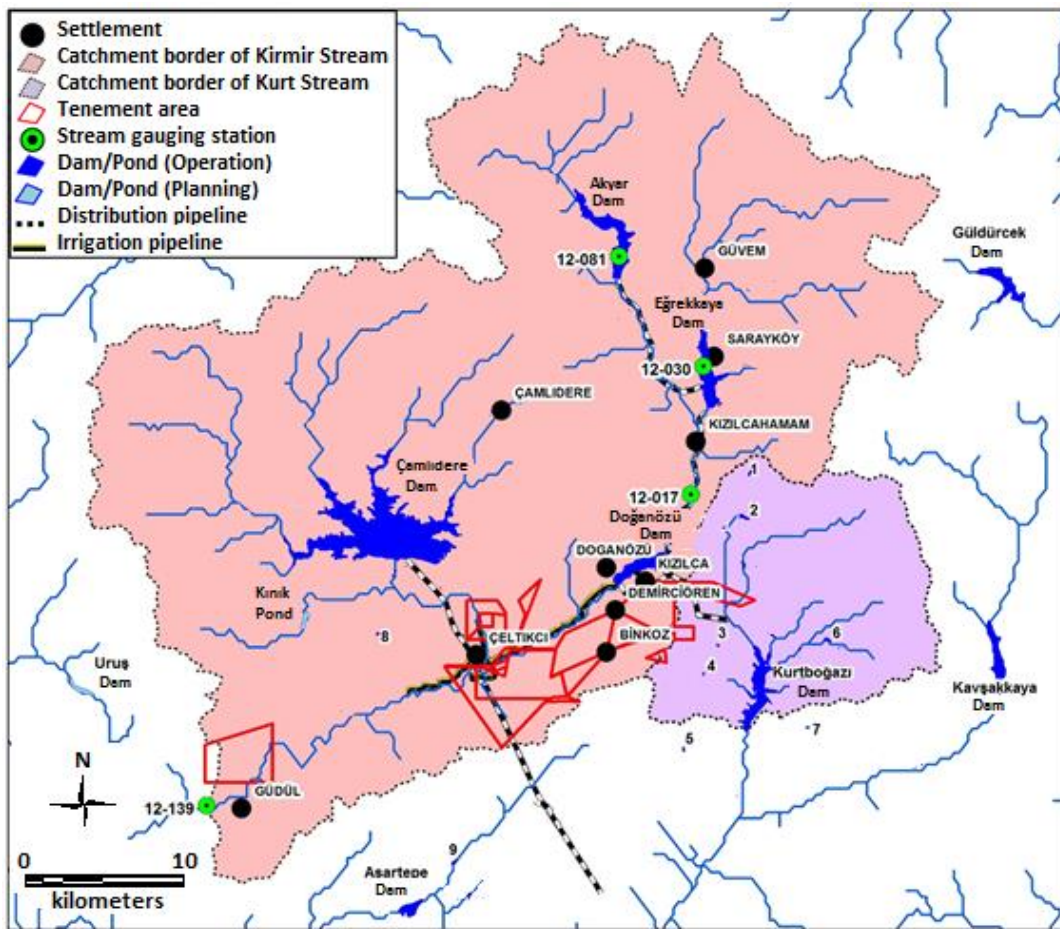


Figure 3.1. Map of catchment basins of Kirmir Stream and Kurt Creek, gauging stations and water structures in the vicinity of the study area

3.2. OBSERVED FLOW DATA

In order to determine the hydrologic nature of the catchment basins and surface water potential of the study area, flow rates of the surface water units are required.

For this purpose, flow rates of stream gauging stations which are operated by the State Hydraulic Works (DSİ) and Electrical Power Resources Survey and Development Administration (EİEİ) were analyzed. In addition, surface water monitoring points having important drainage areas were established. Instantaneous flow measurements have been conducted once a month from these monitoring points.

3.2.1. Stream Gauging Stations

Daily average flow rates were obtained from four stream gauging stations which are operated by the State Hydraulic Works and Electrical Power Resources Survey and Development Administration in the catchment basins of the study area (Figure 3.1, Table 3.1). Table 3.1 shows data inventory of the gauging stations. As can be seen in this figure, Kızılcahamam - Mandra (12017) station has been operated since 1959. Only 4-years of data are not recorded (1964, 1965, 2000 and 2001). The data belonging to this station is important because it is located at the upstream of the Kirmir Stream when compared to the location of the tenements. Other stations having daily average flow data have been operated shorter time than the Kızılcahamam - Mandra station (Figure 3.2).

The hydrograph of the daily average flow rates of the Kızılcahamam - Mandra (12-012) station is presented in Figure 3.3. Flow rate axis of this hydrograph is presented in arithmetic scale in Figure 3.3-a, and in logarithmic scale in Figure 3.3-b. High flow rates can be easily seen in arithmetic scale and low flow rates can be easily inspected in logarithmic scale hydrographs. As can be seen in Figure 3.3-a, flow rates show the seasonality at Kızılcahamam – Mandra (12-017) station. Especially in spring months (February-May), flow rates increase abruptly under the influence of snow melting. In summer months (June-September) low flow rates are dominant. The highest flow rate in this hydrograph is measured as 540 m³/s on 12 March 1968 and lowest flow rate is measured as 0.05 m³/s on 23 August 1963. Also, there is a decrease of the flow rates since 1985 as it can be seen from this hydrograph. These decreases became more evident with the start of the operation of the Eğrekkaya and Akyar Dams in 1992 and 2001, respectively. Moreover, in 2006-2008 years when the precipitation was low, significant decreases of the flow rates can be clearly observed.

Table 3.1. Data of stream gauging stations

No.	Institution	Station No.	Station Name	Stream/Pond Name	Data Type	Data Periods	Coordinates *		Elevation *	Precipitation Area *
							Easting	Northing		
1	DSİ/ EİEİ	12-017	Mandra	Kızılcahamam Creek	Daily Average Flow	April 1959-September 1963 October 1965-September 1999 October 2001-September 2013	40,4350	32,6500	903	907,5
2	DSİ	12-139	Güdül	Kirmir Stream	Daily Average Flow	October 1976-September 1999	40,2140	32,2430	780	2239
3	DSİ	12-030	Saray	Sey Creek	Daily Average Flow	October 1960-September 1965 October 1972-September 1980 October 1982-September 1989	40,5239	32,6606	957	384,2
4	DSİ	12-081	Derince	Bulak Stream	Daily Average Flow	October 1966-September 1969 October 1980-September 1991	40,6000	32,5833	1080	274

* Data from DSİ

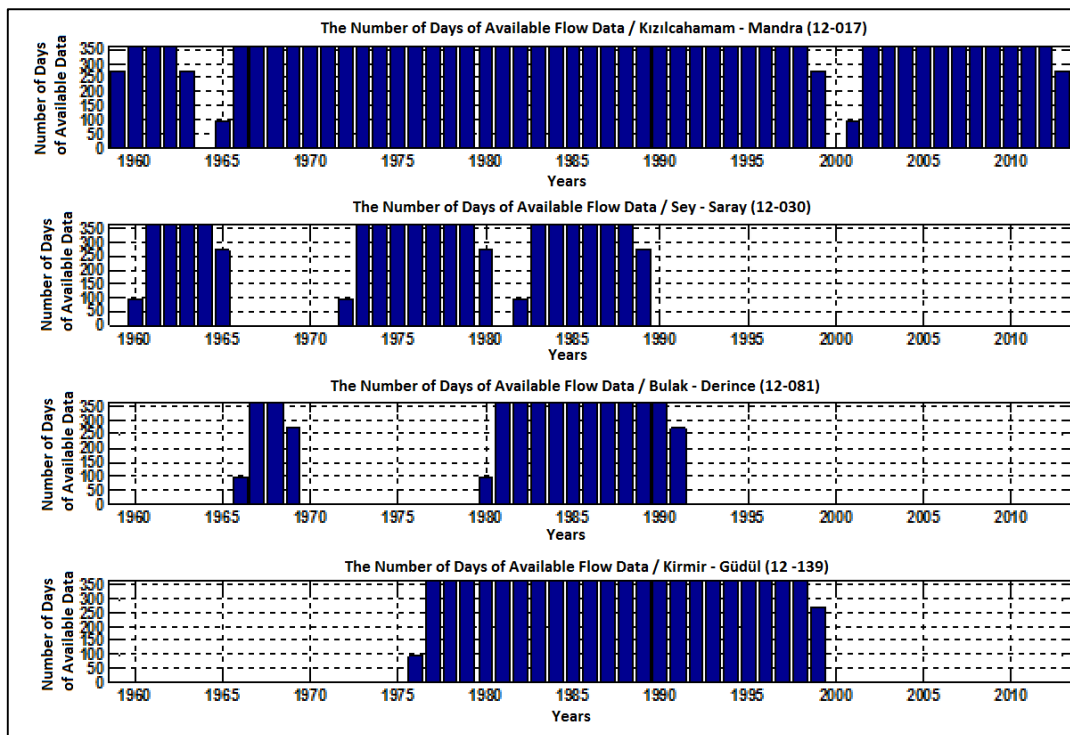


Figure 3. 2. Information of number of days of available data of stream gauging stations

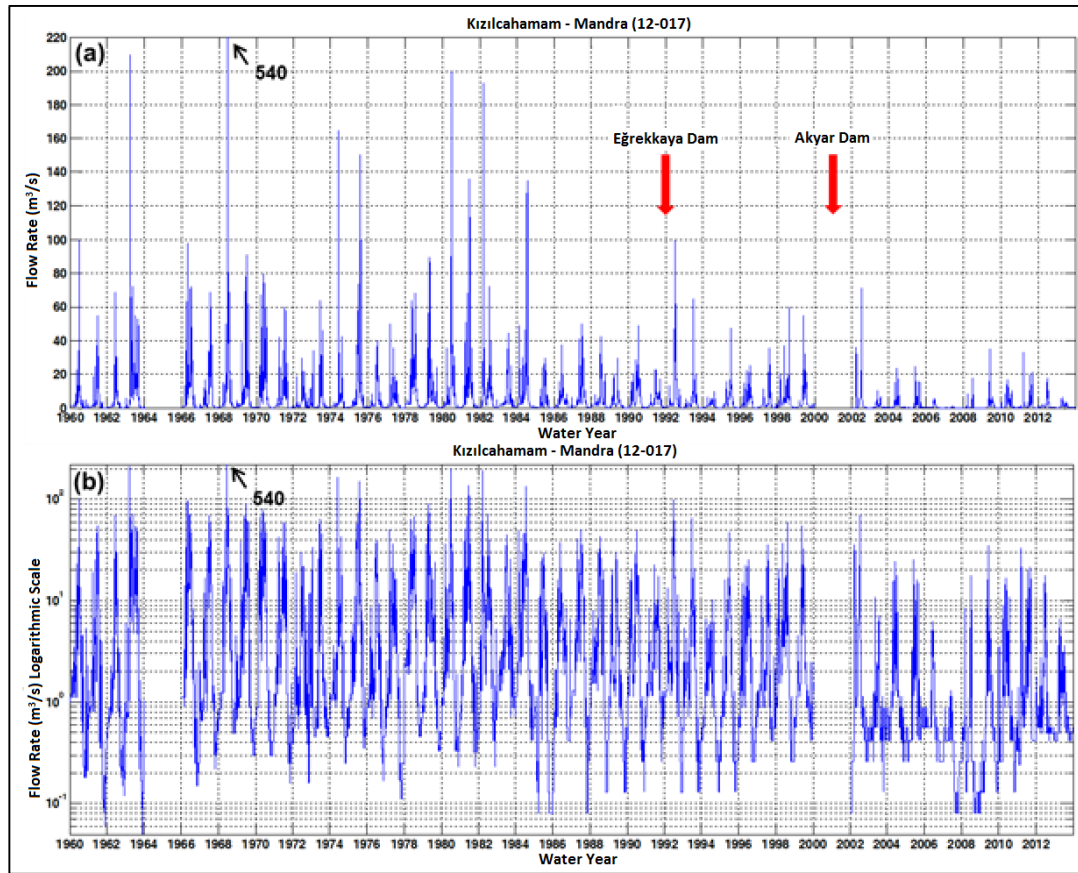


Figure 3.3. Hydrograph of the daily average flow rates of Kızılcahamam – Mandra (12-017) station (a) arithmetic scale, (b) logarithmic scale

Monthly average flow rates were calculated by using available data between 1960 and 2013 (Figure 3.4). Monthly average flow rates were calculated by using the average of the daily average flow rates in each month for all years. In view of all monitoring period of the Kızılcahamam – Mandra (12-017) station, it is seen that there is seasonality of the flow rates; the maximum monthly average flow rates are observed in March and April months as $15.4 \text{ m}^3/\text{s}$ and $15.2 \text{ m}^3/\text{s}$. Following these months the flow rates generally decrease rapidly and in summer months they become very low. When the uncontrolled (natural) flow which occurred between 1960-1991 is analyzed, the same seasonality in monthly average flow rates is observed but with higher discharge rates, especially in March-April with the average flow rates of $18.9 \text{ m}^3/\text{s}$ and $18.5 \text{ m}^3/\text{s}$, respectively. The flow rates during which controlled flow has taken place (1992-2013) were however significantly lower in winter and spring

seasons. In this period, the highest monthly average flow rate was seen in April with $9.3 \text{ m}^3/\text{s}$.

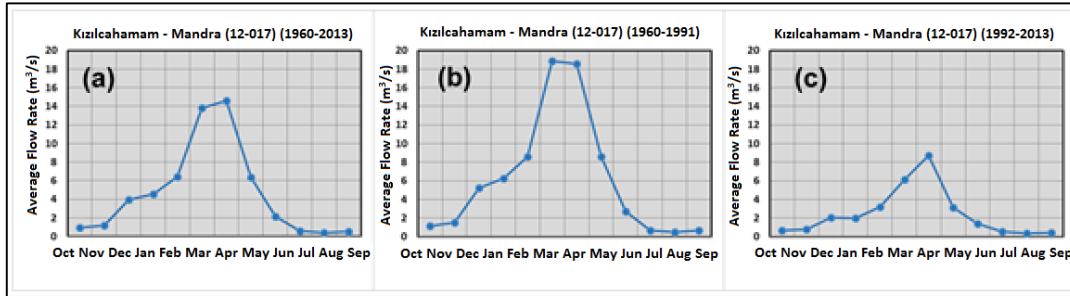


Figure 3.4. Monthly average flow rates of Kızılcahamam – Mandra (12-017) station (a) 1960-2013 water years, (b) 1960-1991 water years (uncontrolled flow), (c) 1992-2013 water years (controlled flow)

Flow duration curves were developed to analyze the distribution of the flow rates of the Kızılcahamam – Mandra (12-017) station for all monitoring periods (Figure 3.5). Flow duration curve shows the probability that the observed flow rates will be exceeded in a specific period of time. The flow rates are presented in arithmetic scale in Figure 3.5-a and in logarithmic scale in Figure 3.5-b. The logarithmic scale shows low flow rates better while the arithmetic scale shows high flow rates clearly. As can be seen in Figure 3.5-b, the flow rates having 5%, 50% and 95% probability of exceedance are $21 \text{ m}^3/\text{s}$, $1.15 \text{ m}^3/\text{s}$ and $0.21 \text{ m}^3/\text{s}$, respectively.

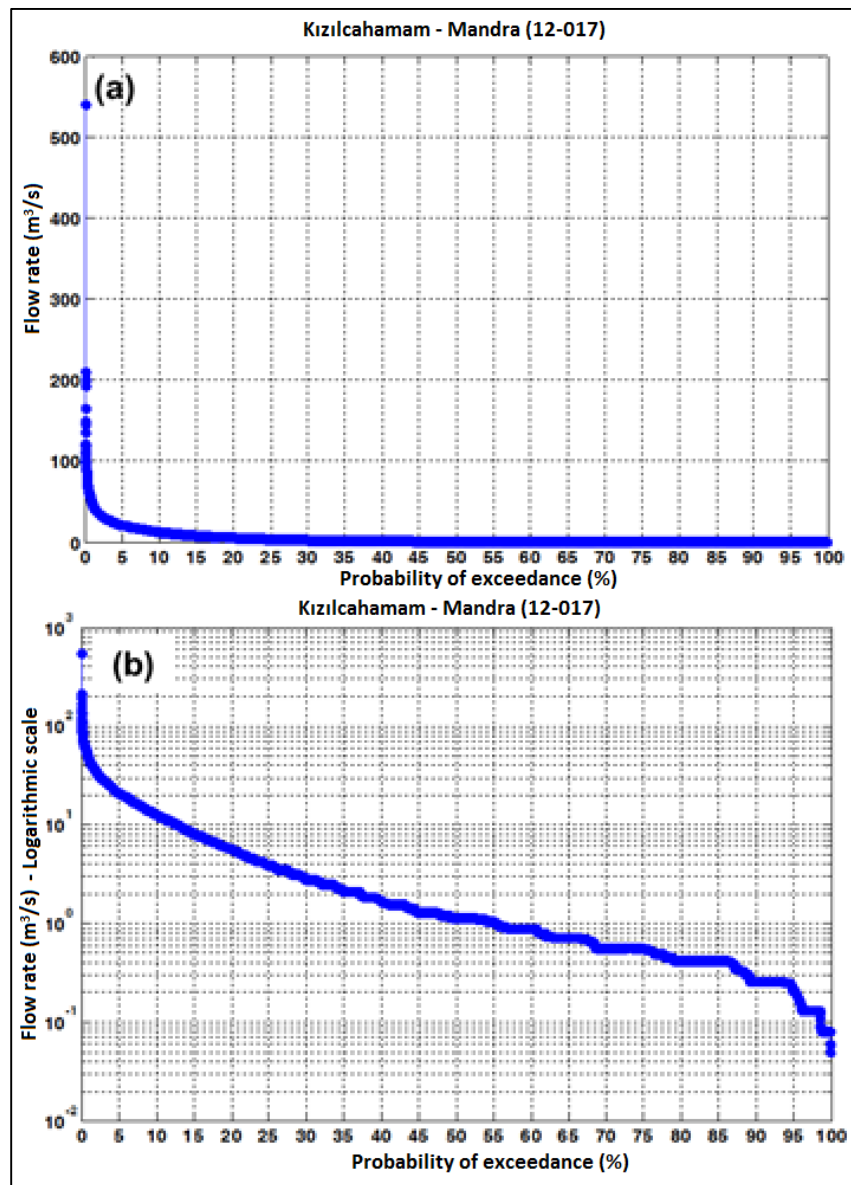


Figure 3.5. Flow duration curve of Kızılcahamam – Mandra (12-017) station (a) arithmetic scale, (b) logarithmic scale (1960-2013)

Low flow analysis was also made for the Kızılcahamam – Mandra (12-017) station. Figure 3.6-a and Figure 3.6-b show the annual lowest daily flow rates and the date of their occurrences, respectively. As it can be seen in Figure 3.6-a, the lowest flow rates vary between 0.05 m³/s and 0.72 m³/s between the years 1960 and 1985. After 1985, the lowest flow rates decreased and varied between 0.13 m³/s and 0.26 m³/s. Figure 3.6-b shows the first date (as day of the water year) of the lowest

daily average flow rates between the years of 1960-2013. For the years 1960-1999, the first water year date of the lowest flow rate regularly occurs from the end July through the end of August. For the years between 2002 and 2013, there is an irregularity of the first date of the lowest flow rate occurrence. During this period, in some years the lowest flow rate is observed in May and in some other years they are observed in October and November. It was thought that this irregularity may occur under the control of dams.

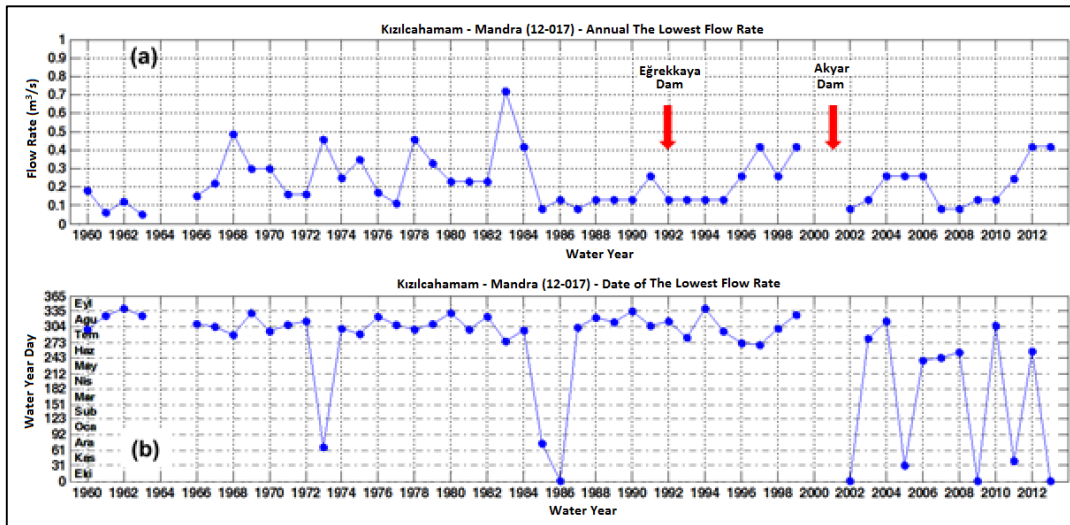


Figure 3.6. (a) Annual lowest flow rate, (b) first date of the lowest flow rate of the Kızılcahamam – Mandra (12-017) station

Low flow duration curves were developed for the Kızılcahamam – Mandra (12-017) station for the years 1960-1991 (uncontrolled flow) and 1992-2013 (controlled flow) (Figure 3.7). For the years between 1960-1991 (uncontrolled flow dominates), the annual lowest flow rate which have 5%, 50% and 95% exceedance probability are $0.5 \text{ m}^3/\text{s}$, $0.2 \text{ m}^3/\text{s}$ and $0.05 \text{ m}^3/\text{s}$, respectively. While for the years 1992-2013 (under the dam control) the annual lowest flow rate which have 5%, 50% and 95% exceedance probability are $0.42 \text{ m}^3/\text{s}$, $0.2 \text{ m}^3/\text{s}$ and $0.08 \text{ m}^3/\text{s}$, respectively. As can be seen from these results, because of the both dam affects and seasonal droughts that occurred after 1992, the annual lowest flow rates decreased, especially for the low flow rates having exceedance probability of 0-15%.

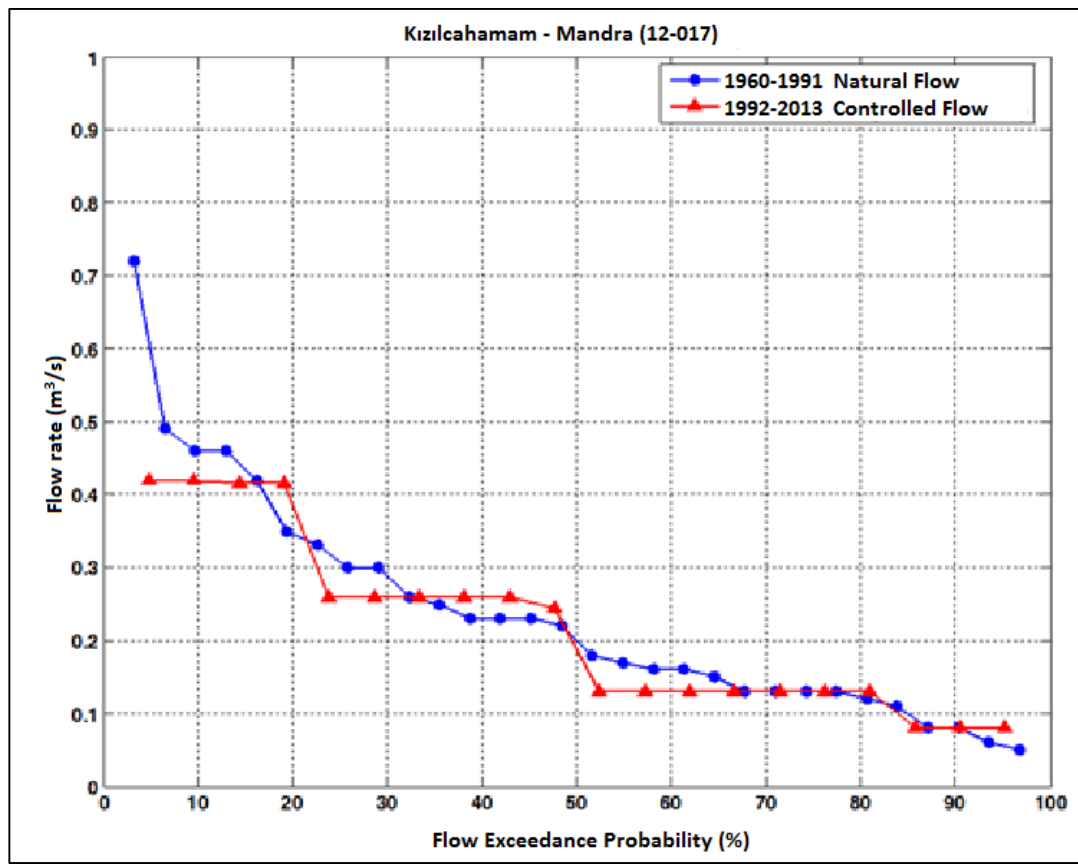


Figure 3.7. Annual flow duration curves by using the lowest flow rates

A low flow threshold value was determined by using the flow duration curve which is presented in Figure 3.5-b. The low flow threshold value was determined as $0.21 \text{ m}^3/\text{s}$ which corresponds to the 95% probability of exceedance (i.e., %5 probability that the flows will be lower than the threshold value) for measured flows between the years 1960 and 2013. The longest low flow duration (i.e., during which the flow remains under this value continually) were calculated for each year by using this low flow threshold value (Figure 3.8-a). As can be seen in Figure 3.8-a, with 110-day period, the daily average flow rates remained under the low flow threshold value ($0.21 \text{ m}^3/\text{s}$) in 2008. Similarly, in 1961, 1963, 1977, 1985, 1992, 2002, 2007 and 2009 years, daily average flow rates continuously remained below the low flow threshold value for more than 30 days. After 2009, number of days during which the low flow threshold value is observed decreased with increasing precipitation. Figure 3.8-b shows that total number of days of daily average flow rates which remain below

the low flow threshold value in a year. As it is seen, Figure 3.8-b and Figure 3.8-a show similarity; however, the total number of days of low flow period increased for some years when compared the longest low flow duration. For instance, daily average flow rates in 2008 remained below the low flow threshold value for a total of 125 days.

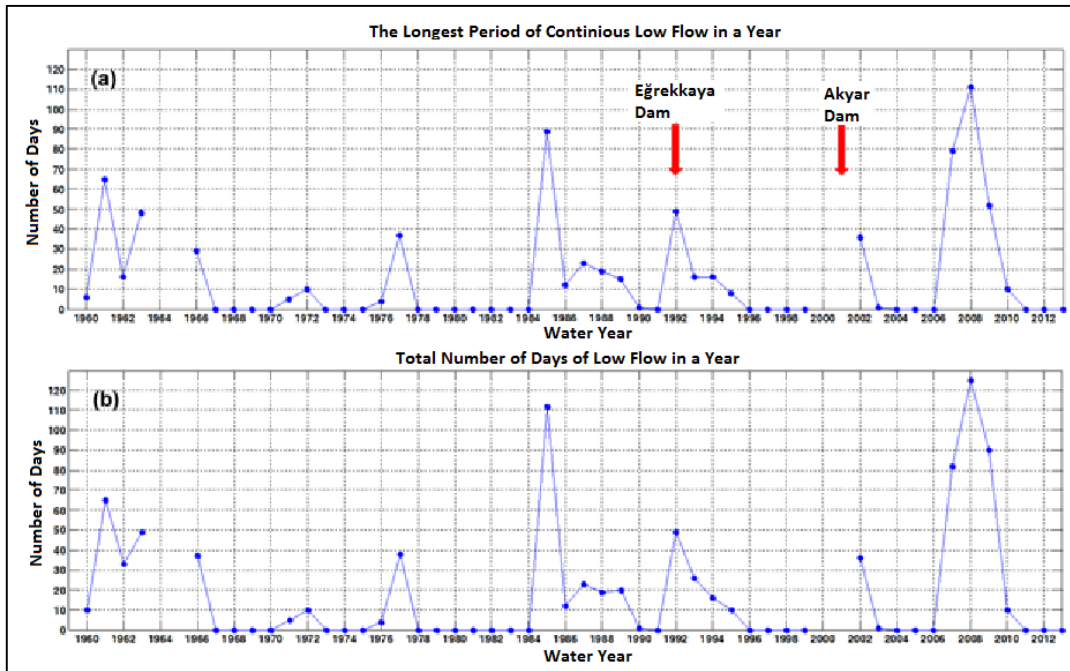


Figure 3.8. For Kızılcahamam – Mandra (12-017) station (a) the longest period of continuous low flow in a year, (b) total number of days of the daily average flow remain under the low flow threshold ($0.21 \text{ m}^3/\text{s}$)

Precipitation-runoff relation for the region was analyzed by comparing the annual average flow data of the Kızılcahamam-Mandra (12-017) gauging station with annual precipitation data measured at Kızılcahamam meteorological station (17664). Figure 3.9 shows that there is a good relation between the annual flow rates and annual precipitation values until the Eğrekkaya Dam started to operate in 1992. Because Eğrekkaya Dam started to hold water, flows at Kızılcahamam – Mandra (12-017) station were decreased irrespective of the increasing precipitation. Decrease of the flows became even more apparent after Akyar Dam started to operate in 2001. Short term flow measurement had been taken at Sey – Saray gauging station (Figure 3.10). Measured annual flows in this station varied in parallel with the annual

precipitation until 1985 after which the flow rates decreased. The measured annual flows at Bulak - Derince (12081) gauging station varied in parallel with the annual precipitation values (Figure 3.11). At Kirmir - Gdl (12139) gauging station however the measured annual average flows decreased after the operation of the amlıdere Dam in 1985 (Figure 3.12). Although the annual total precipitation shows increasing trend after 1994, increases of annual flows at Kirmir - Gdl gauging station have been quite low. As a result, precipitation-runoff relation is affected negatively with holding water by dams in the vicinity of the study area.

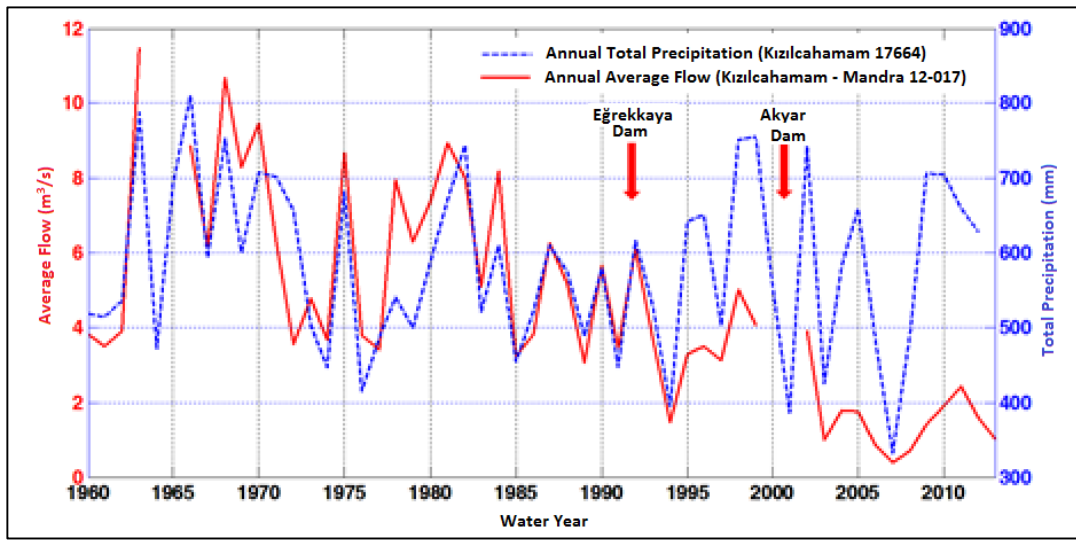


Figure 3.9. Data of annual total precipitation measured at Kızılcahamam (17664) and annual average flow measured at Kızılcahamam – Mandra (12-017) stations

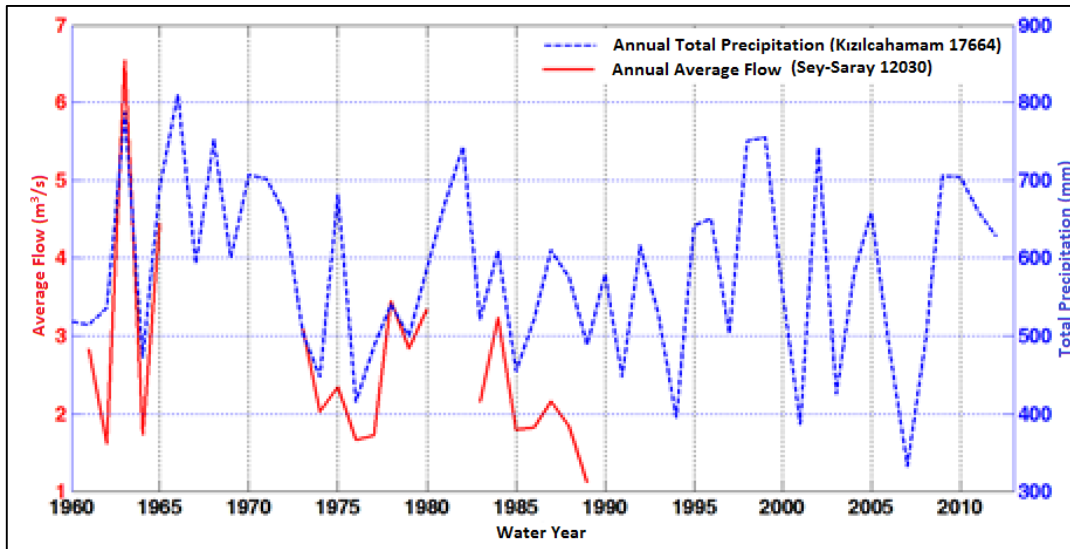


Figure 3.10. Data of annual total precipitation measured at Kızılcahamam (17664) and annual average flow measured at Sey - Saray (12-030) stations

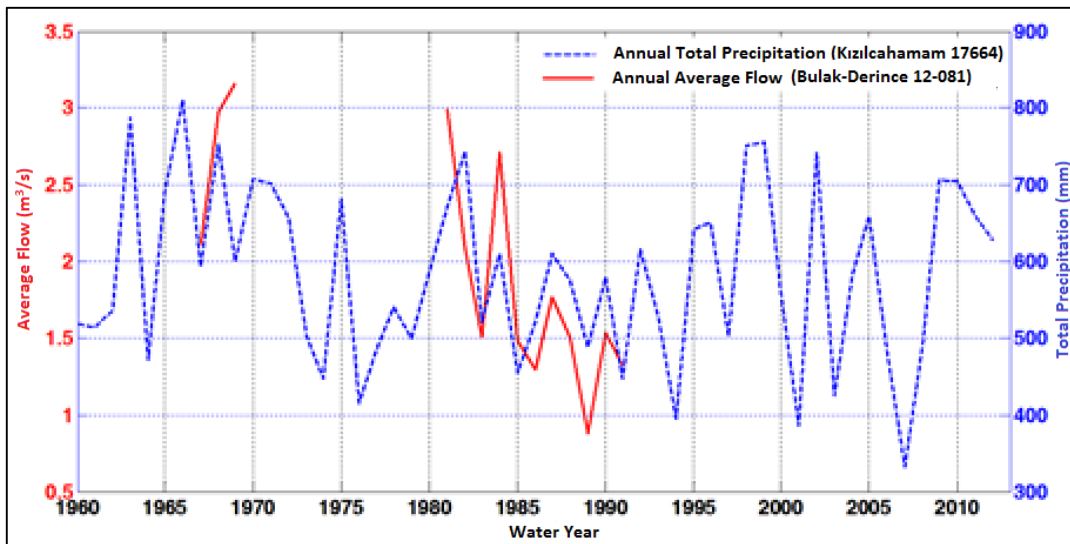


Figure 3.11. Data of annual total precipitation measured at Kızılcahamam (17664) and annual average flow measured at Bulak - Derince (12-081) stations

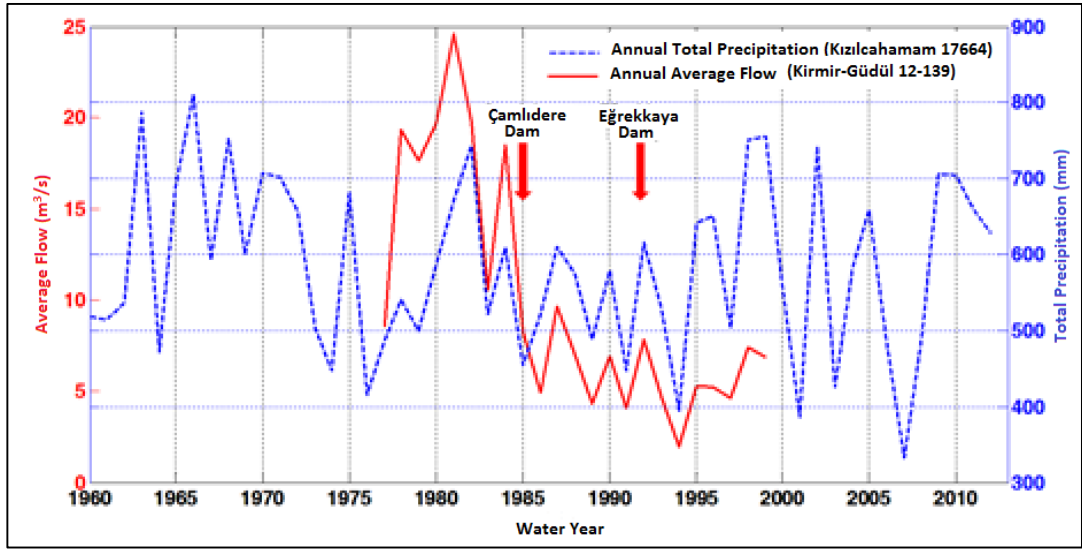


Figure 3.12. Data of annual total precipitation measured at Kızılcahamam (17664) and annual average flow measured at Kirmir - Güdül (12-139) stations

3.2.2. Surface Water Monitoring Points

Twenty-one surface water monitoring points were determined by conducting office and field works which were presented in Monitoring Plan Report by Yazıcıgil et al. (2012) in January 2012 and Progress Report which was presented in April 2013 by Yazıcıgil et al. (2013). Monthly instantaneous flow rates have been measured at these monitoring points since March 2012. Drainage network, surface water monitoring points and catchment basins are presented in Figure 3.13.

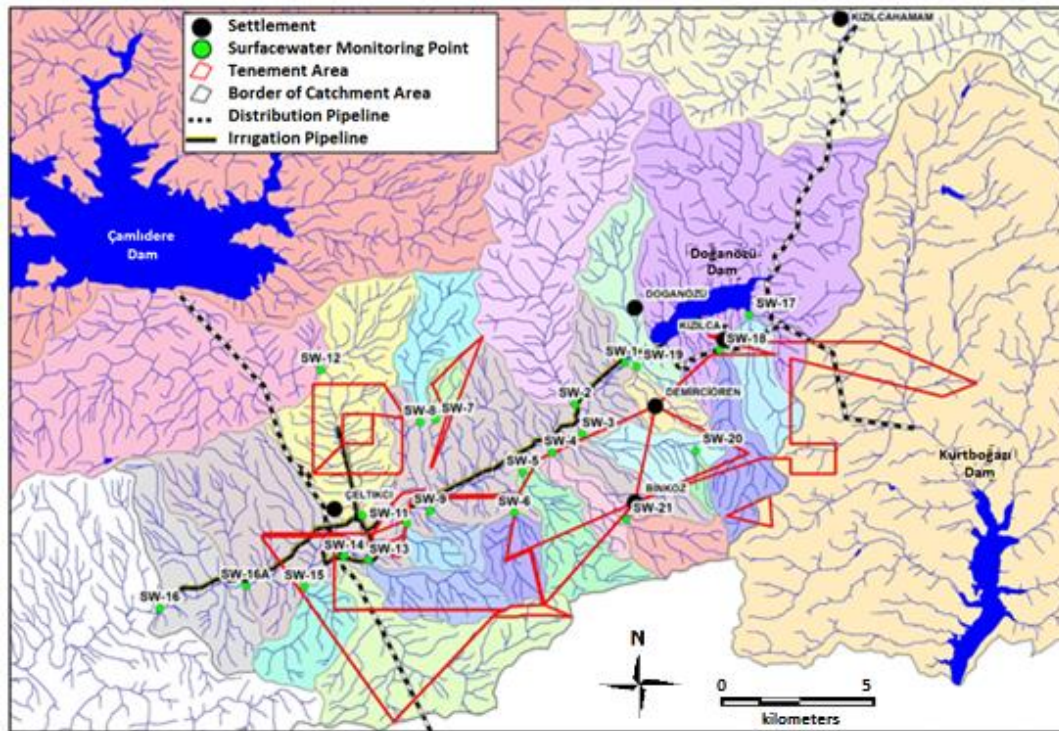


Figure 3.13. Catchment area of the surface water monitoring points in the study area

Among these monitoring points, SW1 and SW16 are on the Kirmir Stream and are located at the upstream and downstream of the study area, respectively. SW11 and SW12 are on the Pazar Stream and they also represent downstream and upstream of the study area, respectively. Other monitoring points were determined on creeks discharging into the Kirmir Stream and have relatively important drainage areas. The monitoring points between SW17 and SW21 which were determined at April 2013 represent the flow from the new tenements. These monitoring points have been monitored after this date. SW17 and SW18 were selected to observe the surface water flow to the Doğanöz Dam Lake. SW19, SW20 and SW21 were selected to observe the surface water flow near the Demirciören village, surface water flow to an artificial lake, and surface water flow near the Binkoz village, respectively. Although SW16A monitoring point had been initially determined as the downstream point of the Kirmir Stream in “Water Source Monitoring Plan” report by Yazıcıgil et al. (2012), because of the changes in cross-sectional areas at high flow rates and

having difficulty at flow measurements, this point was shifted to SW16 (embankment). There is 1% difference between the total catchment basins and 2% difference between the catchment basins uncontrolled by dams between SW16 and SW16A. Thus, it is not expected that there will be a significant difference between the flow measurements at SW16 and SW16A. Measurements were conducted at SW16 or SW16A monitoring points based on the suitability of the measurement conditions.

Flow measurements have been conducted once a month at all surface water monitoring points. Coordinates of the monitoring points, flow rates, measurement date and methods are presented in Table 3.2.

Surface water monitoring points and surface areas of the catchment basins of the water structures are listed in Table 3.3. In this table, total area represents the area of the natural catchment basin and uncontrolled area represents the areas which are not affected by any water structure. Doğanözü Dam started to hold water in November 2012 and it was not used in the calculation of the uncontrolled area. For example, the total catchment area of SW1 is 967.33 km² while the uncontrolled area of this point is 328.44 km². This value is obtained by subtracting the catchment areas of Eğrekkaya (385.29 km²) and Akyar (253.60 km²) Dams from the total catchment area. As can be seen in this table, SW20 (0.88 km²) has the smallest catchment area and SW2 (36.32 km²) has the largest catchment area among the all monitoring points.

Monthly instantaneous flow measurements for all monitoring period (March 2012 – December 2013) were presented graphically in Figure 3.14. In this figure, monitoring points on the Kirmir Stream drainage network and their relation with water structures are schematically presented.

Table 3.2. Instantaneous flow measurement data of surface water monitoring points

Station no.	Easting	Northing	Mar-12			Apr-12			May-12			Jun-12			Jul-12			Aug-12			Sep-12		
			Flow rate (m ³ /s)	Measurement Method	Measurement Date	Flow rate (m ³ /s)	Measurement Method	Measurement Date	Flow rate (m ³ /s)	Measurement Method	Measurement Date	Flow rate (m ³ /s)	Measurement Method	Measurement Date	Flow rate (m ³ /s)	Measurement Method	Measurement Date	Flow rate (m ³ /s)	Measurement Method	Measurement Date	Flow rate (m ³ /s)	Measurement Method	Measurement Date
SW1	463455	4468701	2.1450	Flow meter	12/03/2012	5.4400	Doppler	12/04/2012	0.5843	Flow meter	14/05/2012	0.4014	Flow meter	12/06/2012	0.0638	Flow meter	23/07/2012	0.1142	Flow meter	07/08/2012	0.2862	Flow meter	20/09/2012
SW2	461794	4467329	0.2690	Flow meter	12/03/2012	1.0469	Flow meter	13/04/2012	0.1042	Flow meter	14/05/2012	0.0347	Flow meter	12/06/2012	0.0000	x	20/07/2012	0.0000	x	07/08/2012	0.0000	x	20/09/2012
SW3	462009	4466306		x		0.0336	Flow meter	18/04/2012	0.0151	Flow meter	14/05/2012	0.0038	Flow meter	12/06/2012	0.0000	x	20/07/2012	0.0000	x	07/08/2012	0.0000	x	20/09/2012
SW4	461011	4465738	0.0702	Flow meter	14/03/2012	0.1867	Flow meter	13/04/2012	0.0255	Flow meter	14/05/2012	0.0126	Flow meter	12/06/2012	0.0025	Volume/Time	20/07/2012	0.0000	x	07/08/2012	0.0000	x	20/09/2012
SW5	460022	4465040	0.0408	Flow meter	14/03/2012	0.1210	Flow meter	13/04/2012	0.0425	Flow meter	14/05/2012	0.0093	Flow meter	12/06/2012	0.0000	x	20/07/2012	0.0000	x	07/08/2012	0.0000	x	20/09/2012
SW6	459768	4463658	0.0001	Volume/Time	14/03/2012	0.0002	Visual	13/04/2012	0.0010	Estimation	14/05/2012	0.0040	Volume/Time	12/06/2012	0.0000	x	20/07/2012	0.0000	x	07/08/2012	0.0000	x	20/09/2012
SW7	457104	4466814	0.0080	Estimation	12/03/2012	0.0000	x	13/04/2012	0.0000	x	14/05/2012	0.0000	x	12/06/2012	0.0000	x	20/07/2012	0.0000	x	07/08/2012	0.0000	x	20/09/2012
SW8	456587	4466625	0.0270	Flow meter	12/03/2012	0.0160	Flow meter	13/04/2012	0.0000	x	14/05/2012	0.0000	x	12/06/2012	0.0000	x	20/07/2012	0.0000	x	07/08/2012	0.0000	x	20/09/2012
SW9	456926	4463768	0.0080	Flow meter	14/03/2012	0.0000	x	13/04/2012	0.0158	Flow meter	14/05/2012	0.0094	Flow meter	12/06/2012	0.0030	Volume/Time	20/07/2012	0.0003	Volume/Time	07/08/2012	0.0000	x	20/09/2012
SW10	456136	4463320	0.0120	Flow meter	14/03/2012	0.0020	Estimation	13/04/2012	0.0025	Estimation	14/05/2012	0.0020	Volume/Time	12/06/2012	0.0020	Volume/Time	20/07/2012	0.0000	x	07/08/2012	0.0000	x	20/09/2012
SW11	454659	4463677	0.9160	Flow meter	13/03/2012	1.3080	Flow meter	13/04/2012	0.1522	Flow meter	15/05/2012	0.1406	Flow meter	12/06/2012	0.4089	Flow meter	23/07/2012	0.4006	Flow meter	07/08/2012	0.0695	Flow meter	20/09/2012
SW12	453410	4468405	0.3530	Flow meter	13/03/2012	1.1700	Doppler	14/04/2012	0.3054	Flow meter	15/05/2012	0.1043	Flow meter	12/06/2012	0.5196	Flow meter	23/07/2012	0.4371	Flow meter	07/08/2012	0.0752	Flow meter	20/09/2012
SW13	454846	4462112	0.0000	x	13/03/2012	0.0000	x	13/04/2012	0.0647	Flow meter	15/05/2012	0.0030	Volume/Time	12/06/2012	0.0004	Volume/Time	20/07/2012	0.0000	x	07/08/2012	0.0000	x	20/09/2012
SW14	454031	4462228	0.0750	Flow meter	13/03/2012	0.0630	Flow meter	13/04/2012	0.0259	Flow meter	15/05/2012	0.0027	Flow meter	12/06/2012	0.0015	Volume/Time	20/07/2012	0.0000	x	07/08/2012	0.0000	x	20/09/2012
SW15	452712	4461214	0.0180	Estimation	13/03/2012	0.0000	x	13/04/2012	0.0067	Flow meter	15/05/2012	0.0000	x	12/06/2012	0.0020	Volume/Time	20/07/2012	0.0000	x	07/08/2012	0.0000	x	20/09/2012
SW16	447825	4460366	5.4860	Flow meter	14/03/2012	8.0200	Flow meter	13/04/2012	4.2794	Flow meter	15/05/2012	1.4813	Flow meter	12/06/2012	1.2180	Flow meter	23/07/2012	1.2229	Flow meter	07/08/2012	x	x	x
SW16A	450750	4461240		x		x	x	x	x	x	x	x	x	x	x	x	x	x	x	x	0.5361	Flow meter	20/09/2012
SW17	467566	4470600																					
SW18	466623	4469137																					
SW19	463839	4468540																					
SW20	465825	4465785																					
SW21	463484	4463464																					
Station no.	Easting	Northing	Oct-12			Nov-12			Dec-12			Jan-13			Feb-13			Mar-13			Apr-13		
			Flow rate (m ³ /s)	Measurement Method	Measurement Date	Flow rate (m ³ /s)	Measurement Method	Measurement Date	Flow rate (m ³ /s)	Measurement Method	Measurement Date	Flow rate (m ³ /s)	Measurement Method	Measurement Date	Flow rate (m ³ /s)	Measurement Method	Measurement Date	Flow rate (m ³ /s)	Measurement Method	Measurement Date	Flow rate (m ³ /s)	Measurement Method	Measurement Date
SW1	463455	4468701	0.1756	Flow meter	30/10/2012	0.0000	x	16/11/2012	0.0000	x	18/12/2012	0.0000	x	17/01/2013	0.0000	x	15/02/2013	0.0000	x	11/03/2013	0.0090	Flow meter	24/04/2013
SW2	461794	4467329	0.0000	x	30/10/2012	0.0000	x	16/11/2012	0.0647	Flow meter	18/12/2012	0.0635	Flow meter	17/01/2013	0.3146	Flow meter	15/02/2013	0.2277	Flow meter	11/03/2013	0.1395	Flow meter	24/04/2013
SW3	462009	4466306	0.0000	x	30/10/2012	0.0000	x	16/11/2012	0.0000	x	18/12/2012	0.0000	x	17/01/2013	0.0000	x	15/02/2013	0.0000	x	11/03/2013	0.0185	Flow meter	24/04/2013
SW4	461011	4465738	0.0000	x	30/10/2012	0.0000	x	16/11/2012	0.0130	Flow meter	18/12/2012	0.0157	Flow meter	17/01/2013	0.0684	Flow meter	15/02/2013	0.1131	Flow meter	11/03/2013	0.0487	Flow meter	24/04/2013
SW5	460022	4465040	0.0000	x	30/10/2012	0.0000	x	16/11/2012	0.0000	x	18/12/2012	0.0062	Flow meter	17/01/2013	0.0319	Flow meter	15/02/2013	0.0267	Flow meter	11/03/2013	0.0332	Flow meter	24/04/2013
SW6	459768	4463658	0.0000	x	30/10/2012	0.0000	x	16/11/2012	0.0000	x	18/12/2012	0.0000	x	17/01/2013	0.0000	x	15/02/2013	0.0000	x	11/03/2013	0.0044	Flow meter	24/04/2013
SW7	457104	4466814	0.0000	x	30/10/2012	0.0000	x	16/11/2012	0.0000	x	18/12/2012	0.0000	x	17/01/2013	0.0000	x	15/02/2013	0.0000	x	11/03/2013	0.0000	x	24/04/2013
SW8	456587	4466625	0.0000	x	30/10/2012	0.0000	x	16/11/2012	0.0000	x	18/12/2012	0.0000	x	17/01/2013	0.0000	x	15/02/2013	0.0000	x	11/03/2013	0.0000	x	24/04/2013
SW9	456926	4463768	0.0000	x	30/10/2012	0.0000	x	16/11/2012	0.0000	x	18/12/2012	0.0000	x	17/01/2013	0.0000	x	15/02/2013	0.0000	x	11/03/2013	0.0000	x	22/04/2013
SW10	456136	4463320	0.0000	x	30/10/2012	0.0000	x	16/11/2012	0.0000	x	18/12/2012	0.0000	x	17/01/2013	0.0000	x	15/02/2013	0.0000	x	11/03/2013	0.0000	x	22/04/2013
SW11	454659	4463677	0.1361	Flow meter	30/10/2012	0.1871	Flow meter	16/11/2012	0.3861	Flow meter	18/12/2012	0.7420	Flow meter	18/01/2013	0.6638	Flow meter	15/02/2013	0.7809	Flow meter	11/03/2013	0.4572	Flow meter	22/04/2013
SW12	453410	4468405	0.1063	Flow meter	30/10/2012	0.0882	Flow meter	16/11/2012	0.2731	Flow meter	18/12/2012	0.7176	Flow meter	18/01/2013	0.6259	Flow meter	15/02/2013	0.6598	Flow meter	11/03/2013	0.3628	Flow meter	22/04/2013
SW13	454846	4462112	0.0000	x	30/10/2012	0.0000	x	16/11/2012	0.0000	x	18/12/2012	0.0000	x	17/01/2013	0.0000	x	15/02/2013	0.0000	x	11/03/2013	0.0000	x	24/04/2013
SW14	454031	4462228	0.0025	Flow meter	30/10/2012	0.0187	Flow meter	16/11/2012	0.3653	Flow meter	18/12/2012	0.0625	Flow meter	18/01/2013	0.0599	Flow meter	14/02/2013	0.0351	Flow meter	11/03/2013	0.0625	Flow meter	22/04/2013
SW15	452712	4461214	0.0000	x	30/10/2012	0.0000	x	16/11/2012	0.0394	Flow meter	18/12/2012	0.0584	Flow meter	18/01/2013	0.0180	Flow meter	14/02/2013	0.0125	Flow meter	11/03/2013	0.0195	Flow meter	22/04/2013
SW16	447825	4460366	x	x	30/10/2012	x	x	x	1.2373	Flow meter	18/12/2012	1.7282	Flow meter	18/01/2013	1.9751	Flow meter	15/02/2013	1.9751	Flow meter	11/03/2013	2.1123	Flow meter	24/04/2013
SW16A	450750	4461240	0.7093	Flow meter	30/10/2012	0.7643	Flow meter	16/11/2012	x	x	x	x	x	x	x	x	x	x	x	x	x	x	x
SW17	467566	4470600																					
SW18	466623	4469137																					
SW19	463839	4468540																					
SW20	465825	4465785																					
SW21	463484	4463464																					

Table 3.2. (continued)

Station no.	Easting	Northing	May-13			Jun-13			Jul-13			Aug-13			Sep-13			Oct-13			Nov-13			Dec-13		
			Flow rate (m ³ /s)	Measurement Method	Measurement Date	Flow rate (m ³ /s)	Measurement Method	Measurement Date	Flow rate (m ³ /s)	Measurement Method	Measurement Date	Flow rate (m ³ /s)	Measurement Method	Measurement Date	Flow rate (m ³ /s)	Measurement Method	Measurement Date	Flow rate (m ³ /s)	Measurement Method	Measurement Date	Flow rate (m ³ /s)	Measurement Method	Measurement Date	Flow rate (m ³ /s)	Measurement Method	Measurement Date
SW1	463455	4468701	0.0181	Flow meter	17/05/2013	0.0649	Flow meter	18/06/2013	0.0934	Flow meter	16/07/2013	0.0271	Flow meter	13/08/2013	0.0152	Flow meter	19/09/2013	0.0115	Flow meter	22/10/2013	0.0000	x	19/11/2013	0.0000	x	13/12/2013
SW2	461794	4467329	0.0624	Flow meter	17/05/2013	0.0000	x	18/06/2013	0.0000	x	16/07/2013	0.0000	x	13/08/2013	0.0000	x	19/09/2013	0.0000	x	22/10/2013	0.0064	Flow meter	19/11/2013	0.0093	Flow meter	13/12/2013
SW3	462009	4466306	0.0040	Flow meter	17/05/2013	0.0000	x	18/06/2013	0.0000	x	17/07/2013	0.0000	x	13/08/2013	0.0000	x	19/09/2013	0.0000	x	23/10/2013	0.0000	x	20/11/2013	0.0000	x	12/12/2013
SW4	461011	4465738	0.0158	Flow meter	17/05/2013	0.0015	Flow meter	18/06/2013	0.0015	Flow meter	17/07/2013	0.0000	x	13/08/2013	0.0000	x	19/09/2013	0.0000	x	23/10/2013	0.0068	Flow meter	20/11/2013	0.0000	x	13/12/2013
SW5	460022	4465040	0.0089	Flow meter	17/05/2013	0.0000	Flow meter	19/06/2013	0.0000	x	17/07/2013	0.0000	x	13/08/2013	0.0000	x	19/09/2013	0.0000	x	23/10/2013	0.0000	x	20/11/2013	0.0000	x	13/12/2013
SW6	459768	4463658	0.0000	x	17/05/2013	0.0000	Flow meter	19/06/2013	0.0000	x	17/07/2013	0.0000	x	13/08/2013	0.0000	x	19/09/2013	0.0000	x	23/10/2013	0.0000	x	20/11/2013	0.0000	x	13/12/2013
SW7	457104	4466814	0.0000	x	16/05/2013	0.0000	x	18/06/2013	0.0000	x	18/07/2013	0.0000	x	13/08/2013	0.0000	x	19/09/2013	0.0000	x	22/10/2013	0.0000	x	21/11/2013	0.0000	x	12/12/2013
SW8	456587	4466625	0.0000	x	16/05/2013	0.0000	x	18/06/2013	0.0000	x	18/07/2013	0.0000	x	13/08/2013	0.0000	x	19/09/2013	0.0000	x	22/10/2013	0.0000	x	21/11/2013	0.0000	x	12/12/2013
SW9	456926	4463768	0.0000	x	16/05/2013	0.0165	Flow meter	18/06/2013	0.0165	Flow meter	17/07/2013	0.0313	Flow meter	14/08/2013	0.0336	Flow meter	19/09/2013	0.0000	x	22/10/2013	0.0000	x	21/11/2013	0.0000	x	12/12/2013
SW10	456136	4463320	0.0000	x	16/05/2013	0.0000	x	18/06/2013	0.0000	x	17/07/2013	0.0000	x	14/08/2013	0.0000	x	19/09/2013	0.0000	x	22/10/2013	0.0000	x	21/11/2013	0.0000	x	12/12/2013
SW11	454659	4463677	0.3221	Flow meter	20/05/2013	0.3580	Flow meter	19/06/2013	0.3580	Flow meter	17/07/2013	0.2994	Flow meter	14/08/2013	0.4424	Flow meter	19/09/2013	0.1505	Flow meter	22/10/2013	0.1403	Flow meter	21/11/2013	0.1395	Flow meter	16/12/2013
SW12	453410	4468405	0.3995	Flow meter	20/05/2013	0.4182	Flow meter	19/06/2013	0.4182	Flow meter	17/07/2013	0.2284	Flow meter	14/08/2013	0.3715	Flow meter	19/09/2013	0.0769	Flow meter	22/10/2013	0.0773	Flow meter	21/11/2013	0.0719	Flow meter	16/12/2013
SW13	454846	4462112	0.0033	Flow meter	20/05/2013	0.0008	x	18/06/2013	0.0008	Flow meter	17/07/2013	0.0000	x	14/08/2013	0.0000	x	19/09/2013	0.0000	x	24/10/2013	0.0000	x	21/11/2013	0.0000	x	16/12/2013
SW14	454031	4462228	0.0000	x	20/05/2013	0.0034	x	19/06/2013	0.0034	Flow meter	17/07/2013	0.0059	Flow meter	14/08/2013	0.0055	x	19/09/2013	0.0026	Flow meter	23/10/2013	0.0067	Flow meter	21/11/2013	0.0000	x	16/12/2013
SW15	452712	4461214	0.0045	Flow meter	20/05/2013	0.0027	Flow meter	19/06/2013	0.0027	Flow meter	17/07/2013	0.0024	Flow meter	14/08/2013	0.0017	Flow meter	19/09/2013	0.0038	Flow meter	23/10/2013	0.0098	Flow meter	21/11/2013	0.0046	Flow meter	16/12/2013
SW16	447825	4460366	1.0753	x	20/05/2013	1.8928	Flow meter	19/06/2013	1.9828	Flow meter	17/07/2013	1.0698	Flow meter	14/08/2013	1.5121	Flow meter	19/09/2013	1.0753	Flow meter	23/10/2013	1.1649	Flow meter	21/11/2013	0.5121	Flow meter	16/12/2013
SW16A	450750	4461240	x	x	x	x	x	x	x	x	x	x	x	x	x	x	x	x	x	x	x	x	x	x	x	x
SW17	467566	4470600	0.0000	x	17/05/2013	0.0000	x	18/06/2013	0.0000	x	16/07/2013	0.0000	x	13/08/2013	0.0000	x	19/09/2013	0.0000	x	22/10/2013	0.0000	x	19/11/2013	0.0000	x	13/12/2013
SW18	466623	4469137	0.0036	Flow meter	17/05/2013	0.0000	x	18/06/2013	0.0000	x	16/07/2013	0.0000	x	13/08/2013	0.0000	x	19/09/2013	0.0000	x	22/10/2013	0.0000	x	19/11/2013	0.0000	x	13/12/2013
SW19	463839	4468540	0.0000	x	17/05/2013	0.0000	x	18/06/2013	0.0000	x	18/07/2013	0.0000	x	13/08/2013	0.0000	x	19/09/2013	0.0000	x	22/10/2013	0.0000	x	19/11/2013	0.0000	x	13/12/2013
SW20	465825	4465785	0.0146	Flow meter	17/05/2013	0.0079	Flow meter	18/06/2013	0.0079	Flow meter	16/07/2013	0.0124	Flow meter	13/08/2013	0.0101	Flow meter	19/09/2013	0.0114	Flow meter	22/10/2013	0.0064	Flow meter	19/11/2013	0.0048	Flow meter	13/12/2013
SW21	463484	4463464	0.0181	Flow meter	17/05/2013	0.0045	Flow meter	18/06/2013	0.0045	Flow meter	16/07/2013	0.0013	Flow meter	13/08/2013	0.0068	Flow meter	19/09/2013	0.0058	Flow meter	23/10/2013	0.0146	Flow meter	19/11/2013	0.0000	Flow meter	13/12/2013

Table 3.3. Catchment area of the surface water monitoring points and water structures

Type	Name/No	Total Area (km ²)	Uncontrolled Area (km ²)	Type	Name/No	Total Area (km ²)	Uncontrolled Area (km ²)
Dam	Akyar Dam	253.6	253.6	Surface Water Monitoring Point	SW9	1.62	1.62
	Eğrekkaya Dam	385.29	385.29		SW10	2.15	2.15
	Doğanözü Dam	953.93	315.04		SW11	893.35	138.72
	Çamlidere Dam	754.63	754.63		SW12	870.16	115.52
Gauging Station	Güdül (12-139)	2271.47	877.95		SW13	6.81	6.81
	Mandra (12-017)	884.05	245.17		SW14	24.44	24.44
Surface Water Monitoring Point	SW1	967.33	328.44		SW15	7.43	7.43
	SW2	36.32	36.32		SW16	2058.89	665.37
	SW3	6.75	6.75		SW16A	2044.19	650.67
	SW4	10.11	10.11		SW17	6.36	6.36
	SW5	8.6	8.6		SW18	8.29	8.29
	SW6	5.11	5.11		SW19	3.34	3.34
	SW7	2.1	2.1		SW20	0.88	0.88
	SW8	8.07	8.07		SW21	5.48	5.48

In the monitoring period of March 2012 – December 2013, the highest flow rates were observed between January – May due to the influence of both snowmelt and high rainfall. Also, highest flow rates have been seen in March or May at the monitoring points having small catchment areas and low flow rates. Some of these points (SW3, SW6, SW7, SW8, SW9, SW10 and SW13) had been dry when the instantaneous flow rate measurements were conducted in winter season (December 2012-March 2013). At the monitoring points which are located on the Kirmir and Pazar Streams having large catchment areas, the highest flow rates were measured in April 2012. At this month, measured flow rates were 5.44 m³/s and 8.08 m³/s at SW1 and SW16 that are at the upstream and downstream of the Kirmir Stream, respectively. After May, with decreasing precipitation in the summer, flow rates have been decreased significantly and creeks which have small catchment areas (all monitoring points except SW1, SW11, SW12 and SW16) have become dry. Also, SW6, SW7 and SW8 monitoring points are generally dry in all year round.

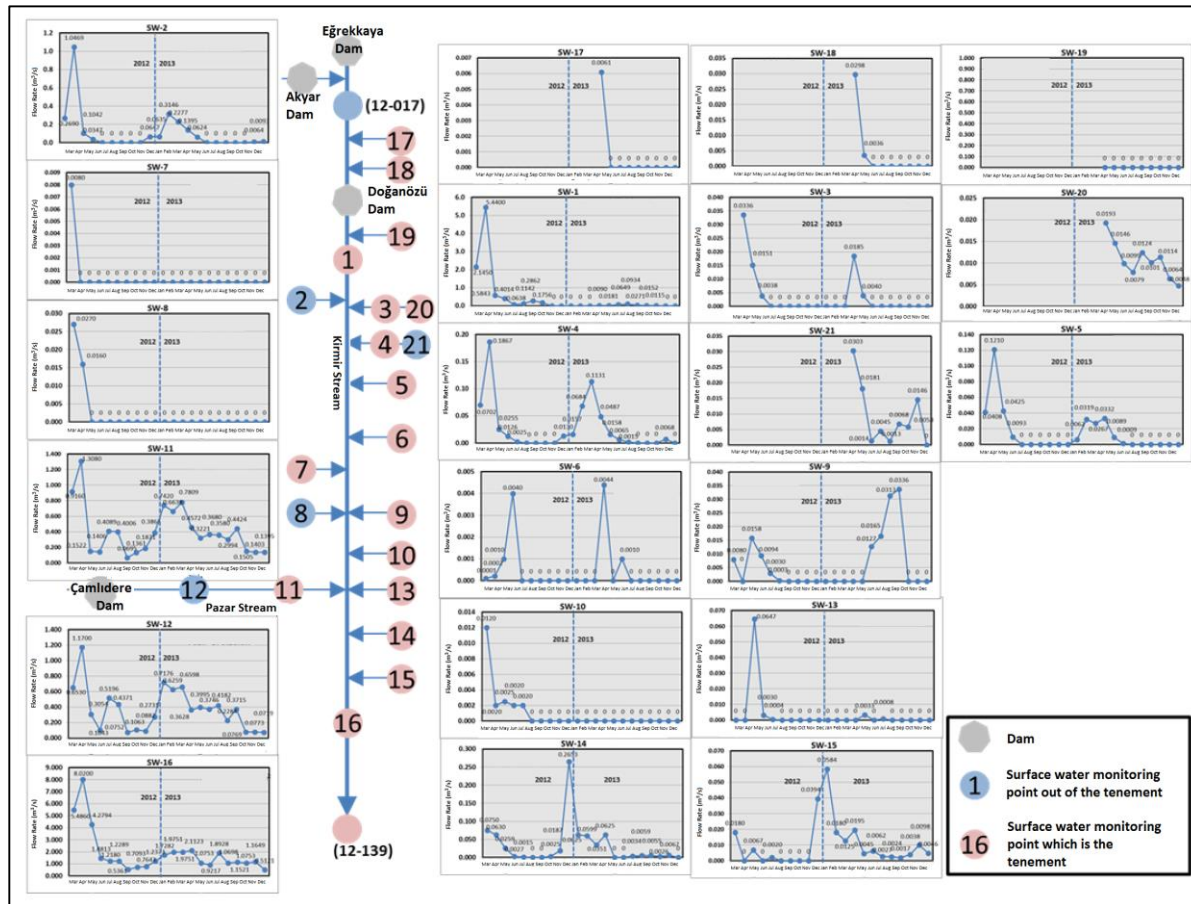


Figure 3.14. Instantaneous flow rate measurement values from surface water monitoring points

The observed increase in flow rates at monitoring points located on the Kirmir Stream (SW1, SW16) and Pazar Stream (SW11, SW12) in July and August months result from the dam operations. After the Doğanözü Dam had been started to hold water in November 2012, flow rates at SW1 were decreased significantly. In winter months SW1 was generally dry while flow rates increased at the other monitoring points. For example in March 2012 before the Doğazözü Dam started to hold water, the instantaneous flow rate at SW1 was $2.145\text{m}^3/\text{s}$ while it was dry in March 2013. By comparison, the flow rates at SW12 on the Pazar stream were almost the same in March 2012 and March 2013; thus, it is clear that the decrease of the flow rates at SW1 is caused by the Doğanözü Dam. Therefore, the flow rates in 2013 winter months were also decreased at SW16 monitoring point which is located on downstream of the Kirmir Stream.

SW20 and SW21 monitoring points which have small catchment areas and drain the area between Demirciören and Binkoz villages, flows have been also observed in the summer season. When the surface water flow measurements and spring locations are analyzed, the contribution from the groundwater system in the catchment areas of these monitoring points can be clearly seen. In order to investigate the springs in the catchment area of SW21 and its downstream SW4 monitoring points, a field study was conducted on 25 April 2013. In this survey, flow rate was measured as 30.3 L/s at SW21. It is understood that the sources of water at this location are the springs located in Hıdırdede and Gürpınar Hills which are on the upstream of SW21 location. Also it is learned that tap water of Binkoz village is taken from Aklan and İkiçörten fountains. In this field study, only a fountain (466130E, 4462400N) could be accessed due to the adverse road conditions and the discharge of this fountain was measured as 1.54 L/s (Figure 3.15). In summary, it is understood that, there is groundwater discharge contribution from highlands in the drainage basins of SW20 and SW21, and this flow decreases due to the infiltration along the streambed and artificial usage as SW3 and SW4 monitoring points are approached.



Figure 3.15. The fountain which was determined at the field study conducted on 25 April 2013

In order to analyze the relation between precipitation-temperature-runoff in the study area, instantaneous flow measurement values with daily precipitation and temperature values observed at Kızılcahamam (January 2012 – May 2013) and Binkoz (June 2013 – December 2013) meteorological stations are evaluated (Figure 3.16). The daily precipitation data of Kızılcahamam station in the period of January 2012 – May 2013 were converted to the representative data of the study area. In this analysis, unit flow data was obtained by normalizing the instantaneous flow measurement data of each monitoring points with the area of the catchment.

As it is seen in Figure 3.16-a, while daily average temperatures are generally below zero in January, February and beginning of March in 2012, they gradually increase after March. Although significant precipitation has not been observed after March 2012, flow rates significantly increase. According to this analysis, increase in flow rates results from the snowmelt. In 2013, temperature had been remaining below zero in only January. From all flow measurements in the study area, the highest flows are observed in February-March period due to the rainfall and snowmelt. SW4, SW5 (Figure 3.16-c), SW9, SW14, SW15 (Figure 3.16-e), SW20 (Figure 3.16-f) which are located in the study area and SW2 (Figure 3.16-e) which is located at the south of the tenements near Mahkemeağacı village have the highest instantaneous unit flow rates measured in monitoring period. The increase of flow

rates in the summer at SW9 indicates the artificial flow. The unit flow rates are generally quite low at the monitoring points located on the Kirmir and Pazar Streams, and reach the highest value in March-May period in 2012. In 2013, these values are lower than 2012. This is caused by having lower precipitation than 2012.



Figure 3.16. Daily precipitation and average temperature data of Kızılcahamam (January 2012-May 2013) and Binkoz (June 2012-December 2013) meteorological stations (a) and flow rates of surface water monitoring points (b-f)

In order to analyze the effect of the Doğanözü dam on the Kirmir Stream, daily flow rates of 12-017 gauging station which is located upstream of the Doğanözü dam and instantaneous flow rates of SW1 monitoring point which is located downstream of the Doğanözü Dam were compared (Figure 3.17). As can be seen in this figure, 12-017 gauging station and SW1 monitoring point flow data were compatible in March-April 2012. However after November 2012 when Doğanözü Dam started to hold water, flow rates at SW1 have been decreased or sometimes it was dry whereas

the flow rates at 12-07 gauging station increase occasionally. The other result which is obtained from this figure is that the measured flow rates in 2013 are lower than the values in 2012. This also indicates that 2013 is drier than 2012.

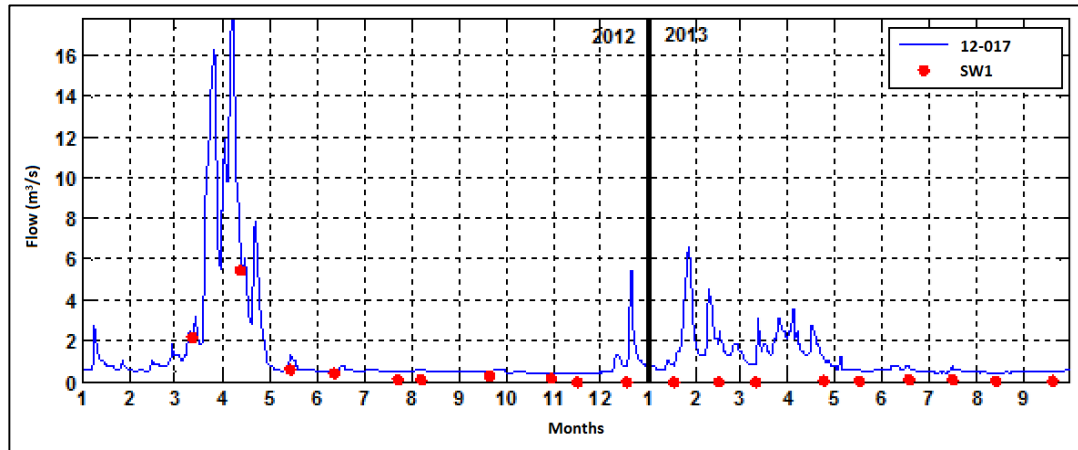


Figure 3.17. Comparison of flow rates at 12-07 and SW1

3.3. CONCEPTUAL WATER BUDGET OF THE STUDY AREA

Total precipitation which falls in an area decomposes into surface runoff, infiltration and evapotranspiration. For hydrologic water budget studies the ratio of these components to the total precipitation is calculated. Components of the hydrologic water budget for the study area were calculated for each month by using the long term average values. Evapotranspiration values and surface water runoff values were calculated by using Thornthwaite and Curve Number (CN) methods, respectively. Remaining portion of the total precipitation is accepted as infiltration.

In order to calculate the potential evapotranspiration by Thornwaite method, monthly average temperature values and latitude of the study area are needed. Long term monthly average temperature data of Kızılcıhamam meteorological station were used for the temperature values in the study area. Monthly potential evapotranspiration corrected according to Thornwaite method (UPET, mm/month) were calculated by this equality:

$$UPET_m = 16x \left(\frac{10t_m}{I} \right)^a \quad (3.1)$$

In this equality m is month index, t is monthly average temperature ($^{\circ}\text{C}$), I is annual temperature index and a is a coefficient depending on temperature index:

$$a = (675 \times 10^{-9})I^3 - (771 \times 10^{-7})I^2 + (179 \times 10^{-4})I + 0.492 \quad (3.2)$$

I is total of monthly temperature indexes, i :

$$i = \left(\frac{t}{5}\right)^{1.514} \quad (3.3)$$

In Curve Number (CN) method which is developed by Soil Conservation Service (SCS, 1964), surface runoff values are calculated in this way: a) direct surface water runoff (or excess precipitation), P_e is equal or less than total precipitation (P), b) soil water retention after the start of the surface runoff (F_a) is equal or less than soil water retention potential (S). Surface water run off can not be seen until the precipitation reaches a significant value (I_a , water retention before the start of water pond); thus potential surface runoff is $P - I_a$. According to Curve Number method, the ratios are equal between two real and two potential values which were identified above.

$$\frac{F_a}{S} = \frac{P_e}{P - I_a} \quad (3.4)$$

Also, according to principles of continuity:

$$P = P_e + I_a + F_a \quad (3.5)$$

By combining the equalities in 3.4 and 3.5, direct surface water runoff (or excess precipitation) is obtained:

$$P_e = \frac{(P - I_a)^2}{P - I_a + S} \quad (3.6)$$

Generally, with the data belonging to small catchment area $I_a = 0.2S$ equality is obtained empirically. According to this equality 3.6 is defined as:

$$P_e = \frac{(P - 0.2S)^2}{P + 0.8S} \quad (3.7)$$

This equation is general equation of the Curve Number method (Chow et al., 1988). Curve Number (CN), is obtained by a curve which is standardized by the relation between P and P_e of many basins. The relation of Curve Number (CN) and

potential soil water retention is defined as $CN:1000/(S+10)$, or $S(\text{inch})=(1000)/CN-10$. Curve Number (CN) can be used for calculation of the potential runoff for a specific soil type and soil cover when there is no soil freezing. High CN value indicates the high potential for surface water runoff. Curve Number varies according to vegetation and land use cover and hydraulic soil groups. Soil hydraulic groups are divided into 4:

- ❖ Group A: Well-drained, have low potential of runoff and high infiltration even if saturated soils (sand, gravel, silt etc.)
- ❖ Group B: Have moderate runoff potential and moderate infiltration soils (sandy loam)
- ❖ Group C: Have high runoff potential and low infiltration soils (clayey loam)
- ❖ Group D: Have very high runoff potential and low infiltration soils (plastic clay)

Land use/vegetation which is needed for calculation of Curve Number is obtained from 1/25000 scale The National Soil Database (NSDB). The soils in the study area have been accepted in Group B which has moderate runoff potential and moderate infiltration. Also, soil slope and depth information were used which are obtained from NSDB. The soils which are located on high slope and low depth is determined as Group C. Land use, vegetation and spatial distribution of hydraulic soil group for all catchment area of the surface water monitoring points were calculated by using a geographic information system. In the light of this information, weighted curve numbers were calculated for each sub-basin (Table 3.4). As calculated curve numbers change between 71 and 77, weighted value is determined as 74 for all sub-basins.

The Curve Number, which is calculated by the method described above, is used to determine the runoff that is formed according to the monthly precipitation. Monthly average precipitation values of the study area have been obtained by the correcting the Kızılcahamam meteorological station precipitation data (See Chapter 2.3.1.1). Thornthwaite method is used for the calculation of the potential evapotranspiration. The remaining part from the total precipitation is accepted as infiltration to groundwater. Consequently, components of the long term hydrologic

water budget have been obtained for each month conceptually as shown in Table 3.5. 1-6 rows in Table 3.5 show the calculation of potential evapotranspiration values with Thorntwaite method.

Table 3.4. Curve Number calculation for sub-basins

Sub-basin No.	Land Use/ Vegetation	Hydraulic Soil Group	CN	Area (km ²)	% Area	%Area x CN/100	Sub-basin CN
SW-2	Settlement	B	88	0.0451	0.12	0.11	71
	Settlement	C	90	0.1342	0.37	0.33	
	Settlement	C	90	0.0467	0.13	0.12	
	Forest	C	67	16.1419	44.45	29.78	
	Forest	C	67	1.8831	5.19	3.47	
	Forest	C	67	0.0167	0.05	0.03	
	Forest	C	67	0.0285	0.08	0.05	
	Forest	C	67	1.7696	4.87	3.26	
	Forest	C	67	0.3988	1.10	0.74	
	Heaths	C	75	7.2638	20.00	15.00	
	Heaths	C	75	1.3156	3.62	2.72	
	Heaths	C	75	3.8387	10.57	7.93	
	Heaths	C	75	0.1138	0.31	0.24	
	Heaths	C	75	0.5598	1.54	1.16	
	Heaths	C	75	0.5414	1.49	1.12	
	Heaths	C	75	0.2018	0.56	0.42	
	Meadow	C	88	0.2207	0.61	0.53	
	Meadow	C	88	0.3705	1.02	0.90	
	Meadow	C	88	0.1746	0.48	0.42	
	Meadow	C	88	0.1901	0.52	0.46	
Irrigated Farming	C	88	0.2037	0.56	0.44		
Irrigated Farming	B	78	0.3385	0.93	0.73		
Irrigated Farming	B	78	0.5187	1.43	1.17		
Forest	C	67	0.6876	11.73	7.86		
Heaths	C	75	3.9350	67.12	50.34		
Heaths	C	75	0.0354	0.60	0.45		
Heaths	C	75	0.6417	10.95	8.21		
Irrigated Farming	B	78	0.4888	8.34	6.50		
Irrigated Farming	B	78	0.0745	1.27	0.99		
SW-3	Settlement	C	90	0.0814	1.76	1.58	74
	Heaths	C	75	2.2202	47.93	35.95	
	Heaths	C	75	0.0007	0.02	0.01	
	Heaths	C	75	0.0009	0.02	0.01	
	Heaths	C	75	1.9554	42.22	31.66	
SW-4	Irrigated Farming	B	78	0.3732	8.06	6.29	76
	Settlement	C	90	0.0388	0.45	0.41	
	Settlement	B	88	0.0080	0.09	0.08	
	Heaths	C	75	6.8582	79.79	59.84	
	Heaths	C	75	0.4785	5.57	4.18	
SW-5	Heaths	C	75	0.4295	5.00	3.75	75
	Irrigated Farming	B	78	0.7711	8.97	7.00	
	Irrigated Farming	B	78	0.0108	0.13	0.10	
	Settlement	C	90	0.0305	0.60	0.54	
	Heaths	C	75	3.9902	78.10	58.58	
SW-6	Heaths	C	75	0.2112	4.13	3.10	76
	Heaths	C	75	0.5761	11.28	8.46	
	Meadow	C	88	0.2818	5.52	4.85	
	Irrigated Farming	B	78	0.0002	0.00	0.00	
	Irrigated Farming	B	78	0.0188	0.37	0.29	
	Settlement	C	90	0.0024	0.12	0.10	
	Heaths	C	75	1.6360	78.05	58.54	
SW-7	Heaths	C	75	0.3664	17.48	13.11	75
	Irrigated Farming	C	82	0.0913	4.35	3.57	
	Settlement	C	90	0.0280	0.35	0.31	
	Forest	C	67	0.6514	0.08	5.41	
SW-8	Forest	C	67	1.6190	20.07	13.45	73
	Forest	C	67	0.3794	4.70	3.15	
	Heaths	C	75	4.4383	55.02	41.26	
	Heaths	C	75	0.0881	1.09	0.82	
	Meadow	C	88	0.0725	0.90	0.79	
	Irrigated Farming	C	82	0.7631	9.46	7.76	
	Irrigated Farming	C	82	0.0273	0.34	0.28	

Sub-basin No.	Land Use/ Vegetation	Hydraulic Soil Group	CN	Area (km ²)	% Area	%Area x CN/100	Sub-basin CN
SW-9	Meadow	C	75	0.1577	9.84	7.38	75
	Meadow	C	75	0.1577	88.44	66.33	
	Meadow	C	88	0.0275	1.72	1.51	
SW-10	Meadow	C	75	0.5277	24.43	18.33	76
	Meadow	C	75	1.4332	67.00	50.25	
	Meadow	C	88	0.1833	8.57	7.54	
SW-13	Settlement	C	90	0.0715	1.05	0.95	75
	Meadow	C	75	2.7757	40.85	30.64	
	Meadow	C	75	0.0124	0.18	0.14	
	Meadow	C	75	3.8976	57.36	43.02	
SW-14	Meadow	C	88	0.0379	0.56	0.49	77
	Settlement	C	90	0.0628	0.26	0.23	
	Settlement	C	90	0.0619	0.25	0.23	
	Meadow	C	75	7.1114	29.12	21.84	
	Meadow	C	75	4.1147	16.85	12.64	
	Meadow	C	75	0.6946	2.84	2.13	
	Meadow	C	75	2.7052	11.08	8.31	
	Meadow	C	75	0.0656	0.27	0.20	
	Meadow	C	75	0.2526	1.06	0.78	
	Meadow	B	75	0.2534	1.04	0.78	
	Meadow	C	88	2.0605	8.44	7.42	
	Meadow	C	88	0.9406	5.85	5.59	
	Irrigated Farming	B	87	0.0165	0.07	0.06	
	Irrigated Farming	B	78	1.5676	6.42	5.01	
	Irrigated Farming	C	82	0.0255	0.10	0.09	
	Irrigated Farming	C	82	1.1224	4.60	3.77	
	Irrigated Farming	B	78	0.7864	3.22	2.51	
Irrigated Farming	B	78	0.0474	0.19	0.15		
SW-15	Meadow	C	75	0.0031	0.04	0.08	75
	Meadow	C	75	2.6173	35.25	26.43	
	Meadow	C	75	1.0417	14.08	10.52	
	Meadow	C	75	1.1547	15.55	11.66	
	Meadow	C	75	2.1121	28.44	21.33	
SW-17	Irrigated Farming	C	82	0.0618	1.10	0.90	71
	Irrigated Farming	C	82	0.4150	5.59	4.58	
	Settlement	C	90	0.0414	0.65	0.59	
	Forest	C	67	1.7354	27.31	18.29	
	Forest	C	67	2.3606	37.14	24.89	
	Meadow	C	75	1.6691	26.26	19.70	
SW-18	Meadow	C	75	0.0141	0.22	0.17	73
	Meadow	C	75	0.0685	1.08	0.81	
	Meadow	B	69	0.0770	1.21	0.84	
	Meadow	B	85	0.3894	6.13	5.27	
	Forest	C	67	1.9557	23.64	15.84	
	Meadow	C	75	0.0002	0.00	0.00	
	Meadow	C	75	4.6772	56.54	42.40	
SW-19	Meadow	C	75	0.2795	5.58	2.58	76
	Meadow	C	75	1.3275	16.06	12.05	
	Meadow	C	88	0.0827	0.39	0.55	
	Settlement	B	88	0.0817	2.44	2.15	
	Forest	C	67	0.3950	11.82	7.92	
	Meadow	C	75	0.6700	20.04	15.03	
	Meadow	C	75	0.0815	2.44	1.83	
SW-20	Meadow	C	75	0.8123	24.30	18.23	74
	Irrigated Farming	B	78	1.2615	37.74	29.44	
	Irrigated Farming	B	78	0.0407	1.22	0.95	
	Forest	C	67	0.0863	9.86	6.61	
	Meadow	C	75	0.5839	66.73	50.05	
SW-21	Meadow	C	75	0.0809	9.25	6.93	75
	Meadow	C	75	0.1239	14.16	10.62	
	Meadow	C	75	3.8332	70.01	52.51	
	Meadow	C	75	0.1402	2.56	1.92	
	Meadow	C	75	0.0078	0.14	0.11	
Meadow	C	75	1.4764	26.96	20.22		
Meadow	C	75	0.0179	0.33	0.25		

Table 3.5. Monthly conceptual water budget of the study area

Row No.	Parameters	Jan	Feb	Mar	Apr	May	Jun	Jul	Aug	Sep	Oct	Nov	Dec	Total	Ratio to Precipitation (%)	
1	Monthly Average Temperature (°C)	-1.0	0.0	4.1	9.3	13.9	17.8	21.1	20.8	16.2	10.8	5.0	1.1			
2	i	0.00	0.00	0.75	2.54	4.72	6.82	8.87	8.65	5.95	3.20	0.99	0.10	42.59		
3	a;	1.2	1.2	1.2	1.2	1.2	1.2	1.2	1.2	1.2	1.2	1.2	1.2	14.4		
4	UPET	0.00	0.00	15.39	39.59	63.79	84.73	103.73	101.73	76.23	47.23	19.17	3.36	554.95		
5	PET	0.00	0.00	15.85	43.94	79.10	105.92	131.73	120.04	79.28	45.34	15.91	2.72	639.83		
6	r: monthly correction coefficient	0.84	0.83	1.03	1.11	1.24	1.25	1.27	1.18	1.04	0.96	0.83	0.81			
7	Precipitation (mm)	58.8	41.6	33.6	38.6	37.2	27.3	14.1	10.4	9.1	31.2	31.2	59.7	392.8		
8	Coefficient of Surface Runoff	1	1	1	1	1	1	0	0	0	1	1	1			
9	Surface Runoff (mm)	12.88	4.99	2.36	3.91	3.45	0.91	0.00	0.00	0.00	1.74	1.74	13.36			
10	Infiltration (I)	45.92	36.61	31.24	34.69	33.75	26.39	14.10	10.40	9.10	29.46	29.46	46.34			
11	I-PET	45.92	36.61	15.38	-9.26	-45.34	-79.52	-117.63	-109.64	-70.18	-15.87	13.55	43.62			
12	TOTAL (P-PET)	0.00	0.00	0.00	-9.26	-54.60	-134.12	-251.76	-361.39	-431.57	-447.45	0.00	0.00			
13	Soil Moisture	100.00	100.00	100.00	91.16	57.92	26.16	8.07	2.69	1.34	1.14	14.69	58.30			
14	Change of Soil Moisture	-4.22	36.61	9.31	-8.84	-33.23	-31.77	-18.09	-5.37	-1.36	-0.2	13.55	43.62			
15	AET	0.00	0.00	15.85	43.53	66.98	58.17	32.19	15.77	10.46	29.66	15.91	2.72	291.25	74%	
16	Excess Precipitation (I-AET)	63.02	4.99	8.43	3.91	3.45	0.91	0.00	0.00	0.00	1.74	1.74	13.36	101.55		
17	Surface Runoff	12.88	4.99	2.36	3.91	3.46	0.91	0.00	0.00	0.00	1.74	1.74	13.36	45.34	12%	
18	Infiltration	50.14	0.00	6.07	0.00	0.00	0.00	0.00	0.00	0.00	0.00	0.00	0.00	56.21	14%	
														Total	392.80	100%

In this table, monthly potential evapotranspiration value (PET) is obtained from UPET value which is calculated in Equality (3.1) by correction with r coefficient according to the longitude of the study area (40°). Runoff values was obtained by using monthly total precipitation (P) and curve number (CN=74) by the help of (3.7) equality. The difference between monthly total precipitation and surface runoff is equal to infiltration (I). Soil water storage (moisture) value was accepted as 100 mm and for each month change in water storage (moisture) value was calculated. By the help of these values, evapotranspiration (AET), surface runoff and groundwater recharge values were calculated. In addition, the sensitivity to the conceptual model of the value of the soil water storage was analyzed. When soil water storage value is accepted as 80 mm, 100 mm and 120 mm, the ratio of infiltration to total precipitation changes as 19%, 14% and 10%, respectively. According to the conceptual water budget which is presented in Table 3.5, 74%, 12% and 14% of annual precipitation are converted to evaporation, surface runoff and infiltration, respectively (Table 3.6).

Table 3.6. Annual water budget results

Hydrologic Component	Amount (mm/year)	Ratio to Annual Precipitation (%)
Precipitation	392.8	100
Evaporation	291.3	74
Surface Runoff	45.3	12
Infiltration	56.2	14

Annual conceptual water budget given above can be checked by using continuous observations (for example precipitation and surface runoff). For this reason, ratio of surface runoff to precipitation for 2013 was calculated. In this calculation precipitation values of the study area in the period of January-May 2013 had been obtained by the correction of the Kızıcahamam meteorological station precipitation data (See Chapter 2.3.1.1). The precipitation values in the period of

June-December 2013 were obtained from the Binkoz meteorological station. Because there is not any gauging station, the monthly instantaneous flow rates of monitoring stations have been accepted as the representative values of the study area. Annual unit surface runoff values of the monitoring points located in the southern part of the Kirmir Stream were calculated (Table 3.7). Flow rates of SW9 monitoring point were not used in calculation because these values show difference from the values measured in other monitoring stations. As can be seen in Table 3.7, surface runoff of the study area in 2013 is 29.25 mm. While considering the total precipitation of the study area in 2013 is 295 mm, it is thought that the 10% of total precipitation turn into surface runoff. These values are consistent with the ratio of surface runoff to annual precipitation of the conceptual water budget which is presented in Table 3.6. Reliability of the water budget calculation will increase with the continuous surface runoff observations in the study area.

Table 3.7. Calculation of total unit surface runoff of the study area in 2013

	SW3	SW4	SW5	SW6	SW10	SW13	SW14	SW15	Total
Unit Surface Runoff (mm)	8.90	70.97	32.26	2.74	0.00	1.61	25.85	50.89	193.02
Area (km²)	6.75	10.11	8.60	5.11	2.15	6.81	24.44	7.43	71.40
Area Weighted Surface Runoff(mm)	0.82	10.05	3.89	0.20	0.00	0.15	8.85	5.30	29.25

3.4. EXISTING AND PLANNED WATER STRUCTURES

The most important surface water unit in the study area is Kirmir Stream. Kirmir Stream is named as Hamam Stream at the upstream of the Doğanözü village. The second important surface water unit is the Pazar Stream which joins the Kirmir Stream at the southern side of the Çeltikçi village. Both Kirmir Stream and Pazar Stream are controlled by important water structures at the upstream of the study area (Figure 3.1, Table 3.8). Kirmir Stream is controlled by three dams which are Akyar Dam on Bulak Stream, Eğrekkaya Dam on Sey Creek and Doğanözü Dam on Kirmir

Stream. These dams supply water for human consumption to Ankara Metropolitan Municipality. In addition, Çamlıdere Dam which is located on the Pazar Stream has the biggest reservoir volume (1226 hm³) in the vicinity of the study area and also it supplies water for human consumption to Ankara Metropolitan Municipality. In order to supply water to Ankara city, these dams store a significant amount of water flow in Kirmir and Pazar Streams, causing dewatering of the streams at downstream of the dams.

Thus, Doğanözü Dam is used for irrigating the lands at both sides of the Kirmir Stream between Doğanözü village and Beypazarı town. As can be seen in Figure 3.1, the pipeline which transmits water from the Çamlıdere Dam to Ankara passes through the project site in north-south direction. Also, Doğanözü Dam irrigation pipeline passes through the study area along the Kirmir Stream. All these pipelines should be considered in mine planning. Stored water in Eğrekkaya, Akyar and partly Doğanözü Dams have been transmitted to Kurtboğazı Dam with water-distribution pipelines. Some parts of the tenements at the eastern side of the study area are located in the catchment of the Kurtboğazı Dam. Kurtboğazı Dam is the other important dam which transmits water to Ankara Metropolitan Municipality. The other important water structure in the vicinity of the study area is Asartepe Dam which is located on İlhan River near the Ayaş town and it is used for irrigation purposes (Table 3.8).

Table 3.8. Information of the dams which are located in the vicinity of the study area

Name	Location	Stream Name	Operation Year	Purpose	Reservoir Volume (hm ³)	Irrigation Area (ha)	Supply Water for Human Consumption (hm ³ /year)	Distance to the Study Area (km)
Doğanözü Dam	Doğanözü	Kirmir Stream	2013	Irrigation + Human	32.7	2777	25	0.7
Çamlıdere Dam	Çamlıdere	Bayındır Stream	1985	Human Consumption	1226	-	142	4.6
Eğrekkaya Dam	Kızılcahamam	Sey Creek	1992	Human Consumption	113	-	79	13.5
Akyar Dam	Kızılcahamam	Bulak Stream	2001	Human Consumption	56	-	45	23.5
Kurtboğazi Dam	Kazan	Kurt Creek	1967	Irrigation + Human	96.9	2800	60	4.1
Kavşakkaya Dam	Kazan	Ova Stream	2007	Human Consumption	64	-	58	18.2
Asartepi Dam	Ayaş	İlhan Stream	1980	Irrigation	20	1500	-	13.4
Güldürcek Dam	Çankırı-Orta	Yazı Stream	1988	Irrigation	53	6200	-	30.1

There are 9 ponds in the study area (Table 3.9). These are used for irrigation purposes and the closest pond to the study area is Çeştepe pond (1.9 km).

In addition, there are two water structures in planning stage (Table 3.10). Uruş Dam will be constructed at the southern side of Beypazarı and it will be used for both irrigation and human consumption. Kınık pond will be established at the northwest of the Çeltikçi and it will be used for irrigation purposes.

Table 3.9. Information of the ponds which are located in the vicinity of the study area

No.	Name	Location	Creek Name	Operation Year	Purpose	Reservoir Volume (hm ³)	Irrigation Area (ha)	Distance to the Study Area (km)
1	Kırköy Pond	Kızılcahamam	Eneğim Creek	1982	Irrigation	0.304	64	8.7
2	Üçbaş Pond	Kızılcahamam	Kavgalının Creek	1968	Irrigation	0.428	76	5.4
3	Çeştepe Pond	Kızılcahamam	Bostan Creek	1985	Irrigation	0.392	143	1.9
4	İğdir Pond	Kızılcahamam	Kayacık Creek	1986	Husbandry Irrigation	0.033	15	2.7
5	Örencik Pond	Kazan	Karanlık Creek	1996	Irrigation	0.2	31	6.8
6	Karagüney Pond	Kızılcahamam	Karagüney Creek	1983	Irrigation	0.505	131	6.2
7	Aşağıkaraören Pond	Kızılcahamam	Kuzoğlu Creek	1978	Irrigation	0.213	49	10.6
8	Aşağıhöyük Pond	Çeltikçi	Ak Creek	1995	Irrigation	0.201	3	6.1
9	Çanlılı Pond	Ayaş	İlhan Stream	1992	Irrigation	0.642	142	9.4

Table 3.10. Information of the dam/pond which are located in the vicinity of the study area

No.	Name	Creek Name	Start-Finish Date	Purpose	Reservoir Volume (hm ³)	Irrigation Area (ha)	Irrigation Area (ha)	Distance to the Study Area (km)
Uruş Dam	Beypazarı	Hamamözü Stream	2014-?	Irrigation + Human Consumption	27.86	2149	?	27.3
Kınık Pond	Çeltikçi	Kavacık Creek	2012-2014	Irrigation	0.602	238	-	11.2

CHAPTER 4

HYDROGEOLOGY

4.1. WATER POINTS

4.1.1. Surface Waters

Kirmir Stream and Pazar Stream are the important surface waters in the study area. Kirmir Stream flows in the direction of north east to south west near the Doğanözü village and Pazar Stream flows from north to south near the Çeltikçi town. These streams join with each other at the southeastern side of the Çeltikçi town and their total watershed area is approximately 2000 km². Both of them are controlled by the water structures which are located at the upstream of the study area. Doğanözü, Eğrekkaya and Akyar Dams control the Kirmir Stream and Çamlıdere Dam controls the Pazar Stream.

Mandra (12-017), Güdül (12-139), Saray (12-030) and Derince (12-081) are the stream gauging stations that are located in the vicinity of the study area. These are operated by the Turkish State Water Works (DSİ) and Electrical Power Resources Survey and Development Administration (EİEİ). In addition to these stations, 21 surface water monitoring points were established to determine the runoff potential in the study area. Monthly instantaneous flow measurements have been conducted at these monitoring points between May 2012 and December 2013. Distribution of the drainage areas in the vicinity of the study area is presented in Figure 4.1.

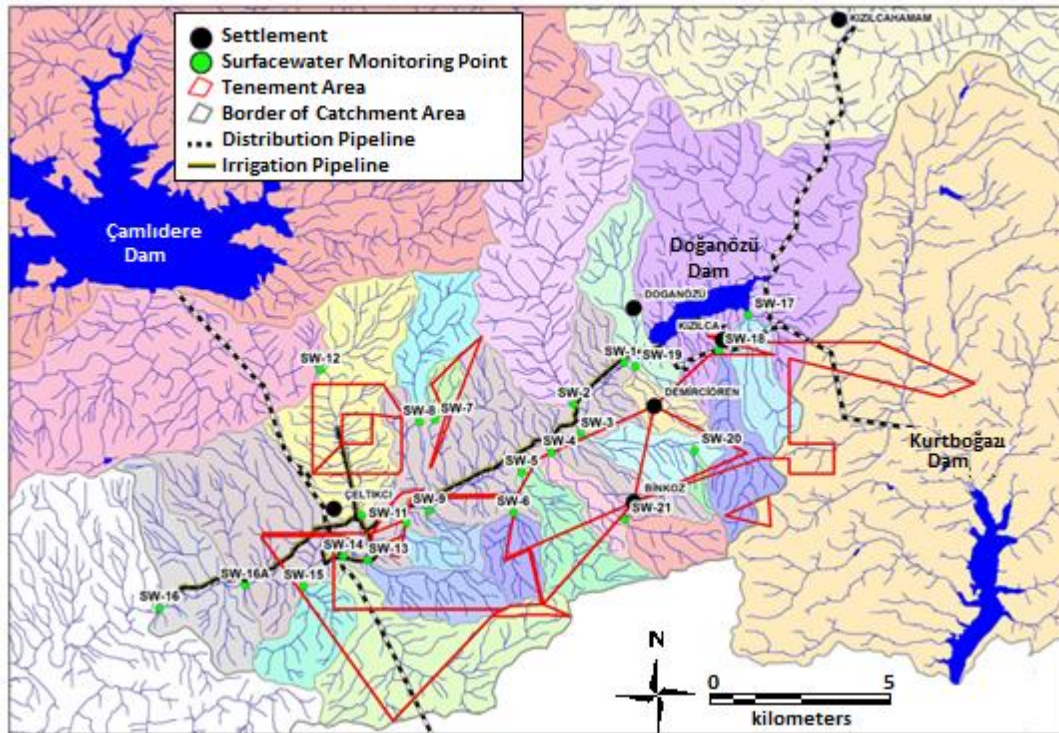


Figure 4.1. Distributions of the drainage areas, water structures and surface water monitoring points

4.1.2. Springs and Fountains

Field studies were conducted in February 2012 and February 2013 to survey the existing springs and fountains in the study area and its vicinity. In total, 44 fountain locations were determined at these studies. These fountains are connected to springs to supply water to villages. Figure 4.2-Figure 4.3 show the locations of the springs on topographic and geological maps, respectively. Information regarding coordinates, elevations, discharges and the name of the host formation are listed in Table 4.1.

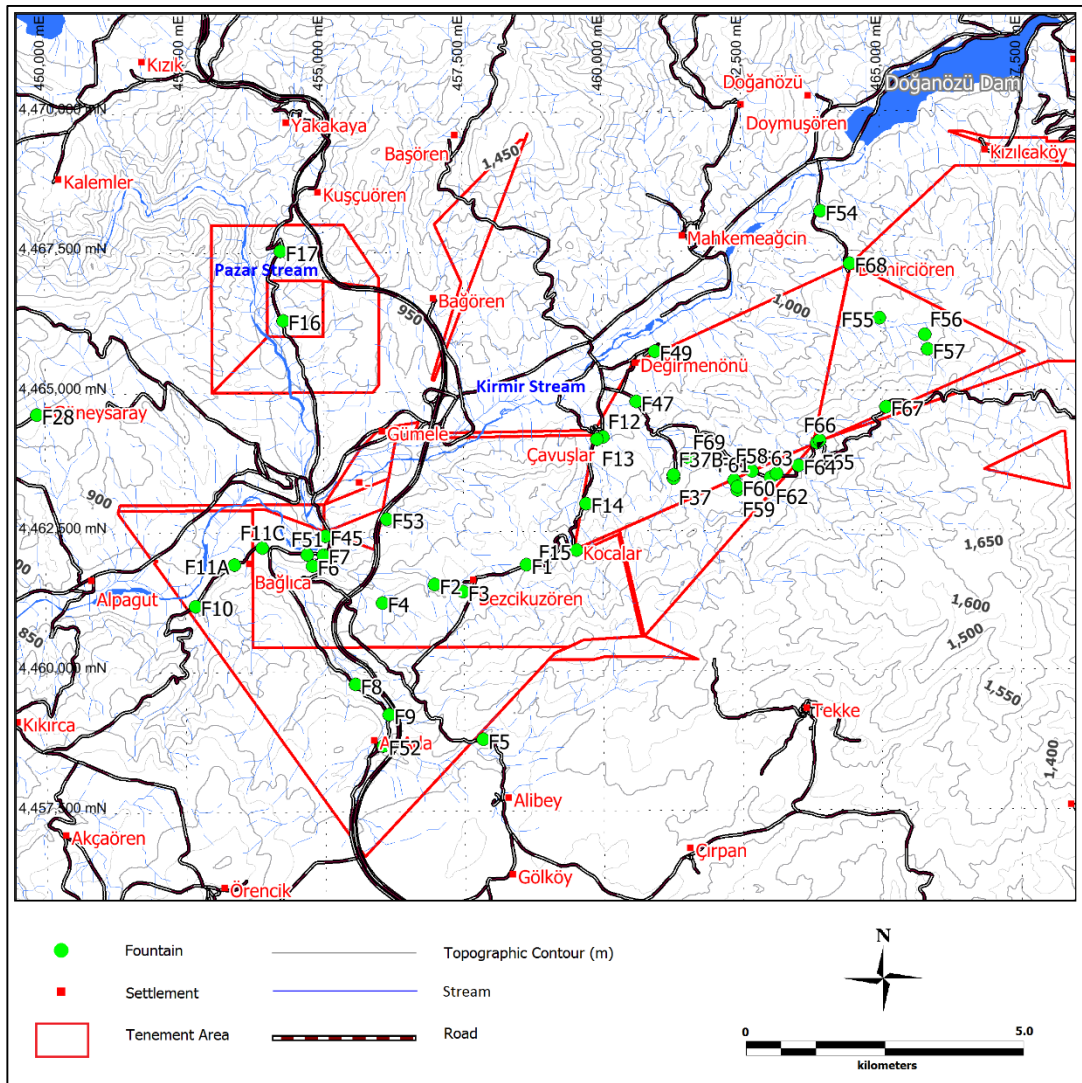


Figure 4.2. Fountain locations on the topographic map

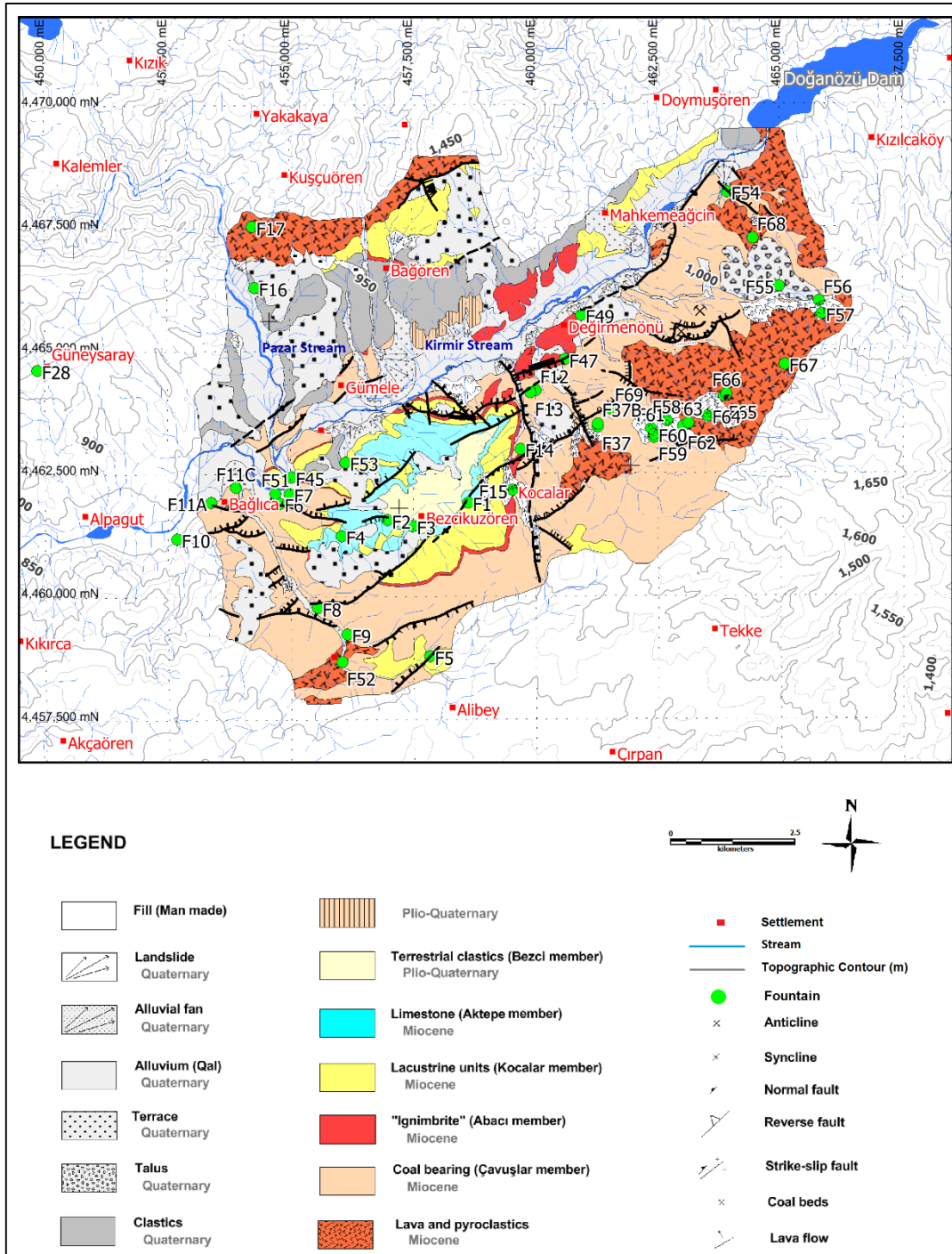


Figure 4.3. Fountain locations on the geological map

Table 4.1. Information of springs in the study area

Monitoring Points	Easting (m)	Northing (m)	Elevation (m)	Lithologic Unit	Quantity (L/s)		
					Minimum	Maximum	Average
F1	458621	4461908	1090	Aktepe member	0.02	0.08	0.06
F2	456969	4461556	1006	Aktepe member	0.08	0.25	0.15
F3	457483	4461431	1024	Aktepe member	0.05	1.45	0.23
F4	456040	4461236	948	Aktepe member	0.10	0.34	0.23
F5	457832	4458783	1090	Kocalar member - Çavuşlar member	0.02	1.68	0.23
F6	454784	4461905	823	Çavuşlar member	0.01	0.06	0.03
F7	454978	4462099	797	Çavuşlar member	0.01	0.05	0.03
F8	455540	4459778	924	Çavuşlar member	0.13	0.27	0.20
F9	456141	4459238	985	Çavuşlar member - Volcanics	0.04	0.09	0.07
F10	452684	4461189	783	?	0.03	0.18	0.08
F11A	453382	4461931	798	Çavuşlar member	0.02	0.10	0.04
F11C	453888	4462232	812	Çavuşlar member	0.04	0.18	0.12
F12	460012	4464187	895	Çavuşlar member	0.05	0.41	0.20
F13	459903	4464144	893	Çavuşlar member	0.03	0.63	0.29
F14	459699	4462994	964	Çavuşlar member	0.00	0.84	0.24
F15	459524	4462160	1056	Çavuşlar member - Abacı member - Kocalar member	0.00	0.49	0.23
F16	454280	4466292	831	?	0.01	1.52	0.19
F17	454243	4467531	895	?	0.00	1.46	0.80
F28	449845	4464638	998	?	2.33	16.87	7.59
F45	455017	4462435	798	Çavuşlar member - Kocalar member	0.03	0.19	0.08
F51	454691	4462106	792	Çavuşlar member - Kocalar member	0.00	0.32	0.18
F52	456035	4458678	980	Volcanics	0.14	1.95	0.83
F53	456117	4462735	874	Kocalar member	0.07	0.29	0.14
F37	461268	4463440	1035	Çavuşlar member	0.00	0.05	0.04
F37B	461268	4463500	1027	Çavuşlar member	0.00	0.27	0.11
F46	457530	4461592	1039	Aktepe member	-	-	0.08
F47	460609	4464813	880	Çavuşlar member	0.00	0.45	0.19
F49	460943	4465714	841	Çavuşlar member	0.06	0.22	0.14
F54	463925	4468208	900	Çavuşlar member - Volcanics	0.00	0.35	0.19
F55	464981	4466294	1102	Volcanics	0.10	1.52	0.69
F56	465792	4465988	1161	Volcanics	0.01	0.23	0.06
F57	465841	4465728	1200	Volcanics	0.04	0.31	0.14
F58	462679	4463557	1137	Çavuşlar member	0.10	0.96	0.43
F59	462413	4463223	1153	Çavuşlar member	0.10	0.41	0.21
F60	462420	4463283	1146	Çavuşlar member	0.00	0.00	0.00
F61	462356	4463400	1136	Çavuşlar member	0.18	0.42	0.29
F62	463008	4463445	1157	Volcanics	0.00	0.00	0.00
F63	463127	4463516	1164	Volcanics	0.05	0.07	0.06
F64	463516	4463658	1190	Volcanics	0.02	0.10	0.05
F65	463851	4464064	1239	Volcanics	0.12	1.89	0.51
F66	463901	4464106	1244	Volcanics	0.02	0.41	0.12
F67	465092	4464703	1394	Volcanics	0.00	0.24	0.11
F68	464449	4467268	1040	Volcanics	0.25	0.51	0.31
F69	461531	4463814	1031	Çavuşlar member	0.07	0.09	0.08

Discharge rates of all fountain monitoring points have been measured once a month regularly to observe the seasonal changes. Minimum, maximum and average discharge rates of the springs are summarized in Table 4.2. Temporal changes of the spring discharge rates and the relation to the precipitation observed in the study area can be seen in Figure 4.4. The monthly precipitation data in this figure after 24.05.2013 represent the precipitation data observed at Binkoz meteorological station. Before this date, the daily precipitation data of the Kızılcahamam meteorological station had been converted to the daily precipitation series by using the monthly percent error rate between Çeltikçi and Kızılcahamam stations (See Chapter 2.3.1.1).

Generally, in the study area discharge rates of the springs are not too much except F28. Average discharge rate of this fountain, which is located at the eastern side of the Pazar Stream, is 7.59 L/s. Discharge rates of the other fountains in the study area changes between 0.03 and 0.83 L/s. No flow was observed at F60 and F62 during the whole monitoring period. Only one measurement has been conducted at F46. As can be seen in Figure 4.4, discharge rates reach the highest value in the spring months while they decrease or dry out in summer months.

Table 4.2. Flow rates of the fountains vicinity of the study area

Monitoring Points	Quantity (L/s)			Monitoring Points	Quantity (L/s)		
	Minimum	Maximum	Average		Minimum	Maximum	Average
F1	0.02	0.08	0.06	F53	0.07	0.29	0.14
F2	0.08	0.25	0.15	F37	0.00	0.05	0.04
F3	0.05	1.45	0.23	F37B	0.00	0.27	0.11
F4	0.10	0.34	0.23	F46	-	-	0.08
F5	0.02	1.68	0.23	F47	0.00	0.45	0.19
F6	0.01	0.06	0.03	F49	0.06	0.22	0.14
F7	0.01	0.05	0.03	F54	0.00	0.35	0.19
F8	0.13	0.27	0.20	F55	0.10	1.52	0.69
F9	0.04	0.09	0.07	F56	0.01	0.23	0.06
F10	0.03	0.18	0.08	F57	0.04	0.31	0.14
F11A	0.02	0.10	0.04	F58	0.10	0.96	0.43
F11C	0.04	0.18	0.12	F59	0.10	0.41	0.21
F12	0.05	0.41	0.20	F60	0.00	0.00	0.00
F13	0.03	0.63	0.29	F61	0.18	0.42	0.29
F14	0.00	0.84	0.24	F62	0.00	0.00	0.00
F15	0.00	0.49	0.23	F63	0.05	0.07	0.06
F16	0.01	1.52	0.19	F64	0.02	0.10	0.05
F17	0.00	1.46	0.80	F65	0.12	1.89	0.51
F28	2.33	16.87	7.59	F66	0.02	0.41	0.12
F45	0.03	0.19	0.08	F67	0.00	0.24	0.11
F51	0.00	0.32	0.18	F68	0.25	0.51	0.31
F52	0.14	1.95	0.83	F69	0.07	0.09	0.08

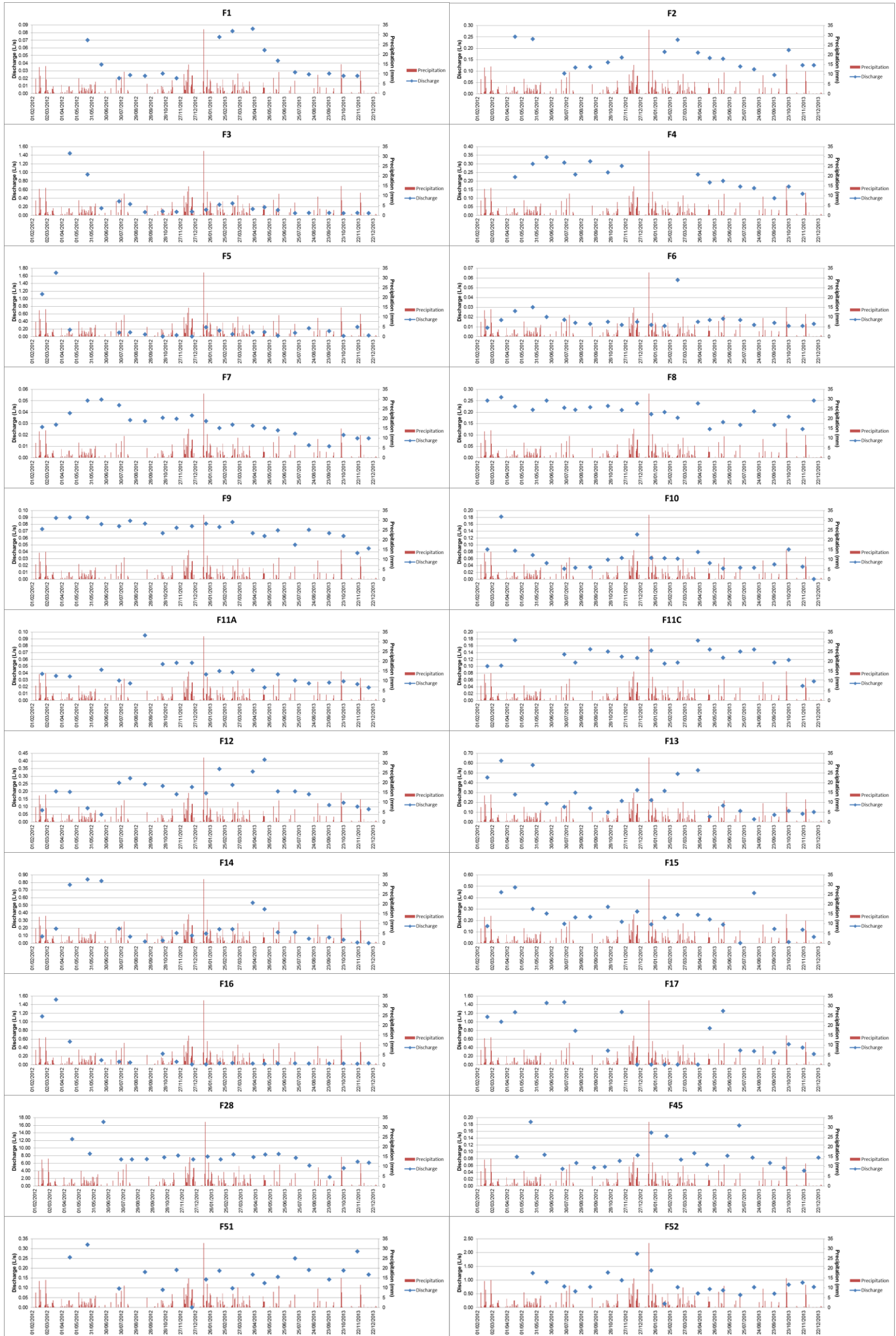


Figure 4.4. Variations of the discharge rates of the fountains

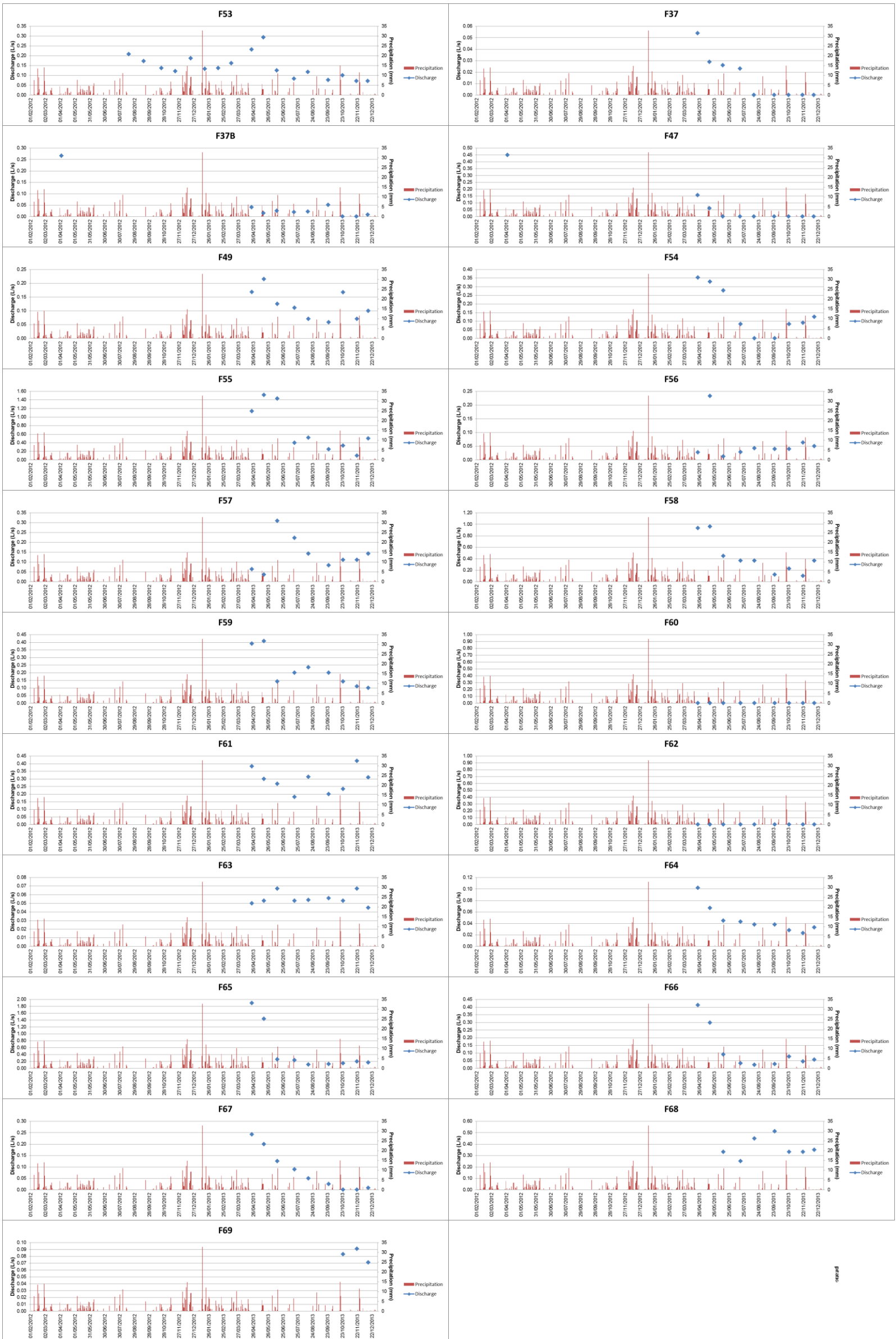


Figure 4.4. (continued)

4.1.3. Wells

Wells located within the study area can be analyzed in four groups. These are: (i) wells which were opened by The Bank of Provinces, (ii) water wells in villages (iii) monitoring wells and (iv) pump wells. Locations of these wells are presented in Figure 4.5.

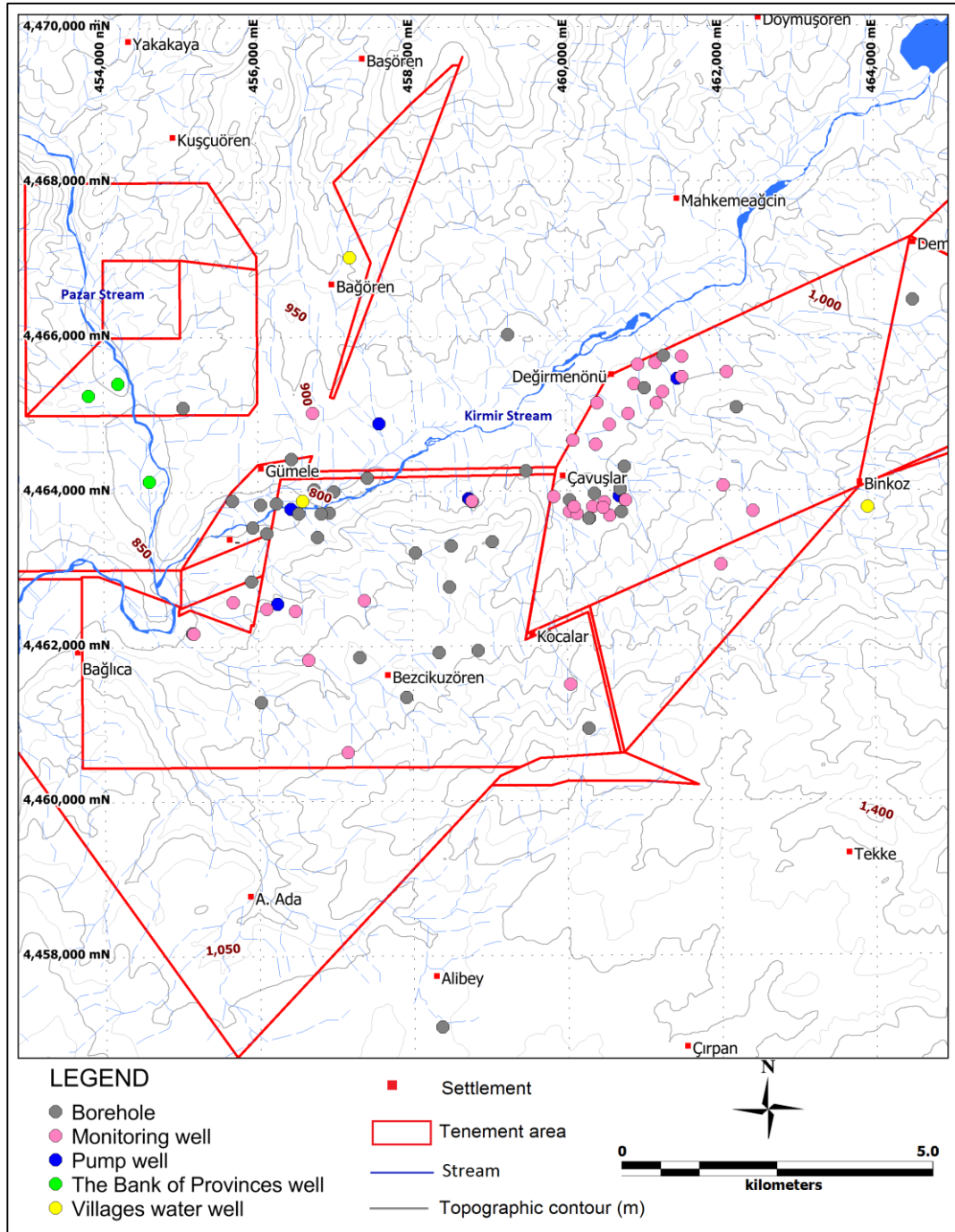


Figure 4.5. Location map of the wells in the study area

4.1.3.1. The Bank of Provinces Wells

In the study area, three wells were opened by The Bank of Provinces in 2007 to supply water to the Çeltikçi town, but these are not currently in use. General information (coordinates, depth, static water level, screen interval etc.) of these wells can be seen in Table 4.3. The results of the pumping tests conducted by the Bank of Provinces were re-evaluated in Chapter 4.2.1.

Table 4.3. Information of the Bank of Provinces Wells

Well ID	Easting (m)	Northing (m)	Elevation (m)	EOH (m)	Screen Top (m)	Screen Bottom (m)	Total Screen Length (m)	Taped Formation	Static Water Level (m)	Dynamic Water Level (m)	Yield (L/s)
L1	453806	4465254	821	42	14	35	13	Alluvium	10,5	30,5	2,5
L2	454189	4465407	810	32	10	18	8	Alluvium	3,6	14,5	4,0
L3	454593	4464137	800	27	10	18	8	Blocky Alluvium	3,2	12,0	4,5

4.1.3.2. Water Wells in Villages

There are water wells in Gümele, Bağören and Binkoz villages. These wells were opened to supply water to these villages. However, the well in Binkoz village is not in use.

4.1.3.3. Monitoring Wells

In the scope of the mining activities, a total of 76 exploration drilling has been conducted in the study area (Figure 4.5). Forty two of these exploration boreholes have been converted to monitoring wells to define hydrogeological conditions and hydraulic parameters, and measure water level, flow discharge and water quality parameters in the study area. Seven of them were completed in 2012, and the remaining 35 of them were completed in 2013. Locations of these wells are presented in Figure 4.6 and well details are listed in Table 4.4. The decision of the which exploration hole would be converted to a monitoring well has been taken by considering the target geological formation, coal bearing units, estimated hydraulic pressure, structural and topographical conditions and border of the tenement areas. The locations of these wells on geological map are also given in Figure 4.7. The monitoring wells are completed either with galvanized steel, PPRC (PoliPropilen

Random Copolymer) or PVC casing and screen after washing them with clean water. Following the gravel pack installment, the borehole annular space made impermeable with bentonite layer.

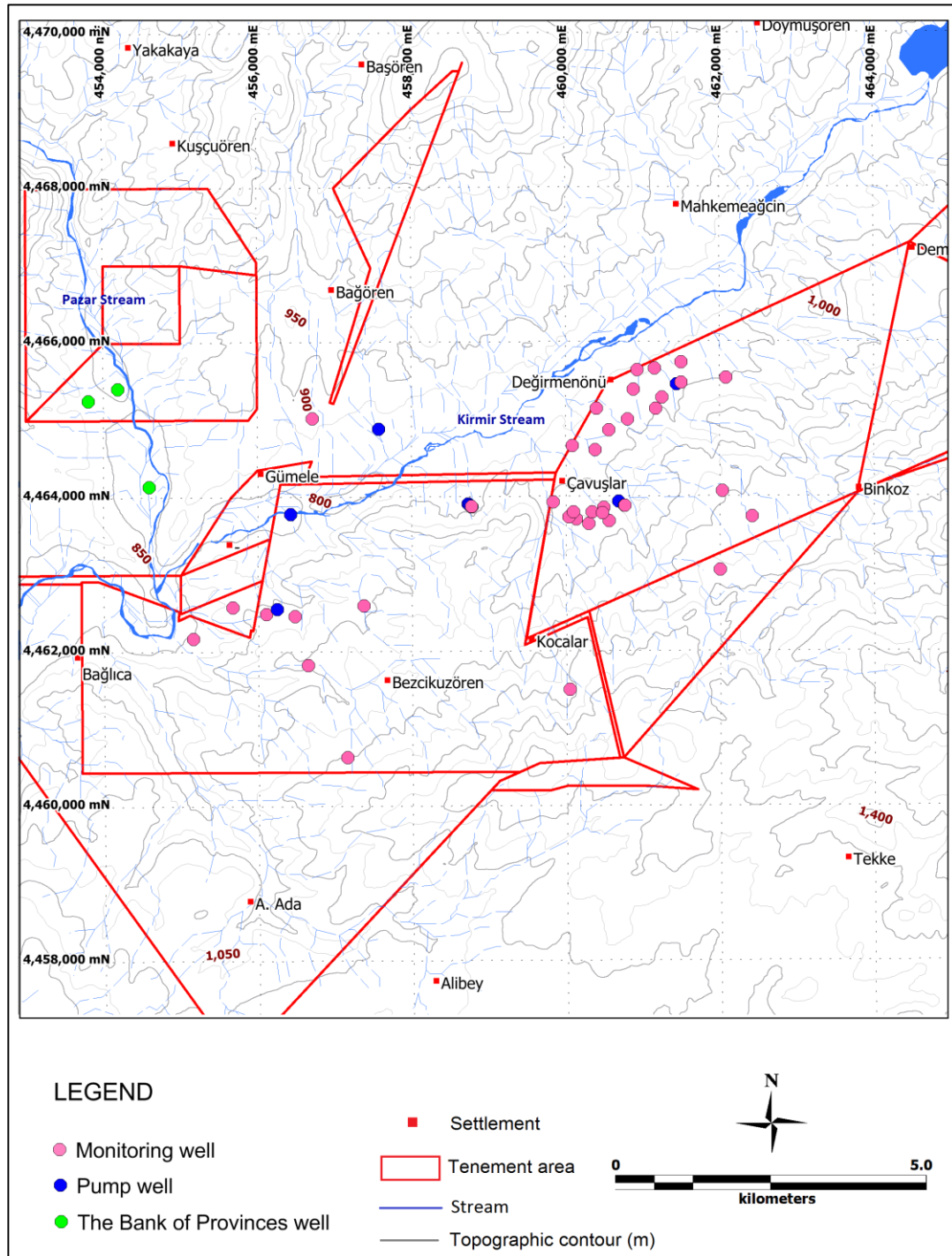


Figure 4.6. Monitoring wells, pump wells and The Bank of Provinces wells in the study area

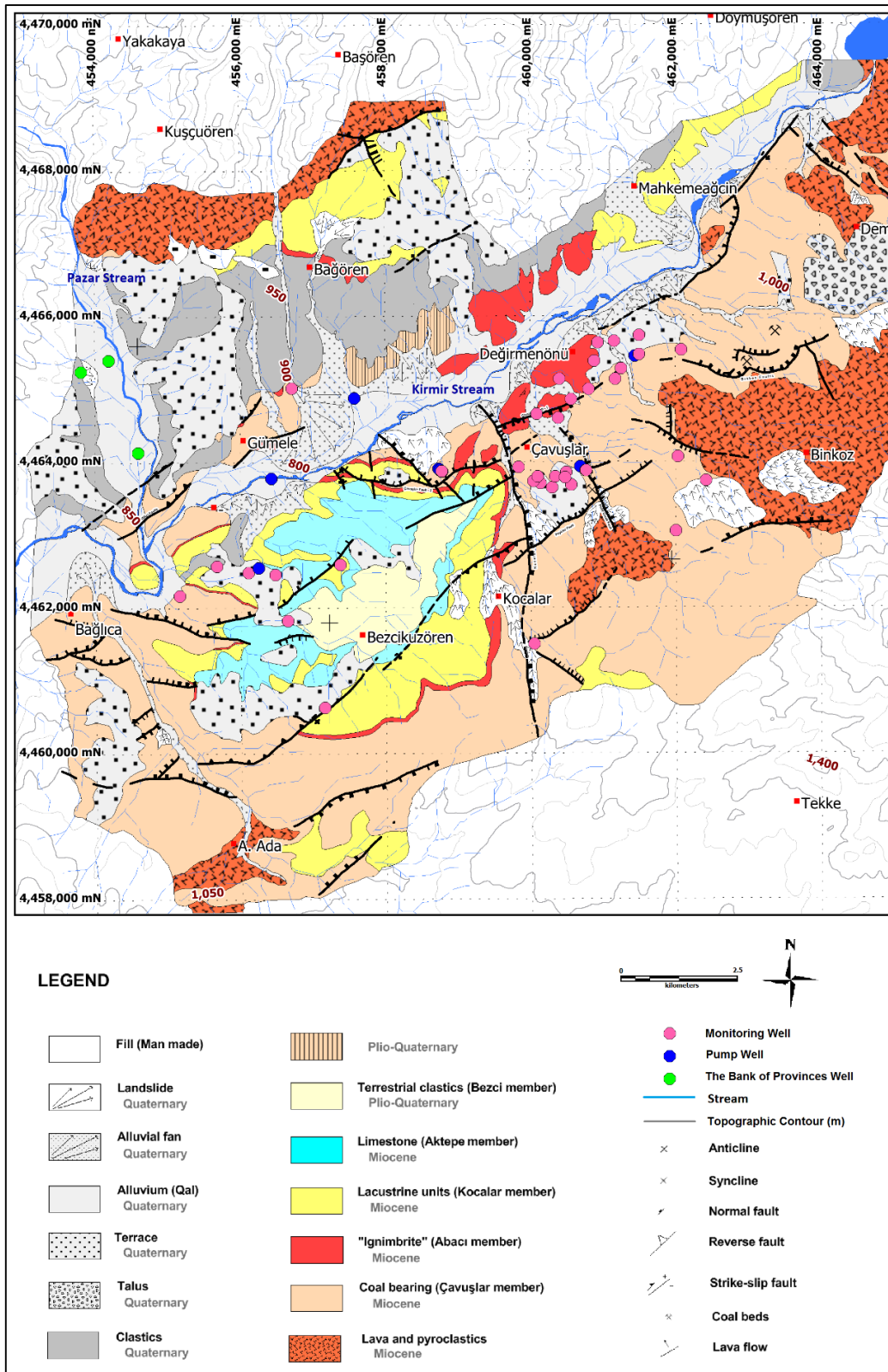


Figure 4.7. Distribution map of the monitoring, pump and The Bank of Provinces Wells on the geological map

The process well completion is ended with cementation and well head construction. The well development process using a compressed air could be done only at large-diameter wells (i.e, diameter greater than 8.5 inches) that are completed with PVC casing.

Water level or water pressure measurements have been conducted at all monitoring wells twice a month. Slug tests have been conducted to determine the hydraulic parameters, like hydraulic conductivity and storativity, at large diameter wells which were completed with PVC casing. Also at some locations, nested wells were opened to determine the vertical hydraulic gradients. In the light of the data which are obtained from the monitoring wells, the hydraulic properties of the various lithologic units were determined.

4.1.3.4. Pump Wells

In addition to the monitoring wells, seven large diameter pump wells were opened at some critical locations to determine the hydraulic parameters. These wells were drilled with rotary system drilling machine by using clean water as circulation fluid. After the completed washing and completion process, these wells were developed by air lifting and submerge pumps. In some of these wells, pump tests were conducted with falling and rising phases. The well at which was observed free flow, only free flow test was performed. The locations of pump wells, their distributions on geological units and well details are presented in Figure 4.6-4.7 and Table 4.4.

Table 4.4. Well detail of pump wells and monitoring wells in the study area

Hole ID	Well Type	Easting (m)	Northing (m)	Elevation (m)	EOH (m)	Screen Top (m)	Screen Bottom (m)	Screen Level	Aquifer Taped
PW1	Pump well	458728.6	4463904.2	865.8	284.0	240.0	272.0	Below the coal	Volcanics
PW4A	Pump well	456424.6	4463781.5	799.0	440.0	390.0	432.0	Below the coal	Volcanics
PW5	Pump well	461440.7	4465444.5	867.7	145.0	113.8	133.3	In the coal	Coal
PW6	Pump well	460682.8	4463932.9	929.3	172.0	144.0	160.0	In the coal	Coal
CEL18	Monitoring well	456477.7	4462460.5	937.6	475.0	446.0	464.0	Below the coal	Volcanics
CEL19A	Monitoring well	458776.0	4463867.2	870.8	235.0	214.0	228.0	Below the coal	Çavuşlar member
CEL19B	Monitoring well	458778.9	4463869.2	870.9	216.0	194.0	210.0	In the coal	Coal
CEL24	Monitoring well	457373.2	4462595.7	971.6	490.0	435.0	450.0	Below the coal	Çavuşlar member
CEL27	Monitoring well	456646.8	4461827.1	1004.3	505.4	481.0	499.0	Below the coal	Volcanics
CEL32	Monitoring well	457149.4	4460631.7	1092.5	441.0	411.0	429.0	Below the coal	Volcanics
CEL33	Monitoring well	460294.3	4463646.1	954.6	387.0	363.0	381.0	Below the coal	Çavuşlar member
CEL35	Monitoring well	460379.6	4464598.2	869.4	303.7	277.0	300.0	Below the coal	Çavuşlar member
CEL36	Monitoring well	460805.8	4464993.7	877.5	302.0	270.0	299.0	Below the coal	Çavuşlar member
CEL37	Monitoring well	459835.7	4463926.8	892.5	385.0	361.0	379.0	Below the coal	Çavuşlar member
CEL38	Monitoring well	460400.9	4465133.4	859.0	330.3	306.0	324.0	Below the coal	Çavuşlar member
CEL39	Monitoring well	460560.3	4463679.0	969.2	223.2	199.0	217.0	Below the coal	Çavuşlar member
CEL42	Monitoring well	460338.7	4463793.2	951.5	314.3	301.0	319.0	Below the coal	Çavuşlar member
CEL43	Monitoring well	461156.8	4465651.7	851.1	240.0	220.0	237.1	Below the coal	Çavuşlar member
CEL44	Monitoring well	461499.6	4465730.7	857.5	202.0	180.5	197.6	Below the coal	Çavuşlar member
CEL46	Monitoring well	460134.9	4463703.4	942.2	352.3	328.0	346.0	Below the coal	Çavuşlar member
CEL47	Monitoring well	461252.8	4465278.7	874.0	392.5	175.7	187.1	Below the coal	Çavuşlar member
CEL47A	Monitoring well	461250.3	4465276.6	874.0	157.0	143.6	152.1	In the coal	Coal
CEL51	Monitoring well	461170.1	4465131.0	887.7	215.5	191.6	205.9	Below the coal	Çavuşlar member
CEL53	Monitoring well	461501.9	4465466.8	868.8	224.7	200.7	218.7	Below the coal	Çavuşlar member
CEL53A	Monitoring well	461501.9	4465466.8	868.8	130.1	106.8	124.8	In the coal	Coal
CEL54	Monitoring well	460039.3	4463732.9	932.9	350.2	336.0	354.0	Below the coal	Çavuşlar member
CEL55	Monitoring well	455672.0	4462576.3	864.7	350.6	326.6	344.6	Below the coal	Volcanics
CEL56	Monitoring well	460097.3	4463795.9	935.5	325.0	300.0	318.0	In the coal	Coal and Çavuşlar member
CEL57	Monitoring well	456106.9	4462490.2	924.0	423.1	391.0	409.0	Below the coal	Volcanics
CEL58	Monitoring well	460087.3	4464655.4	857.7	310.3	286.0	304.0	Below the coal	Çavuşlar member
CEL59	Monitoring well	460762.4	4463877.7	919.2	206.0	169.0	199.0	Below the coal	Çavuşlar member
CEL59A	Monitoring well	460761.3	4463881.0	919.1	130.0	106.0	124.0	In the coal	Coal
CEL61	Monitoring well	460488.2	4463855.7	958.8	255.0	237.8	252.1	Below the coal	Çavuşlar member
CEL62	Monitoring well	460931.4	4465632.0	844.1	260.3	236.0	254.0	Below the coal	Çavuşlar member
CEL63	Monitoring well	455159.0	4462170.6	811.4	270.0	246.0	264.0	Below the coal	Volcanics
CEL64	Monitoring well	460474.8	4463784.0	958.5	265.0	245.0	262.1	Below the coal	Çavuşlar member
CEL66	Monitoring well	460880.4	4465382.6	862.6	241.8	218.0	236.0	In the coal	Coal
CEL68	Monitoring well	460558.8	4464855.0	873.2	275.0	251.0	269.0	In the coal	Coal and Çavuşlar member
CEL69	Monitoring well	456711.0	4465015.7	849.7	361.0	337.0	355.0	Below the coal	Çavuşlar member
CEL75	Monitoring well	462082.0	4465531.0	895.0	88.6	64.6	82.6	Below the coal	Çavuşlar member

4.2. HYDROGEOLOGY OF THE STUDY AREA

Hydrogeology of the study area is determined utilizing information obtained from field works and studies, pump wells and monitoring wells, and spring and fountains in the study area. Locations of the monitoring points which are used in evaluation is shown in Figure 4.8.

The basement of the study area is composed of the volcanic rocks which consist of Miocene aged andesitic, andesitic-basaltic lavas and pyroclastic materials.

These units, also exposed over large areas outside the study area, carry water along fractures and joints. These volcanics show the confined aquifer behavior in the area to the west of the Kocalar fault. Groundwater temperatures reach up to 40°C in some wells. At some locations in the Kirmir stream valley, free flow conditions are also observed. The volcanics exposed at large areas on the eastern side of the Kocalar fault near the Binkoz village show the unconfined aquifer property at this side.

The Çavuşlar member of the Çeltikçi formation is exposed almost all places in the study area. The member is composed of cream-white-light green mudrocks with sandstones, tuffs and organic-coal bearing levels. This important unit that carries water behaves jointly with the volcanics in the study area. It shows confined aquifer properties at the west of the Kocalar fault. On the other hand, it shows unconfined aquifer properties on the eastern and southern side of the Kocalar fault. Free flow conditions are observed in some places where sharp changes in the topography occurs. The thickness of the Çavuşlar member changes between 200-300 m. It is overlain by the Abacı ignimbrite at the western side of the Kocalar fault. A massive silicified tuff level which underlies the Abacı ignimbrites forms an impervious layer over the Çavuşlar member, causing it to behave in a confined manner together with the underlying volcanics in the western side of the Kocalar fault. This aquifer system is called as “Volcanics-Çavuşlar” aquifer in this study. A second aquifer system is present over this aquifer in a synclinal basin at the western side of the Kocalar fault. This upper aquifer consists of the mudrocks of the Kocalar member having sandstone and tuffaceous levels, limestones and dolomitic mudrocks of the Aktepe member, and sandstones and siltstones of the Bezci member. In this study, this aquifer system which behaves as an unconfined aquifer is called “Bezci-Aktepe-Kocalar” aquifer. The coal layers are found in the lower aquifer system that is confined.

At the northern side of the study area, Quaternary aged alluvium that lies along the Kirmir and Pazar streams forms an unconfined aquifer system. However, it should be noted that this aquifer system is a weak aquifer due to its limited areal extent and shallow thickness (15-20 m). The hydrogeological map of the study area is shown in Figure 4.8.

4.2.1. Hydraulic Parameters

The major hydraulic parameters which affect the groundwater flow are hydraulic conductivity and storativity. These parameters can be obtained from aquifer tests such as pump test, slug test, and free flow test. For this reason, pump tests have been conducted at each pump well if there is sufficient water, and if not, slug test have been conducted. Also slug tests have been performed at some monitoring wells that have sufficient diameter.

The pump and monitoring wells have been filtered at different target zones which are determined by considering the various geological units existing in the study area. The various targeted geological units and the position of the screen with respect to the coal seams for each well are summarized in Table 4.5. Alluvium in the study area could not be tested because of the absence of the monitoring well filtered in the alluvium only. Thus, the pump test results of the Bank of Provinces wells in the Pazar Stream alluviums were used to determine the hydrogeological parameters of the alluvium.

Table 4.5. Aquifer tests and target geological units

Hole ID	Easting (m)	Northing (m)	Elevation (m)	Pump/Slug Tests	Screen Level	Aquifer Taped
PW1	458728.6	4463904.2	865.8	Pump Test	Below the coal	Volcanics
PW2	458747.6	4463892.2	867.9	Slug Test	Above the coal	Çavuşlar member
PW3	456244.4	4462551.7	906.4	Pump Test	Above the coal	Aktepe and Kocalar member
PW4A	456424.6	4463781.5	799.0	Free Flow Test	Below the coal	Volcanics
PW5	461440.7	4465444.5	867.7	Pump Test	In the coal	Coal
PW6	460682.8	4463932.9	929.3	Pump Test	In the coal	Coal
PW7	457574.03	4464880.44	828.525	Pump Test	Above the coal	Alluvium and Çavuşlar member
CEL19A	458776.0	4463867.2	870.8	Pump Test (Monitoring Well)	Below the coal	Çavuşlar member
CEL25	460043.1	4461502.6	1177.3	Slug Test	No coal	Volcanics
CEL36	460805.8	4464993.7	877.5	Slug Test	Below the coal	Çavuşlar member
CEL43	461156.8	4465651.7	851.1	Slug Test	Below the coal	Çavuşlar member
CEL44	461499.6	4465730.7	857.5	Slug Test	Below the coal	Çavuşlar member
CEL47	461252.8	4465278.7	874.0	Pump Test (Monitoring Well)	Below the coal	Çavuşlar member
CEL47A	461250.3	4465276.6	874.0	Pump Test (Monitoring Well)	In the coal	Coal
CEL49	462033.3	4464065.6	1091.6	Slug Test	No coal	Volcanics
CEL50	462416.6	4463736.1	1114.9	Slug Test	No coal	Volcanics
CEL51	461170.1	4465131.0	887.7	Slug Test	Below the coal	Çavuşlar member
CEL52	461501.9	4465466.8	868.8	Slug Test	No coal	Volcanics
CEL53A	461501.9	4465466.8	868.8	Pump Test (Monitoring Well)	In the coal	Coal
CEL59	460762.4	4463877.7	919.2	Pump Test (Monitoring Well)	Below the coal	Çavuşlar member
CEL59A	460761.3	4463881.0	919.1	Pump Test (Monitoring Well)	In the coal	Coal
CEL59B	460763.2	4463880.2	919.1	Pump Test (Monitoring Well)	Above the coal	Çavuşlar member
CEL61	460488.2	4463855.7	958.8	Slug Test	Below the coal	Çavuşlar member
CEL64	460474.8	4463784.0	958.5	Slug Test	Below the coal	Çavuşlar member

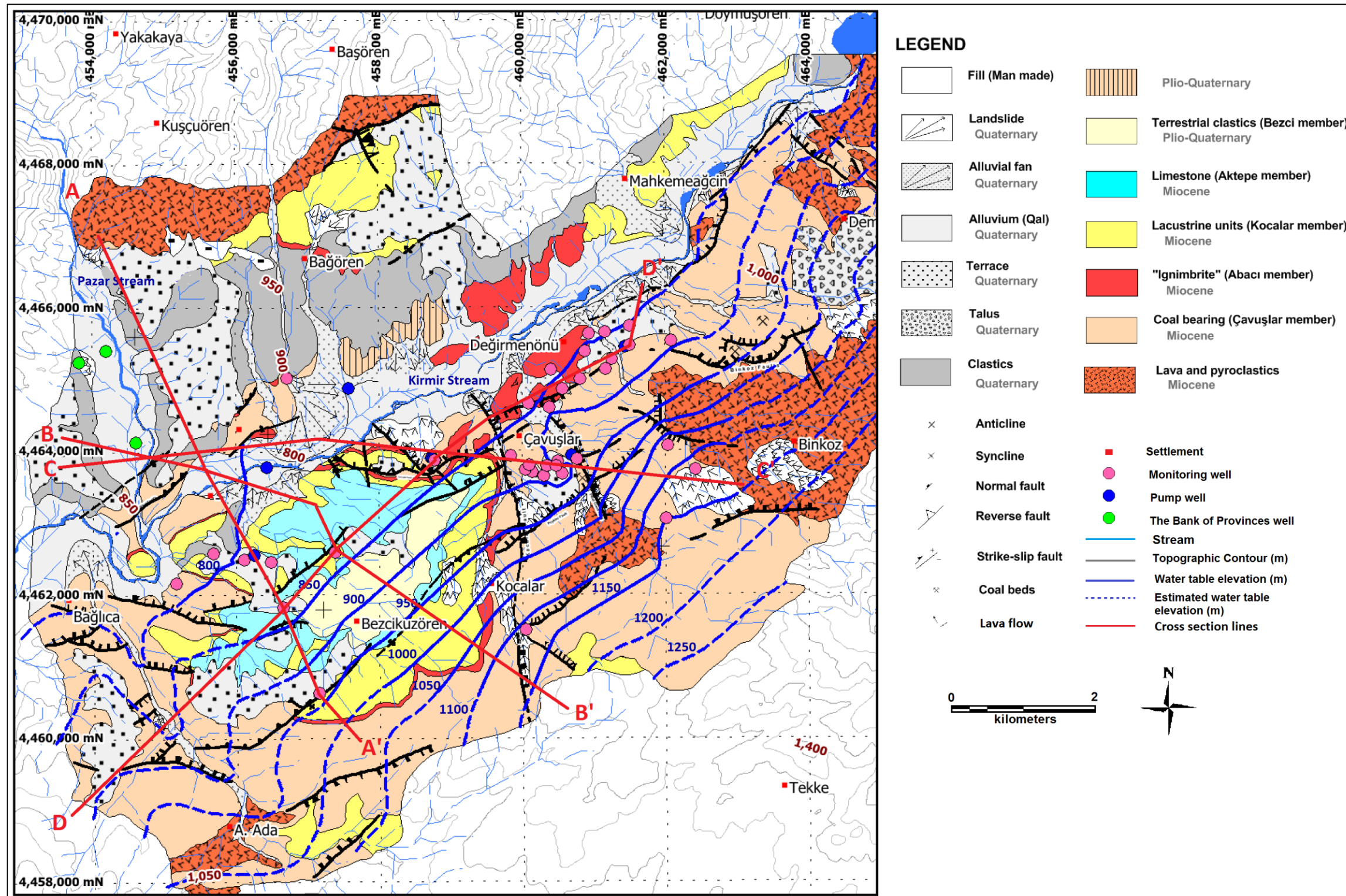


Figure 4. 8. Groundwater elevation contours on geological map of the study area

The location of the wells in which pump tests are conducted is presented in Figure 4.9. The pump tests were performed at PW1 and PW3 in 2012, and at PW5, PW6 and PW6 in 2013. Also, a free flow test was conducted at PW4A in 2013. A slug test was conducted at only PW2 among all the pump wells due to the insufficient water yield at this well. Other slug tests were conducted at 10 monitoring wells in the study area in 2013. The information gathered from pump tests, free flow test and slug tests were analyzed with Aquifer Test Pro 4.2 Software. Calculated aquifer parameters from these wells are listed in Table 4.6.

Aquifers test results which had been conducted at a total of 27 wells were evaluated. Calculated hydraulic conductivity and storativity values were grouped in accordance with the target geological unit and the minimum, maximum and arithmetic as well as the geometric averages of the values are presented in Table 4.7. The examination of the results in Table 4.7 shows that the alluvium, coal and the Çavuşlar member under the coal layer have higher hydraulic conductivity values. The pump test results of The Bank of Provinces wells were used to define the hydraulic properties of the alluvium in the study area. Calculated hydraulic conductivity values for the alluvium vary between 4.27×10^{-6} m/s and 5.59×10^{-5} m/s and the geometric mean of the hydraulic conductivity is 1.22×10^{-5} m/s. Among the wells screened in the coal layer (PW5, PW6, CEL47A, CEL53A and CEL59A), PW6 has the lowest (1.26×10^{-7} m/s) and CEL53A has the highest (2.26×10^{-6} m/s) hydraulic conductivity value. Their geometric mean is 6.77×10^{-7} m/s. The hydraulic conductivity values of 9 wells (CEL19A, CEL36, CEL43, CEL44, CEL47, CEL51, CEL59, CEL61 and CEL64) which were screened in the Çavuşlar member under the coal layer vary between 5.52×10^{-9} m/s and 7.59×10^{-5} m/s. Their geometric mean is calculated as 9.40×10^{-7} m/s.

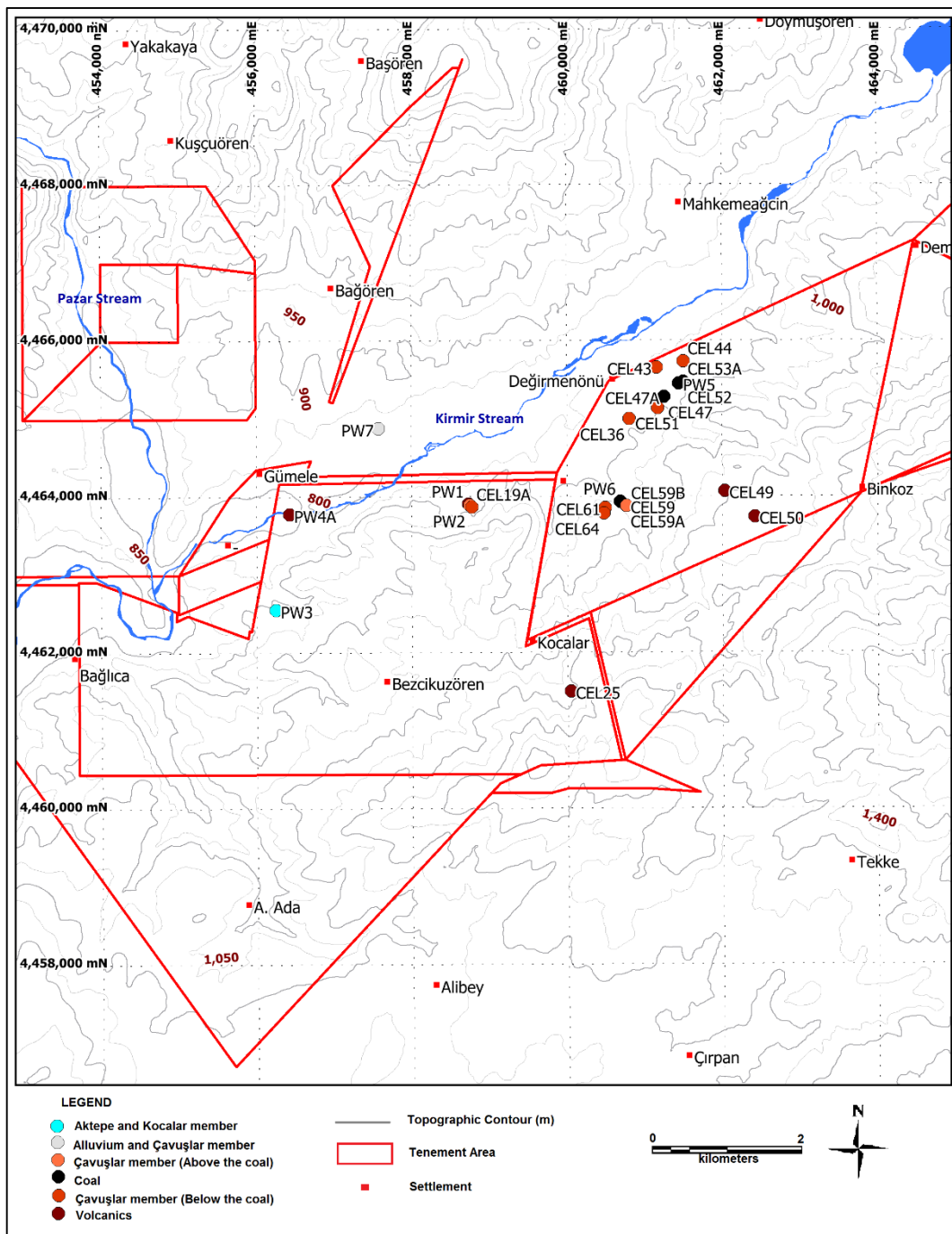


Figure 4. 9. Locations of the wells which were conducted aquifer tests

Table 4.6. Aquifer test results

Well ID	Test Type	Method	Filtered Level		Transmissivity (m ² /s)	Hydraulic Conductivity (m/s)	Storativity	Hydraulic Conductivity (m/s)	
								Aritmetic Mean	Geometric Mean
PW1	Pump Test	Cooper & Jacob	Below the Coal	Volcanics	8.82E-04	2.00E-05		1.44E-05	1.14E-05
		Theis			5.90E-04	1.34E-05			
		Hantush			2.24E-04	5.09E-06			
		Hantush (with Storage)			2.19E-04	4.98E-06			
		Theis Recovery			1.26E-03	2.86E-05			
PW2	Pump Test	Hvorslev(Falling Head Phase)	Above the Coal	Çavuşlar		2.37E-08		1.84E-08	1.79E-08
		Bouwer&Rice(Falling Head Phase)				1.50E-08			
		Hvorslev(Rising Head Phase)				2.18E-08			
		Bouwer&Rice(Rising Head Phase)				1.31E-08			
PW3	Pump Test	Cooper & Jacob	Above the Coal	Aktepe and Kocalar	1.02E-04	1.26E-06		9.11E-07	8.30E-07
		Theis (with Jacob correction)			7.08E-05	8.73E-07			
		Neuman			3.88E-05	4.79E-07			
		Boulton			4.26E-05	5.25E-07			
		Theis Recovery			1.15E-04	1.42E-06			
PW4A		Cooper & Jacob	Below the Coal	Volcanics		1.56E-07		1.56E-07	1.56E-07
PW5	Pump Test	Theis	In the Coal	Coal	2.21E-05	6.69E-07		1.05E-06	9.45E-07
		Cooper&Jacob			5.77E-05	1.75E-06			
		Theis Recovery			2.38E-05	7.20E-07			
PW6	Pump Test	Theis	In the Coal	Coal	5.29E-06	1.26E-07		3.98E-07	3.29E-07
		Cooper&Jacob			2.36E-05	5.62E-07			
		Theis Recovery			2.12E-05	5.05E-07			
PW7	Pump Test	Cooper&Jacob	Above the Coal	Alluvium and Çavuşlar	3.50E-05	5.34E-07		3.06E-07	2.70E-07
		Theis Recovery			9.89E-06	1.51E-07			
		Neuman			1.49E-05	2.27E-07			
		Theis (with Jacob correction)			2.90E-05	4.43E-07			
		Boulton			1.15E-05	1.76E-07			
CEL19A	Pump Test	Cooper & Jacob	Below the Coal	Çavuşlar	3.09E-03	7.02E-05	2.01E-02	5.37E-05	5.00E-05
		Theis			2.25E-03	5.11E-05	1.89E-02		
		Hantush			1.08E-03	2.45E-05	1.60E-02		
		Hantush (with Storage)			2.06E-03	4.68E-05	1.86E-02		
		Theis Recovery			3.34E-03	7.59E-05			
CEL25	Slug Test	Hvorslev(Falling Head Phase)	No Coal	Volcanics		4.89E-09		5.93E-09	5.84E-09
		Hvorslev(Rising Head Phase)				6.97E-09			
CEL36	Slug Test	Hvorslev(Falling Head Phase)	Below the Coal	Çavuşlar		6.67E-07		5.96E-07	5.94E-07
		Bouwer&Rice(Falling Head Phase)				5.51E-07			
		Hvorslev(Rising Head Phase)				6.33E-07			
		Bouwer&Rice(Rising Head Phase)				5.34E-07			
CEL43	Slug Test	Hvorslev(Falling Head Phase)	Below the Coal	Çavuşlar		5.52E-09		9.76E-09	8.79E-09
		Hvorslev(Rising Head Phase)				1.40E-08			
CEL44	Slug Test	Hvorslev(Falling Head Phase)	Below the Coal	Çavuşlar		9.46E-07		8.07E-07	8.02E-07
		Bouwer&Rice(Falling Head Phase)				8.25E-07			
		Hvorslev(Rising Head Phase)				7.41E-07			
		Bouwer&Rice(Rising Head Phase)				7.14E-07			
CEL47	Pump Test	Theis	Below the Coal	Çavuşlar	1.91E-05	5.78E-07	2.24E-05	1.15E-06	1.05E-06
		Cooper&Jacob			5.53E-05	1.68E-06	4.02E-05		
		Theis Recovery			3.93E-05	1.19E-06			
CEL47A	Pump Test	Theis	In the Coal	Coal	1.91E-05	5.78E-07	2.18E-05	1.10E-06	1.02E-06
		Cooper&Jacob			5.13E-05	1.56E-06	4.38E-05		
		Theis Recovery			3.81E-05	1.16E-06			
CEL49	Slug Test	Hvorslev(Falling Head Phase)	No Coal	Volcanics		1.04E-08		1.09E-08	1.08E-08
		Hvorslev(Rising Head Phase)				1.13E-08			
CEL50	Slug Test	Hvorslev(Falling Head Phase)	No Coal	Volcanics		7.90E-09		1.08E-08	1.04E-08
		Hvorslev(Rising Head Phase)				1.36E-08			
CEL51	Slug Test	Hvorslev(Falling Head Phase)	Below the Coal	Çavuşlar		1.53E-06		1.57E-06	1.57E-06
		Hvorslev(Rising Head Phase)				1.61E-06			
CEL52	Slug Test	Hvorslev(Falling Head Phase)	No Coal	Volcanics		1.55E-07		1.48E-07	1.47E-07
		Hvorslev(Rising Head Phase)				1.40E-07			
CEL53A	Pump Test	Theis	In the Coal	Coal	3.21E-05	9.72E-07	2.16E-05	1.40E-06	1.29E-06
		Cooper&Jacob			7.46E-05	2.26E-06	6.07E-05		
		Theis Recovery			3.21E-05	9.72E-07			
CEL59	Pump Test	Cooper&Jacob	Below the Coal	Çavuşlar	3.19E-04	7.61E-06	4.15E-03	7.52E-06	7.52E-06
		Theis Recovery			3.12E-04	7.43E-06			
CEL59A	Pump Test	Theis	In the Coal	Coal	6.13E-06	1.46E-07	3.84E-05	4.16E-07	3.51E-07
		Cooper&Jacob			2.67E-05	6.35E-07	1.54E-04		
		Theis Recovery			1.97E-05	4.68E-07			
CEL59B	Pump Test	Cooper&Jacob	Above the Coal	Çavuşlar	6.50E-05	1.55E-06	3.15E-04	1.55E-06	1.55E-06
CEL61	Slug Test	Hvorslev(Falling Head Phase)	Below the Coal	Çavuşlar		1.23E-06		1.36E-06	1.35E-06
		Hvorslev(Rising Head Phase)				1.49E-06			
CEL64	Slug Test	Hvorslev(Falling Head Phase)	Below the Coal	Çavuşlar		1.51E-07		1.64E-07	1.63E-07
		Hvorslev(Rising Head Phase)				1.77E-07			
L1	Pump Test	Boulton	Above the Coal	Alluvium	1.39E-04	5.68E-06		4.98E-06	4.92E-06
		Neuman			1.05E-04	4.27E-06			
L2	Pump Test	Boulton	Above the Coal	Alluvium	2.33E-04	1.68E-05		2.84E-05	2.28E-05
		Neuman			1.75E-04	1.26E-05			
		Theis (with Jacob correction)			7.78E-04	5.59E-05			
L3	Pump Test	Boulton	Above the Coal	Alluvium	2.47E-04	1.73E-05		1.62E-05	1.61E-05
		Neuman			2.01E-04	1.40E-05			
		Theis (with Jacob correction)			2.47E-04	1.73E-05			

Table 4.7. Hydraulic conductivity and storativity values of the each geological unit

Hydraulic Conductivity (m/s)					
Tested Unit	Minimum Value	Maximum Value	Aritmetic Mean	Geometric Mean	Wells involved in calculation
Alluvium	4.27E-06	5.59E-05	1.65E-05	1.22E-05	L1-L2-L3
Aktepe and Kocalar	4.79E-07	1.42E-06	9.11E-07	8.30E-07	PW3
Çavuşlar (Above the Coal Layer)	1.31E-08	1.55E-06	6.17E-07	1.95E-07	PW2-PW7-CEL59B
Coal	1.26E-07	2.26E-06	8.72E-07	6.77E-07	PW5-PW6-CEL47A-CEL53A-CEL59A
Çavuşlar (Below the Coal Layer)	5.52E-09	7.59E-05	7.43E-06	9.40E-07	CEL19A-CEL36-CEL43-CEL44-CEL47-CEL51-
Volcanics	4.89E-09	2.86E-05	2.46E-06	7.46E-08	PW1-PW4A-CEL25-CEL49-CEL50-CEL52
Storativity S					
Tested Unit	Minimum Value	Maximum Value	Aritmetic Mean	Geometric Mean	Wells involved in calculation
Çavuşlar (Above the Coal Layer)	3.15E-04	3.15E-04	3.15E-04	3.15E-04	CEL59B
Coal	2.18E-05	1.54E-04	5.67E-05	4.65E-05	CEL47A-CEL53A-CEL59A
Çavuşlar (Below the Coal Layer)	2.24E-05	2.01E-02	7.53E-03	1.32E-03	CEL19A-CEL57-CEL59

The highest geometric mean of the storativity values (1.32×10^{-3}) was obtained for the Çavuşlar member below the coal layer and the lowest geometric mean value (4.65×10^{-5}) was calculated for the coal layer itself.

The hydraulic conductivity values presented numerically in Table 4.7 are shown graphically in Figure 4.10. The examination of this figure shows that the alluvium has the highest hydraulic conductivity while the volcanics and the Çavuşlar member above the coal layer have the lowest hydraulic conductivity. The Çavuşlar member below the coal layer, Aktepe and Kocalar members and the coal layer itself have similar hydraulic conductivity values. While considering minimum and maximum hydraulic conductivity values of each geological unit, it is observed that Çavuşlar member and volcanics have the maximum variations within these values. Thus, it can be said that these members show nonhomogeneous properties with

respect to the hydraulic conductivity distribution. However, enough tests to support the heterogeneity have not been conducted for Bezci, Aktepe and Kocalar members, yet.

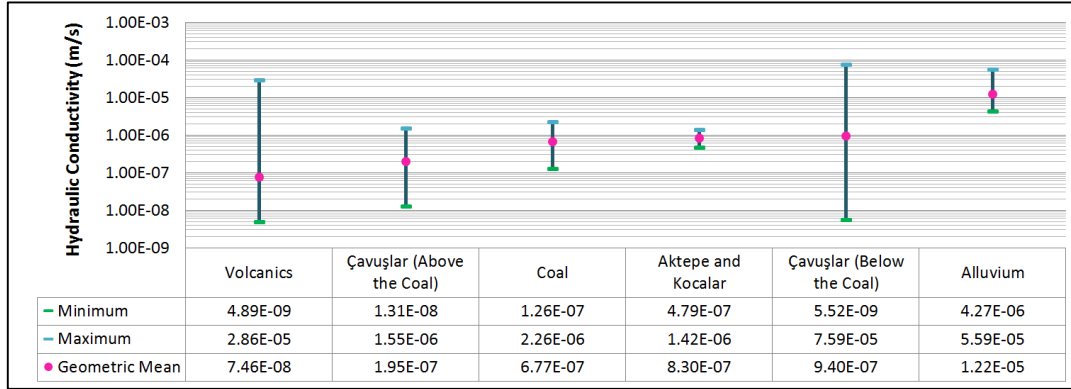


Figure 4.10. Calculated hydraulic conductivity values of the study area

Anisotropy ratios (the ratio of vertical hydraulic conductivity to horizontal hydraulic conductivity) were calculated at some wells (Table 4.8). According to the calculations, PW3 which is filtered in Aktepe and Kocalar members have the lowest value (10^{-5}). It varies between 10^{-1} and 10^{-2} for CEL19A and CEL47 which are filtered below the coal layer in the Çavuşlar member. Anisotropy ratio of PW1 which is filtered in volcanics is 10^{-1} and the wells which are completed in the alluvium have anisotropy ratios varying between 10^{-2} and 10^{-3} .

Table 4.8. Anisotropy ratio of the wells

Formation	Well ID	K_v/K_h	
Volcanics	PW1	1.00E-01	1/10
Çavuşlar (Below the Coal Layer)	CEL19A	3.16E-02	1/32
Aktepe and Kocalar	PW3	1.00E-05	1/100000
Çavuşlar (Below the Coal Layer)	CEL47	1.00E-01	1/10
Alluvium	L1	3.03E-02	1/30
Alluvium	L2	2.54E-03	1/450
Alluvium	L3	3.15E-02	1/32

4.2.2. Groundwater Elevations

4.2.2.1. Spatial Change of Groundwater Elevations

Groundwater level map can only be prepared for the Volcanics-Çavuşlar aquifer system which is widely distributed in the study area. It was not possible to map the groundwater level of the Bezci-Aktepe-Kocalar aquifer because of the insufficient number of observation wells in this aquifer. Similarly, a water-table map could not be developed for the alluvium of the Kirmir Stream. The map which was created using the groundwater levels gathered from monitoring wells in the Volcanics-Çavuşlar aquifer system is presented in Figure 4.11. The water level data corresponding to the December 2013 monitoring values was used while preparing the groundwater level map. Furthermore, groundwater levels belonging to the monitoring wells filtered in the coal seam and above the coal were ignored.

In the study area, groundwater flows from the higher elevations in the southeast toward the Kirmir Stream in the northwest (Figure 4.11). Groundwater levels are decreasing from 1200-1250 m in the southeast to 800-850 m in the north of the study area. Because of this reason, the eastern and southern boundaries of the study area correspond to the recharge zones. Groundwater flows from the recharge zones to the Kirmir Stream. There is not enough data in the northern part of the Kirmir Stream, so the groundwater level map could not be prepared for this area. The northwest oriented groundwater flow direction in the study area is controlled by some fault lines. For instance, along the Kocalar fault which divides the study area hydrogeologically into two, and Polatcreek fault groundwater discharge take place. The hydraulic gradient is more at the eastern side of the Kocalar fault (0.15) and less at the western side of this fault (0.1). The hydraulic gradient decreases toward the discharge zone along the Kirmir Stream.

The depth to groundwater level change between 150 m and 300 m at the western side of the Kocalar fault. Toward the north it decreases to 50 m with decreasing topographic elevations. Free flow is observed at PW4A well which is located near the Kirmir Stream; thus, groundwater level is above the ground surface. At the eastern side of the Kocalar fault, general depth of the groundwater changes between 50 m and 100 m. Groundwater elevations are over the topography and free

flow conditions occur at the wells opened near the Polatcreek fault (CEL35, CEL59A, CEL59B and CEL68). In a similar way, the local changes in topography cause free flow conditions in the region around the wells CEL47A, CEL53A and PW5.

4.2.2.2. Temporal Changes in Groundwater Elevations

Groundwater elevations have been measured in 15-days periods to characterize the project area and observe the temporal changes and spatial distributions of groundwater. Groundwater elevations of all monitoring and pump wells till the end of 2013 are presented as hydrographs in Figure 4.12. The precipitation data was added to these hydrographs to observe the relations between precipitation and groundwater elevations (Figure 4.12). The Binkoz meteorological station was installed on 24.05.2013 and started to record meteorological data after this date. Before that time, the Kızılcahamam metrological station daily precipitation data were corrected using the monthly %bias between the Çeltikçi and Kızılcahamam meteorological station precipitation data (See Chapter 2.3.1.1).

The abrupt changes observed in groundwater elevations are generally caused by the pump tests or development activities conducted at the surrounding nearby wells. The groundwater level measurements at the monitoring and pump wells had been mostly in year 2013; therefore, there was not much opportunity to observe the effect of the year 2012 which received more precipitation.

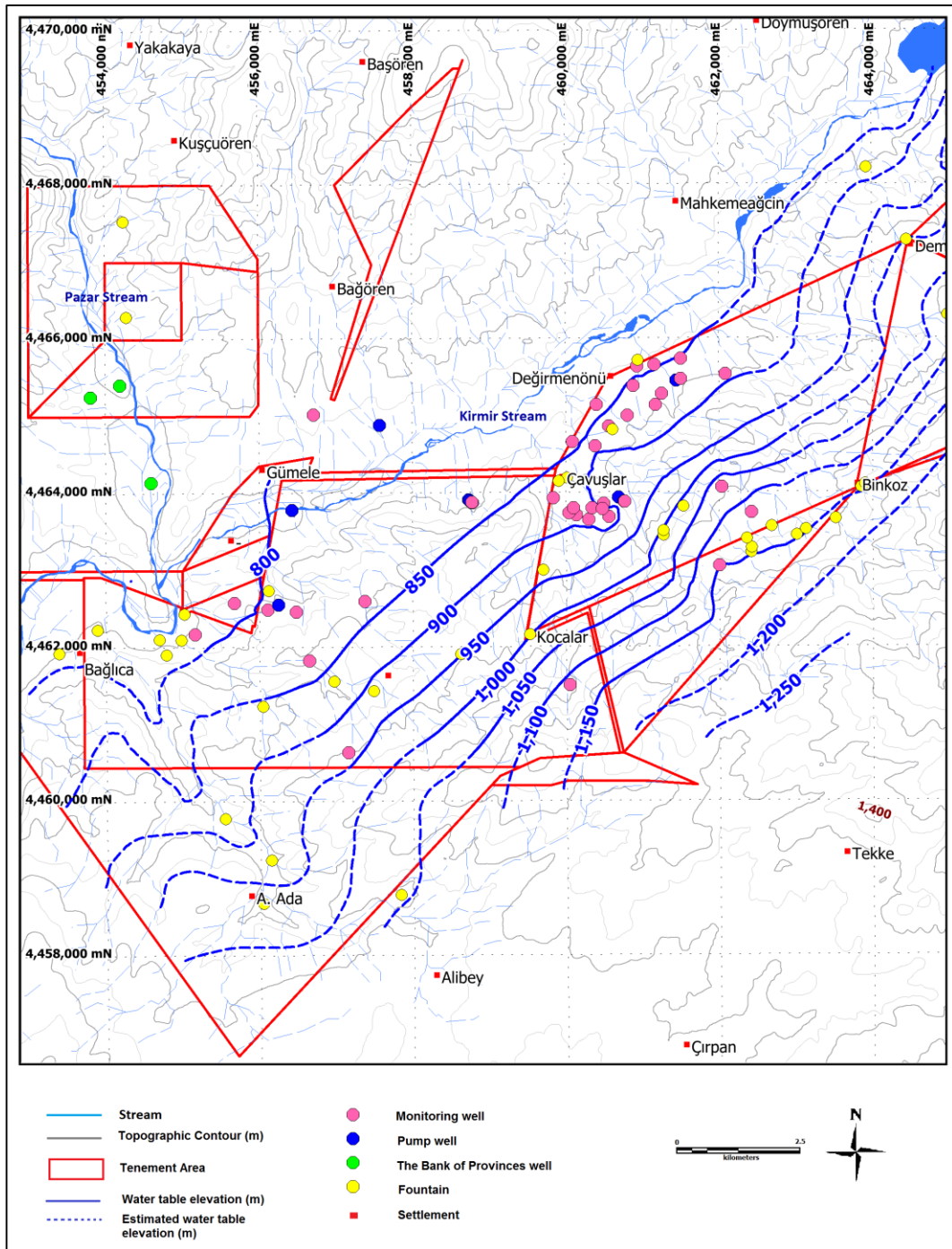


Figure 4.11. Groundwater elevation map of the study area

In the pump wells, except for PW3, almost no fluctuations were observed at the groundwater elevations. Groundwater level at PW3 decreased in June 2013. After that date, groundwater levels remained almost the same. Groundwater levels could be measured only in December 2013 at PW5, PW6 and PW7 wells.

By examining the hydrographs of the monitoring wells, it can be concluded that groundwater levels did not change much over time in the study area (Figure 4.13). However, the rapid increase of the groundwater level in CEL32 produced approximately 70 m rise in groundwater level after August 2013. It is thought that the reason of this much increase which was not seen in none of the other wells is the smaller radius of the well casing and the closeness of the CEL32 to the fault zone. Also, 8-10 m fluctuations were observed in groundwater levels at CEL35 and CEL36. It was observed that the groundwater levels increased at CEL35 while the levels decreased at CEL36. The reason for this decrease in groundwater level at CEL36 is believed to be produced by the development activity conducted with air compressor in this well.

In the study area, nested wells had been opened to determine the hydraulic relation between the various zones above the coal, below the coal and in the coal. The temporal changes of the groundwater levels of these nested wells were analyzed. In this context, hydrograph of the PW1/PW2, CEL47/CEL47A, CEL19A/CEL19B/CEL19D and CEL59/CEL59A/CEL59B were examined together. According to the hydrograph of PW1 and PW2 wells which are located at the west of the Kocalar fault, groundwater levels below the coal zone is 15 m higher than the above the coal (Figure 4.13). Also in this area, when the groundwater levels of the wells screened below the coal (CEL19A), in the coal (CEL19B) and above the coal (CEL19D) were analyzed, it is seen that, the groundwater elevations are almost same in wells below the coal and in the coal layers, but they are higher than the above the coal layer (Figure 4.14). Hence, for this area, it can be said that there is a vertical hydraulic gradient from below the coal to above the coal. The CEL47 and CEL47A wells which are located at the east of the Kocalar fault, were filtered below the coal and in the coal, respectively. While, the measured groundwater levels in the coal

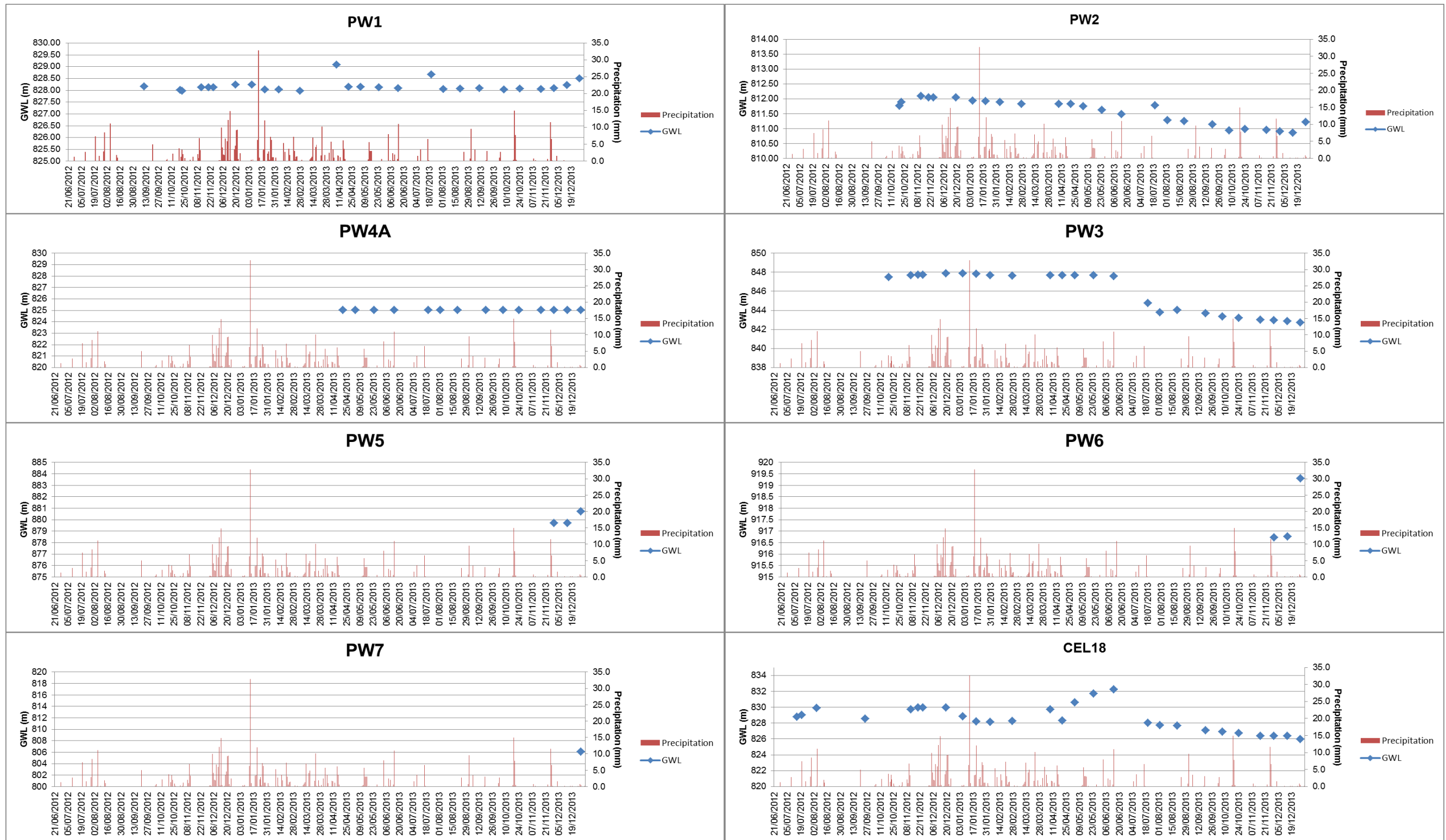


Figure 4.12. Temporal changes of the groundwater measurements at pump and monitoring wells

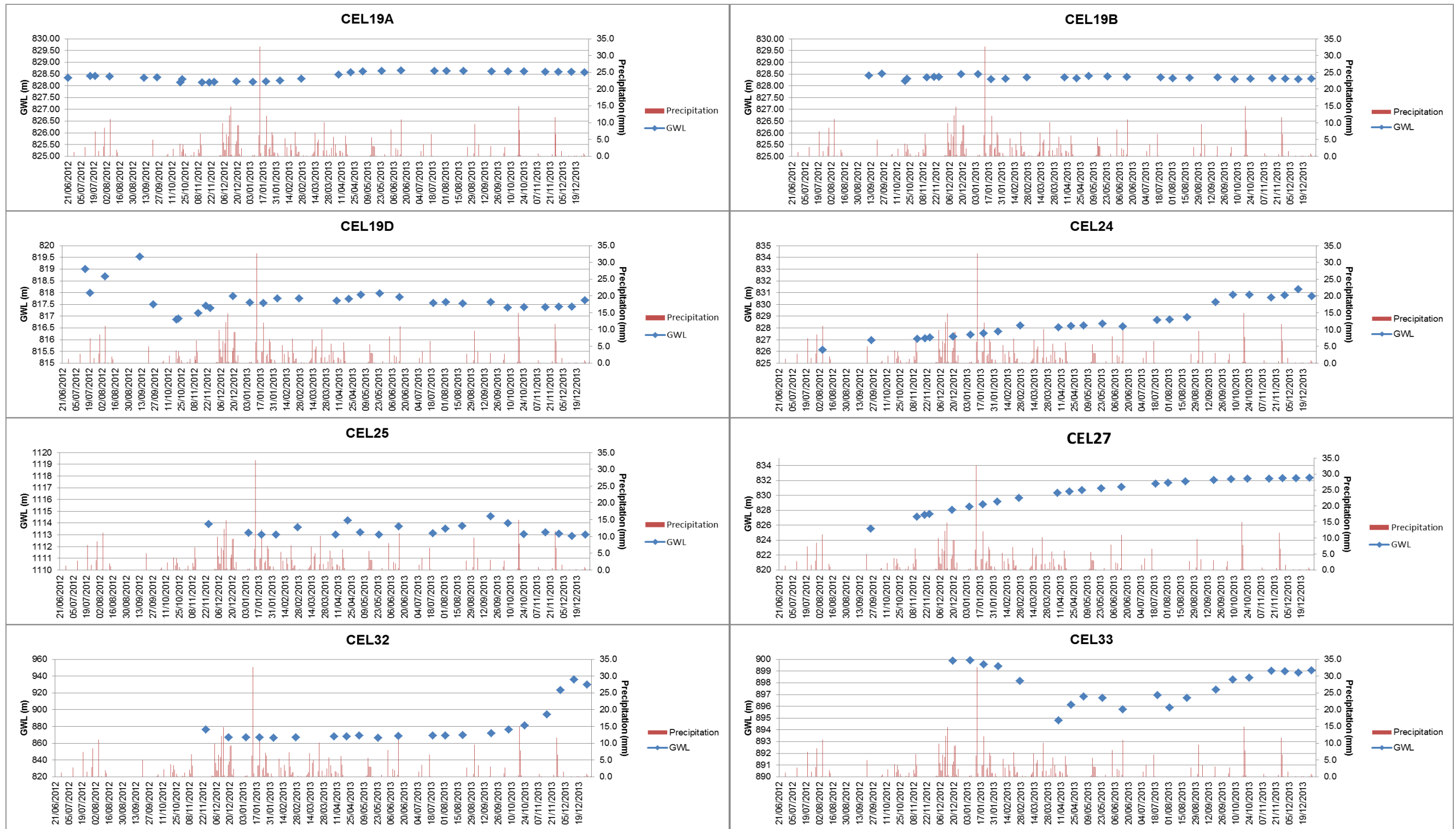


Figure 4.12. (continued)

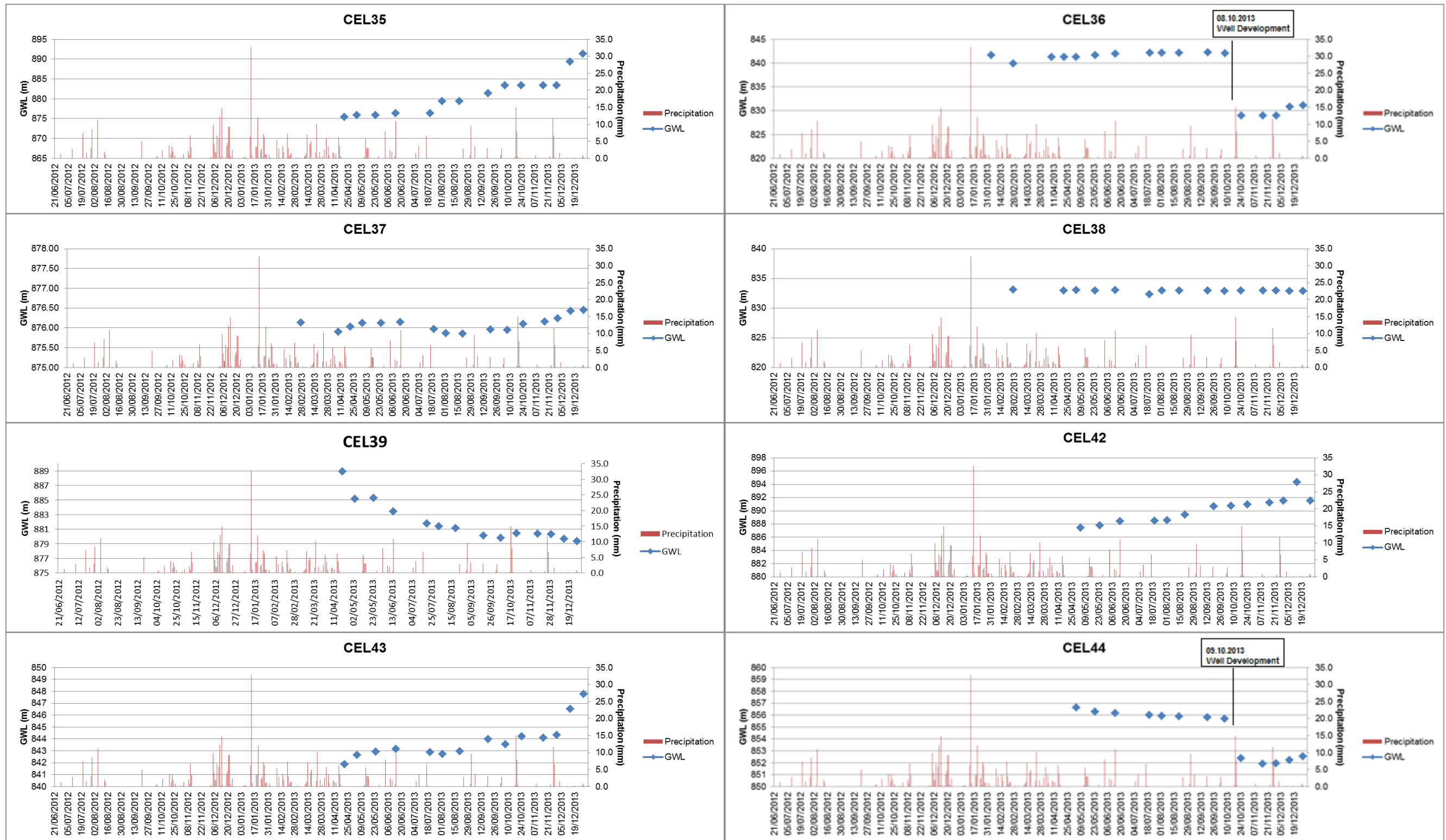


Figure 4.12. (continued)

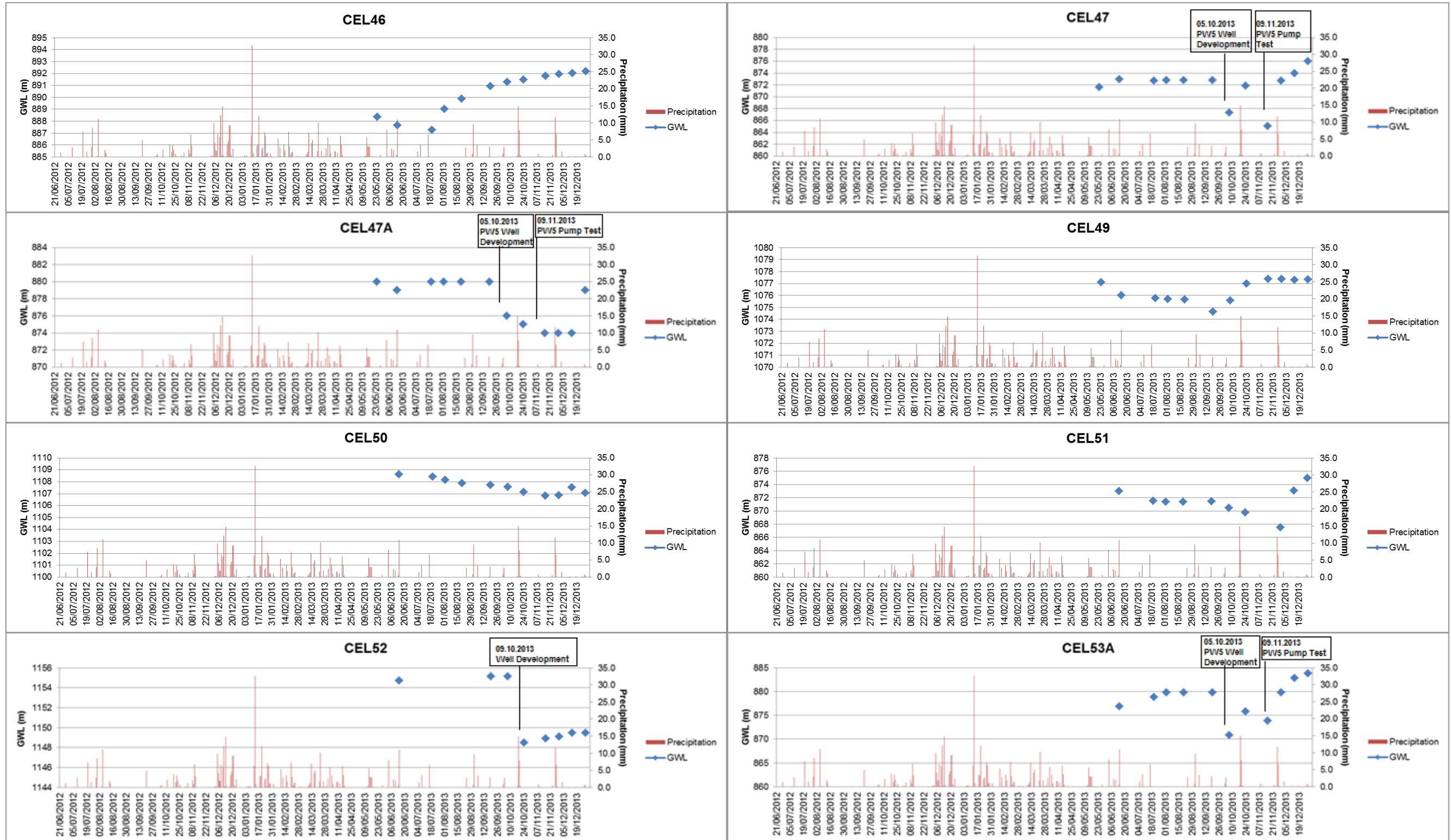


Figure 4.12. (continued)

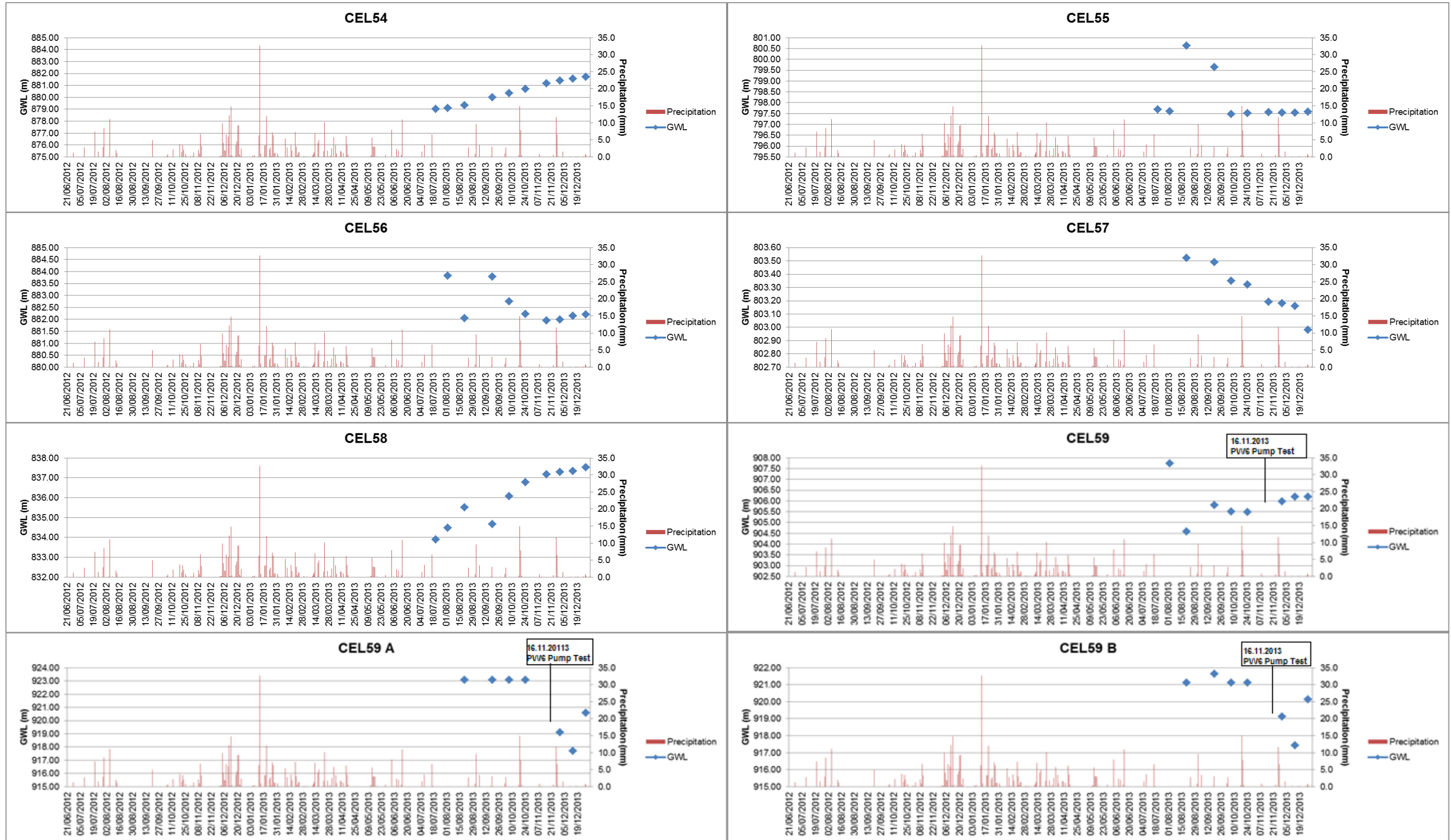


Figure 4.12. (continued)

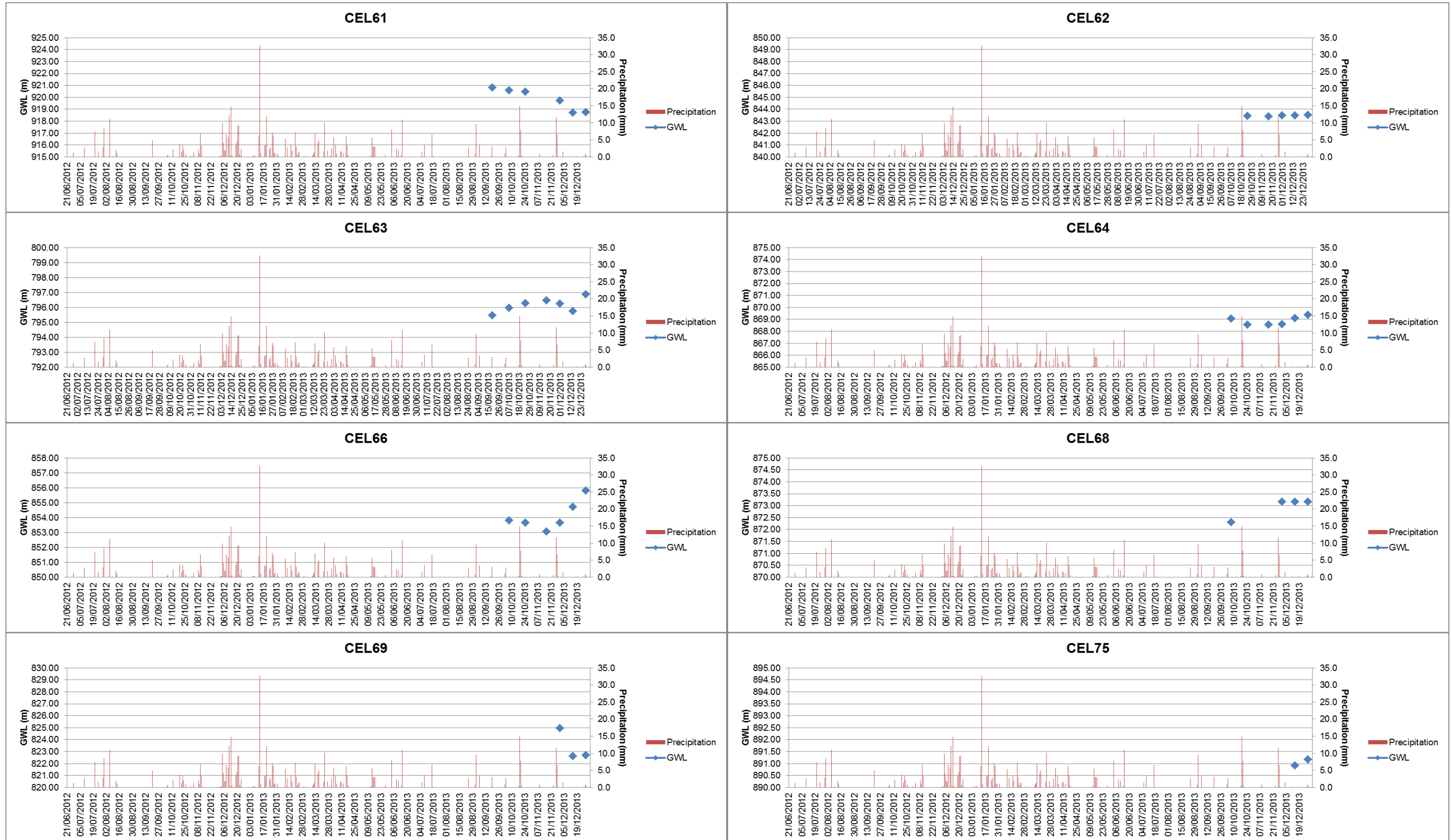


Figure 4.12. (continued)

seam have been higher than the levels below the coal, this difference has gradually declined after the pump test at PW5 (Figure 4.15). Similarly, CEL59, CEL59A and CEL59B wells which are located at the east of the Kocalar fault were screened below the coal seam, in the coal seam and above the coal seam, respectively. The groundwater levels of these nested wells show that the groundwater levels above the coal and in the coal seam are the same and they are higher than below the coal seam (Figure 4.16). But the presence of the short-term monitoring data precludes any solid explanations as to the cause of this difference in water levels. To summarize, groundwater level measurements of the pump and monitoring wells should be continued and also compared with the precipitation data.

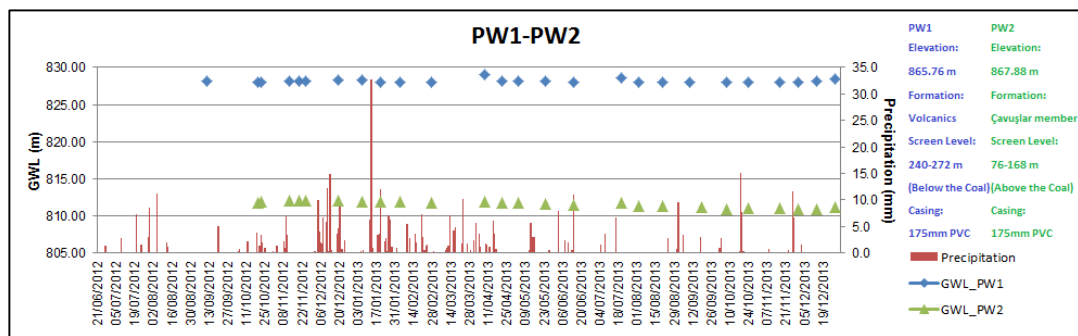


Figure 4.13. Temporal changes of the groundwater levels at PW1-PW2

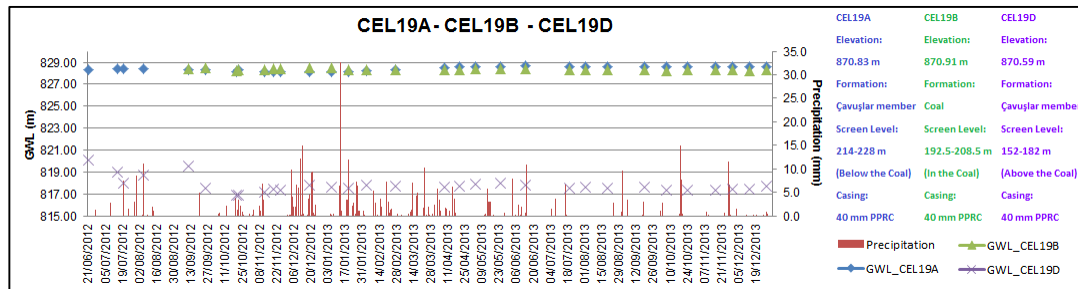


Figure 4.14. Temporal changes of the groundwater levels at CEL19A-CEL19B-CEL19D

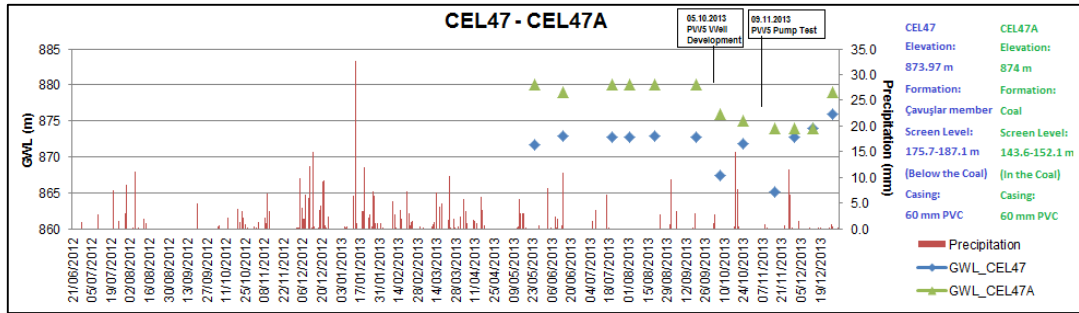


Figure 4.15. Temporal changes of the groundwater levels at CEL47-CEL47A

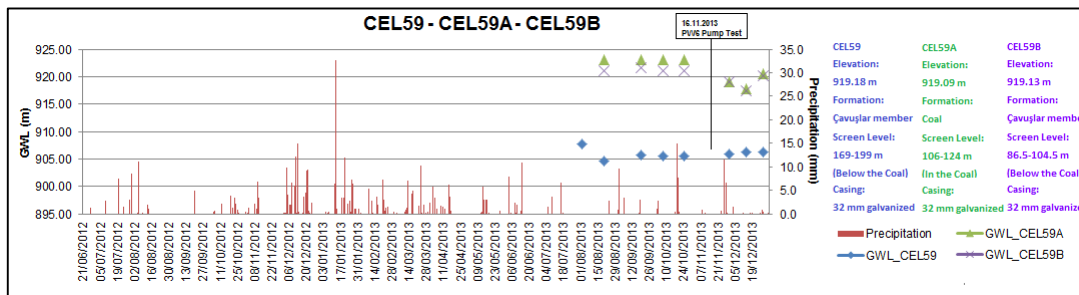


Figure 4.16. Temporal changes of the groundwater levels at CEL59-CEL59A-CEL59B

4.2.3. Hydrogeological Cross-sections

The hydrogeological cross sections were prepared to enhance the hydrogeological understanding of the study area. For this reason, geological information from all wells including exploration, monitoring and pump wells had been used. Geology of the study area had been studied by Bora Rojay (See Chapter 2.4). Cross section lines and locations of the wells are presented in Figure 4.8 and prepared 4 cross sections can be seen in Figure 4.17-4.20.

The surface geology, structural elements and borehole logs had been used while drawing the cross sections. Groundwater levels on the cross sections were obtained from the groundwater elevation map (Figure 4.11). The groundwater level of the Bezci-Aktepe-Kocalar aquifer at the western side of the Kocalar fault was determined from the groundwater levels at PW3 and the spring locations at that area.

It can be clearly seen from the A-A', B-B' and D-D' hydrogeological cross sections that the Bezci-Aktepe-Kocalar unconfined aquifer which occurs in a synclinal basin is located at the western side of the Kocalar fault. Although there is not enough information about the water table of the Bezci-Aktepe-Kocalar unconfined aquifer, it is seen that the groundwater level of this aquifer is higher than

the Volcanic-Çavuşlar confined aquifer. Based on this information, it is thought that there is discharge from the upper aquifer (Bezci-Aktepe-Kocalar unconfined aquifer) to the lower aquifer (Volcanic-Çavuşlar confined aquifer).

It can be seen from C-C' and D-D' hydrogeological cross sections that there is a single aquifer (Volcanic-Çavuşlar aquifer) at the eastern side of the Kocalar fault. This aquifer acts as an unconfined aquifer at this side, but groundwater levels exceed the topographic elevations at some locations due to the sudden changes in the topography.

4.2.4. Fluid Pressure under the Coal Seam

In the study area, coal bearing Çavuşlar member and Volcanics act together and constitute the most important water bearing unit (Volcanic-Çavuşlar aquifer). This unit shows the confined aquifer behavior at the western side of the Kocalar fault. The information gathered from the monitoring wells which were completed in the coal seam and below the coal layer shows that this unit has high fluid pressures (Table 4.9).

As can be seen in the hydrogeological cross sections of the study area, the coal seam is 300 – 400 m below the ground surface at the western side of the Kocalar fault. The fluid pressures at the monitoring wells which were screened in the coal seam and below the coal seam were calculated to give an idea of the expected fluid pressures when the coal is removed from the system (Figure 4.21). In some wells, screened segment is in the coal seam and in some of them screened section is 50 – 100 meter below the coal layer. Thus, the fluid pressures were calculated separately for the coal seam and the layers below the seam. Elevation of the midpoint of the screen length and bottom of the coal seam had been subtracted from the topographic elevation to calculate the pressure heads. As can be seen in Figure 4.21, the fluid pressures vary between 0.68 MPa (CEL75) and 4.31 MPa (PW4A) at the midpoint of the screened sections, and 0.40 MPa (CEL75) and 3.54 MPa (PW4A) immediately below the coal seam.

For the study area, the distribution of the fluid pressures below the coal seam is presented in Figure 4.21. As can be seen in this figure, the fluid pressure below the coal seam is 3 MPa near the Kirmir Stream and this value increases up to 4 MPa near the Bezcikuzören village and decreases to 0.5 MPa at the higher elevations at

the southern side. The fluid pressure at the eastern side of the Kocalar fault between the Binkoz and Demirciören villages is 0 MPa because the coal seam rises to the ground surface around that area. The fluid pressure however increases up to 2.5 MPa toward the Kirmir Stream at this side.

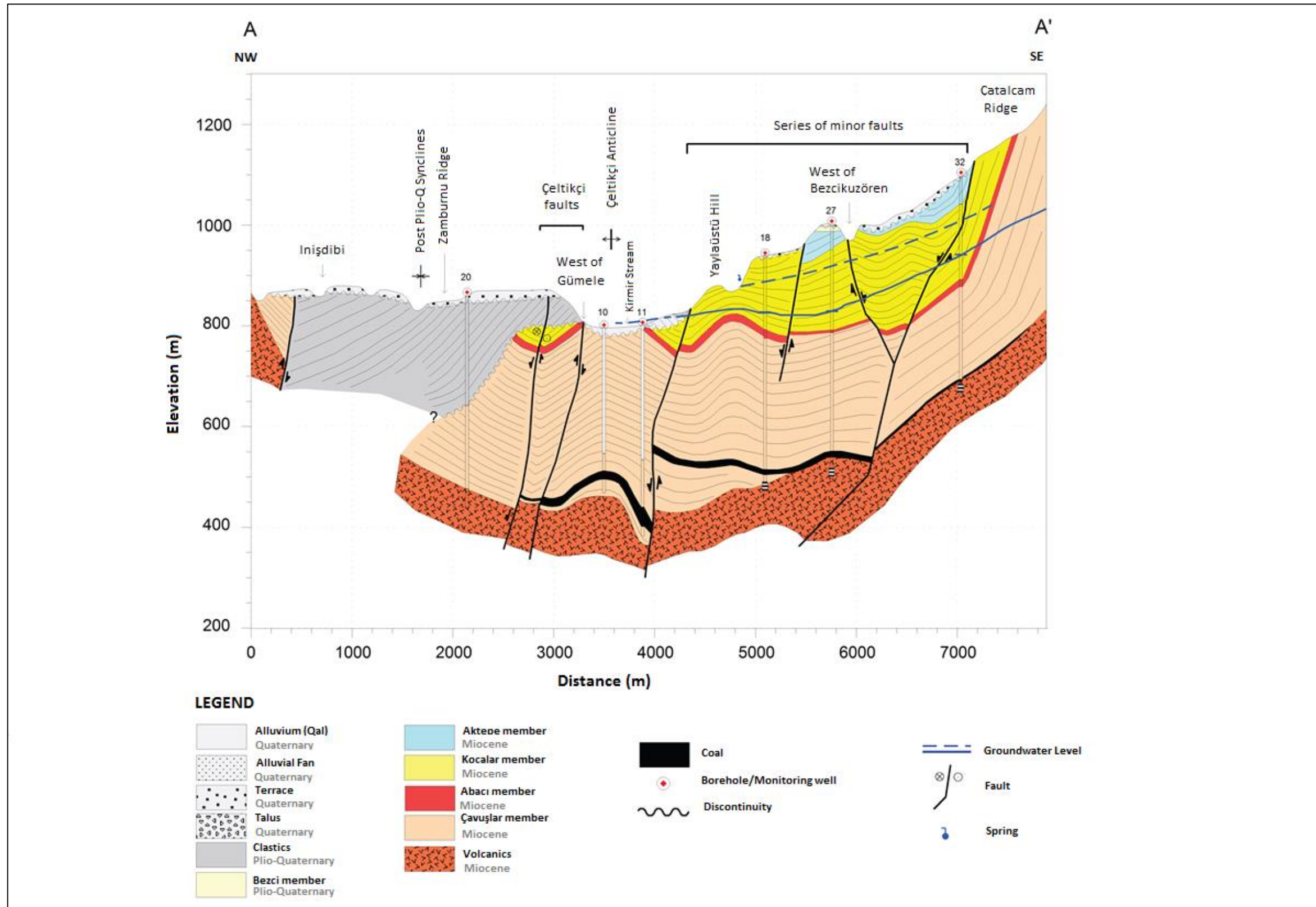


Figure 4.17. A-A' cross section

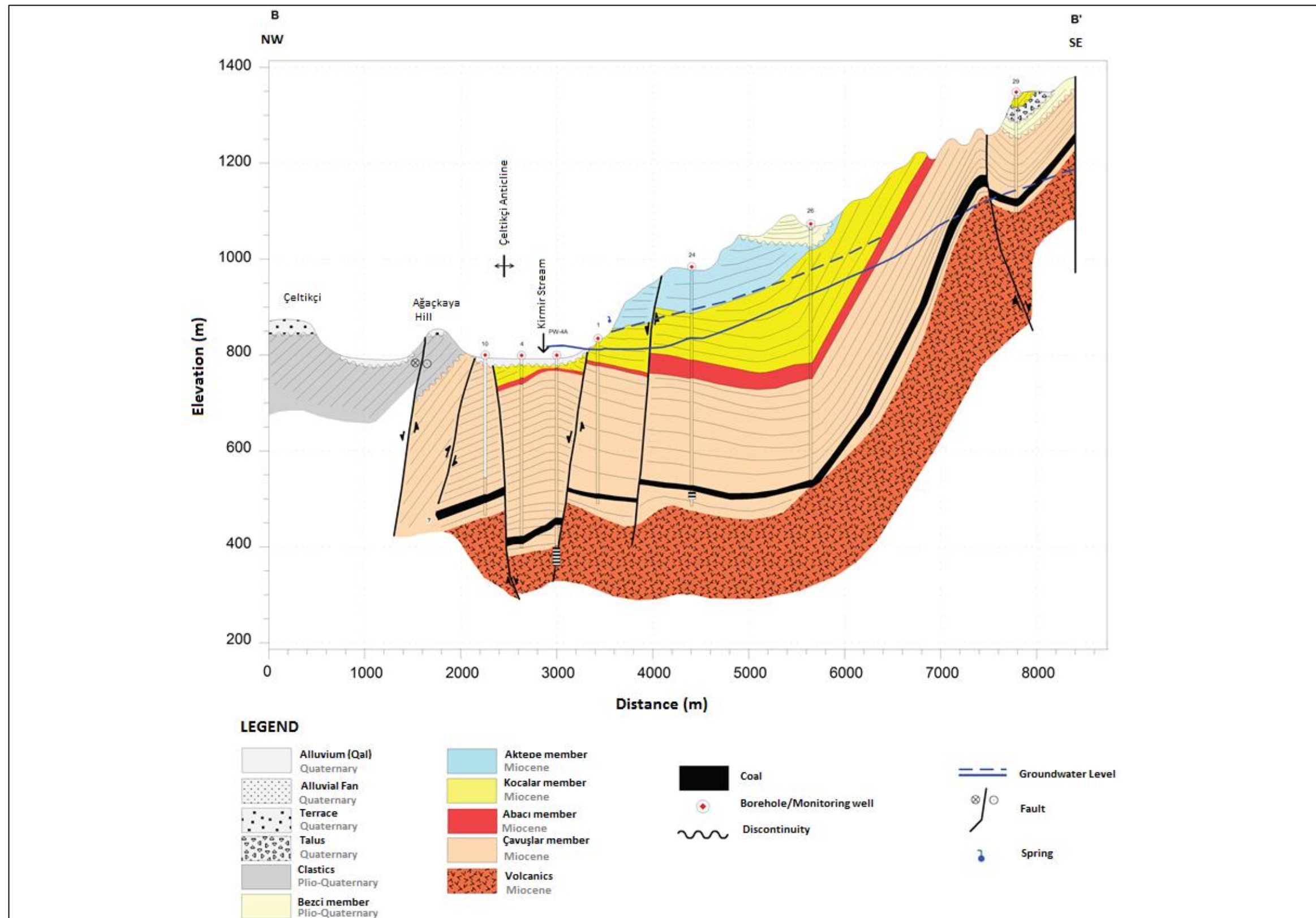


Figure 4.18. B-B' cross section

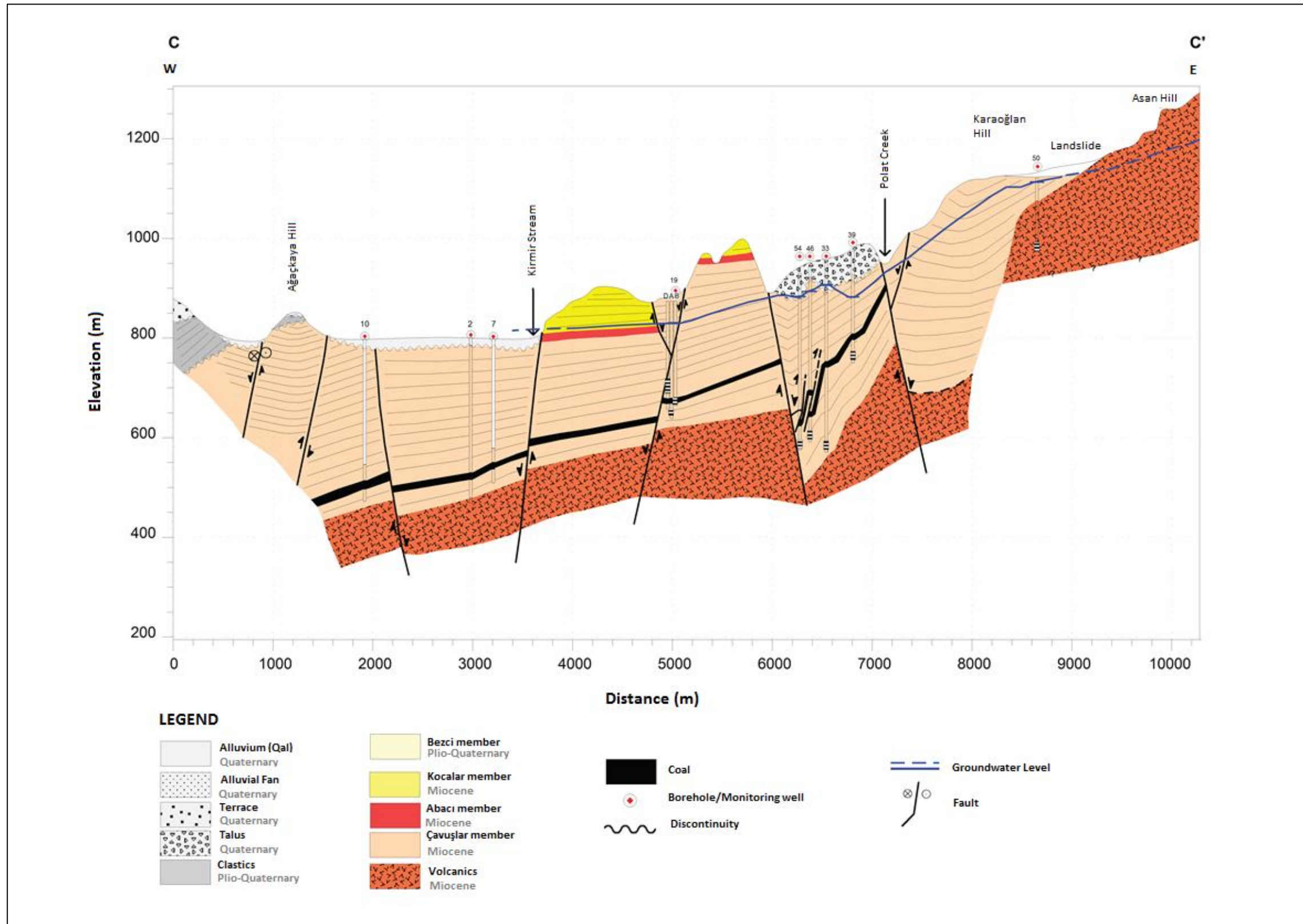


Figure 4.19. C-C' cross section

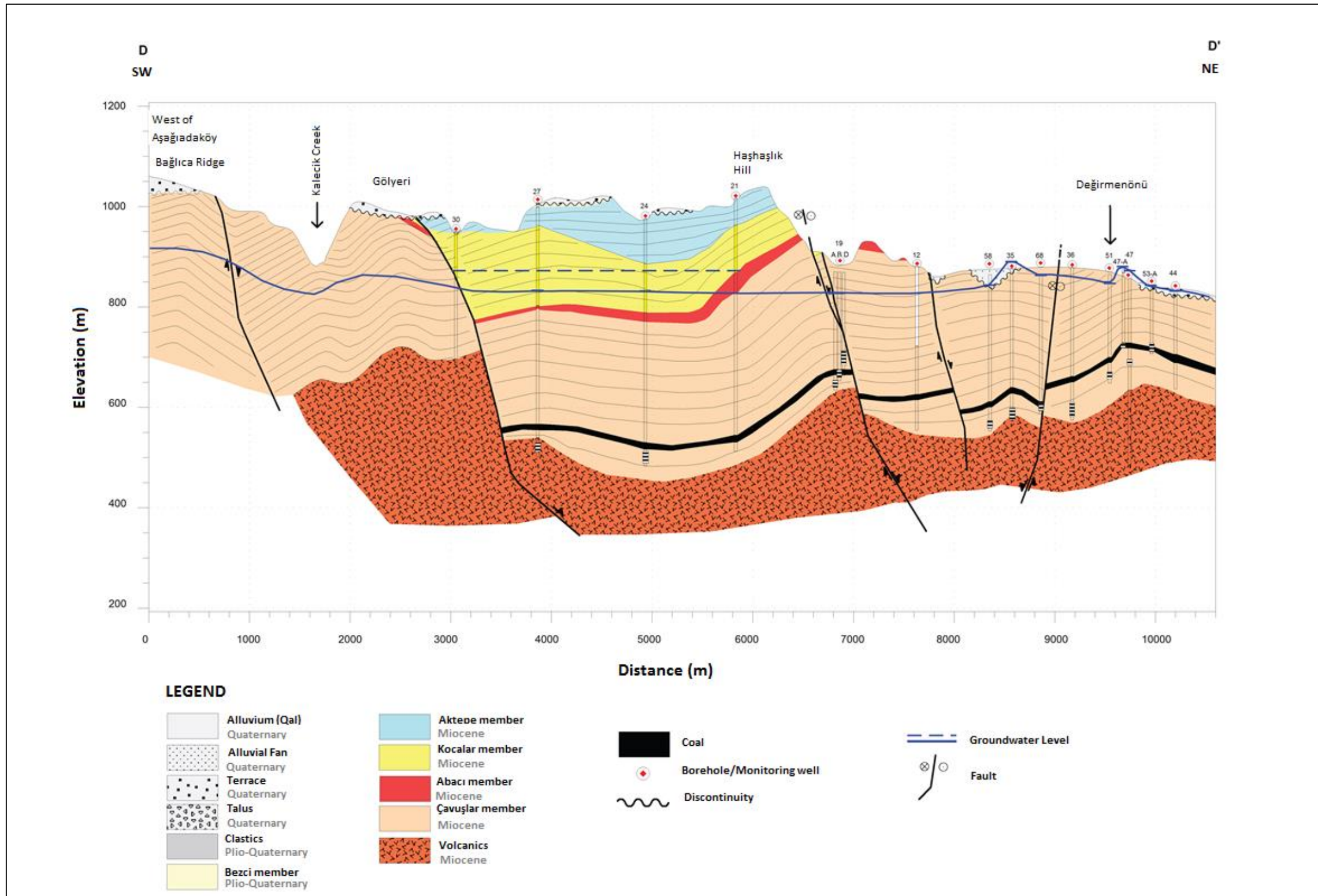


Figure 4.20. D-D' cross section

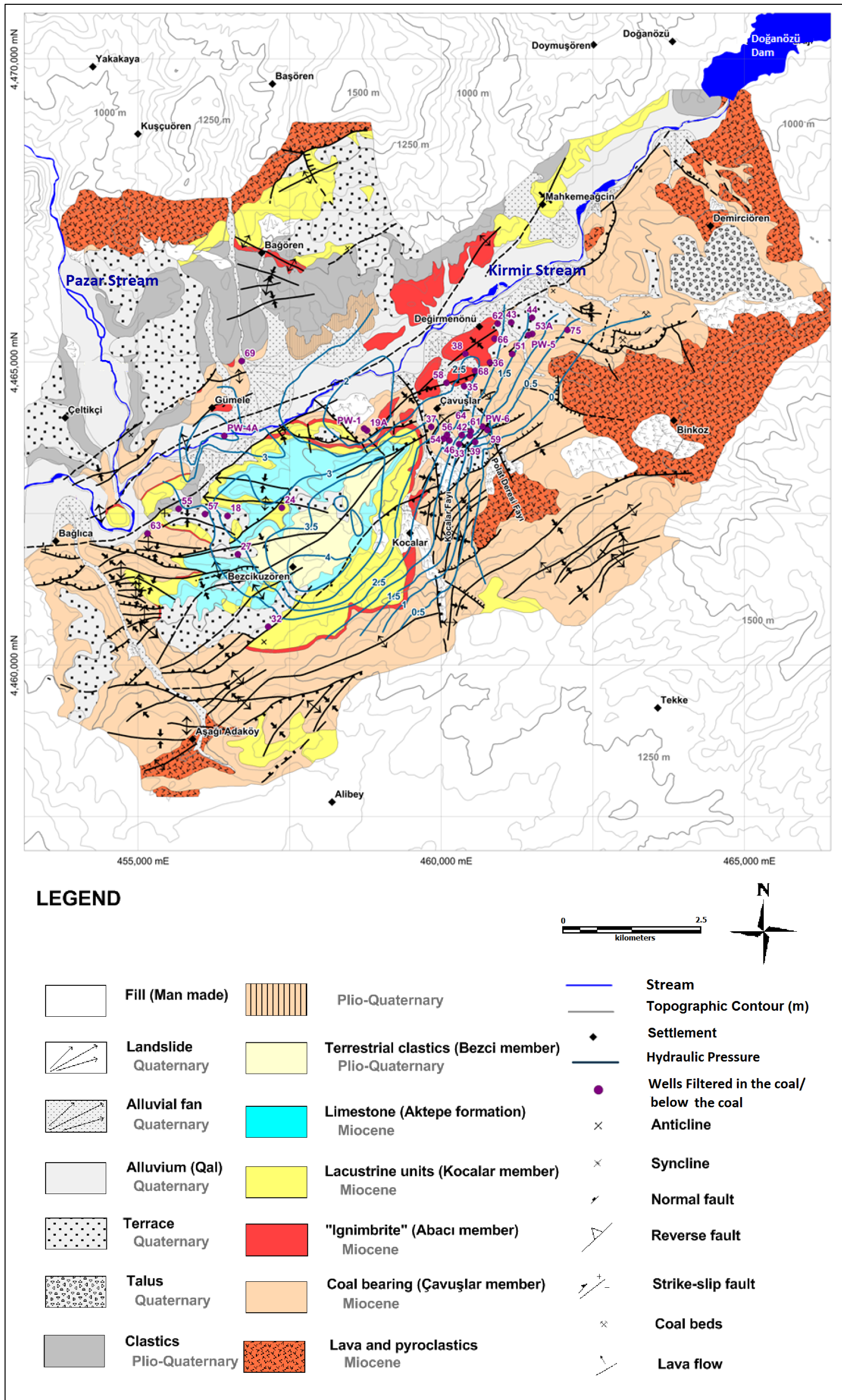


Figure 4.21. Hydraulic pressure distribution of the study area

Table 4.9. Fluid pressures calculated at the wells

Hole ID	Screen Level	Aquifer Taped	Depth to Bottom of the Seam 3 (m)	Depth to Midpoint of the Screen Level (m)	Depth to Water Table (m)	Midpoint of the Screen Level		Bottom of the Seam 3	
						Pressure Head (m)	Hydraulic Pressure (Mpa)	Pressure Head (m)	Hydraulic Pressure (Mpa)
CEL18	Below the coal	Volcanics	434.27	455.00	109.05	345.95	3.39	325.22	3.19
CEL19A	Below the coal	Çavuşlar member	200.75	221.00	42.41	178.59	1.75	158.34	1.55
CEL24	Below the coal	Çavuşlar member	456.46	472.00	143.03	328.97	3.23	313.43	3.07
CEL27	Below the coal	Volcanics	457.74	490.00	174.05	315.95	3.10	283.69	2.78
CEL32	Below the coal	Volcanics	408.62	420.50	212.87	207.63	2.04	195.75	1.92
CEL33	Below the coal	Çavuşlar member	217.14	372.00	56.76	315.24	3.09	160.38	1.57
CEL35	Below the coal	Çavuşlar member	249.86	289.35	-11.64	300.99	2.95	261.50	2.56
CEL36	Below the coal	Çavuşlar member	228.35	284.78	39.37	245.41	2.41	188.98	1.85
CEL37	Below the coal	Çavuşlar member	333.37	370.00	16.37	353.63	3.47	317.00	3.11
CEL38	Below the coal	Çavuşlar member	276.70	315.00	26.12	288.88	2.83	250.58	2.46
CEL39	Below the coal	Çavuşlar member	174.09	208.00	87.21	120.79	1.18	86.88	0.85
CEL42	Below the coal	Çavuşlar member	251.70	310.00	61.46	248.54	2.44	190.24	1.87
CEL43	Below the coal	Çavuşlar member	187.67	228.56	7.31	221.25	2.17	180.36	1.77
CEL44	Below the coal	Çavuşlar member	145.12	189.05	2.96	186.09	1.82	142.16	1.39
CEL46	Below the coal	Çavuşlar member	301.01	337.00	51.85	285.15	2.80	249.16	2.44
CEL47	Below the coal	Çavuşlar member	154.00	181.40	2.10	179.30	1.76	151.90	1.49
CEL47A	In the coal	Coal	154.00	147.85	-3.58	151.43	1.48	157.58	1.54
CEL51	Below the coal	Çavuşlar member	172.64	198.77	16.22	182.55	1.79	156.42	1.53
CEL53A	In the coal	Coal	123.42	115.80	-9.55	125.35	1.23	132.97	1.30
CEL54	Below the coal	Çavuşlar member	309.57	345.00	52.44	292.56	2.87	257.13	2.52
CEL55	Below the coal	Volcanics	313.72	335.60	66.59	269.01	2.64	247.13	2.42
CEL56	In the coal	Çavuşlar member	305.81	309.00	52.92	256.08	2.51	252.89	2.48
CEL57	Below the coal	Volcanics	364.70	400.00	120.69	279.31	2.74	244.01	2.39
CEL58	Below the coal	Çavuşlar member	261.02	295.00	21.64	273.36	2.68	239.38	2.35
CEL59	Below the coal	Çavuşlar member	125.50	184.00	13.25	170.75	1.67	112.25	1.10
CEL59A	In the coal	Coal	125.50	115.00	-2.26	117.26	1.15	127.76	1.25
CEL61	Below the coal	Çavuşlar member	239.43	244.99	38.94	206.05	2.02	200.49	1.97
CEL62	Below the coal	Çavuşlar member	210.92	245.00	0.67	244.33	2.40	210.25	2.06
CEL63	Below the coal	Volcanics	222.52	255.00	15.20	239.80	2.35	207.32	2.03
CEL64	Below the coal	Çavuşlar member	213.45	253.56	89.61	163.95	1.61	123.84	1.21
CEL66	In the coal	Coal	231.28	227.00	8.48	218.52	2.14	222.80	2.18
CEL68	In the coal	Çavuşlar member	260.81	260.00	0.22	259.78	2.55	260.59	2.55
CEL69	Below the coal	Çavuşlar member	314.61	346.00	26.28	319.72	3.13	288.33	2.83
CEL75	Below the coal	Çavuşlar member	45.09	73.60	3.96	69.64	0.68	41.13	0.40
PW1	Below the coal	Volcanics	204.30	256.00	37.61	218.39	2.14	166.69	1.63
PW4A	Below the coal	Volcanics	335.00	413.05	-26.00	439.05	4.30	361.00	3.54
PW5	In the coal	Coal	132.00	123.55	-12.33	135.88	1.33	144.33	1.42
PW6	In the coal	Coal	160.00	152.00	11.69	140.31	1.38	148.31	1.45

4.3. CONCEPTUAL GROUNDWATER BUDGET

There are mainly three aquifers in the study area. One of them is the Bezci – Aktepe – Kocalar unconfined aquifer overlying the Abacı ignimbrites at the west of the Kocalar Fault which is formed of sandstones and tuff banded mudstones of the

Kocalar member, limestone and dolomitic mudstones of the Aktepe member and sandstone –siltstone alternations of the Bezci member. The second aquifer which is observed in almost all around the project area is the Volcanic-Çavuşlar aquifer. This aquifer consists of the cream-white- light green colored mudstones of the Çavuşlar member and fractured sections of the volcanic rock unit forming the basement in the project area. Although this aquifer shows the property of being confined at the west of the Kocalar Fault, it is unconfined aquifer at the east of Kocalar fault. The third aquifer at the project area is the Quaternary age alluvium along the Kirmir and Pazar Streams formed by clay, silt, sand and gravel.

The conceptual groundwater budget depicting the recharge and discharge amounts for the Bezci-Aktepe-Kocalar and Volcanic-Çavuşlar aquifers is calculated as shown in Table 4.10. The groundwater budget for the Quaternary Alluvium aquifer was not calculated because of the insufficient number of monitoring wells for measuring the water level changes in that aquifer. Table 4.10 shows the conceptual groundwater budgets for two aquifers separately.

Table 4.10. Conceptual Groundwater Budget of the study area

Bezci - Aktepe - Kocalar Aquifer			
Recharge (m ³ /year)		Discharge (m ³ /year)	
Recharge From Rainfall	8.09x10 ⁵	Discharge From Springs	5.55x10 ⁴
		Discharge From Volcanic - Çavuşlar Aquifer	7.53x10 ⁵
Total	8.09x10⁵	Total	8.09x10⁵
Volcanic - Çavuşlar Aquifer			
Recharge (m ³ /year)		Discharge (m ³ /year)	
Recharge From Rainfall	2.11x10 ⁶	Discharge From Springs	1.9x10 ⁵
Recharge From Bezci - Aktepe - Kocalar Aquifer	7.53x10 ⁵	Lateral outflow	6.36x10 ⁶
Lateral inflow	3.48x10 ⁶		
Total	6.35x10⁶	Total	6.55x10⁶

The surface area of the Bezci-Aktepe-Kocalar aquifer is approximately 14.39 km² at the west of the Kocalar Fault. According to the details of the conceptual water budget of the project area, 14 % of the annual rainfall (56 mm/year) percolates downward to the groundwater system. Under the light of these data, recharge from the rainfall is calculated as 8.09x10⁵ m³/year for the Bezci-Aktepe-Kocalar aquifer.

The discharge components of this aquifer are discharge from the springs and discharge to the underlying Volcanic-Çavuşlar aquifer. For the determination of the amount of discharge from the springs, the average total discharge of the nine springs (F1, F2, F3, F4, F5, F6, F7, F45, F51 and F53) that are located within the aquifer boundaries is calculated as 1.13 L/s based upon the monitoring program. Furthermore, nine more springs which are located within aquifer boundaries, but not included in the monitoring program are also determined on topographic map. Accepting that the average discharge amount from each of these springs is 0.07 L/s, the total discharge from the springs is calculated as 1.76 L/s and it is shown in the budget as 5.55×10^4 m³/years. Darcy's equation is used to determine the amount of discharge from the Bezci-Aktepe-Kocalar aquifer to the underlying Volcanic-Çavuşlar aquifer. In this equation, vertical hydraulic conductivity is accepted as 500 times smaller than the horizontal hydraulic conductivity. The value of the hydraulic gradient is calculated by dividing the difference in groundwater levels at the only well PW3 drilled in this aquifer and at CEL18 drilled in the Volcanic-Çavuşlar aquifer into thickness of the silicified tuff which separates the two aquifers. Amount of discharge from the Bezci-Aktepe-Kocalar to the Volcanic-Çavuşlar aquifer is calculated as 7.53×10^5 m³/year and together with springs the total discharge amounts to 8.09×10^5 m³/year.

The Volcanic-Çavuşlar aquifer which is confined at the west of the Kocalar Fault and unconfined at the east of Kocalar Fault is recharged from rainfall, Bezci-Aktepe-Kocalar aquifer and lateral inflow. Its discharge components are springs and lateral outflows. The total surface area of this aquifer is 52 km², 37.61 km² of which is being recharged from rainfall. Annual recharge from rainfall was calculated as 56.2 mm. Thus, recharge from rainfall into this aquifer amounts to 2.11×10^6 m³/year. The calculated discharge amount from the Bezci-Aktepe-Kocalar aquifer (7.53×10^5 m³/year) becomes recharge to the Volcanic – Çavuşlar aquifer in the budget. As it can be seen from the groundwater level map given Figure 4.11, there is recharge to the system from south- southeast part of the study area in the form of lateral inflow. In order to calculate this recharge amount, two different recharge amounts were calculated for east and west side of the Kocalar Fault by using Darcy's equation.

There exists recharge from the volcanic unit to the system at the west of Kocalar Fault. During the calculation of this recharge amount, the average hydraulic conductivity calculated for the volcanic units is used. The hydraulic gradient and recharge area were obtained from groundwater level map and hydrogeological cross-sections, respectively. At the east of the Kocalar Fault, however there exists recharge not only from the volcanic units but also from the Çavuşlar member. Therefore, the geometric average of the hydraulic conductivities calculated for these two formations were taken as hydraulic conductivity and hydraulic gradient and recharge area were determined by using groundwater level map and hydrogeological cross sections, respectively. Thus, the lateral inflow is calculated as $4.71 \times 10^5 \text{ m}^3/\text{year}$ and $3.01 \times 10^6 \text{ m}^3/\text{year}$ at the west and at the east of the Kocalar Fault, respectively. The total lateral inflow is $3.48 \times 10^6 \text{ m}^3/\text{year}$. Thus, total recharge to the Volcanic-Çavuşlar aquifer is determined as $6.35 \times 10^6 \text{ m}^3/\text{year}$.

Among the groundwater discharge components of the Volcanic-Çavuşlar aquifer, discharge from the springs is calculated as $1.9 \times 10^5 \text{ m}^3/\text{year}$ with the help of the average flow rate (6.02 L/s) of 28 springs located within the aquifer boundaries that were monitored during the study. Another discharge from the system is the lateral outflow from the aquifer toward the Kirmir Stream. For determination of the lateral outflow, the groundwater system is separated into two parts as west and east of the Kocalar Fault and discharge amounts were calculated separately. Average hydraulic conductivity values calculated in CEL44 and CEL36 wells are used to determine the amount of outflow at the east of the Kocalar Fault and discharge area and hydraulic gradient values were determined by using groundwater level map and hydrogeological cross sections. The lateral outflow amount from this area is $4.47 \times 10^6 \text{ m}^3/\text{year}$. The hydraulic conductivity values calculated in PW1 and PW4A ($1.14 \times 10^{-5} \text{ m/s}$ and $1.56 \times 10^{-7} \text{ m/s}$ respectively) wells cannot be used because of wide range but it is accepted as $5 \times 10^{-7} \text{ m/s}$ for the determination of the amount of outflow at the west of Kocalar Fault. The discharge area and hydraulic gradient values were determined by using groundwater level map and hydrogeological cross-sections. The outflow from this area is calculated as $1.89 \times 10^6 \text{ m}^3/\text{year}$. Therefore, the total

discharge from the Volcanic-Çavuşlar aquifer system is calculated as 6.55×10^6 m³/year.

Conceptually calculated groundwater budget is based on some assumptions. To verify these assumptions, a numerical flow model of the study area is needed which will help to understand the relation between the aquifer systems in detail and to simulate the reactions of these systems under different conditions.

4.4. EXISTING AND PLANNED GROUNDWATER USAGE

The groundwater in the study area is currently utilized as drinking and domestic water for nearby settlements. According to information gathered from individuals and headmen of 12 settlements that are located either within or on the borders of the tenements, the water needs of the peasants are generally satisfied by springs that are canalized into village water depots. Every village in the vicinity excluding Aşağıdaköy and Kocalar has at least one water depot. For Aşağıdaköy and Kocalar villages, water is supplied by nearby or in-settlement water fountains. In addition to water depots, Binkoz, Bağören and Gümele villages also have water wells. Despite the fact that Binkoz village had been the site of water well drilled by ASKİ, the water emerged from the well was found to be unusable and thus, is not used. Bağören village uses water well due to water in its local water depot not meeting quality standards for drinking water. In Gümele, water is pumped from the water well to the village depot and distributed whenever needed. The depots and water sources for settlements within the tenements can be seen in Figure 4.22. There is no planned usage of groundwater in the study area.

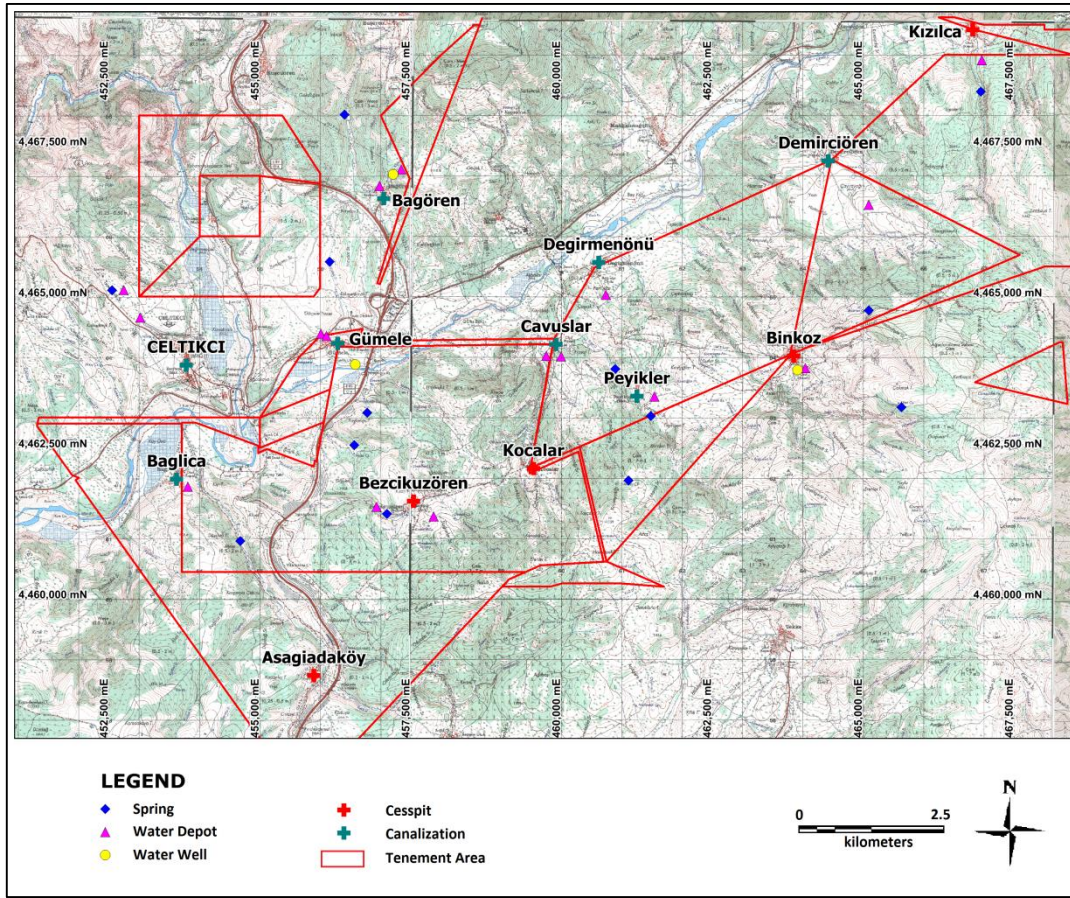


Figure 4.22. Water supply locations in or vicinity of the study area

4.5. THERMAL WATER RESOURCE

Neighbored by the surrounding villages in the project area, Kızılcahamam area is abundant in thermal sources. A temperature of 75-86°C is measured in the geothermal field exploration of Kızılcahamam (MTA, 2005). A geothermal water well drilled by MTA is located within the project area (Figure 4.23). According to information obtained, this drill hole reaches a depth of 1500 m and the temperature of the water had been measured to be 70°C.

Apart from the wells drilled by the General Directorate of Mineral Research and Exploration, at PW1 and PW4A pumping wells with the depth of 284 m and 440 m respectively measured groundwater temperature is 39.6°C and 43.8°C at screened depths (250 m and 410 m). Thus, the study area has a geothermal potential. On the

other hand, the temperature of the spring water (around 22°C) shows thermal properties at the fountain numbered F28 located in the west side of the project area. Water points which are thermally important inside the study area are shown in the Figure 4.23.

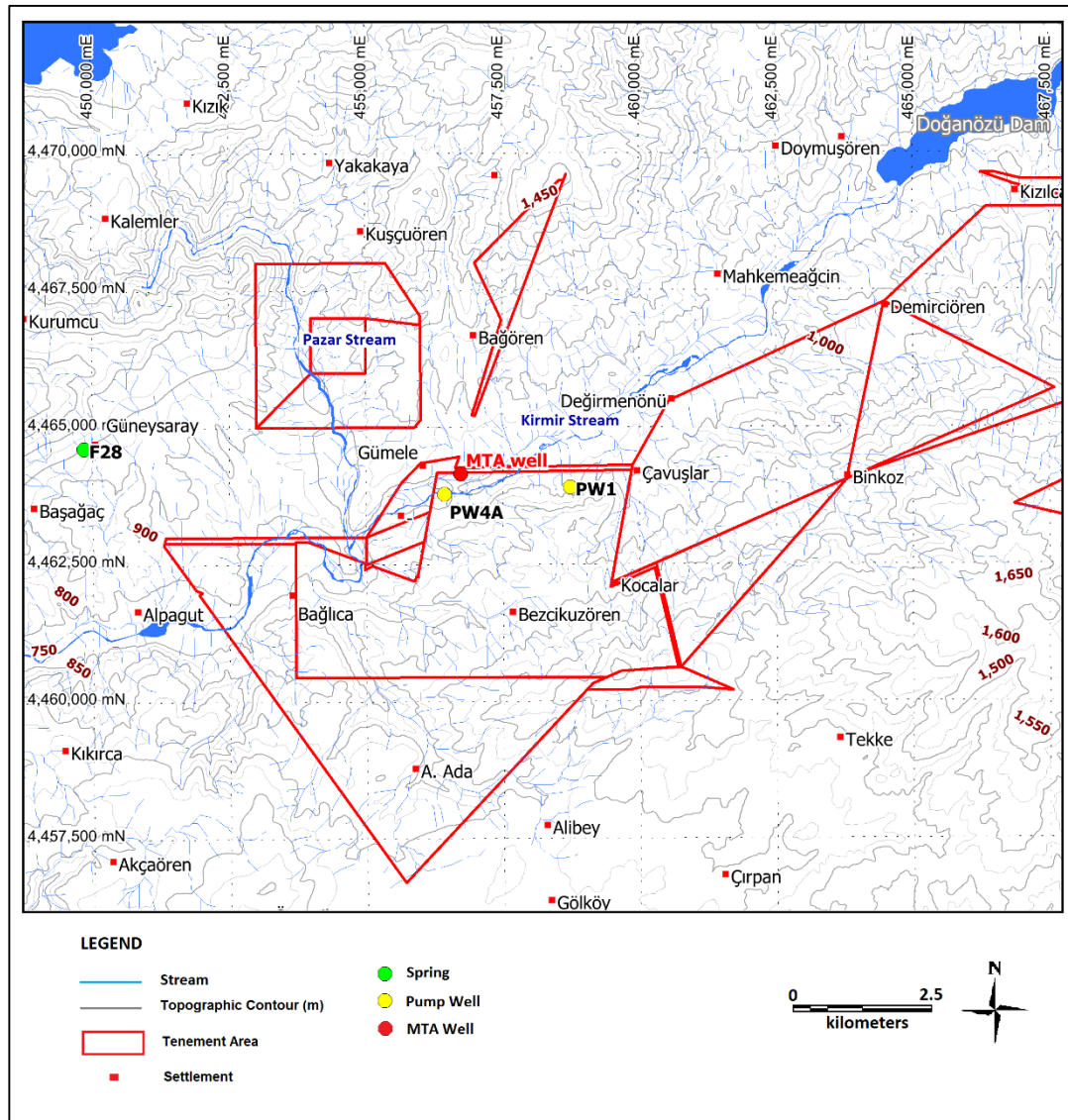


Figure 4.23. Water points which have thermal potential in the study area

CHAPTER 5

HYDROCHEMISTRY AND WATER QUALITY

5.1. STUDIES CONDUCTED

In the scope of the hydrochemical monitoring program, the field studies had been conducted between February 2012 and December 2013. From all surface water, spring/fountain monitoring points monthly field parameters; temperature (T), electrical conductivity (EC), salinity (S), total dissolved solid (TDS), pH, oxidation-reduction potential (ORP) (after December 2012), dissolved oxygen (DO) and discharge (Q) parameters had been measured. Also, pH, EC and T measurements had been conducted during the pump tests at pump wells. In addition to this, EC-T profiles had been taken from all pump wells and proper monitoring wells which were completed with 60 mm PVC pipe. Also, field parameters measurements, samplings which represent both dry and wet season had been conducted at May 2012, September 2012, June 2013 and September 2013. Villages' water depots had been added in the sampling programs. All these samples had been collected according to international standards and analyzed at ALS Group which has international accreditation laboratories in Vancouver, Canada.

5.2. SURFACE WATER HYDROCHEMISTRY

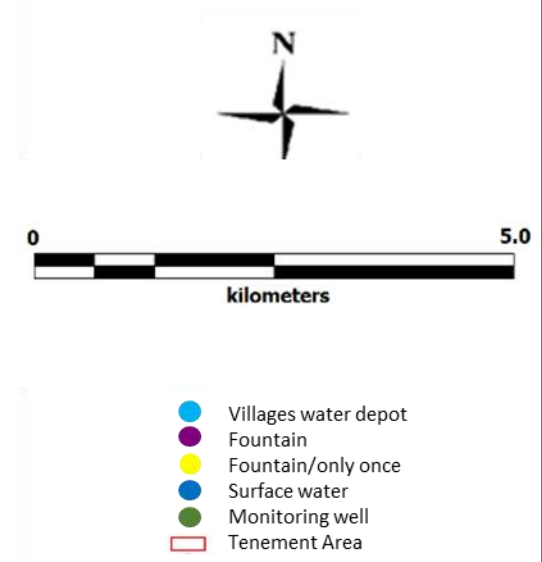
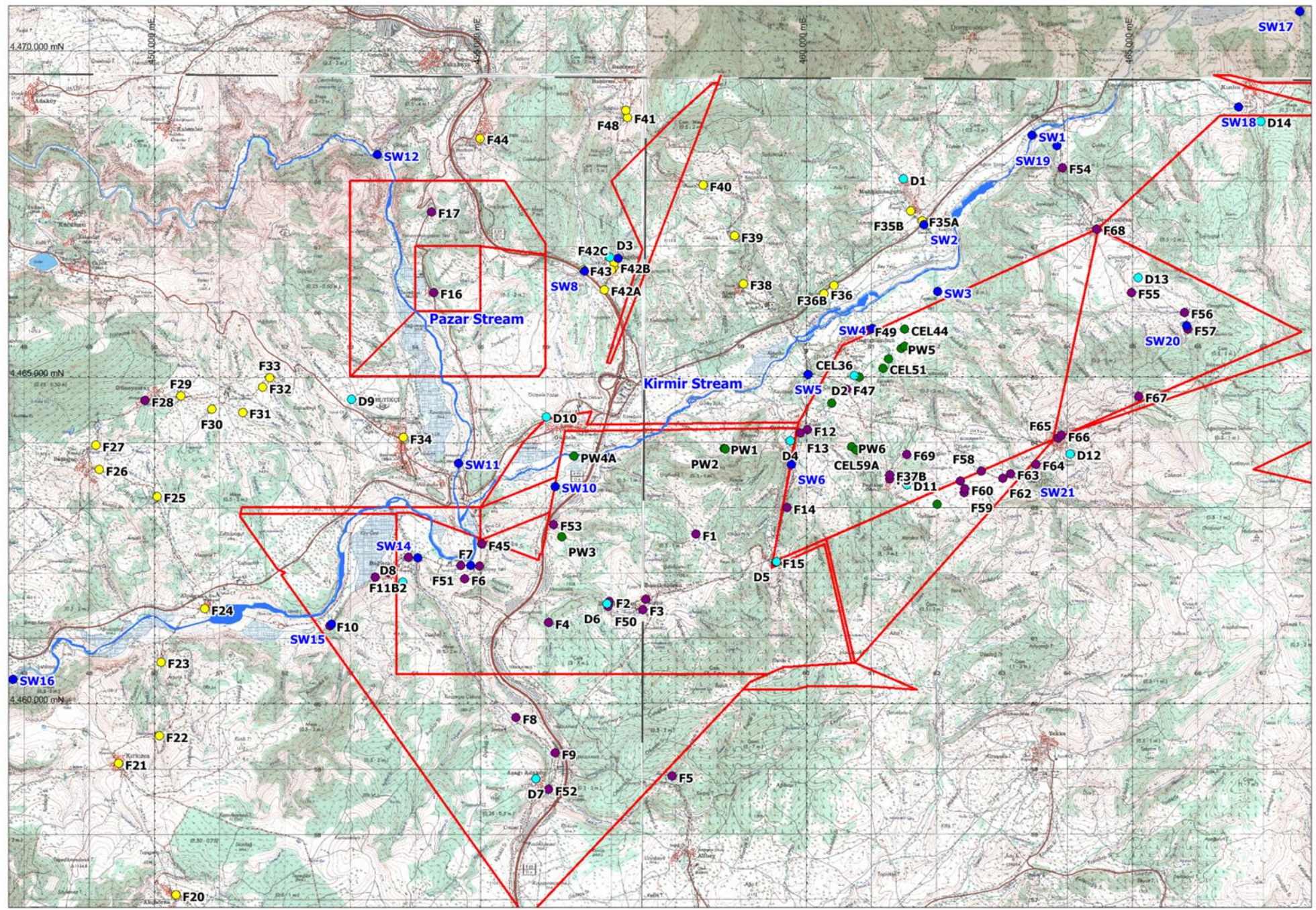
In or in the vicinity of the study area, 21 important surface water monitoring points (SW) were determined. Areal distribution of the surface water monitoring points is presented in Figure 5.1. SW1 and SW16 are located on Kirmir Stream and SW12 and SW11 are located on Pazar Stream. These pairs of sampling points represent the upstream and downstream of the study area, respectively. Other surface

water monitoring points having important drainage areas were also selected. SW17-SW21 surface water monitoring points were added on February 2013 after the tenements had been enlarged.

5.2.1. Analysis of Field Parameters

Average values pH, EC, DO and ORP parameters are listed in Table 5.1 and graphically presented in Figure 5.2. All surface waters in the study area show the alkaline characteristic and average pH values vary between 8.00 and 8.86. From upstream to the downstream of Kirmir and Pazar Streams, pH values slightly decrease (SW1 to SW16 and SW12 to SW11).

Average normalized electrical conductivity values vary between 213-560 $\mu\text{S}/\text{cm}$. Total dissolved solid and salinity values which depend on electrical conductivity, change between 76-515 mg/l and 0.1-0.4 ppt, respectively.



- Villages water depot
- Fountain
- Fountain/only once
- Surface water
- Monitoring well
- Tenement Area

Figure 5.1. Surface water, groundwater and water depot monitoring points

Table 5.1. Average hydrochemical field parameters analysis result of surface water monitoring points (nm: not measurement, sm: single measurement)

Average (%Ave dev)	T(°C)	pH	ORP (mv)	EC (mS/cm)	EC 25°C (mS/cm)	S (ppt)	TDS (mg/l)	DO (mg/l)	DO (%)
SW1	18.7 (%26)	8.58 (%4.0)	162 (%14)	499.1 (%26)	560.0 (%23)	0.27 (%28)	363.9 (%23)	8.76 (%24)	99.1 (%18)
SW2	12.0 (%48)	8.53 (%3.7)	186 (%9)	232.0 (%37)	294.7 (%33)	0.15 (%33)	195.6 (%31)	10.50 (%35)	97.8 (%22)
SW3	16.8 (%12)	8.69 (%2.5)	199 (%1)	433.6 (%11)	530.0 (%5)	0.28 (%11)	344.5 (%5)	7.63 (%10)	85.3 (%7)
SW4	12.9 (%49)	8.86 (%2.4)	186 (%19)	399.7 (%26)	505.7 (%16)	0.26 (%18)	329.7 (%16)	9.06 (%14)	97.3 (%12)
SW5	17.4 (%29)	8.91 (%2.3)	187 (%22)	536.3 (%11)	630.4 (%2)	0.30 (sm)	409.6 (%2)	7.51 (%22)	85.1 (%16)
SW6	17.0 (%20)	8.00 (%2.3)	176 (%7)	566.7 (%30)	792.3 (%6)	0.38 (%7)	515.0 (%6)	8.30 (%29)	85.5 (%11)
SW7	13.8 (sm)	8.56 (sm)	nm	202.8 (sm)	261.8 (sm)	0.10 (sm)	170.1 (sm)	11.80 (sm)	127.3 (sm)
SW8	9.8 (%34)	8.33 (%1.9)	nm	294.6 (%17)	423.5 (%18)	0.17 (%27)	275.4 (%18)	11.13 (%11)	104.6 (%7)
SW9	19.8 (%20)	8.27 (%2.5)	118 (%28)	495.9 (%18)	549.0 (%14)	0.28 (%10)	356.6 (%14)	6.53 (%35)	75.8 (%33)
SW10	22.6 (%3)	8.27 (%1.8)	nm	499.8 (%5)	526.8 (%3)	0.27 (%17)	341.7 (%3)	6.91 (%6)	88.0 (%4)
SW11	14.3 (%39)	8.34 (%3.1)	175 (%19)	292.2 (%26)	364.5 (%19)	0.18 (%19)	236.8 (%19)	8.63 (%23)	94.5 (%19)
SW12	14.3 (%36)	8.58 (%3.3)	185 (%9)	201.6 (%20)	256.6 (%20)	0.12 (%30)	167.1 (%20)	8.77 (%18)	98.0 (%20)
SW13	23.0 (%6)	8.27 (%5.0)	173 (%15)	516.8 (%9)	545.0 (%8)	0.28 (%11)	362.1 (%4)	6.50 (%15)	77.9 (%12)
SW14	14.9 (%34)	8.63 (%2.0)	198 (%11)	405.9 (%15)	506.8 (%8)	0.25 (%22)	329.0 (%8)	7.98 (%22)	85.7 (%18)
SW15	15.2 (%40)	8.49 (%2.3)	192 (%11)	321.4 (%38)	382.4 (%28)	0.17 (%31)	248.6 (%28)	7.02 (%22)	77.0 (%19)
SW16	15.3 (%41)	8.31 (%3.6)	195 (%6)	454.3 (%25)	549.2 (%16)	0.26 (%19)	356.9 (%16)	8.54 (%17)	94.6 (%17)
SW17	11.6 (sm)	7.69 (sm)	260 (sm)	85.0 (sm)	116.0 (sm)	0.10 (sm)	75.7 (sm)	7.80 (sm)	76.5 (sm)
SW18	14.7 (%22)	8.36 (%0.2)	218 (%11)	174.0 (%22)	213.1 (%15)	0.10 (sm)	138.6 (%15)	7.50 (%17)	80.8 (%10)
SW20	12.1 (%33)	8.62 (%2.6)	165 (%22)	348.3 (%10)	452.5 (%2)	0.20 (%1)	294.0 (%2)	8.21 (%22)	82.5 (%19)
SW21	14.0 (%27)	8.70 (%1.3)	178 (%14)	405.0 (%9)	504.7 (%5)	0.23 (%17)	328.1 (%5)	8.63 (%13)	91.8 (%12)

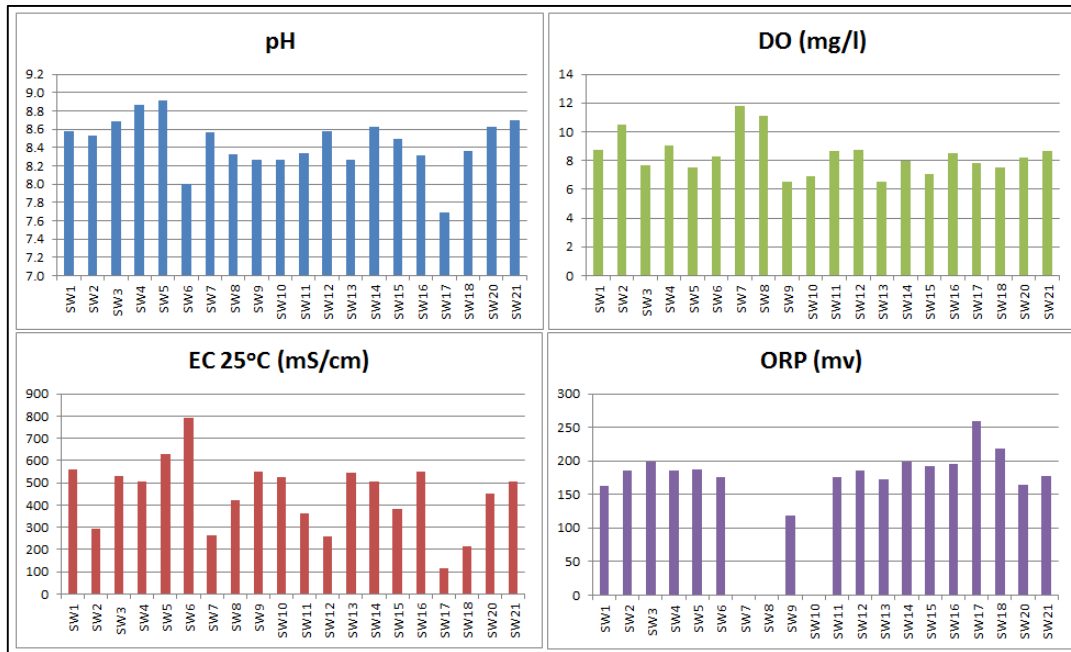


Figure 5.2. Average pH, EC, DO and ORP parameters (single measurement at SW7 and SW17)

Average dissolved oxygen amount is between 6.5 and 11.8 mg/l and average oxidation reduction potential varies between 118 and 260 mV. SW9, SW10, SW13 and SW15 have the lowest; SW2, SW7 (single measurement) and SW8 have the highest dissolved oxygen values, relatively. Also, SW17 and SW18 have the lowest, SW9 has the highest oxidation-reduction value in the study area.

Variation of field parameters in the monitoring period is analyzed with percentage average deviation [% average deviation = (sum of the absolute values of difference between data and average / number of data) x (100/ average)]. These values were calculated for all surface water monitoring points as shown in Table 5.1. From highest to lowest, the % average deviation values were determined for temperature (29%), dissolved oxygen (20%), oxidation-reduction potential (14%), electrical conductivity (14%) and pH (3%).

5.2.2. Analysis of Laboratory Parameters

In 2012 and 2013, water samples have been collected from surface water monitoring points twice a year representing dry and wet seasons. These samples have

been analyzed at ALS Laboratory. Sampling could not be conducted at SW7, SW8, SW17, SW18 and SW19 monitoring points because the flow were not observed at these locations during sampling periods. Detailed chemical analysis results were evaluated.

Water facieses which were determined according to the major ion concentrations are presented in Figure 5.3 and facieses distribution in the study area is presented in Figure 5.4. According to average concentrations of anions, all surface waters are in HCO_3 facieses. According to the average concentrations of cations, the waters at the upstream of the Kirmir Stream are in Na facies, while at the downstream they are in mixed facies. SW11, SW12 (Pazar Stream), SW20 and SW2 have calcium characteristics. On the other hand, the waters of SW3, SW5 and SW6 are in Mg facies, SW4, SW21 are in mixed facies (at the southeast of Kirmir Stream), SW10, SW13 are in Ca facies and SW14, SW15 are in mixed facies (at the west of Kirmir Stream).

The relation between the geologic units within the drainage basins and water facies in the southern reach of the Kirmir Stream was analyzed. It is observed that there is an interaction between carbonate water (SW10, SW13) with Aktepe member, Bezci member and Kocalar member; manganese water (SW3, SW5, SW6) with Çavuşlar member and mixed water with all these members and volcanics.

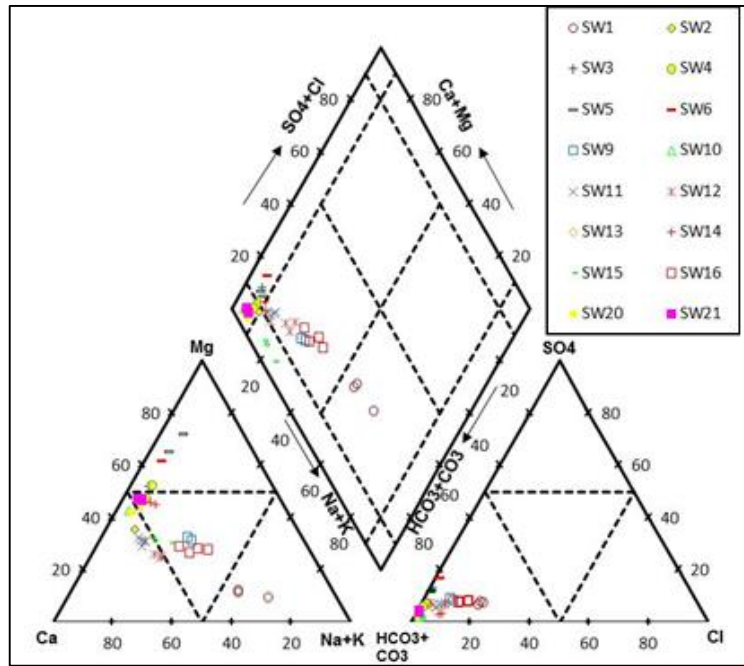


Figure 5.3. Relative distributions of the major ion concentrations of the surface water in 2012 and 2013

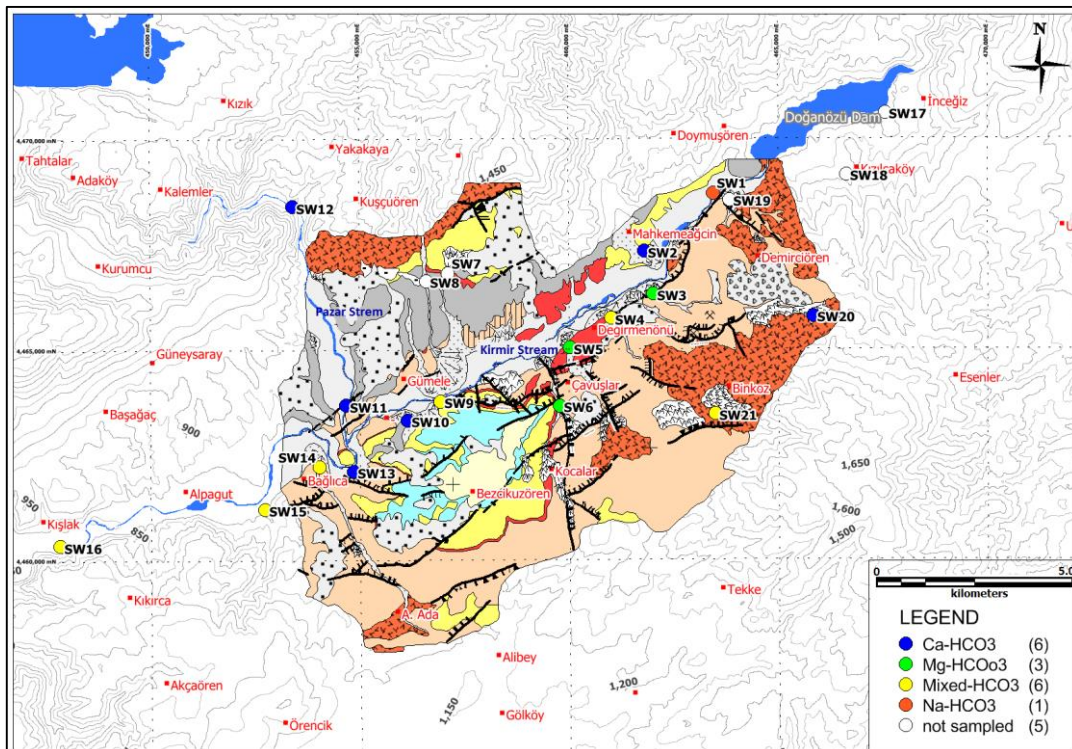


Figure 5.4. Hydrochemical facies distribution according to surface water major ion average concentrations

5.3. GROUNDWATER HYDROCHEMISTRY

A total of 47 fountain locations, 14 villages water depots and 16 pump/monitoring wells had been added into the monitoring program. From these, water depots and wells were taken in only sampling program while fountains were incorporated in monthly monitoring program. Thirty-one fountain locations which are out of the tenements were determined and field parameters were measured at one time only. Some of fountain monitoring points were added after February 2013. All groundwater monitoring locations can be seen on the topographic map in Figure 5.1.

5.3.1. Spring and Fountains

A total of 78 fountain locations were determined in or in the vicinity of the study area. Among these 31 fountain location were monitored only once while other 47 have been monitored regularly. The monitoring points, which are out of the tenements, were monitored only once. Others are in the tenement area except F28. Twenty of them were added after February 2013. F60 and F62 monitoring points had been dry in all monitoring period.

5.3.1.1. Analysis of Field Parameters

Average values of the field parameters (Discharge, pH, EC, DO and ORP) of the regular fountain monitoring points and their average deviations are presented in Table 5.2. Also these field parameters are presented graphically in Figure 5.5.

Discharges of the fountains are generally lower than 0.3 L/s except for F28 (7.6 L/s). However, discharge of F17 (north of the study area), F52 (near the Aşağıadaköy village), and F55, F58, F65 (in the additional points) are greater than 0.3 L/s and vary between 0.4 and 0.8 L/s.

Routine fountain monitoring points have alkaline properties; average pH values vary between 7.29 and 8.21. Generally, waters in magnesium facies (fountains fed from Çavuşlar member dolomitic mudstone) are more basic than waters in calcium facies (fountains fed from Bezci member clayey carbonates, Aktepe member clayey limestone, Kocalar member mudstone, tuffaceous sandstone and volcanic

unit). According to interaction of the rocks, average values of pH in volcanics is 7.64, Çavuşlar member at the layers above the coal is 7.65 and Çavuşlar member at the layers below the coal is 7.87.

The normalized electrical conductivity values (EC at 25 °C) of the fountain monitoring points vary between 207 and 1058 $\mu\text{S}/\text{cm}$. Average EC values according to the probable unit which interact with the water of the fountain from low to high are determined as 519 $\mu\text{S}/\text{cm}$ in volcanics, 557 $\mu\text{S}/\text{cm}$ in carbonates and 692 $\mu\text{S}/\text{cm}$ in Çavuşlar member. Total dissolved solid and salinity values depend on the electrical conductivity values and the values vary between 135-691 mg/l and 0.1-0.5 ppt, respectively.

Average values of the dissolved oxygen values of the fountains vary between 4.8 and 9.3 mg/l. Variations with the interacting units are the same as in pH and EC values. From low to high, they can be listed as 6.79 mg/l in volcanics, 6.82 mg/l in carbonates and 7.32 mg/l in Çavuşlar member.

Average values of the oxidation-reduction potential range between 171 and 232 mv and all waters show oxidation properties. In similar trend with the other field parameters, average ORP values can be listed from low to high as 196 mv in volcanics, 206 mv in carbonates and 216 mv in Çavuşlar member.

Table 5.2. Average hydrochemical field parameters analysis result of fountains (nm: not measurement, sm: single measurement)

Average (%AveDev)	T(°C)	pH	ORP (mv)	EC (mS/cm)	EC 25°C (mS/cm)	S (ppt)	TDS (mg/l)	DO (mg/l)	DO (%)	Q (L/s)	Average (%AveDev)	T(°C)	pH	ORP (mv)	EC (mS/cm)	EC 25°C (mS/cm)	S (ppt)	TDS (mg/l)	DO (mg/l)	DO (%)	Q (L/s)	
F1	15.7 (%22)	7.51 (%2.7)	204 (%23)	461.1 (%9)	559.9 (%2)	0.30 (0)	364.0 (%2)	5.31 (%23)	66.7 (%23)	0.06 (%79)	F45	15.1 (%20)	7.77 (%3.0)	200 (%19)	465.9 (%8)	579.5 (%3)	0.30 (%2)	376.6 (%3)	8.01 (%18)	90.7 (%16)	0.08 (%36)	
F2	15.2 (%14)	7.58 (%2.6)	209 (%16)	439.8 (%6)	543.0 (%5)	0.29 (%9)	355.7 (%4)	6.45 (%18)	74.6 (%19)	0.15 (%27)	F46	12.1 (%44)	7.75 (%2.2)	nm	370.6 (%13)	501.2 (%1)	0.20 (0)	325.7 (%1)	9.30 (%24)	96.7 (%15)	0.08 (0)	
F3	13.9 (%14)	7.70 (%3.0)	205 (%19)	451.3 (%4)	578.8 (%4)	0.30 (%2)	376.0 (%4)	6.89 (%14)	77.3 (%17)	0.23 (%85)	F47	11.9 (%16)	7.95 (%1.3)	224 (%2)	447.9 (%10)	603.7 (%5)	0.30 (0)	391.5 (%4)	7.23 (%18)	72.0 (%18)	0.19 (%57)	
F4	15.4 (%8)	7.62 (%2.9)	192 (%18)	469.0 (%4)	567.9 (%5)	0.30 (0)	377.6 (%3)	7.31 (%13)	84.4 (%16)	0.36 (%70)	F49	15.2 (%30)	7.58 (%1.9)	195 (%16)	867.4 (%13)	1,057.8 (%5)	0.53 (%10)	690.6 (%6)	6.84 (%26)	74.9 (%27)	0.14 (%46)	
F5	14.2 (%19)	7.71 (%2.5)	221 (%14)	374.8 (%8)	478.7 (%4)	0.20 (%5)	308.5 (%3)	7.58 (%21)	83.3 (%22)	0.23 (%100)	F50	14.6 (sm)	7.50 (sm)	nm	585.0 (sm)	745.0 (sm)	0.40 (sm)	484.0 (sm)	7.30 (sm)	90.1 (sm)	nm	
F6	13.5 (%35)	7.89 (%2.7)	207 (%14)	499.6 (%16)	621.4 (%3)	0.30 (%1)	412.4 (%5)	7.89 (%16)	87.3 (%17)	0.03 (%90)	F51	16.9 (%17)	7.60 (%2.4)	195 (%18)	565.0 (%10)	681.6 (%4)	0.32 (%11)	444.0 (%4)	4.88 (%41)	56.3 (%40)	0.18 (%27)	
F7	14.9 (%35)	8.19 (%2.4)	190 (%16)	521.2 (%14)	636.1 (%6)	0.30 (%1)	421.2 (%3)	8.06 (%14)	89.7 (%13)	0.03 (%29)	F52	15.4 (%6)	7.80 (%2.8)	215 (%11)	391.5 (%5)	481.4 (%5)	0.21 (%8)	346.9 (%19)	6.70 (%16)	80.0 (%19)	0.83 (%35)	
F8	15.5 (%18)	8.21 (%2.6)	208 (%16)	343.2 (%7)	421.9 (%2)	0.20 (%1)	274.1 (%2)	7.50 (%17)	86.9 (%16)	0.20 (%16)	F53	14.0 (%8)	7.62 (%3.1)	211 (%17)	525.4 (%5)	667.9 (%3)	0.30 (%1)	433.9 (%4)	5.78 (%20)	64.9 (%21)	0.14 (%33)	
F9	15.8 (%7)	7.63 (%2.4)	219 (%19)	547.6 (%7)	663.3 (%7)	0.31 (%7)	430.5 (%7)	7.32 (%21)	83.6 (%14)	0.07 (%14)	F54	13.4 (%18)	7.69 (%2.0)	191 (%15)	514.1 (%8)	663.3 (%4)	0.30 (%2)	430.8 (%4)	4.82 (%10)	51.7 (%10)	0.19 (%57)	
F10	15.2 (%33)	7.65 (%2.9)	219 (%13)	464.6 (%13)	573.8 (%5)	0.30 (0)	372.8 (%5)	5.47 (%29)	58.6 (%51)	0.08 (%51)	F55	13.5 (%9)	7.51 (%1.8)	203 (%13)	476.2 (%6)	614.6 (%3)	0.31 (%6)	399.7 (%3)	6.35 (%21)	65.4 (%20)	0.69 (%65)	
F11A	14.9 (%37)	8.07 (%3.5)	206 (%12)	478.1 (%16)	587.5 (%3)	0.29 (%7)	381.9 (%3)	7.58 (%19)	82.1 (%30)	0.04 (%30)	F56	13.0 (%24)	7.71 (%1.6)	199 (%23)	418.2 (%12)	540.9 (%5)	0.29 (%6)	351.6 (%5)	5.56 (%19)	58.7 (%18)	0.06 (%66)	
F11B1	15.6 (%26)	7.65 (%1.6)	nm	478.0 (%8)	587.5 (%2)	0.30 (0)	382.0 (%2)	6.83 (%6)	74.1 (%2)	0.12 (%2)	F57	12.8 (%13)	8.03 (%1.6)	209 (%13)	408.6 (%7)	540.7 (%3)	0.29 (%5)	351.5 (%3)	8.52 (%27)	92.5 (%30)	0.14 (%45)	
F11B2	13.1 (%8)	7.68 (%1.2)	nm	455.6 (%1)	594.5 (%2)	0.30 (0)	387.0 (%2)	7.70 (%12)	79.0 (%14)	0.20 (%83)	F58	13.4 (%12)	7.91 (%1.6)	222 (%9)	590.6 (%7)	761.2 (%4)	0.40 (%5)	494.8 (%4)	7.32 (%11)	77.1 (%13)	0.43 (%54)	
F11C	17.7 (%17)	7.81 (%2.3)	229 (%14)	501.9 (%9)	586.3 (%4)	0.30 (%2)	385.8 (%2)	6.26 (%19)	75.7 (%23)	0.12 (%20)	F59	13.5 (%12)	8.00 (%0.6)	232 (%14)	495.5 (%6)	637.7 (%4)	0.30 (%3)	414.3 (%4)	7.39 (%14)	136.2 (%75)	0.21 (%40)	
F12	13.8 (%25)	7.79 (%2.4)	213 (%23)	531.0 (%9)	673.3 (%3)	0.42 (%54)	440.3 (%2)	7.52 (%16)	83.3 (%16)	0.20 (%35)	F61	12.9 (%6)	7.85 (%1.4)	228 (%15)	542.6 (%5)	704.9 (%4)	0.39 (%6)	461.1 (%4)	7.53 (%19)	77.4 (%22)	0.29 (%21)	
F13	12.8 (%27)	7.60 (%3.1)	227 (%18)	721.6 (%11)	930.1 (%7)	0.49 (%5)	624.7 (%5)	6.38 (%19)	69.3 (%17)	0.29 (%66)	F63	13.4 (%12)	7.63 (%1.6)	218 (%15)	521.6 (%6)	670.4 (%3)	0.30 (%1)	435.4 (%3)	5.99 (%20)	61.0 (%16)	0.06 (%10)	
F14	12.4 (%28)	7.92 (%4.4)	225 (%12)	618.2 (%13)	817.5 (%7)	0.40 (%4)	531.5 (%7)	7.54 (%17)	79.9 (%19)	0.24 (%85)	F64	13.3 (%14)	7.62 (%2.7)	196 (%21)	484.2 (%7)	625.3 (%4)	0.30 (%3)	406.7 (%4)	7.60 (%14)	79.9 (%16)	0.82 (%168)	
F15	11.9 (%18)	7.88 (%2.4)	208 (%20)	380.8 (%11)	502.9 (%7)	0.25 (%19)	326.8 (%7)	7.08 (%22)	74.7 (%22)	0.23 (%38)	F65	13.6 (%14)	7.29 (%2.4)	186 (%28)	190.0 (%17)	245.0 (%14)	0.10 (0)	158.8 (%14)	6.93 (%11)	73.4 (%13)	0.51 (%102)	
F16	13.5 (%38)	7.56 (%3.1)	213 (%21)	590.6 (%11)	773.5 (%17)	0.37 (%21)	503.2 (%17)	7.03 (%17)	74.0 (%23)	0.19 (%131)	F66	13.2 (%10)	7.33 (%3.0)	188 (%22)	160.5 (%15)	207.0 (%12)	0.10 (%4)	135.1 (%12)	7.01 (%14)	73.9 (%16)	0.12 (%89)	
F17	16.7 (%18)	7.55 (%3.0)	217 (%16)	458.0 (%8)	544.6 (%2)	0.30 (%3)	354.4 (%2)	7.65 (%13)	89.6 (%3)	0.80 (%50)	F67	12.4 (%13)	8.01 (%1.5)	181 (%14)	345.1 (%6)	455.4 (%4)	0.20 (%1)	296.5 (%4)	7.75 (%22)	84.8 (%25)	0.11 (%67)	
F28	22.2 (%6)	7.47 (%2.9)	186 (%17)	343.4 (%4)	370.3 (%3)	0.20 (%3)	240.0 (%3)	3.94 (%22)	50.6 (%21)	7.59 (%27)	F68	14.1 (%10)	7.67 (%1.4)	171 (%16)	405.7 (%6)	511.8 (%4)	0.29 (%8)	332.1 (%4)	5.13 (%27)	55.6 (%27)	0.31 (%30)	
F37	12.8 (%13)	7.84 (%1.6)	219 (%13)	608.0 (%7)	801.6 (%3)	0.42 (%8)	520.8 (%3)	7.41 (%12)	75.4 (%14)	0.04 (%48)	F69	13.1 (%12)	8.18 (%1.5)	218 (%3)	393.1 (%11)	510.2 (%8)	0.27 (%13)	331.6 (%8)	8.37 (%11)	80.0 (%10)	0.08 (%9)	
F37B	14.6 (%25)	8.03 (%1.9)	201 (%18)	472.0 (%14)	588.1 (%5)	0.29 (%4)	382.2 (%5)	7.32 (%15)	79.8 (%15)	0.11 (%121)												

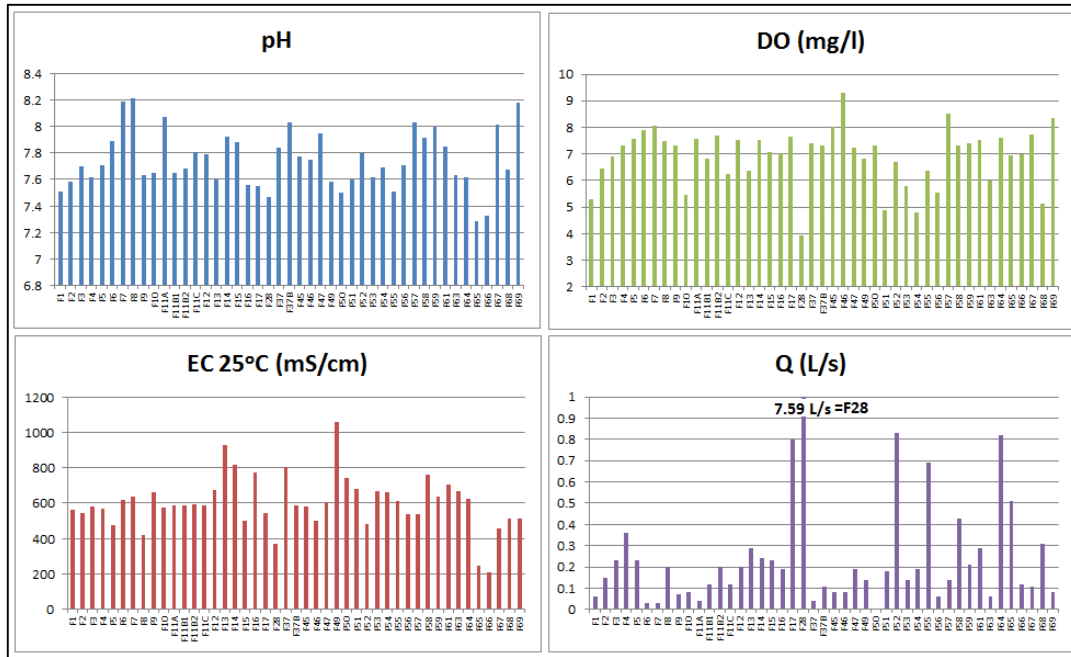


Figure 5. 5. Average pH, EC, DO and ORP parameters of fountain monitoring points

Percentage average deviations from averages values of the field parameters were calculated of the waters of the routine monitoring points and they are presented in Table 5.2. Deviations from high to low were determined as 53.5% in discharge, 18% in temperature, 17.8% in dissolved oxygen, 16% in oxidation reduction potential, 4.6 % in electrical conductivity and 2.3 % in pH values.

The field parameters of the secondary monitoring points which are located out of the tenement areas were measured at once and their values are listed in Table 5.3.

Table 5.3. Field parameters of the fountain monitoring points which are located out of the tenements

ID	Date	T(°C)	pH	EC (mS/cm)	EC 25°C (mS/cm)	S (ppt)	TDS (mg/l)	DO (mg/l)	DO (%)	Q (L/s)
F18	Apr-12	13.0	7.13	439.8	571.7	0.3	371.5	6.30	68.9	0.820
F19	Apr-12	10.3	7.59	376.1	524.3	0.3	340.7	6.70	64.6	1.136
F20	Apr-12	8.5	7.59	361.1	546.8	0.3	355.5	8.50	81.3	2.910
F21	Apr-12	10.8	7.71	286.1	396.1	0.2	257.2	8.00	82.2	0.685
F22	Apr-12	12.2	7.57	466.4	617.2	0.3	400.9	7.00	72.9	0.510
F23	Apr-12	12.6	7.91	454.1	607.3	0.3	364.9	8.10	83.7	0.314
F24	Apr-12	11.1	7.54	359.0	494.5	0.2	321.0	5.50	55.1	1.000
F25	Apr-12	9.2	7.36	351.3	508.8	0.2	330.9	4.20	40.0	0.319
F26	Apr-12	9.2	7.27	388.7	564.2	0.3	366.5	6.80	66.9	0.073
F27	Apr-12	14.5	8.12	318.4	401.5	0.2	261.2	6.10	66.6	0.174
F29	Apr-12	20.1	7.36	325.4	364.7	0.2	237.2	4.50	54.2	0.862
F30	Apr-12	11.2	7.75	403.0	564.7	0.3	367.0	7.10	73.7	0.145
F31	Apr-12	13.4	7.59	373.7	489.8	0.2	318.0	6.30	59.8	0.100
F32	Apr-12	11.3	7.35	423.5	584.3	0.3	379.7	6.40	66.9	0.081
F33	Apr-12	9.4	7.41	205.3	299.9	0.1	194.6	7.20	73.0	0.848
F34	Apr-12	9.2	7.50	176.0	252.6	0.1	164.1	7.30	72.0	0.625
F35B	Apr-12	9.9	7.52	441.6	634.4	0.3	415.4	7.20	71.4	0.455
F36	Apr-12	14.5	7.48	590.0	746.0	0.4	485.0	5.30	57.8	0.040
F36B	Apr-12	14.0	7.31	558.0	709.0	0.3	461.0	4.00	42.0	0.057
F38	Apr-12	14.2	7.94	662.0	862.0	0.4	561.0	6.70	65.7	0.358
F39	Apr-12	11.7	7.57	647.0	892.0	0.4	580.0	6.30	67.1	0.016
F40	Apr-12	9.8	7.49	218.0	309.5	0.1	201.2	7.10	74.4	0.490
F41	Apr-12	9.5	7.27	57.0	81.0	0.0	52.6	6.80	74.2	0.446
F42A	Apr-12	9.2	7.52	294.7	429.1	0.2	278.7	7.60	66.9	0.500
F42B	Apr-12	12.5	7.59	341.0	458.0	0.2	297.5	6.40	67.4	0.556
F42C	Apr-12	9.0	7.78	257.8	377.8	0.2	245.4	7.40	72.9	2.261
F42D	Apr-12	11.1	7.53	381.7	523.8	0.3	340.0	6.20	57.3	0.289
F43	Apr-12	12.5	7.36	519.0	689.0	0.3	448.0	3.70	36.0	nm
F44	Feb-12	8.9	8.30	222.4	321.5	0.2	209.1	7.00	67.5	0.146
F48	Apr-12	11.0	7.45	57.5	78.7	0.0	51.1	6.40	66.6	0.075

5.3.1.2. Analysis of Laboratory Parameters

Water sampling had been conducted at fountain monitoring points in dry and wet seasons in 2012 and 2013. Because F47, F62 and F60 were dry and F69 was added after sampling periods, these points were not sampled.

According to average major ion concentrations, water facies and distributions in the study area are presented in Figure 5.6-5.7, respectively. Possible rock units which interact with the waters were determined by considering the chemical properties of the water and lithological information. With respects to the anion content, all fountain waters in the study area are in HCO₃ facies. According to cation content, the fountain waters in the study area were divided into three; Mg facies, Ca facies and mixed facies. In detail, the fountain waters which are fed from Çavuşlar

member which constitutes the lacustrine sedimentary rocks (mudstone, claystone, siltstone, bituminous shale and tuff) are in Mg facies. Those fountains fed from Bezci member (sandstone, claystone and clayey carbonates), Aktepe member (clayey limestone), Kocalar member (mudstone, tuffaceous sandstone) and lava and pyroclastics (except for F67) are in Ca facies. The fountains that have been affected from some of these units are in mixed facies.

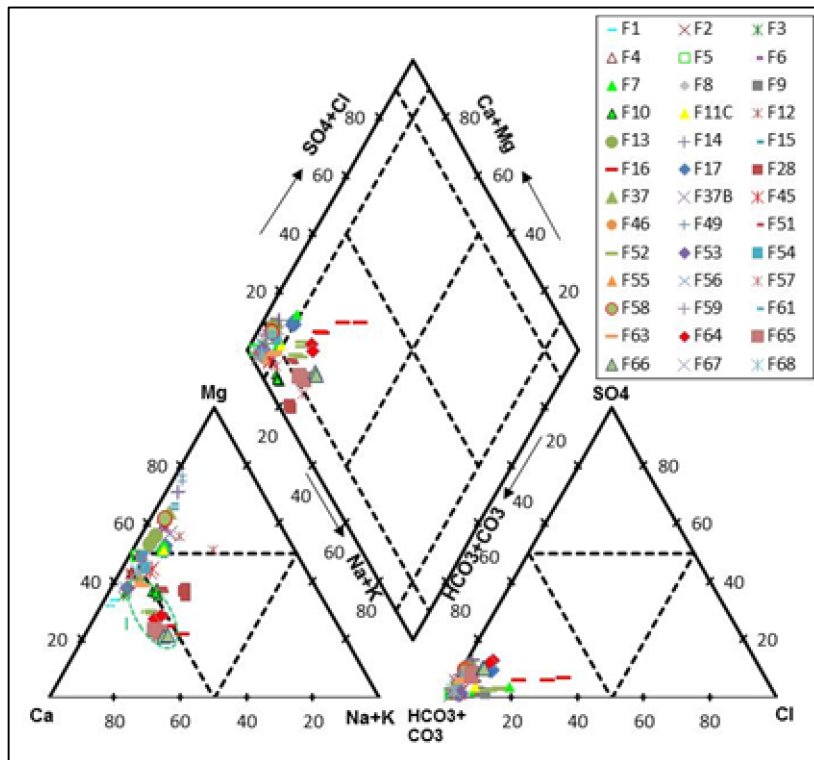


Figure 5.6. Relative distributions of the major ion concentrations of the fountains in 2012 and 2013

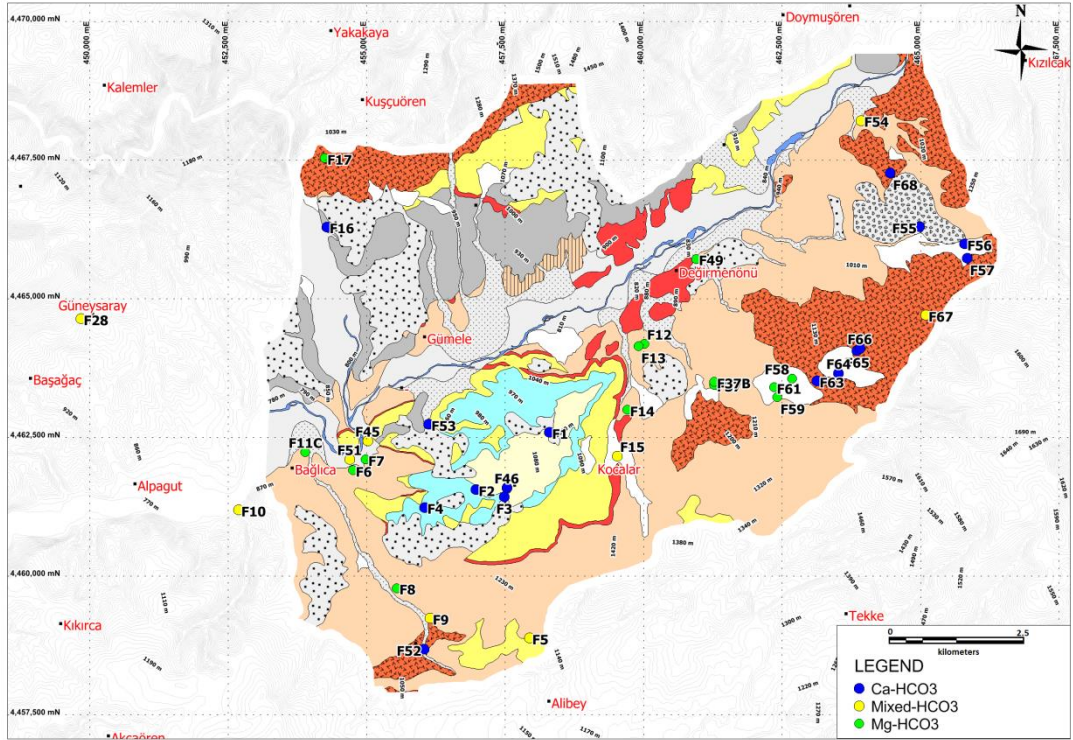


Figure 5.7. Areal distributions of hydrochemical facies according to major ion average concentrations of fountain monitoring points

Table 5.4. Probable lithological units which interact with fountain water and cation facies of the fountain monitoring points

ID	Possible Units Which Interact with Water	Cation Facies	ID	Possible Units Which Interact with Water	Cation Facies
F1	Bezci member	Ca	F45	Çavuşlar member and Kocalar m..	Mixed
F2	Aktepe member (Bezci m.?)	Ca	F46	Aktepe member	Ca
F3	Kocalar m. and Aktepe m.	Ca	F49	Çavuşlar m.	Mg
F4	Aktepe m.	Ca	F51	Çavuşlar member and Kocalar m..	Mixed
F5	Kocalar m. and Çavuşlar m.	Mixed	F52	Volcanics	Ca
F6	Çavuşlar m.	Mg	F53	Kocalar m. and Aktepe m.?	Ca
F7	Çavuşlar m.	Mg	F54	Çavuşlar m. and Volcanics	Mixed
F8	Çavuşlar m.	Mg	F55	Volcanics	Ca
F9	Çavuşlar m. and Volcanics	Mixed	F56	Volcanics	Ca
F10	?	Mixed	F57	Volcanics	Ca
F11C	Çavuşlar m.	Mg	F58	Çavuşlar m.	Mg
F12	Çavuşlar m.	Mg	F59	Çavuşlar m.	Mg
F13	Çavuşlar m.	Mg	F61	Çavuşlar m.	Mg
F14	Çavuşlar m.	Mg	F63	Volcanics?	Ca
F15	Çavuşlar m., Abacı m., Kocalar m.?	Mixed	F64	Volcanics	Ca
F16	?	Ca	F65	Volcanics	Ca
F17	?	Mg	F66	Volcanics	Ca
F28	?	Mixed	F67	Çavuşlar m. and Volcanics	Mixed
F37	Çavuşlar m.	Mg	F68	Volcanics	Ca
F37B	Çavuşlar m.	Mg			

Clayey carbonates in Bezci member, mudstones in Kocalar member and clayey limestones in Aktepe member bring in calcium facies to the water. It is expected that the waters which are fed from volcanic lavas and pyroclastics should have been in the sodium facies, but they show the calcium facies properties. This is more likely due to the shallow circulation of waters and their reaction with the clayey levels in pyroclastics (Table 5.4).

5.3.2. Wells

Field parameters could be measured from wells generally at sampling periods because it was difficult to take fresh aquifer water from wells at routine monthly monitoring. In addition, in some of the wells in which pump tests (PW1, PW3, PW5 and PW6) were conducted, field parameters were measured during these tests. Free flow is observed at some of the sampled wells (PW4A, CEL35, CEL47A, CEL53A, CEL59A, PW5 and CEL59B). Also, electrical conductivity (EC at 25°C) and temperature (T) profiles were taken at some monitoring wells. A summary of the

field parameters measured is presented in Table 5.5. Measurements at the end of the screen at PW2 and CEL43 and at the start and end of the screen at PW4A could not be taken. Hence, the best fit linear equations of the measurements were used to represent these levels. Location of the wells at which field parameters are measured or sampling is conducted is shown in Figure 5.1.

5.3.2.1. Analyses of Field Parameters

Temperature values generally increase linearly down to the screen level in all the wells. The average temperature values at the screen levels in the wells are listed in Table 5.6 and presented graphically in Figure 5.8. The temperatures at deeply circulating groundwaters of the volcanics penetrated by PW4A and PW1 reach 43.8 °C and 39.6 °C, respectively. These wells have the highest groundwater temperatures observed in the study area. The temperature of the waters at the bottom of the coal layers in Çavuşlar member (CEL35 and CEL36) is approximately 33 °C. If an average 3°C temperature gradient at each 100 meter depth and a near surface water temperature of 14 °C are assumed, then water temperatures at the screen depths are about 17 °C higher than the gradient temperatures in PW4A and PW1 wells. The same condition is also noted at CEL35 and CEL36 wells, but the water temperatures are about 10 °C higher than the gradient temperatures. This indicates that deeply circulating groundwater in the study area shows geothermal characteristics. The preliminary geothermometer calculation conducted using the data of PW4A indicates that the reservoir temperatures is in the range of 75-106 °C. The temperatures of 75-86 °C is observed at the deep geothermal wells in the Kızılcahamam town which is located 20 km away from the study area (MTA, 2005).

Electrical conductivity values at the screen levels in the monitoring wells are listed in Table 5.6 and presented graphically in Figure 5.99. EC values vary between 400 and 3217 µS/cm in the monitoring wells. The highest electrical conductivity values were observed at the wells which screen the volcanics and the lowest values were observed at the wells which screen the units above the Çavuşlar member. The anomalously high electrical conductivity observed at PW2 which is screened above the coal layer in the Çavuşlar member is attributed to the low value of the hydraulic conductivity ($K=1.84 \times 10^{-8}$ m/s) causing a long duration for rock-water reaction.

Table 5.5. Hydrochemical field parameters of the monitoring wells which were measured at sampling

Well ID	Date	T (°C)	pH	ORP (mv)	EC (mS/cm)	EC (mS/cm) 25 °C	S (ppt)	TDS (mg/l)	DO (mg/l)	DO%	Lithological Unit	
PW3	Average	17.9-19*	7.97-8.08*	135	405	473-490*	0.3	307	2.9	32.3	Aktepe m. and Kocalar m.	
CEL59B	Sep-13	15.9	9.28	127	740	904	0.4	588	1.0	10.1	Çavuşlar m.	Above the Çoal
PW2	Oct-12	23.7	9.76	149	4473	4587	2.5	2980	1.2	16.2	Çavuşlar m.	Above the Çoal
CEL47A	Sep-13	17.9	8.49	120	740	861	0.4	560	0.4	4.3	Çavuşlar m.	In the Çoal
CEL53A	Sep-13	17.9	8.45	181	814	911	0.5	592	0.6	7.1	Çavuşlar m.	In the Çoal
CEL59A	Sep-13	18.0	8.32	115	818	964	0.5	627	0.8	9.2	Çavuşlar m.	In the Çoal
PW5	Nov-13	22.4*	8.57*	nm	846	891*	0.4	578.0	1.3	14.8	Çavuşlar m.	In the Çoal
PW6	Nov-13	20.5*	8.99*	nm	787	874*	0.4	565.0	1.9	20.1	Çavuşlar m.	In the Çoal
CEL35	Sep-13	15.3	8.11	107	707	870	0.4	565	0.6	6.2	Çavuşlar m.	Below the Çoal
CEL44	Oct-13	15.2	9.24	0	634	784	0.4	509	9.2	95.8	Çavuşlar m.	Below the Çoal
CEL51	Oct-13	19.7	9.40	0	689	767	0.4	499	7.3	84.6	Çavuşlar m.	Below the Çoal
CEL36	Oct-13	17.4	10.59	0	692	820	0.4	533	8.6	94.1	Çavuşlar m.	Below the Çoal
CEL47	Oct-13	14.5	10.47	0	587	737	0.4	479	4.8	48.2	Çavuşlar m.	Below the Çoal
PW1	Average	36.2-38.3*	7.49-7.57*	328	3023	2488-2675*	1.3	1617	1.0	14.0	Volcanics	Below the Çavuşlar m.
PW4A	Sep-13	25.9	8.05	127	3225	3206	1.7	208	0.9	12.9	Volcanics	Below the Çavuşlar m.
CEL52	Oct-13	13.7	8.67	0	971	1259	0.6	818	7.6	79.1	Volcanics	Below the Çavuşlar m.

*Measurement at pump tests

Table 5.6. Electrical conductivity (EC) and Temperature (T) values of the wells at the bottom and top of the screen level

Well ID	Depth to Top of the Screen Level (m)	Depth to Bottom of the Screen Level (m)	Measurement Depth of Top of the Screen Level (m)	T °C	EC (µS/cm) 25 °C	Measurement Depth of Bottom of the Screen Level (m)	T °C	EC (µS/cm) 25 °C	Average T °C	Average EC (µS/cm) 25 °C	Lithological Unit	
PW3	36.0	128.0	36	15.7	388.6	130	17.9	410	16.8	399	Aktepe m. and Kocalar m.	
CEL59B	86.5	104.5				nm					Çavuşlar m.	Above the Coal
PW2	76.0	168.0	77	21	2011	168	30.3	?	25.7	2011	Çavuşlar m.	Above the Coal
CEL47A	143.6	152.1	140	23.2	810	150	23.6	812	23.4	811	Çavuşlar m.	In the Coal
CEL53A	106.8	124.8	110	22	831	120	22.2	845	22.1	838	Çavuşlar m.	In the Coal
CEL59A	106.0	124.0				nm					Çavuşlar m.	In the Coal
PW5	114.0	133.0	114	22.5	855	140	23	882	22.8	869	Çavuşlar m.	In the Coal
PW6	144.0	160.0	144	22.5	937	160	23.4	949	23.0	943	Çavuşlar m.	In the Coal
CEL61	237.8	252.1	240	28.2	1138	250	29.1	1148	28.7	1143	Çavuşlar m.	Below the Coal
CEL35	277.0	300.0	270	32.4	844	300	33.9	911	33.2	878	Çavuşlar m.	Below the Coal
CEL44	180.5	197.6	180	24.6	722	200	25.5	736	25.1	729	Çavuşlar m.	Below the Coal
CEL51	191.6	205.9	190	25.3	1221	210	26.5	833	25.9	1027	Çavuşlar m.	Below the Coal
CEL43	220.0	237.1	220	27.9	2568	237	29.5	1561	28.7	2065	Çavuşlar m.	Below the Coal
CEL64	245.0	262.1	250	23.7	1099	265	30.2	1096	27.0	1098	Çavuşlar m.	Below the Coal
CEL36	270.0	299.0	270	31.5	1194	300	32.8	770	32.2	982	Çavuşlar m.	Below the Coal
CEL47	175.7	187.1	170	24.9	614	190	25.8	717	25.4	666	Çavuşlar m.	Below the Coal
CEL52	180.4	194.7	180	25.3	1161	190	26.8	1331	26.1	1246	Volcanics	Below the Çavuşlar m.
CEL25	195.0	210.0	190	24.5	616	210	26	596	25.3	606	Volcanics	Below the Çavuşlar m.
CEL50	131.0	148.1	130	20.1	1293	149	21.4	1710	20.8	1502	Volcanics	Below the Çavuşlar m.
PW1	240.0	272.0	240	38.8	2407	270	40.4	2432	39.6	2420	Volcanics	Below the Çavuşlar m.
PW4A	390.0	432.0	390	43.2	3205.9	432	44.4	3228.8	43.8	3217	Volcanics	Below the Çavuşlar m.

Highlighted values were calculated from the best fit equation

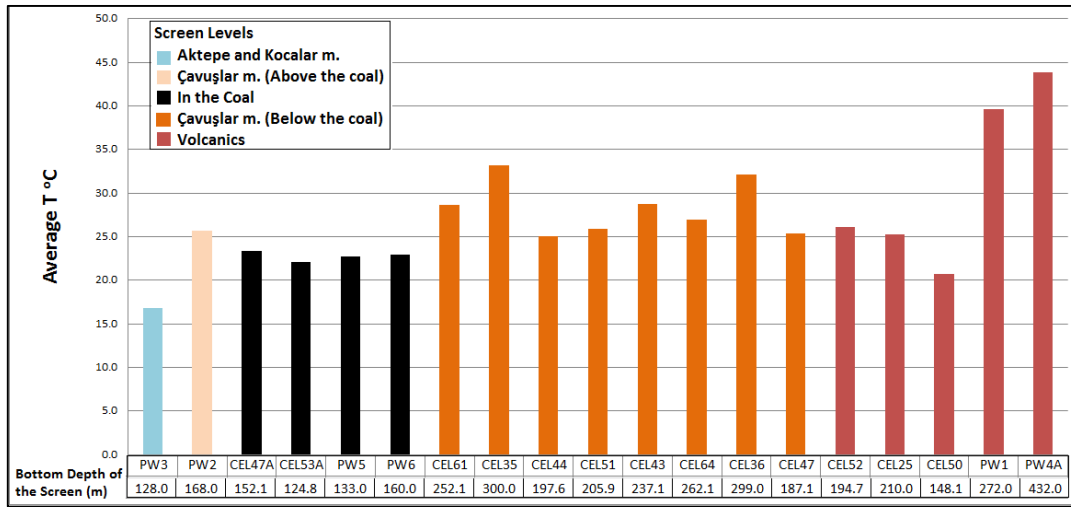


Figure 5.8. Distribution of the average temperature of the wells in the screen level

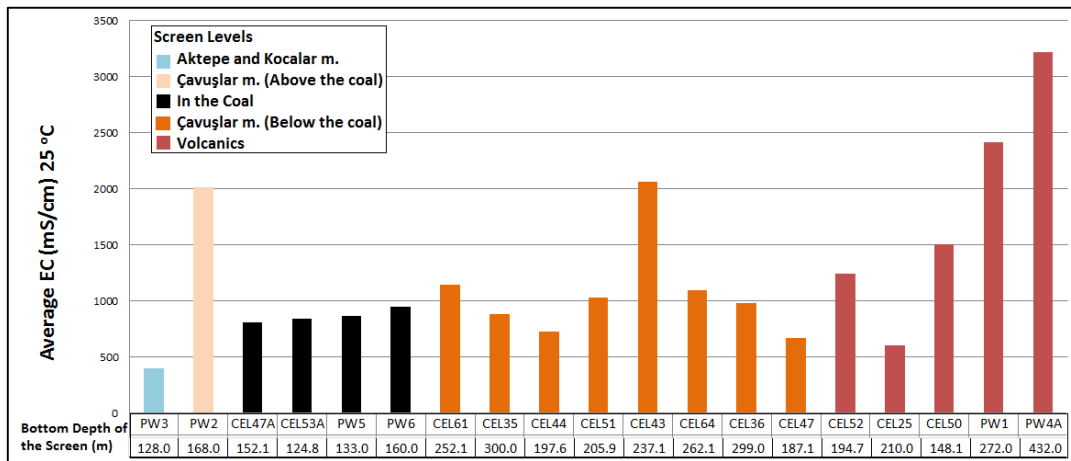


Figure 5.9. Distribution of the average electrical conductivity of the wells in the screen level

Well waters have basic properties and pH values range between 7.49 and 10.59 (Table 5.5). According to the lithological unit distribution, deeply circulating volcanic unit groundwater (PW1 and PW4A) and groundwater in well PW3 screened in Kocalar and Aktepe members have relatively low pH values (7.49-8.05). Groundwater in the coal seam is more basic and pH values vary between 8.32 and 8.49. Groundwater in the wells in Çavuşlar member filtered at above or below the coal zone is much more basic (9.24-10.59) except for CEL35.

The dissolved oxygen amount in the groundwater is in the range between 0.4-9.2 mg/l. Groundwater in the Çavuşlar member below the coal and volcanics which is relatively shallow circulating have the highest dissolved oxygen values (4.8 and 9.2 mg/l). Whereas groundwater of deeply circulating volcanics, coal zone and Çavuşlar member above the coal have less dissolved oxygen values (0.6-1.3 mg/l). Dissolved oxygen value of the groundwater of the units which overlie the Çavuşlar member is approximately 3 mg/l.

Oxidation-reduction potential could be measured only from a few well. The highest value was recorded at PW1 with 328 mv. The other values vary between 107-150 mv. In addition, measured ORP values from the well waters in the study area show the oxidation characteristics.

5.3.2.2. Analyses of Laboratory Parameters

Water sampling campaign for monitoring wells was conducted in 2012 (only PW1 and PW3 well) and 2013. Figure 5.10 shows the distributions of the well waters in Piper Diagram according to the major ion concentration. Their areal distribution is presented in Figure 5.11. According to anion content, all well waters are in HCO_3 facieses, except for PW2 which is in Cl facies. According to cation content, waters in wells screened in volcanics (PW4A, PW1, CEL52) are in Na facies, those screened in Çavuşlar member below the coal zone are in Mg (CEL35, CEL44, CEL51) or Na (CEL36, CEL47) facieses. The well waters screened in the coal seam are in Na (PW6, CEL47A, CEL59A, and CEL53A) or Mg (PW5) facieses. The well waters screened in Çavuşlar member above the coal zone are in Na (PW2, CEL59B) facieses. PW3 well which is screened in Kocalar and Aktepe member overlying the Çavuşlar member is in mixed facies according to cation content.

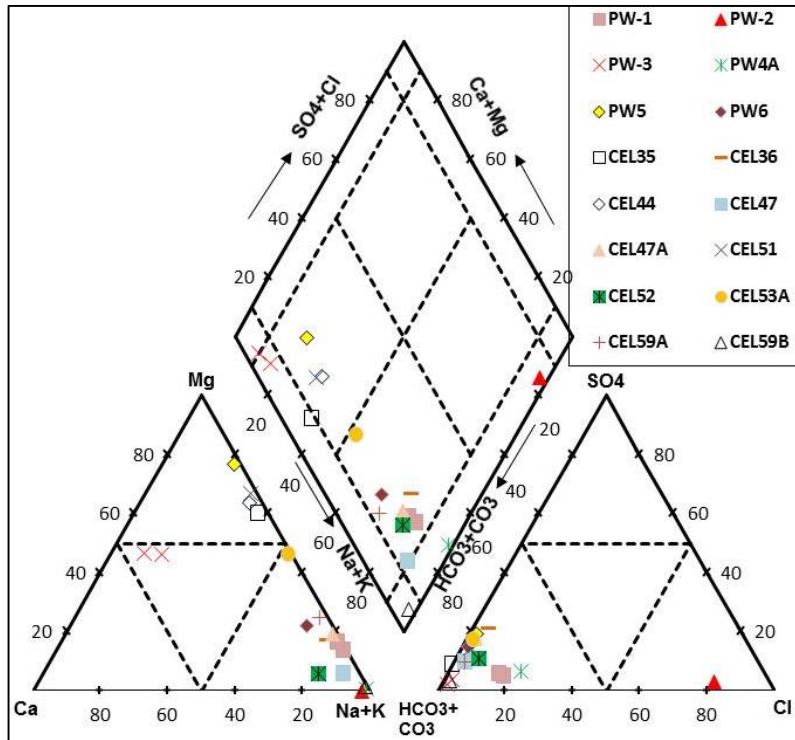


Figure 5.10. Relative distributions of the major ion concentrations of the well waters in 2012 and 2013

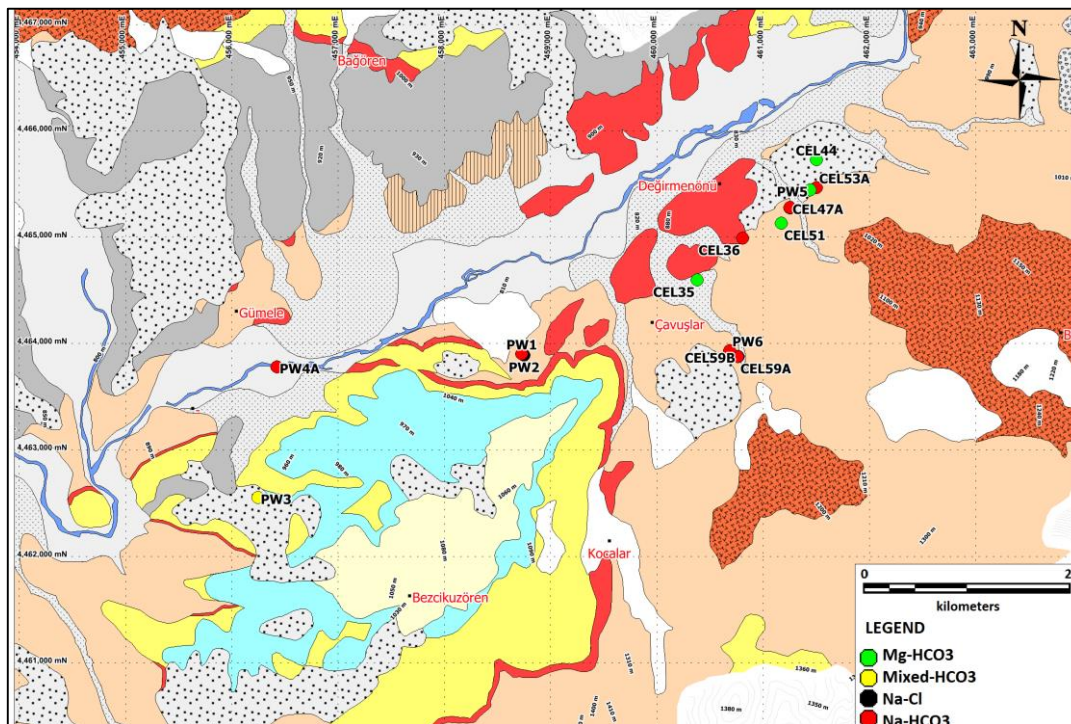


Figure 5.11. Areal distributions of hydrochemical facies according to major ion average concentrations of well monitoring points

There is a coherency of Mg facies water observed in the wells which is screened in Çavuşlar member, below the coal (CEL35, CEL44 and CEL 51) and in the coal (PW5) and fountain waters which are fed from these units. This coherency probably comes from interaction with mudstone. The reason why water of CEL36 which is screened in Çavuşlar member, below the coal is in Na facies is that this well is either mixed from the units in Na facies and/or there is a rock-water reaction within the unit. Likewise, it is thought that the reason for Na facies of the well waters of CEL47 which is screened in Çavuşlar member below the coal seam, CEL47A, CEL53A, CEL59A, PW6 which are screened in the coal seam and CEL59B which is screened in Çavuşlar member above the coal seam is probably caused by mixing and/or reactions.

The Na-Cl facies seen in PW2 well which is screened in Çavuşlar member above the coal seam is probably caused by the low hydraulic conductivity ($K=1.84 \times 10^{-8}$ m/s) producing a longer duration for rock water interaction. Measured high electrical conductivity values (EC at 25°C=2011µS/cm) also supports this comment.

5.3.3. Villages Water Depots

Field parameters were measured from the villages' water depots at the sampling periods. D11-D14 water depots were added in 2013 monitoring period after the expanding of the tenement area. Figure 5.1 shows the location of the water depot monitoring points.

5.3.3.1. Field Parameters

Average values of the field parameters (pH, EC, DO and ORP) of the villages' water depots and their average deviations are presented in Table 5.7. Domestic water of the villages is basic and their pH values are in the range between 7.72 and 8.42. Normalized electrical conductivity values (EC at 25 °C) change between 196-968 µS/cm. The salinity (S) and total dissolved solid (TDS) values which change with electrical conductivity are in the range between 0.2-0.5ppt and 126-614 mg/l, respectively. Average values of oxygen values change between 5.5-11.1 mg/l and average values of oxidation reduction potential are in the range between 128-230 mv. All waters have oxidation property. These values are graphically presented in

Figure 5.12. From high to low, the percentage average deviation are determined in the following order: dissolved oxygen (21.2), oxidation-reduction potential (9), temperature (4), electrical conductivity (3) and pH (3).

Table 5.7. Hydrochemical field parameters of the village water depots

Average (%AveDev)	T (°C)	pH	ORP (mv)	EC (mS/cm)	EC 25°C (mS/cm)	S (ppt)	TDS (mg/l)	DO (mg/l)	DO (%)
D1	20.1 (%4)	8.10 (%2.8)	162 (%1)	384.7 (sm)	413.9 (%5)	0.20 (sm)	283.5 (%1)	5.48 (%14)	63.7 (%15)
D2	17.8 (sm)	8.07 (%3.3)	165 (%2)	805.5 (%4)	865.8 (%5)	0.45 (%11)	592.0 (sm)	7.10 (%28)	83.0 (%32)
D3	17.3 (%5)	8.42 (%0.5)	200 (%28)	468.1 (%5)	546.1 (%3)	0.30 (sm)	362.0 (%3)	8.85 (%37)	99.2 (%39)
D4	17.6 (%1)	8.19 (%2.1)	161 (%4)	801.5 (%3)	967.8 (%4)	0.50 (sm)	614.0 (%3)	6.90 (%26)	80.6 (%28)
D5	14.2 (%5)	7.74 (%1.9)	128 (%22)	420.7 (%3)	533.3 (%3)	0.28 (%14)	346.6 (%3)	6.98 (%20)	80.1 (%20)
D6	19.4 (%5)	8.19 (%1.3)	130 (sm)	627.0 (%1)	701.5 (%1)	0.35 (%14)	461.0 (%1)	9.10 (%1)	108.2 (%4)
D7	20.6 (sm)	8.14 (%3.4)	180 (sm)	527.0 (sm)	569.0 (%3)	0.30 (sm)	385.0 (sm)	11.10 (sm)	138.4 (sm)
D8	20.4 (%5)	7.88 (%3.4)	211 (%2)	540.5 (sm)	594.8 (%3)	0.30 (sm)	389.5 (sm)	6.60 (%45)	80.2 (%49)
D9	22.9 (sm)	7.83 (%4.2)	230 (sm)	172.7 (sm)	195.7 (%1)	0.10 (sm)	126.4 (sm)	8.10 (sm)	92.5 (sm)
D10	18.0 (%1)	8.15 (%1.5)	211 (%4)	579.0 (%3)	662.8 (%4)	0.30 (sm)	429.0 (sm)	8.10 (%40)	96.4 (%44)
D11	15.7 (%3)	8.01 (%0.5)	125 (%15)	502.2 (%2)	611.9 (%1)	0.30 (sm)	397.8 (%1)	7.10 (%35)	76.8 (%35)
D12	16.7 (%5)	7.99 (%0.5)	139 (sm)	425.0 (%2)	512.4 (sm)	0.25 (%20)	333.0 (sm)	8.03 (%2)	90.8 (%4)
D13	18.6 (%7)	8.10 (%1.1)	132 (%22)	402.8 (%1)	467.2 (sm)	0.20 (sm)	303.9 (sm)	7.80 (%28)	94.7 (%33)
D14	18.9 (%10)	7.93 (%4.5)	223 (%31)	450.0 (sm)	541.4 (sm)	0.30 (sm)	352.0 (sm)	6.50 (%29)	70.9 (%29)

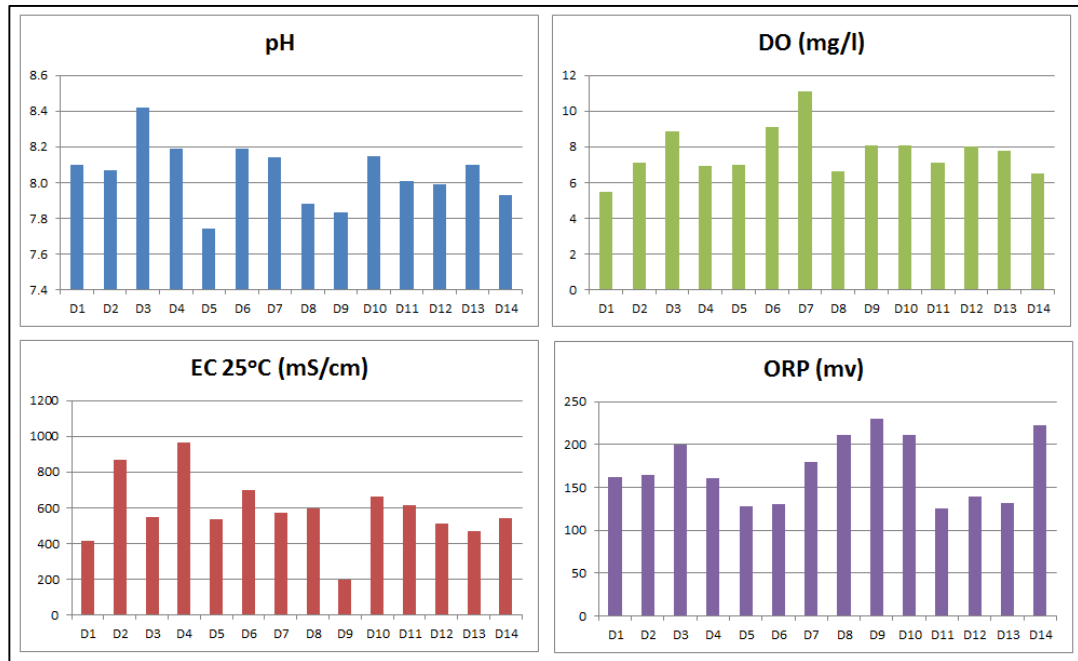


Figure 5.12. Average pH, EC, DO and ORP parameters of village water depots

5.3.3.2. Laboratory Parameters

Water facieses of the depots which are determined according to the major ion concentrations are shown in Figure 5.13. Bezcikuzören (D6), Çeltikçi (D9), Binkoz (D12), Demirciören (D13) and Kızılca (D14) waters are in Ca-HCO₃ facies, Değirmenönü (D2), Bağören (D3), Çavuşlar (D4), Aşağıada (D7) and Peykler (D11) waters are in Mg-HCO₃ facies, and Mahkemeağacı (D1), Bağlıca (D8) and Gümele (D10) waters are in Mixed-HCO₃ facies.

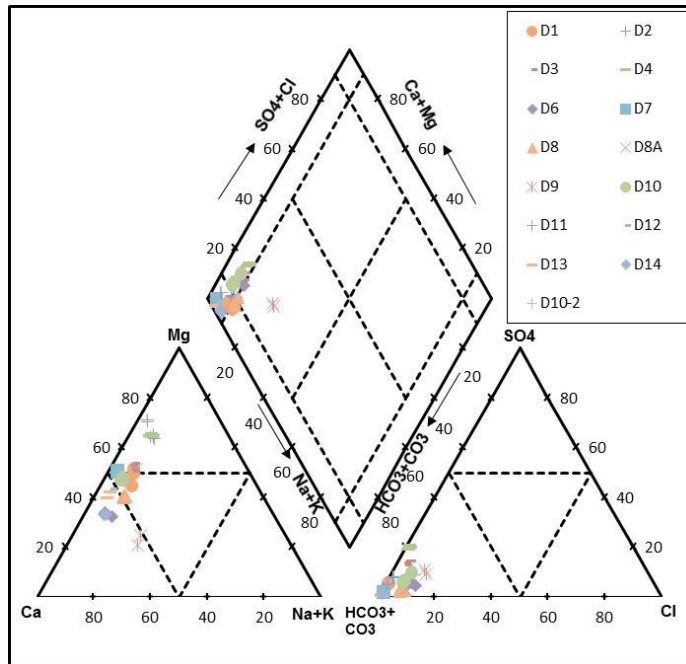


Figure 5.13. Relative distributions of the major ion concentrations of the water depots in the villages

5.4. WATER QUALITY

Water quality assessments were evaluated based on inland water resources classification (YSKYY, 2012) for surface waters, inland water resources groundwater classification (SKKY, 2008; YKBKK, 2012), irrigation water classification (AATTUT, 2010) and limits for human consumptions (İTAS, 2005; EU, 1998).

5.4.1. Surface Water

Surface water quality classifications were evaluated according to inland water resources surface water classification and drinking water limits for human consumptions. Their summary is presented in Table 5.8 and areal distribution of the water classifications according to inland water classification can be seen in Figure 5.14.

When average concentrations were evaluated according to inland water resources limits, it is seen that upstream of the Kirmir Stream (SW1) is in Class IV and downstream of Kirmir Stream (SW16) is in Class III due to NO_2 . Upstream of

the Pazar Stream (SW12) is in Class IV due to color and downstream of this stream (SW11) is in Class III due to fecal coliform. Other surface waters, SW20, SW21 are in Class III and SW4, SW5, SW9, SW14, SW15 are in Class IV. The surface waters which were sampled only in May; SW2, SW3 are in Class III and SW6, SW10, SW13 are in Class II.

Table 5.8. Surface water quality classification

ID	Date	Inland Water Resources Surface Water Classification	Irrigation Water Classification	Human Consumption	Human Consumption Indicator Parameters
SW1	May-12	CLASS IV- N-NO2, pH	CLASS III- pH, TSS, Na	As, NO2	
	Sep-12	CLASS IV- N-NO2, pH, P	CLASS III- Coli.F., pH, TSS, Na, Na	As, B, NO2	
	Sep-13	CLASS III- pH, P	CLASS III- Na	As	
	Average	CLASS IV- N-NO2	CLASS III- Coli.F., TSS, Na, Na	As, NO2	
SW2	May-12	CLASS III- pH	CLASS III- TSS	As	
SW3	May-12	CLASS III- pH	CLASS II- SAR-EC, Na	As	
SW4	May-12	CLASS III- pH	CLASS III- TSS, Na	As	
	Jun-13	CLASS IV- Color	CLASS III- Coli.F., Coli.F., Na	As	
	Average	CLASS IV- Color	CLASS III- Coli.F., Coli.F., TSS, Na	As	
SW5	May-12	CLASS III- pH	CLASS III- Mo, TSS, Na	As	
	Jun-13	CLASS IV- Color	CLASS III- Mo, TSS, Na	As	
	Average	CLASS IV- Color	CLASS III- Mo, TSS, Na	As	
SW6	May-12	CLASS II- EC, O2	CLASS III- Mo, Na	As	
SW9	Jun-13	CLASS IV- Color	CLASS III- Coli.F., Coli.F., TSS, Na	As	
	Sep-13	CLASS IV- Color	CLASS III- Na	As	
	Average	CLASS IV- Color	CLASS III- Coli.F., Coli.F., Na	As	
SW10	May-12	CLASS II- EC, O2	CLASS III- TSS, TSS	As	
SW11	May-12	CLASS II- EC, N-NO2, O2, P	CLASS III- TSS, Na	As	
	Sep-12	CLASS III- O2	CLASS III- TSS, Na	As	O2
	Jun-13	CLASS IV- Color	CLASS III- Coli.F., Coli.F., Na	As	
	Sep-13	CLASS II- EC, N-NO2, P	CLASS III- TSS, Na	As	
	Average	CLASS III- Coli.(F)	CLASS III- Coli.F., Coli.F., TSS, Na	As	
SW12	May-12	CLASS III- N-NO2	CLASS III- Na	As	
	Sep-12	CLASS III- pH	CLASS III- Na	As	
	Jun-13	CLASS IV- Color	CLASS III- Coli.F., Na	As	
	Sep-13	CLASS IV- Color	CLASS III- Na	As	
	Average	CLASS IV- Color	CLASS III- Coli.F., Na	As	
SW13	May-12	CLASS II- EC, N-NO2, N-NO3, P	CLASS III- TSS, TSS	As	
SW14	Jun-13	CLASS IV- Coli.(F)	CLASS III- Coli.F., Coli.F., TSS, TSS, Na	As	
	Sep-13	CLASS III- pH	CLASS III- TSS, TSS, Na	As	
	Average	CLASS IV- Coli.(F)	CLASS III- Coli.F., Coli.F., TSS, TSS, Na	As	
SW15	May-12	CLASS II- EC, O2	CLASS III- Na	As	
	Jun-13	CLASS IV- Color	CLASS III- Coli.F., Coli.F., Na	As	
	Sep-13	CLASS IV- Color	CLASS III- Na	As	
	Average	CLASS IV- Color	CLASS III- Coli.F., Coli.F., Na	As	
SW16	May-12	CLASS III- P	CLASS III- TSS, TSS, Na	As	
	Sep-12	CLASS II- EC, N-NO2, P	CLASS III- TSS, Na	As	
	Jun-13	CLASS IV- Color, N-NO2	CLASS III- Coli.F., TSS, Na	As	
	Sep-13	CLASS IV- COD	CLASS III- TSS, Na	As	
	Average	CLASS III- N-NO2	CLASS III- Coli.F., TSS, Na	As	
SW20	Jun-13	CLASS III- pH	CLASS III- Coli.F., TSS	As	Al, Fe, Mn
	Sep-13	CLASS III- O2, pH	CLASS III- TSS	As	
	Average	CLASS III- pH	CLASS III- Coli.F., TSS	As	Al, Fe
SW21	Jun-13	CLASS IV- Color	CLASS III- Coli.F., TSS	As	
	Sep-13	CLASS III- pH	CLASS II- SAR-EC, Na	As	
	Average	CLASS III- pH	CLASS III- Coli.F., TSS	As	

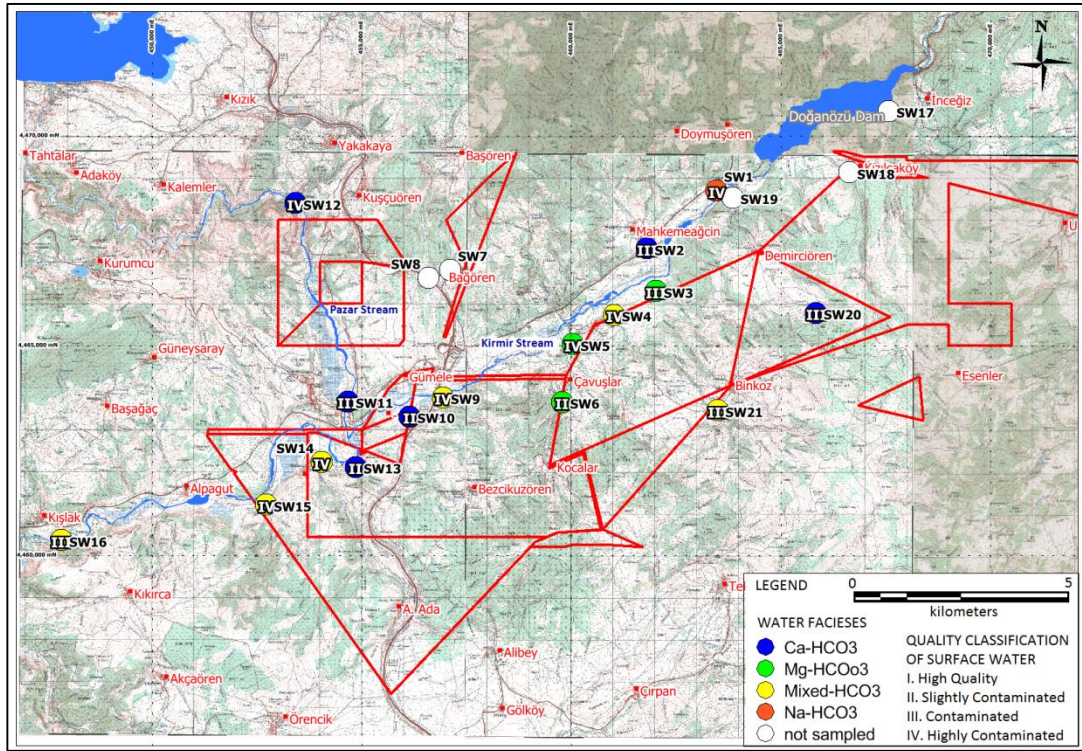


Figure 5.14. Areal distribution of the surface water monitoring points according to inland water classification

5.4.2. Spring and Fountain

Waters of fountain monitoring points were classified according to inland water classification, irrigation water classification and limits of human consumption. Summary of these classifications and areal distributions of inland water classes of these monitoring points are presented in Table 5.9 and Figure 5.15, respectively.

According to this evaluation, all water samples from fountains are in medium and low quality groundwater classes (Class II and Class III). Parameters which cause these classes for each fountain monitoring points are listed in Table 5.9.

Table 5.9. Water quality classification of fountain monitoring points

ID	Date	Inland Water Resources Surface Water Classification	Irrigation Water Classification	Human Consumption	Human Consumption Indicator Parameters	ID	Date	Inland Water Resources Surface Water Classification	Irrigation Water Classification	Human Consumption	Human Consumption Indicator Parameters
F1	May-12	CLASS II- EC, N-NO3, O2	CLASS II- SAR-EC, Na			F28	May-12	CLASS III- O2	CLASS III- Na		O2
	Sep-12	CLASS III- O2	CLASS II- SAR-EC, Na		O2		Sep-12	CLASS III- O2	CLASS III- Na		O2
	Average	CLASS III- O2	CLASS II- SAR-EC, Na		O2		Jun-13	CLASS III- O2	CLASS III- Na		
F2	May-12	CLASS II- EC, O2	CLASS II- SAR-EC, Na			F37	Sep-13	CLASS III- O2	CLASS III- Na		O2
	Sep-12	CLASS II- EC, O2	CLASS II- SAR-EC, Na				Average	CLASS III- O2	CLASS III- Na		O2
	Average	CLASS II- EC, O2	CLASS II- SAR-EC, Na				Jun-13	CLASS II- EC	CLASS III- Na		
F3	May-12	CLASS II- As, EC, N-NO3, O2	CLASS II- SAR-EC, Na	As		F37B	Jun-13	CLASS III- As	CLASS III- Na	As	
	Sep-12	CLASS II- As, EC, N-NO3	CLASS II- SAR-EC, Na	As			Sep-13	CLASS III- As, O2	CLASS III- Na	As	
	Jun-13	CLASS II- As, EC, N-NO3, O2	CLASS II- SAR-EC, Na	As			Average	CLASS III- As	CLASS III- Na	As	
	Sep-13	CLASS II- As, EC, N-NO3, O2	CLASS II- SAR-EC, Na	As			May-12	CLASS II- As, EC	CLASS III- Na	As	
F4	May-12	CLASS II- EC, O2	CLASS II- SAR-EC, Na			F45	Sep-12	CLASS II- As, EC	CLASS III- Na	As	
	Sep-12	CLASS II- EC	CLASS II- SAR-EC, Na				Average	CLASS II- As, EC	CLASS III- Na	As	
	Average	CLASS II- EC	CLASS III- TSS, TSS				May-12	CLASS II- As, EC	CLASS II- SAR-EC, Na	As	
	Jun-13	CLASS III- TSS, TSS					Jun-13	CLASS III- As, EC	CLASS III- Mo	As	
F5	May-12	CLASS II- EC, O2	CLASS II- SAR-EC	As		F49	Sep-13	CLASS III- As, EC, O2	CLASS III- F, Mo	As	O2
	Sep-12	CLASS II- EC	CLASS II- SAR-EC	As			Average	CLASS III- As, EC	CLASS III- Mo	As	
	Jun-13	CLASS II- EC	CLASS II- SAR-EC	As			May-12	CLASS III- O2	CLASS III- Na	As	O2
	Sep-13	CLASS II- EC	CLASS II- SAR-EC	As			Sep-12	CLASS II- As, EC	CLASS III- Na	As	
F6	May-12	CLASS II- EC, N-NO2, O2	CLASS II- SAR-EC, Na			F51	Jun-13	CLASS III- O2	CLASS III- Na	As	O2
	Sep-12	CLASS II- EC	CLASS II- SAR-EC, Na				Average	CLASS III- O2	CLASS III- Na	As	O2
	Average	CLASS II- EC, O2	CLASS II- SAR-EC, Na				May-12	CLASS II- EC, P	CLASS III- Na	As	
	May-12	CLASS II- EC	CLASS III- Na	As			Sep-12	CLASS II- EC, P	CLASS III- Na	As	
F7	Sep-12	CLASS II- EC	CLASS III- Na	As		F52	Jun-13	CLASS II- EC, Hg, N-NO2, P	CLASS III- Na	As	
	Jun-13	CLASS II- EC	CLASS III- Na	As			Sep-13	CLASS II- EC, O2, P	CLASS III- Na	As	
	Sep-13	CLASS II- EC, O2	CLASS III- Na	As			Average	CLASS II- EC, P	CLASS III- Na	As	
	Average	CLASS II- EC	CLASS III- Na	As			Sep-12	CLASS III- O2	CLASS II- EC, Na	As	
F8	May-12	CLASS II- EC	CLASS II- SAR-EC, Na	As		F53	Jun-13	CLASS II- EC, N-NO2	CLASS II- SAR-EC, Na	As	
	Sep-12	CLASS II- EC	CLASS III- TSS	As			Sep-13	CLASS III- O2	CLASS II- SAR-EC, Na	As	O2
	Jun-13	CLASS III- Fe	CLASS II- SAR-EC, Na	As	Fe		Average	CLASS II- EC, N-NO2, O2	CLASS II- SAR-EC, Na	As	
	Sep-13	CLASS II- EC	CLASS II- SAR-EC, Na	As			Jun-13	CLASS III- O2	CLASS III- Na	As	
F9	May-12	CLASS II- Cl, EC	CLASS II- SAR-EC, Na	As		F54	Jun-13	CLASS II- As, EC, N-NO2, O2, P	CLASS II- SAR-EC, Na	As	
	Sep-12	CLASS II- EC	CLASS II- SAR-EC, Na	As			Sep-13	CLASS III- O2	CLASS II- SAR-EC, Na	As	O2
	Average	CLASS II- Cl, EC	CLASS II- SAR-EC, Na	As			Average	CLASS III- O2	CLASS II- SAR-EC, Na	As	O2
	May-12	CLASS II- Cl, EC	CLASS II- SAR-EC, Na	As			Jun-13	CLASS III- O2	CLASS II- SAR-EC, Na	As	O2
F10	May-12	CLASS III- O2	CLASS III- Na	As	O2	F55	Sep-13	CLASS III- O2	CLASS II- SAR-EC, Na	As	O2
	Sep-12	CLASS III- O2	CLASS III- Na	As			Average	CLASS III- O2	CLASS II- SAR-EC, Na	As	O2
	Jun-13	CLASS II- As, EC, O2, TOC	CLASS III- Na	As			Jun-13	CLASS III- O2	CLASS II- SAR-EC, Na	As	O2
	Sep-13	CLASS III- O2	CLASS III- Na	As	O2		Sep-13	CLASS III- O2	CLASS II- SAR-EC, Na	As	O2
F11C	May-12	CLASS II- EC	CLASS III- Na	As		F56	Average	CLASS III- O2	CLASS II- SAR-EC, Na	As	O2
	Sep-12	CLASS III- As	CLASS III- Na	As			Jun-13	CLASS II- EC	CLASS II- SAR-EC, Na	As	
	Sep-12	CLASS II- As, EC	CLASS III- Na	As			Sep-13	CLASS III- O2	CLASS II- SAR-EC, Na	As	O2
	Jun-13	CLASS II- EC	CLASS III- Na	As			Average	CLASS III- O2	CLASS II- SAR-EC, Na	As	O2
F12	May-12	CLASS III- As	CLASS III- Na	As		F57	Jun-13	CLASS III- As	CLASS III- Mo	As	
	Sep-12	CLASS III- As	CLASS III- Na	As			Sep-13	CLASS II- As, EC, O2	CLASS III- Mo	As	
	Sep-12	CLASS II- As, EC	CLASS III- Na	As			Average	CLASS III- As	CLASS III- Mo	As	
	Jun-13	CLASS II- EC	CLASS III- Na	As			Jun-13	CLASS II- As, EC, COD, N-NO2	CLASS II- SAR-EC, Na	As	
F13	May-12	CLASS III- As	CLASS III- Na	As		F58	Sep-13	CLASS II- As, EC, P	CLASS II- SAR-EC, Na	As	
	Sep-12	CLASS III- As, O2	CLASS III- As, Na	As			Average	CLASS II- As, EC, N-NO2, P	CLASS II- SAR-EC, Na	As	
	Average	CLASS III- As, O2	CLASS III- As, Na	As			Jun-13	CLASS III- N-NO2	CLASS III- TSS	As	
	May-12	CLASS II- As, EC, O2, TDS	CLASS III- Mo	As			Sep-13	CLASS II- As, EC, N-NO2, O2	CLASS II- EC, Na	As	
F14	Sep-12	CLASS II- As, EC, O2, P, TDS	CLASS III- Mo	As		F59	Average	CLASS II- As, EC, N-NO2	CLASS III- TSS	As	
	Average	CLASS II- As, EC, O2, P, TDS	CLASS III- Mo	As			Jun-13	CLASS III- O2	CLASS III- Na	As	O2
	May-12	CLASS III- As	CLASS II- SAR-EC	As			Sep-13	CLASS III- O2%	CLASS III- Na		
	Sep-12	CLASS III- As	CLASS II- SAR-EC	As			Average	CLASS III- O2	CLASS III- Na		
F15	Jun-13	CLASS III- As	CLASS II- SAR-EC	As		F63	Jun-13	CLASS III- N-NO2	CLASS III- Na		
	Sep-13	CLASS III- As, O2	CLASS II- SAR-EC, Na	As	O2		Sep-13	CLASS II- EC, N-NO2, N-NO3, P	CLASS III- Na		
	Average	CLASS III- As	CLASS II- SAR-EC	As			Average	CLASS II- EC, N-NO2, N-NO3, P	CLASS III- Na		
	May-12	CLASS II- Cl, EC, P	CLASS III- Na	As			Jun-13	CLASS III- Al, P	CLASS II- SAR-EC, Na	As	Al, Fe
F16	Sep-12	CLASS II- Cl, EC, O2, P	CLASS III- Na	As		F64	Sep-13	CLASS III- P	CLASS II- SAR-EC, Na	As	
	Jun-13	CLASS II- Cl, EC, P	CLASS III- Na	As			Average	CLASS III- P	CLASS II- SAR-EC, Na	As	Al, Fe
	Sep-13	CLASS II- Cl, EC, O2, P	CLASS III- Na	As			Jun-13	CLASS III- O2, P	CLASS II- SAR-EC, Na	As	
	Average	CLASS II- Cl, EC, O2, P	CLASS III- Na	As			Sep-13	CLASS III- P	CLASS II- SAR-EC, Na	As	
F17	May-12	CLASS II- EC, O2, P	CLASS III- Na	As		F65	Average	CLASS III- O2%, P	CLASS II- SAR-EC, Na	As	
	Sep-12	CLASS II- EC, O2, P	CLASS III- Na	As			Jun-13	CLASS II- As, EC	CLASS II- SAR-EC, Na	As	
	Jun-13	CLASS II- EC, P	CLASS III- Na	As			Sep-13	CLASS II- As, EC	CLASS II- SAR-EC, Na	As	
	Sep-13	CLASS II- EC, P	CLASS III- Na	As			Average	CLASS II- As, EC	CLASS II- SAR-EC, Na	As	
F18	May-12	CLASS II- EC, P	CLASS III- Na	As		F66	Jun-13	CLASS II- EC, O2	CLASS II- SAR-EC, Na	As	
	Sep-12	CLASS II- EC, P	CLASS III- Na	As			Sep-13	CLASS III- O2	CLASS II- SAR-EC, Na	As	O2
	Jun-13	CLASS II- EC, P	CLASS III- Na	As			Average	CLASS III- O2	CLASS II- SAR-EC, Na	As	
	Average	CLASS II- EC, P	CLASS III- Na	As			Jun-13	CLASS II- As, EC	CLASS II- SAR-EC, Na	As	

Table 5.10. Water quality classification of well samples

ID	Date	Inland Water Resources Surface Water Classification	Irrigation Water Classification	Human Consumption	Human Consumption Indicator Parameters
PW1	Oct-12	CLASS III- B, EC, Temperature, Na, TDS	CLASS III- B, F, Na, Cl	As, B	EC, Na, NH4
	Sep-13	CLASS III- B, EC, Temperature, Na, O2	CLASS III- B, F, Na, Cl	As, B	Na, O2, NH4
	Average	CLASS III- B, EC, Temperature, Na, O2	CLASS III- B, F, Na, Cl	As, B	Na, O2, NH4
PW2	Sep-13	CLASS III- As, B, Cl, EC, COD, N(Kjel) , Na, N-NH4, O2, pH, TDS, TOC	CLASS III- As, B, Cl, EC, Mo, pH, TSS, TDS, Na, Cl	As, B	Cl, EC, Na, O2, NH4, pH
PW3	Oct-12	CLASS II- As, EC, Cr	CLASS III- Na	As	
	Sep-13	CLASS III- O2	CLASS II- SAR-EC, Na	As	O2
	Average	CLASS III- O2	CLASS III- Na	As	O2
PW4A	Sep-13	CLASS III- B, Cl, EC, Temperature, Na, O2, TDS	CLASS III- B, EC, Mo, TDS, Na, Cl	As, B	Cl, EC, Fe, Na, O2
PW5	Nov-13	CLASS III- O2, pH	CLASS III- Na	As	O2, NH4
PW6	Nov-13	CLASS III- Al, B, Na, O2, pH	CLASS III- TSS, Na,	B	Al, Fe, O2, NH4
CEL35	Sep-13	CLASS III- O2	CLASS III- Na,		Mn, O2, NH4
CEL36	Oct-13	CLASS III- B, N(Kjel) , Na, N-NH4, N-NO2, pH, TOC	CLASS III- pH, TSS, Na	B	NH4, pH
CEL44	Oct-13	CLASS III- N-NO2, pH	CLASS III- pH, TSS, Na		Mn, NH4
CEL47	Oct-13	CLASS III- N(Kjel) , Na, N-NH4, N-NO2, O2, pH	CLASS III- Mo, pH, TSS, Na	As	Al, Fe, O2, NH4, pH
CEL47A	Oct-13	CLASS III- B, O2, P	CLASS III- Na	B	Mn, O2, NH4
CEL51	Oct-13	CLASS III- pH, P	CLASS III- pH, TSS, Na		Mn, NH4
CEL52	Oct-13	CLASS III- EC, COD, Cr, Mn, Na, pH, TOC	CLASS III- Cr, Mn, TSS, Na	Cr	Fe, Mn, Na, NH4
CEL53A	Oct-13	CLASS III- Na, O2	CLASS III- Na	As	O2, NH4
CEL59A	Oct-13	CLASS III- Cr, Na, O2	CLASS III- Na	Cr	Mn, O2, NH4
CEL59B	Oct-13	CLASS III- B, Na, N-NH4, O2, pH, P	CLASS III- F, pH, SAR-EC, Na	As, B	Na, O2, NH4

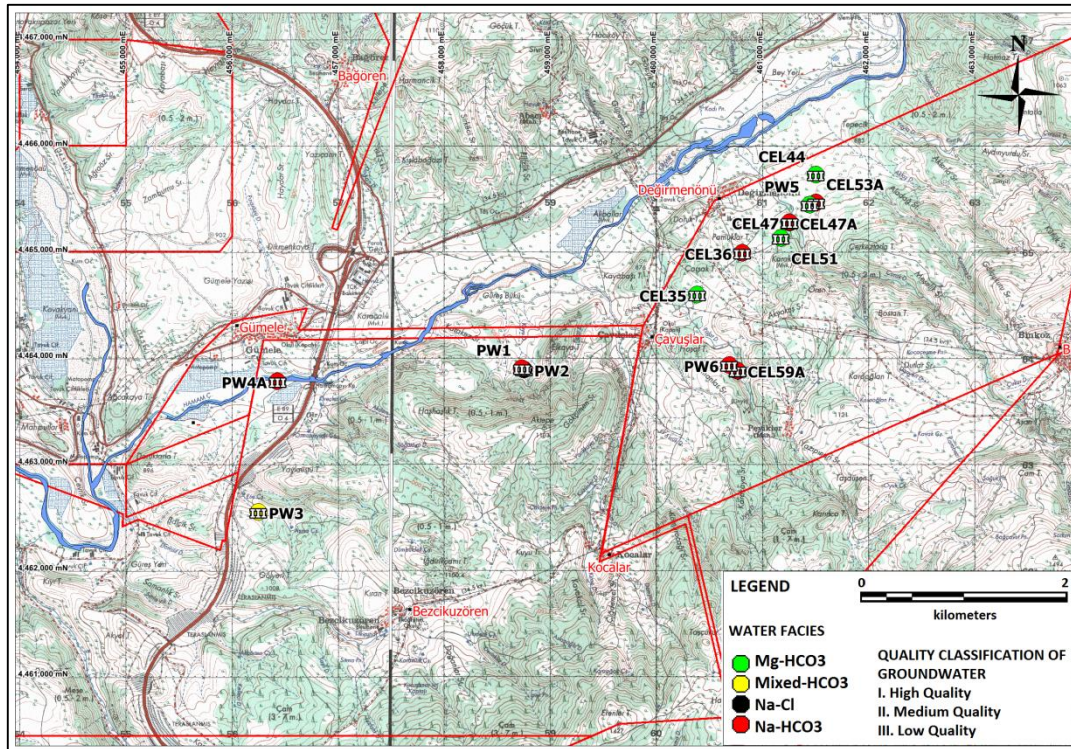


Figure 5.16. Areal distribution of the well monitoring points according to inland water classification

5.4.4. Water Depots

Analysis of water depots of the villages were evaluated according to limits of human consumption. Results of this evaluation are summarized in Table 5.11. There are not any water depots in Kocalar and Aşağıadaköy villages, thus the fountains which supply water to villages were sampled. Sampling could not be conducted from Çeltikçi town in September 2012, June 2013 due to water cut and Aşağıadaköy village in September 2013 due to infrastructure works. D11, D12, D13 and D14 had been added in sampling program after adding new tenements.

According to this assessment, due to elevated values of arsenic (higher than 0.01 mg/l), the waters of the depots are not suitable for drinking except for Kızılcaköy village. In addition, water of the Bezcikuzören village water depot is not suitable for drinking due to high nitrate concentration. There is no change in quality in the monitoring period.

Table 5.11. Water quality classification of water depots of the villages

ID	Date	Human Consumption	Human Consumption Indicator Parameters	ID	Date	Human Consumption	Human Consumption Indicator Parameters	
D1 Mahkemeağacı	May-12	As		D7 Aşağıada	May-12	As		
	Sep-12	As			Sep-12	As		
	Jun-13	As			Jun-13	As		
	Sep-13	As	O2		Average	As		
	Average	As			Average	As		
D2 Değirmenönü	May-12	As		D8 Bağlıca	May-12	As		
	Sep-12	As			Sep-12	As		
	Jun-13	As			Jun-13	As		
	Sep-13	As			Sep-13	As	O2	
	Average	As			Average	As		
D3 Bağören	May-12	As		D8A Bağlıca	Jun-13	As		
	Sep-12	As			D9 Çeltikçi	May-12	As	A1
	Jun-13	As				Sep-13	As	
	Sep-13	As				Average	As	
	Average	As				May-12	As	
D4 Çavuşlar	May-12	As		D10 Gümele		Sep-12	As	
	Sep-12	As			Jun-13	As		
	Jun-13	As			Sep-13	As	O2	
	Sep-13	As			Average	As		
	Average	As			Jun-13	As		
D5 Kocalar	May-12	As		D11 Peykler	Sep-13	As	O2	
	Sep-12	As			Average	As		
	Jun-13	As			Jun-13	As		
	Sep-13	As	O2		Sep-13	As		
	Average	As			Average	As		
D6 Bezcikuzören	May-12	As, NO3		D12 Binkoz	Jun-13	As		
	Sep-12	As, NO3			Sep-13	As		
	Jun-13	As, NO3			Average	As		
	Sep-13	As, NO3			Jun-13	As		
	Average	As, NO3			Sep-13	As		
D13 Demirciören	May-12	As, NO3		D13 Demirciören	Average	As		
	Sep-12	As, NO3			Jun-13			
	Jun-13	As, NO3			Sep-13			
	Sep-13	As, NO3			Average			
	Average	As, NO3			Jun-13			
D14 Kızılca	May-12	As, NO3		D14 Kızılca	Sep-13		O2	
	Sep-12	As, NO3			Average			
	Jun-13	As, NO3			Jun-13			
	Sep-13	As, NO3			Sep-13			
	Average	As, NO3			Average			

CHAPTER 6

CONCLUSIONS AND RECOMMENDATIONS

6.1. CONCLUSIONS

In this study, various site specific data was collected and analyzed to make hydrogeological characterization of the Çeltikçi coal basin. Study area is located on a steep and rough terrain. Elevation values change between 760-780 m near the Kirmir Stream and 1690 m at the Hıdırdede Hill which is at the eastern side of the study area. The most important surface waters in the study area are Kirmir Stream and Pazar Stream. These two important surface waters are controlled by the important water structures. According to Thorntwaite climate classification, climate class of the region was determined as semi-arid – low humid. Regionally, study area is located in the southern part of the volcanic region which is named as “Galatian Volcanic Province” (GVP). The units which outcrop at the surface from bottom to top are; Miocene aged volcanics, Miocene aged Çeltikçi formation, Plio-Quaternary and Quaternary units. Coal layers are in the Miocene aged Çeltikçi formation. According to the conceptual water budget of the study area, 74%, 12% and 14% of total precipitation transform to the evaporation, surface runoff and groundwater percolation, respectively.

There are three main aquifers in the study area. First of them is the Bezci-Aktepe-Kocalar unconfined aquifer which is composed of mudstone with tuff layers (Kocalar member), limestone and dolomitic mudstone (Aktepe member) and sandstone-siltstone (Bezci member). The second one is the Volcanic-Çavuşlar aquifer which is composed of cream-white-light green colored mudstone with sandstone-tuff-coal layers (Çavuşlar member) and the volcanics forming the basement of the study area. This aquifer is an unconfined aquifer at the eastern side of the Kocalar fault while it acts as a confined aquifer at the western side of this fault. The third

aquifer in the study area is the Quaternary aged alluvium which is composed of clay, silt, sand and gravel lying along the Kirmir and Pazar Streams.

A total of 76 exploration wells have been opened as part of the exploration activities. Forty-two of them were converted to monitoring wells in order to determine hydraulic conditions and hydraulic parameters, measure the groundwater levels, flow rate and water quality parameters and monitor their changes. In addition to these wells, seven pump wells were drilled in the study area in order to determine the hydraulic parameters of the aquifers by conducting aquifer tests. According to the geometric mean of all analysis result of the aquifer tests; alluvium has the highest hydraulic conductivity with 1.22×10^{-5} m/s. Çavuşlar member below the coal has the second highest hydraulic conductivity values (9.40×10^{-7} m/s). Third one is Aktepe and Kocalar members (8.30×10^{-7}), fourth one is Coal Seam (6.77×10^{-7} m/s), and fifth one is Çavuşlar member above the coal (6.77×10^{-7} m/s). Volcanics has the lowest hydraulic conductivity with 7.46×10^{-8} m/s.

Groundwater in the Çavuşlar-Volcanic aquifer generally flows from the highlands at the southeast of the study area toward the Kirmir Stream which flows through NE-SW. Groundwater levels decrease from 1200-1250 m at the southeast to 800-900 m at the Kirmir Stream. Northwest oriented general groundwater flow direction is modified locally by some fault lines. Hydraulic gradient is higher at the eastern side of the Kocalar fault (0.15) compared to the western side of it (0.1). Hydraulic gradient decreases toward the discharge area along the Kirmir Stream.

Kirmir Stream is highly contaminated both at the upstream and downstream due to the elevated values of NO_2 . Upstream of the Pazar Stream is highly contaminated due to color parameter and downstream of this Stream is also contaminated due to fecal coliform. All surface waters are not suitable for human consumption due to elevated arsenic value. In addition, according to irrigation water criteria, all surface waters are in hazardous class. According to the inland groundwater classification criteria, some spring waters are low quality and some are medium quality due to low O_2 and high As values. Groundwater in the monitoring wells is in low quality. CEL35, CEL44 and CEL51 are not suitable for human consumption due to high As/B/Cr concentrations. Waters which appear as suitable for human consumption, Mn and NH_4 indicator parameters are high. With respect to

irrigation water criteria, all well waters are in hazardous water quality. Also because of the high As concentration, water depots are not suitable for human consumption except for the Kızılca village water depot.

6.2. RECOMMENDATIONS

- ❖ Binkoz meteorological station should be operated continuously. In order to avoid to data loss, data should be downloaded regularly and quality control of the measurements should be conducted. All sensors in the station should be calibrated by an accredited institution.
- ❖ Geology of the study area should be extended to the north and south borders of the catchment.
- ❖ Groundwater level and pressure measurements at all monitoring and pump wells should be continued. Also, discharge measurements should be conducted with pressure measurements at the wells that have the free flow conditions.
- ❖ In order to determine the water table of the Bezci-Aktepe-Kocalar aquifer and the relation between the underlying Volcanic-Çavuşlar aquifer, monitoring and pump wells should be drilled at the selected locations.
- ❖ Conceptual hydrologic model and conceptual water budget should be continuously updated with new data.
- ❖ 3-D groundwater flow model should be developed for using in both mining activities and Environmental Assessment Impact (EAI) studies.
- ❖ There is a need to test how to reduct water pressures below the coal seam. Also it is recommended to conduct a similar research for dewatering in the planned open-pit area. In this context, 3-D groundwater flow model should be used.
- ❖ In addition to the existing hydrochemical monitoring points, the monitoring wells should be opened in Bezci, Aktepe, Kocalar and Abacı members in order to determine the hydrochemical properties of the groundwater at these units.

REFERENCES

AATTUT, 2010, Atıksu Arıtma Tesisleri Teknik Usuller Tebliği, Resmi Gazete No: 27527.

Agusti, J., Cabrera, L., Garces, M., Krijgsman, W., Oms, O. and Pares, J. M., 2001. A calibrated mammal scale for the Neogene of Western Europe. State of the art, *Earth-Sci. Reviews*, 52, 247-260.

Akyol, E., 1968, Ankara-Kızılcahamam, Çeltikçi civarında bulunan kömür zuhurlarının 1/25000 ölçekli detay jeolojik etüdü hakkında rapor, MTA, Report no. 4405, 14p.

Chow V.T., Maidment, D.R., Mays, L.W., 1988, *Applied Hydrology*, McGraw Hill Publishing, 572p.

Ercan, T., Yeğingil, Z., Bigazzi, G., Oddone, M., and Özdoğan, M., 1990, Kuzeybatı Anadolu, obsidiyen buluntularının kaynak belirleme çalışmaları, *Jeoloji Mühendisliği*, 36, 19-32.

EU, 1998. On quality of water intended for human consumption, Council Directive 98/83/EC of 3 November 1998. *Official Journal of European Communities*.

Gürbüz, M., 1981. İnönü (KB Ankara) Orta Miosendeki Hemicyon sansaniensis (Ursidae) türünün tanımlanması ve stratigrafik yayılımı. *TJK Bulletin*, 24, 2, 85-90.

İnci, U., Helvacı, C., and Yağmurlu, F., 1988, Stratigraphy of the Beypazarı Neogene basin, Central Anatolia, Turkey, *Newsl. Stratigr.*, 18, 165-182.

İTAS, 2005. İnsani Tüketim Amaçlı Sular Hakkında Yönetmelik, Resmi Gazete No: 25730.

Keller, J., Jung, D., Eckhard, F., J., and Kreuzer, H., 1992, Radiometric ages and chemical characterization of the Galatian andesite massif, Pontus, Turkey, *Acta Vulcanologica*, 2, 267-276.

Koçyiğit, A., 1991. Changing Stress Orientation in Progressive Intracontinental Deformation as Indicated by the Neotectonics of the Ankara Region (NW Central Anatolia), TPJD Bulletin, 3/1, 43-55.

Koçyiğit, A., Winchester, J. A., Bozkurt, E. and Holland, G., 2003. Saraçköy Volcanic Suite: implications for the subductional phase or arc evolution in the Galatian Arc Complex, Ankara, Turkey. Geological Journal, 38, 1-14.

MTA, 2005. Türkiye Jeotermal Kaynakları Envanteri. Envanter Serisi 201, Maden Tetkik ve Arama Genel Müdürlüğü.

Ozansoy, F., 1961. Ankara Bölgesi Fauna Teakubu Etüdünün Esaslı Sonuçları, MTA Bulletin, 56, 86-95.

Öngür, T., 1976, Kızılcahamam, Çamlıdere, Çeltikçi, Kazan dolayının jeoloji durumu ve jeotermal enerji olanakları, MTA Report no. 3273, 34p.

Rojay, F. B., 2013. Structural evolution of Çeltikçi – Gümele area during post Miocene, METU Report, 38 p.

SKKY, 2008. Su kirliliği Kontrol Yönetmeliğinde Değişiklik Yapılmasına Dair Yönetmelik, Resmi Gazete No: 267856.

Soil Conservation Service (SCS), 1964, SCS National Engineering Handbook, Section 4: Hydrology, Updated 1972, U.S. Department of Agriculture, Washington D.C.

Şen, Ş. and Rage, J. C., 1979. Çalta (Ankara) Pliyosen Omurgalı Faunası, TJK Bulletin, 22, 1, 155-160.

Tankut, A., Wilson, M. and Yihunie, T., 1998. Geochemistry and tectonic setting of Tertiary volcanism in the Güvem area, Anatolia, Turkey: J. of Volcanology and Geothermal Research, 85, 285-301.

Tankut, A., Akıman, O., Türkmenoğlu, A., Güleç, N., Göker, T. T., 1990, Tertiary volcanic rocks in NW-Central Anatolia, In: Savaşçın, Y., Eronat, A.H., (eds), IESCA 1990 Proceedings 2, 450–466.

Tatlı, S., 1975, KızılcaKirmircayı Doğu Alanının Jeolojisi ve Jeotermal Enerji Olanakları, MTA Report no. 5749, 42p.

Tekkaya, İ., 1973. Orta Sinaptaki Yeni Bir Gazella Türü. MTA Bulletin, 80, 113-136.

Tekkaya, İ., 1974a. The Bovidae fauna of middle Sinap of Turkey. TJK Bulletin, 17, 1, 173-186.

Tekkaya, İ., 1974b. A new species of Tortonian Anthropoid (primate, mammalia) from Anatolia. MTA Bulletin, 83, 148-165.

Toprak, V., Savaşçın Y., Güleç, N. and Tankut, A., 1996. Structure of the Galatian volcanic province. Int. Geology Review, 38, 747-758.

Turgut, A.T., 1978, Kızılcahamam (Ankara) – Çeltikçi ve Çamlıdere Neojen havzalarının linyit olanakları, MTA Report No., 6173, 20p.

TÜİK, 2012. Adrese dayalı nüfus kayıt sistemi (ADNKS) veri tabanı, Ankara ili, Belde ve köyler nüfusu.

Türkecan, A., Hepşen, N., Papak, İ., Akbaş, B., Dinçel, A., Karataş, S., Özgür, İ.B., Akay, E., Bedi, Y., Sevin, M., Mutlu, G., Sevin, D., Ünay, E., ve Saraç, G., 1991, Seben-Gerede (Bolu)- Güdül- Beypazarı (Ankara) ve Çerkeş- Orta-Kurşunlu (Çankırı) yörelerinin (Köroğlu Dağları) jeolojisi ve volkanik kayaların petrolojisi, MTA Report no. 9193, 118p.

Wilson, M., Tankut, A. and Güleç, N., 1997. Tertiary volcanism of the Galatia province, north-west Central Anatolia, Turkey. Lithos, 42, 105-121.

Yazıcıgil, H., Çamur, M.Z., Süzen, M.L., Yılmaz K.K., Kahraman, C., Sayıt A., 2014. Final Report, Çeltikçi Kömür Havzasının Hidrojeolojik Etüdü ve Karakterizasyonu, ODTÜ; Project No. 11-03-09-2-00-36.

YSKYY, 2012. Yüzeysel su kalitesi yönetimi yönetmeliği, Resmi Gazete No: 28483.

YKBKK, 2012. Yeraltısularının Kirlenme ve Bozulmaya Karşı Korunması Hakkında Yönetmelik, Resmi Gazete No. 28257.